



**TRANSITIONAL FLOW OF NON-NEWTONIAN FLUIDS IN OPEN CHANNELS OF
DIFFERENT SHAPES**

by

CHRISTINE MAHEMBA WA KABWE

**Thesis submitted in fulfilment of the requirements for the degree
Master of Technology: Chemical Engineering**

in the Faculty of Engineering

at the Cape Peninsula University of Technology

**Supervisor: Prof R Haldenwang
Co-supervisor: Prof V Fester**

**Cape Town
November 2014**

CPUT copyright information

The dissertation/thesis may not be published either in part (in scholarly, scientific or technical journals), or as a whole (as a monograph), unless permission has been obtained from the University

DECLARATION

I, CHRISTINE MAHEMBA WA KABWE, declare that the contents of this dissertation/thesis represent my own unaided work, and that the dissertation/thesis has not previously been submitted for academic examination towards any qualification. Furthermore, it represents my own opinions and not necessarily those of the Cape Peninsula University of Technology.

Signed

Date

ABSTRACT

Open channels are widely used in the mining industries where homogeneous non-Newtonian slurries have to be transported around plants (Sanders *et al.*, 2002). As water becomes scarcer and more costly due to legislative limitations, higher concentrations of slurries have to be transported. Very little work had been done to predict the laminar-turbulent transition flow of non-Newtonian fluids in open-channels. The effect of open channel on flow of non-Newtonian fluids in the transition region is not well understood. A systematic study on the effect of open channel shape on transitional flow for different non-Newtonian fluids has as far as can be ascertained not been conducted to date.

This work investigated the effect of the channel cross-sectional shape on transitional flow of non-Newtonian fluids.

There are a number of analytical and empirical methods available for the prediction of transitional flow in open channels. However, there are no conclusive guidelines in the literature that would predict the transitional flow for different shapes.

A large experimental database for non-Newtonian flow produced by the Flow Process Research Centre at the Cape Peninsula University of Technology in rectangular, trapezoidal, semi-circular and triangular channels at slopes varying from 1° to 5° was used to achieve the objective. The test fluids consisted of bentonite and kaolin clay suspensions, and solutions of carboxymethyl cellulose (CMC) of various concentrations. The shear stress - shear rate behaviour of each test fluid was measured using in-line tube viscometry.

To evaluate predictive models of transitional flow in various channel shapes, a comparison of critical actual velocities with models velocities was conducted for power law, Bingham plastic and yield-shear thinning fluids. After comparison of various models in different flume shapes, Haldenwang's critical Reynolds number for rectangular channels was deemed to be the best predictive model. To improve Haldenwang's critical Reynolds number, new correlations based on Haldenwang's (2003) method were developed for each shape studied and their corresponding critical velocities were compared.

By combining all the transition data for the four shapes a new correlation "combined model" was developed for onset of transition and onset of full turbulence which can adequately accommodate the four different channel shapes for all fluids tested.

ACKNOWLEDGEMENTS

I wish to thank:

- My supervisor, Prof. Rainer Haldenwang, for his support and professional guidance throughout the whole research process.
- My co-supervisor, Prof. Veruscha Fester for her constructive criticism.
- The Cape Peninsula University of Technology, as well as the Flow Process and Rheology Center, for the opportunity to join this world-recognised research unit.
- My colleagues and friends for their moral support and assistance.

DEDICATION

This thesis is dedicated to:

The Almighty God: for his unconditional love

My father, Mr. Kabwe Ka Mahango Louis Rufin, for his love, encouragement and believing in me

My mother, Ms. Jacqueline Fatuma wa Kaite, for her love, support and wise words

My nephews and nieces, for your love and support

My friends, colleagues and family, for your continuous support and prayers

TABLE OF CONTENTS

| | |
|---|-------------|
| DECLARATION | II |
| ABSTRACT | III |
| ACKNOWLEDGEMENTS | IV |
| DEDICATION | V |
| TABLE OF CONTENTS | VI |
| LIST OF FIGURES | IX |
| LIST OF TABLES | XIII |
| GLOSSARY | XVI |
| NOMENCLATURE | XVII |
| CHAPTER 1: INTRODUCTION | 1 |
| 1.1 INTRODUCTION..... | 1 |
| 1.2 PROBLEM STATEMENT | 2 |
| 1.3 OBJECTIVE | 2 |
| 1.4 METHODOLOGY..... | 2 |
| 1.5 DELINEATION | 3 |
| 1.6 SUMMARY..... | 3 |
| CHAPTER 2: LITERATURE REVIEW | 4 |
| 2.1 INTRODUCTION..... | 4 |
| 2.2 GEOMETRY OF OPEN CHANNELS | 4 |
| 2.3 FLOW REGIMES | 6 |
| 2.3.1 <i>Reynolds number</i> | 6 |
| 2.3.2 <i>Laminar flow</i> | 7 |
| 2.3.3 <i>Transitional flow</i> | 7 |
| 2.3.4 <i>Turbulent flow</i> | 7 |
| 2.3.5 <i>Froude number</i> | 7 |
| 2.3.6 <i>Types of flow in open channels</i> | 8 |
| 2.3.6.1 Uniform and varied flow | 9 |
| 2.3.6.2 Steady and unsteady flow..... | 9 |
| 2.3.7 <i>The most efficient shape for open channels</i> | 9 |
| 2.4 FLUID RHEOLOGY | 10 |
| 2.4.1 <i>Newtonian fluid behaviour</i> | 10 |
| 2.4.2 <i>Non-Newtonian fluid behaviour</i> | 11 |
| 2.4.3 <i>Time independent models</i> | 12 |
| 2.4.4 <i>Rheometry for non-Newtonian fluids</i> | 14 |
| 2.4.4.1 Rotary viscometer | 14 |
| 2.4.4.2 Tube viscometer | 14 |
| 2.5 NEWTONIAN OPEN CHANNEL FLOW | 16 |
| 2.5.1 <i>Laminar flow</i> | 17 |
| 2.5.2 <i>Turbulent flow</i> | 18 |
| 2.5.2.1 Chézy..... | 18 |
| 2.5.2.2 Manning or Gauckler-Manning..... | 18 |
| 2.5.2.3 Blasius | 19 |
| 2.5.2.4 Colebrook-White | 19 |
| 2.5.3 <i>Laminar-Turbulent Transition</i> | 20 |
| 2.6 NON-NEWTONIAN OPEN CHANNEL FLOW..... | 22 |

| | | |
|---|---|-----------|
| 2.6.1 | <i>Laminar flow</i> | 22 |
| 2.6.1.1 | Work done by Kozicki and Tiu | 22 |
| 2.6.1.2 | Work done by Hao and Zhenghai | 23 |
| 2.6.1.3 | Work done by Coussot | 24 |
| 2.6.1.4 | Abulnaga's approach | 25 |
| 2.6.1.5 | De Kee et al.'s thin film approach | 26 |
| 2.6.1.6 | Work done by Haldenwang | 27 |
| 2.6.1.7 | Work done by Burger | 28 |
| 2.6.1.8 | Experimental procedure used by Haldenwang and Burger | 28 |
| 2.6.2 | <i>Turbulent flow</i> | 30 |
| 2.6.2.1 | Kozicki and Tiu approach | 30 |
| 2.6.2.2 | Torrance pipe flow model adapted | 32 |
| 2.6.2.3 | Slatter's pipe flow model adapted | 32 |
| 2.6.2.4 | Naik's model | 33 |
| 2.6.2.5 | Abulnaga's approach | 34 |
| 2.6.2.6 | Yang and Zhao's model | 35 |
| 2.6.2.7 | Haldenwang's turbulent model | 36 |
| 2.7 | PREVIOUS WORK DONE IN THE LAMINAR-TURBULENT TRANSITION REGION | 36 |
| 2.7.1 | <i>Work done by Hao and Zhengai</i> | 36 |
| 2.7.2 | <i>Work done by Naik</i> | 37 |
| 2.7.3 | <i>Wilson's work</i> | 38 |
| 2.7.4 | <i>Work done by Coussot</i> | 38 |
| 2.7.5 | <i>Work by Slatter and Wasp</i> | 39 |
| 2.7.6 | <i>Work done by Haldenwang</i> | 39 |
| 2.7.7 | <i>Work done by Fitton</i> | 40 |
| 2.7.8 | <i>Slatter's work</i> | 41 |
| 2.7.9 | <i>Wan and Wang's model</i> | 43 |
| 2.7.10 | <i>Yang and Zhao's model</i> | 43 |
| 2.8 | NON-NEWTONIAN OPEN CHANNEL FLOW EXPERIMENTAL STUDIES | 44 |
| 2.9 | AVAILABILITY OF DATA IN THE LITERATURE | 47 |
| 2.10 | CONCLUSION | 49 |
| CHAPTER 3: METHODOLOGY USED FOR DATA ANALYSIS | | 50 |
| 3.1. | FLOW BEHAVIOUR | 50 |
| 3.2. | CRITICAL VELOCITY | 51 |
| 3.3. | STATISTICAL ANALYSIS | 53 |
| 3.4. | ADAPTATION OF HALDENWANG'S (2003) MODEL TO OTHER CHANNEL SHAPES | 53 |
| CHAPTER 4: HALDENWANG (2003) TRANSITIONAL FLOW MODELS ADAPTED FOR SHAPE EFFECT | | 63 |
| 4.1 | INTRODUCTION | 63 |
| 4.2 | TRIANGULAR FLUME | 63 |
| 4.3 | TRAPEZOIDAL FLUME | 66 |
| 4.4 | SEMI-CIRCULAR FLUME | 70 |
| 4.5 | COMBINED MODEL | 73 |
| 4.6 | CONCLUSION | 76 |
| CHAPTER 5: COMPARISON OF THE ADAPTED MODELS WITH THOSE FOUND IN THE LITERATURE | | 77 |
| 5.1. | INTRODUCTION | 77 |
| 5.2. | TRANSITIONAL FLOW | 77 |
| 5.2.1 | <i>Work done by Straub et al. (1958) for Newtonian fluids</i> | 78 |
| 5.2.2 | <i>Evaluation of power law fluids</i> | 78 |
| 5.2.2.1 | Work done by Haldenwang | 78 |

| | | |
|--|--|------------|
| 5.2.2.2 | Work done by Fitton..... | 81 |
| 5.2.2.3 | Work done by Slatter (2013)..... | 84 |
| 5.2.3 | <i>Evaluation of Bingham plastic fluids</i> | 90 |
| 5.2.3.1 | Work done by Hao and Zhenghai..... | 90 |
| 5.2.3.2 | Work done by Naik..... | 91 |
| 5.2.3.3 | Work done by Haldenwang..... | 92 |
| 5.2.3.4 | Work done by Fitton..... | 94 |
| 5.2.4 | <i>Evaluation of yield shear-thinning fluids</i> | 96 |
| 5.2.4.1 | Work done by Coussot..... | 96 |
| 5.2.4.2 | Work done by Haldenwang..... | 98 |
| 5.2.4.3 | Work done by Fitton..... | 101 |
| 5.2.4.4 | Work done by Slatter..... | 104 |
| 5.2.5 | <i>Comparison between models</i> | 110 |
| 5.2.5.1 | Comparison between Haldenwang and Fitton's models for power law fluids..... | 110 |
| 5.2.5.2 | Comparison between Haldenwang and Fitton's models for Bingham plastic fluids..... | 112 |
| 5.2.5.3 | Comparison between Coussot, Haldenwang, Fitton and Slatter's models for yield shear-thinning fluids..... | 114 |
| 5.3. | END OF TRANSITIONAL FLOW (ONSET OF TURBULENT FLOW)..... | 116 |
| 5.3.1 | <i>Power law fluids</i> | 116 |
| 5.3.2 | <i>Bingham plastic fluids</i> | 117 |
| 5.3.3 | <i>Yield shear-thinning fluids</i> | 119 |
| 5.4. | COMPARISON OF THE ADAPTED TRANSITIONAL MODELS..... | 120 |
| 5.4.1 | <i>Onset of transitional flow: Rectangular flume</i> | 120 |
| 5.4.2 | <i>End of transitional flow: Rectangular flume</i> | 122 |
| 5.4.3 | <i>Onset of transitional flow: Triangular flume</i> | 123 |
| 5.4.4 | <i>End of transitional flow: Triangular flume</i> | 125 |
| 5.4.5 | <i>Onset of transitional flow: Semi-circular flume</i> | 127 |
| 5.4.6 | <i>End of transitional flow: Semi-circular flume</i> | 128 |
| 5.4.7 | <i>Onset of transitional flow: Trapezoidal flume</i> | 130 |
| 5.4.8 | <i>End of transitional flow: Trapezoidal flume</i> | 131 |
| 5.5. | CONCLUSIONS..... | 133 |
| CHAPTER 6: CONCLUSIONS AND RECOMMENDATIONS..... | | 135 |
| 6.1 | INTRODUCTION..... | 135 |
| 6.2 | SUMMARY..... | 135 |
| 6.3 | CONTRIBUTIONS..... | 137 |
| 6.4 | CONCLUSION..... | 138 |
| 6.5 | RECOMMENDATIONS..... | 138 |
| REFERENCES..... | | 139 |
| APPENDICES..... | | 144 |
| APPENDIX A: RECTANGULAR FLUME DATA..... | | 145 |
| APPENDIX B: SEMI-CIRCULAR FLUME DATA..... | | 160 |
| APPENDIX C: TRAPEZOIDAL FLUME DATA..... | | 168 |
| APPENDIX D: TRIANGULAR FLUME DATA..... | | 176 |

LIST OF FIGURES

| | |
|---|----|
| Figure 2.1: Types of flow (Chaudhry, 2008) | 8 |
| Figure 2.2: Shear stress and velocity gradient in a fluid (Coulson & Richardson, 1999) | 11 |
| Figure 2.3: Flow curve models | 12 |
| Figure 2.4: The f - Re relationship for flow in smooth channels (Chow, 1959) | 21 |
| Figure 2.5: 10 m flume rig (Haldenwang, 2003)..... | 30 |
| Figure 2.6: In-line pipe viscometer (Haldenwang, 2003)..... | 30 |
| Figure 2.7: Friction factor vs. Re_{Zhang} and Re_n plot for a rectangular channel showing the effect of roughness upon laminar, transitional and turbulent flow (Zhang and Ren, 1982) | 45 |
| Figure 2.8: Friction factors for idealised tailings slurries flowing in the SRC 150 mm flume . | 46 |
| Figure 2.9: Fitton's small flume experimental data | 47 |
| Figure 3.1: 6% kaolin suspension flowing in a rectangular channel set at 3 degrees slope .. | 51 |
| Figure 3.2: 7.1% kaolin suspension flowing in a 150 mm trapezoidal channel set at 4 degrees slope | 52 |
| Figure 3.3: 7.1% kaolin suspension flowing in a 150 mm trapezoidal channel set at 4 degrees slope | 52 |
| Figure 3.4: Onset of transition locus for 4.6% bentonite slurry in a 150 mm trapezoidal flume | 54 |
| Figure 3.5: Onset of "full turbulence" for 4.6 % bentonite slurry in a 150 mm trapezoidal flume | 55 |
| Figure 3.6: Moody diagram for 5.3% CMC in water solution flowing in a 150 mm semi-circular flume at 5 degrees slope..... | 58 |
| Figure 3.7: Rectangular flume experimental data at 3 degree slope..... | 59 |
| Figure 3.8: A f vs. Re_H plot for experimental data in a triangular flume at a 3 degree slope.. | 60 |
| Figure 3.9: A f vs. Re_H plot for experimental data in a semi-circular flume at a 3 degree slope | 60 |
| Figure 3.10: A f vs. Re_H plot for experimental data in a trapezoidal flume at a 3 degree slope | 61 |
| Figure 4.1: Onset of transition locus – relationship of m-values with apparent viscosity at 100 s^{-1} for all fluids flowing in a 300 mm triangular flume | 63 |
| Figure 4.2: Onset of transition locus – relationship of y-intercept values with apparent viscosity at 100 s^{-1} for all fluids flowing in a 300 mm triangular flume | 64 |
| Figure 4.3: Onset of 'Full turbulence' locus – relationship of m-values with apparent viscosity at 500 s^{-1} for all fluids flowing in a 300 mm triangular flume | 65 |
| Figure 4.4: Onset of 'Full turbulence' locus – relationship of c-values with apparent viscosity at 500 s^{-1} for all fluids flowing in a 300 mm triangular flume | 65 |
| Figure 4.5: Evaluation of the adapted triangular models at the onset and end of transition . | 66 |
| Figure 4.6: Onset of transition locus – relationship of m-values with apparent viscosity at 100 s^{-1} for all fluids flowing in 75 and 150 mm trapezoidal flumes | 67 |
| Figure 4.7: Onset of transition locus – relationship of y-intercept values with apparent viscosity at 100 s^{-1} for all fluids flowing in 75 and 150 mm trapezoidal flumes | 67 |
| Figure 4.8: Onset of 'Full turbulence' locus – relationship of m-values with apparent viscosity at 500 s^{-1} for all fluids flowing in 75 and 150 mm trapezoidal flumes | 68 |
| Figure 4.9: Onset of 'Full turbulence' locus – relationship of y-intercept values with apparent viscosity at 500 s^{-1} for all fluids flowing in 75 and 150 mm trapezoidal flumes | 69 |
| Figure 4.10: Evaluation of the adapted transition models for trapezoidal flume at the onset and end of transition | 70 |

| | |
|---|----|
| Figure 4.11: Onset of transition locus – relationship of m-values with apparent viscosity at 100 s ⁻¹ for all fluids flowing in 150 and 300 mm semi-circular flumes | 70 |
| Figure 4.12: Onset of transition locus – relationship of c-values with apparent viscosity at 100 s ⁻¹ for all fluids flowing in 150 and 300 mm semi-circular flumes | 71 |
| Figure 4.13: Onset of ‘Full turbulence’ locus – relationship of m-values with apparent viscosity at 500 s ⁻¹ for all fluids flowing in 150 and 300 mm semi-circular flumes | 72 |
| Figure 4.14: Onset of ‘Full turbulence’ locus – relationship of y-intercept values with apparent viscosity at 500 s ⁻¹ for all fluids flowing in 150 and 300 mm semi-circular flumes | 72 |
| Figure 4.15: Evaluation of the transition models at the onset and end of transition in the semi-circular flume | 73 |
| Figure 4.16: Onset of transition locus – relationship of m-values with apparent viscosity at 100 s ⁻¹ for all fluids in all flumes used..... | 74 |
| Figure 4.17: Onset of transition locus – relationship of y-intercept values with apparent viscosity at 100 s ⁻¹ for all fluids in all flumes used | 74 |
| Figure 4.18: Onset of ‘Full turbulence’ locus – relationship of m-values with apparent viscosity at 500 s ⁻¹ for all fluids in all flumes used | 75 |
| Figure 4.19: Onset of ‘Full turbulence’ locus – relationship of y-intercept values with apparent viscosity at 500 s ⁻¹ for all fluids in all flumes used | 75 |
| Figure 4.20: Evaluation of the combined transition models at the onset and end of transition in a 150 mm rectangular flume..... | 76 |
| Figure 5.1: Prediction of transition. 3.8% CMC suspension flowing in a 150 mm rectangular shape at 4° slope..... | 78 |
| Figure 5.2: Prediction of transition. 2.8% CMC suspension flowing in a 150 mm rectangular shape at 5° slope..... | 79 |
| Figure 5.3: Haldenwang’s transition model for 2.8% and 3.8% CMC solutions flowing in a 150 mm rectangular flume | 81 |
| Figure 5.4: Prediction of transition showing the intersection between the laminar flow and the turbulent flow Fanning friction factors. 3.8% CMC solution flowing in a 300 mm semi-circular channel at 4° slope | 82 |
| Figure 5.5: Fitton’s transition model for 3.8% CMC solution..... | 84 |
| Figure 5.6: Slatter’s transition model for 3.8% CMC solution | 85 |
| Figure 5.7: Slatter’s transition model for 3.8% CMC solution flowing in a 300 mm rectangular flume at 3 degrees slope..... | 86 |
| Figure 5.8: Slatter’s transition model for 3.8% CMC solution flowing in a 300 mm rectangular flume at 4 degrees slope..... | 86 |
| Figure 5.9: Slatter’s transition model for 3.8% CMC solution flowing in a 300 mm rectangular flume at 5 degrees slope..... | 87 |
| Figure 5.10: Slatter’s transition model for 2.8% CMC solution flowing in a 300 mm rectangular flume | 87 |
| Figure 5.11: Slatter’s transition model for 2.8% CMC solution flowing in a 300 mm rectangular flume at 3 degrees slope..... | 88 |
| Figure 5.12: Slatter’s transition model for 2.8% CMC solution flowing in a 300 mm rectangular flume at 4 degrees slope | 88 |
| Figure 5.13: Slatter’s transition model for 2.8% CMC solution flowing in a 300 mm rectangular flume at 5 degrees slope | 89 |
| Figure 5.14: Slatter’s transition model for 1%, 1.8%, 2.8% and 3.8% CMC solutions flowing in a 300 mm rectangular flume | 90 |

| | |
|---|-----|
| Figure 5.15: 6% bentonite slurry flowing in a 300 mm rectangular flume at slopes 2-5 degrees..... | 91 |
| Figure 5.16: Prediction of transition. 4.5% bentonite in water slurry flowing in a 150 mm rectangular flume at 5° slope..... | 92 |
| Figure 5.17: Prediction of transition. 4.5% bentonite in water slurry flowing in a 300 mm rectangular flume at 5° slope..... | 92 |
| Figure 5.18: Haldenwang's transition model for 4.5% bentonite in water slurry flowing in a 150 mm and 300 mm rectangular channel | 94 |
| Figure 5.19: Fitton's transition model for 4.5% bentonite in water slurry | 96 |
| Figure 5.20: Coussot's transition model for kaolin in water slurries | 98 |
| Figure 5.21: Prediction of transition. 5.3% kaolin in water slurry flowing in a 150 mm rectangular flume at 3° slope..... | 99 |
| Figure 5.22: Prediction of transition. 5.3% kaolin in water slurry flowing in a 300 mm rectangular shape at 3° slope..... | 99 |
| Figure 5.23: Haldenwang's transition model for kaolin in water slurries..... | 101 |
| Figure 5.24: Prediction of transition. 7.2% kaolin in water slurry flowing in a 150 mm rectangular channel | 101 |
| Figure 5.25: Fitton's transition model for kaolin in water slurries | 104 |
| Figure 5.26: 5.3% kaolin in water slurry flowing in a 300 mm rectangular flume | 105 |
| Figure 5.27: Slatter's transition model for 5.3% kaolin in water slurry flowing in a 300 mm rectangular flume at 3 degrees slope | 106 |
| Figure 5.28: Slatter's transition model for 5.3% kaolin in water slurry flowing in a 300 mm rectangular flume at 4 degrees slope | 106 |
| Figure 5.29: Slatter's transition model for 5.3% kaolin in water slurry flowing in a 300 mm rectangular flume at 5 degrees slope | 107 |
| Figure 5.30: 4.5% kaolin in water slurry flowing in 300 mm rectangular flume..... | 108 |
| Figure 5.31: Slatter's transition model for 4.5% kaolin in water slurry flowing in a 300 mm rectangular flume at 3 degrees slope | 108 |
| Figure 5.32: Slatter's transition model for 4.5% kaolin in water slurry flowing in a 300 mm rectangular flume at 4 degrees slope | 109 |
| Figure 5.33: Slatter's transition model for 4.5% kaolin in water slurry flowing in a 300 mm rectangular flume at 5 degrees slope | 109 |
| Figure 5.34: Slatter's transition models ($Re_4=700$ and V_c criteria) for 4.5% & 5.3% kaolin in water slurries in a 300 mm rectangular flume..... | 110 |
| Figure 5.35: Comparison between Haldenwang, Fitton and Slatter models for transition for power law fluids | 111 |
| Figure 5.36: Comparison between critical models for power law fluids..... | 112 |
| Figure 5.37: Comparison between Fitton and Haldenwang models for transition for Bingham plastic fluids | 113 |
| Figure 5.38: Comparison between critical velocity models for Bingham plastic fluids | 113 |
| Figure 5.39: Comparison between the Coussot, Fitton, Haldenwang and Slatter models for transition velocity for yield shear-thinning fluids..... | 114 |
| Figure 5.40: Comparison between critical velocity models for yield shear-thinning fluids .. | 115 |
| Figure 5.41: Haldenwang (2010) model for end of transition | 116 |
| Figure 5.42: Haldenwang's prediction for end of transitional flow of a power law fluid | 117 |
| Figure 5.43: Haldenwang (2010) model for end transition | 118 |
| Figure 5.44: Haldenwang's prediction for end of transitional flow of a Bingham plastic fluid | 118 |

| | |
|---|-----|
| Figure 5.45: Haldenwang (2010) model for end of transition | 119 |
| Figure 5.46: Haldenwang's prediction for end of transitional flow of a yield shear-thinning fluid | 120 |
| Figure 5.47: Model comparison for the onset of transition in a rectangular flume | 121 |
| Figure 5.48: Onset of transitional flow in rectangular flume: model comparison | 121 |
| Figure 5.49: Model comparison for the end of transition in a rectangular flume..... | 122 |
| Figure 5.50: End of transitional flow in rectangular flume: model comparison | 123 |
| Figure 5.51: Model comparison for the onset of transition in a triangular flume | 124 |
| Figure 5.52: Onset of transitional flow in triangular flume: model comparison | 124 |
| Figure 5.53: Model comparison for the end of transition in a triangular flume..... | 126 |
| Figure 5.54: End of transitional flow in triangular flume: model comparison | 126 |
| Figure 5.55: Model comparison for the onset of transition in a semi-circular flume..... | 127 |
| Figure 5.56: Onset of transitional flow in semi-circular flume: model comparison..... | 128 |
| Figure 5.57: Model comparison for the end of transition in a semi-circular flume | 129 |
| Figure 5.58: End of transitional flow in semi-circular flume: model comparison | 129 |
| Figure 5.59: Model comparison for the onset of transition in a trapezoidal flume | 130 |
| Figure 5.60: Onset of transitional flow in trapezoidal flume: model comparison | 131 |
| Figure 5.61: Model comparison for the end of transition in a trapezoidal flume | 132 |
| Figure 5.62: End of transitional flow in trapezoidal flume: model comparison..... | 132 |

LIST OF TABLES

| | |
|--|-----|
| Table 2.1: Various channel shapes characteristics | 5 |
| Table 2.2: Differences between pipe and open channel flow of an incompressible fluid (Chanson, 2004) | 10 |
| Table 2.3: The equivalent roughness height (Chanson, 2004)..... | 20 |
| Table 2.4: Summary of laminar-turbulent transition open channel models..... | 44 |
| Table 3.1: Determination of laminar flow in semi-circular flumes | 56 |
| Table 3.2: Determination of turbulent flow in semi-circular flumes | 57 |
| Table 3.3: Determination of transitional flow in semi-circular flumes..... | 58 |
| Table 3.4: Summary of published work by various authors (transitional flow) | 62 |
| Table 5.1: Haldenwang's transition model for 3.8% CMC solution flowing in a 150 mm rectangular channel..... | 80 |
| Table 5.2: Haldenwang's transition model for 2.8% CMC solution flowing in a 150 mm rectangular channel..... | 80 |
| Table 5.3: 3.8% CMC solution flowing in a 150 mm rectangular channel shape | 82 |
| Table 5.4: 3.8% CMC solution flowing in a 150 mm semi-circular channel shape..... | 83 |
| Table 5.5: 3.8% CMC solution flowing in a 150 mm trapezoidal channel shape | 83 |
| Table 5.6: 3.8% CMC solution flowing in a 300 mm triangular channel shape | 83 |
| Table 5.7: Haldenwang's transition model for 4.5% bentonite in water slurry flowing in 150 mm rectangular channel | 93 |
| Table 5.8: Haldenwang's transition model for 4.5% bentonite in water slurry flowing in 300 mm rectangular channel | 93 |
| Table 5.9: 4.5% bentonite in water slurry in a 300 mm rectangular channel shape..... | 94 |
| Table 5.10: 4.5% bentonite in water slurry in a 300 mm semi-circular channel shape | 95 |
| Table 5.11: 4.5% bentonite in water slurry in a 150 mm trapezoidal channel shape | 95 |
| Table 5.12: 4.5% bentonite in water slurry in a 300 mm triangular channel shape..... | 95 |
| Table 5.13: 5.3% kaolin in water slurry flowing in a 300 mm rectangular channel shape | 97 |
| Table 5.14: 5.3% kaolin in water slurry flowing in a 150 mm trapezoidal channel shape | 97 |
| Table 5.15: Haldenwang's transition model for 5.3% kaolin in water slurry flowing in a 150 mm rectangular channel | 100 |
| Table 5.16: Haldenwang's transition model for 5.3% kaolin in water slurry flowing in a 300 mm rectangular channel | 100 |
| Table 5.17: 5.3% kaolin in water slurry flowing in a 300 mm rectangular channel shape ... | 102 |
| Table 5.18: 5.3% kaolin in water slurry flowing in a 300 mm semi-circular channel shape. | 102 |
| Table 5.19: 5.3% kaolin in water slurry flowing in a 150 mm trapezoidal channel shape ... | 103 |
| Table 5.20: 5.3% kaolin in water slurry flowing in a 300 mm triangular channel shape | 103 |
| Table 5.21: Statistical analysis for power law models | 112 |
| Table 5.22: Statistical analysis for Bingham plastic models | 114 |
| Table 5.23: Statistical analysis for yield shear-thinning models | 115 |
| Table 5.24: Statistical analysis for Haldenwang's upper critical velocity model for a power law fluid | 117 |
| Table 5.25: Statistical analysis for Haldenwang's upper critical model for a Bingham plastic fluid | 119 |
| Table 5.26: Statistical analysis for Haldenwang's upper critical model for a yield shear- thinning fluid..... | 120 |

| | |
|---|-----|
| Table 5.27: Statistical analysis for the onset of transition in a rectangular flume | 122 |
| Table 5.28: Statistical analysis for the end of transition in a rectangular flume | 123 |
| Table 5.29: Statistical analysis for the onset of transition in a triangular flume | 125 |
| Table 5.30: Statistical analysis for the end of transition in a triangular flume | 127 |
| Table 5.31: Statistical analysis for the onset of transition in a semi-circular flume | 128 |
| Table 5.32: Statistical analysis for the end of transition in a semi-circular flume | 130 |
| Table 5.33: Statistical analysis for the onset of transition in a trapezoidal flume | 131 |
| Table 5.34: Statistical analysis for the end of transition in a trapezoidal flume | 133 |
| Table 5.35: Overall performance of transitional flow models used for different flume shapes | 134 |
| Table A.1: 1% CMC in water solution flowing in a 300 mm rectangular flume | 145 |
| Table A.2: 1.8% CMC in water solution flowing in a 300 mm rectangular flume | 145 |
| Table A.3: 2.8% CMC in water solution flowing in a 300 mm rectangular flume | 146 |
| Table A.4: 3.8% CMC in water solution flowing in a 300 mm rectangular flume | 146 |
| Table A.5: 1% CMC in water solution flowing in a 150 mm rectangular flume | 147 |
| Table A.6: 1.8% CMC in water solution flowing in a 150 mm rectangular flume | 147 |
| Table A.7: 2.8% CMC in water solution flowing in a 150 mm rectangular flume | 148 |
| Table A.8: 3.8% CMC in water solution flowing in a 150 mm rectangular flume | 148 |
| Table A.9: 4.5% Bentonite in water suspension flowing in a 300 mm rectangular flume.... | 149 |
| Table A.10: 6% Bentonite in water suspension in a 300 mm rectangular flume..... | 149 |
| Table A.11: 4.5% Bentonite in water suspension in a 150 mm rectangular flume..... | 150 |
| Table A.12: 4.5% Bentonite in water suspension in a 150 mm rectangular flume..... | 150 |
| Table A.13: 6% Bentonite in water suspension in a 150 mm rectangular flume..... | 151 |
| Table A.14: 3% kaolin in water suspension in a 150 mm rectangular flume | 152 |
| Table A.15: 4.5% kaolin in water suspension in a 150 mm rectangular flume | 152 |
| Table A.16: 5.3% kaolin in water suspension in a 150 mm rectangular flume | 153 |
| Table A.17: 6% kaolin in water suspension in a 150 mm rectangular flume | 153 |
| Table A.18: 7% kaolin in water suspension in a 150 mm rectangular flume | 154 |
| Table A.19: 8% kaolin in water suspension in a 150 mm rectangular flume | 154 |
| Table A.20: 9% kaolin in water suspension in a 150 mm rectangular flume | 155 |
| Table A.21: 10% kaolin in water suspension in a 150 mm rectangular flume | 155 |
| Table A.22: 3% kaolin in water suspension in a 300 mm rectangular flume | 156 |
| Table A.23: 4.5% kaolin in water suspension in a 300 mm rectangular flume | 156 |
| Table A.24: 5.3% kaolin in water suspension in a 300 mm rectangular flume | 157 |
| Table A.25: 6% kaolin in water suspension in a 300 mm rectangular flume | 157 |
| Table A.26: 7.1% kaolin in water suspension in a 300 mm rectangular flume | 158 |
| Table A.27: 8% kaolin in water suspension in a 300 mm rectangular flume | 158 |
| Table A.28: 10% kaolin in water suspension in a 300 mm rectangular flume | 159 |
| Table B.1: 1.5% CMC in water solution in a 300 mm semi-circular flume | 160 |
| Table B.2: 3% CMC in water solution in a 300 mm semi-circular flume..... | 160 |
| Table B.3: 1.5% CMC in water solution in a 150 mm semi-circular flume | 161 |
| Table B.4: 3% CMC in water solution in a 150 mm semi-circular flume..... | 161 |
| Table B.5: 4% CMC in water solution in a 150 mm semi-circular flume..... | 162 |
| Table B.6: 5.3% CMC in water solution in a 150 mm semi-circular flume | 162 |
| Table B.7: 4.6% Bentonite in water suspension in a 300 mm semi-circular flume | 163 |
| Table B.8: 6.2% Bentonite in water suspension in a 300 mm semi-circular flume | 163 |
| Table B.9: 4.6% Bentonite in water suspension in a 150 mm semi-circular flume | 164 |
| Table B.10: 6.2% Bentonite in water suspension in a 150 mm semi-circular flume | 164 |

| | |
|--|-----|
| Table B.11: 3.5% kaolin in water suspension in a 300 mm semi-circular flume | 165 |
| Table B.12: 5.3% kaolin in water suspension in a 300 mm semi-circular flume | 165 |
| Table B.13: 7.1% kaolin in water suspension in a 300 mm semi-circular flume | 166 |
| Table B.14: 5.3% kaolin in water suspension in a 150 mm semi-circular flume | 166 |
| Table B.15: 7.14% kaolin in water suspension in a 150 mm semi-circular flume | 167 |
| Table B.16: 9% kaolin in water suspension in a 150 mm semi-circular flume | 167 |
| Table C.1: 4% CMC in water solution in a 150 mm trapezoidal flume..... | 168 |
| Table C.2: 1.5% CMC in water solution in a 75 mm trapezoidal flume..... | 169 |
| Table C.3: 3% CMC in water solution in a 75 mm trapezoidal flume..... | 169 |
| Table C.4: 4% CMC in water solution in a 75 mm trapezoidal flume..... | 170 |
| Table C.5: 1.5% CMC in water solution in a 150 mm trapezoidal flume..... | 170 |
| Table C.6: 3% CMC in water solution in a 150 mm trapezoidal flume..... | 171 |
| Table C.7: 4.6% Bentonite in water suspension in a 75 mm trapezoidal flume | 171 |
| Table C.8: 6.2% Bentonite in water suspension in a 75 mm trapezoidal flume | 172 |
| Table C.9: 4.6% Bentonite in water suspension in a 150 mm trapezoidal flume | 172 |
| Table C.10: 6.2% Bentonite in water suspension in a 150 mm trapezoidal flume | 173 |
| Table C.11: 5.4% kaolin in water suspension in a 75 mm trapezoidal flume..... | 173 |
| Table C.12: 7.2% kaolin in water suspension in a 75 mm trapezoidal flume..... | 174 |
| Table C.13: 5.4% kaolin in water suspension in a 150 mm trapezoidal flume | 174 |
| Table C.14: 7.1% kaolin in water suspension in a 150 mm trapezoidal flume | 175 |
| Table D.1: 2% CMC in water solution in a 300 mm triangular flume | 176 |
| Table D.2: 3.1% CMC in water solution in a 300 mm triangular flume | 177 |
| Table D.3: 4% CMC in water solution in a 300 mm triangular flume | 177 |
| Table D.4: 4.9% CMC in water solution in a 300 mm triangular flume | 178 |
| Table D.5: 3.5% Bentonite in water suspension in a 300 mm triangular flume..... | 178 |
| Table D.6: 4.6% Bentonite in water suspension in a 300 mm triangular flume..... | 179 |
| Table D.7: 5.4% Bentonite in water suspension in a 300 mm triangular flume..... | 179 |
| Table D.8: 3.4% kaolin in water suspension in a 300 mm triangular flume | 180 |
| Table D.9: 5% kaolin in water suspension in a 300 mm triangular flume | 180 |
| Table D.10: 7% kaolin in water suspension in a 300 mm triangular flume | 181 |
| Table D.11: 9.2% kaolin in water suspension in a 300 mm triangular flume | 181 |

GLOSSARY

- Apparent viscosity:** The point value of the ratio of shear stress to shear rate at a given shear rate.
- Bingham plastic fluid:** Fluid characterised by a linear relationship between shear stress and shear rate with a yield stress.
- Flume:** Artificial open channel transporting fluids, slurries or tailings.
- Froude number:** Dimensionless number which is the ratio of inertial to gravitational forces.
- Laminar flow:** The flow regime in which viscous forces are greater than inertial forces.
- Launder:** The term launder is often used interchangeably with the terms flume and open channel to express the same thing.
- Newtonian fluid:** Fluid which has a linear relationship between shear stress and shear rate that passes through the origin.
- Non-Newtonian fluid:** Any fluid that does not have a linear relationship between shear stress and shear rate and/or does not pass through the origin.
- Open channel:** Natural or artificial conduit for transporting fluids with a free surface open to the atmosphere.
- Reynolds number:** Dimensionless number which is the ratio of inertial to viscous forces.
- Rheology:** Science of deformation and flow of matter.
- Transition region:** It is an unstable flow regime where the laminar and turbulent flow regimes are mixed.
- Turbulent flow:** The flow regime is characterised by fluid particles moving in very irregular paths where inertial forces dominate over viscous forces.

NOMENCLATURE

| Symbol | Description | S.I. Units |
|---|--|----------------------------------|
| A | Area | m ² |
| a | Geometric coefficient for channel shape | - |
| A ₀ | Velocity function (Naik) | - |
| B | Breadth of channel | m |
| b | Geometric coefficient for channel shape | - |
| c* | Function defined by Eqn. | 2.57 - |
| C _{Chézy} | Chézy constant | m ^{1/2} s ⁻¹ |
| D | Tube diameter | m |
| d | Particle diameter | μm |
| d _x | Representative particle size of the solids | μm |
| D _{charac} | Characteristic geometry dimension | m |
| e | Hydraulic roughness | m |
| <i>f</i> | Friction factor | - |
| <i>f_D</i> | Darcy friction factor | - |
| <i>f_F</i> | Fanning friction factor | - |
| <i>f_L</i> | Fanning friction factor for laminar flow | - |
| <i>f_T</i> or <i>f_{turb}</i> | Fanning friction factor for turbulent flow | - |
| F | Force | N |
| Fr | Froude number | - |
| g | Gravitational acceleration | m/s ² |
| h | Height | m |
| H _b | Herschel Bulkley number | - |
| He | Hedström number | - |
| He* | Hedstrom number defined by Eqn. 2.58 | - |
| k | Fluid consistency index | Pa.s ⁿ |

| | | |
|---------------------------------|--|--------------------|
| K | Open channel shape constant | - |
| K' | Apparent sheet flow fluid consistency defined by Eqn. 2.92 | Pa.s ⁿ |
| L | Pipe or channel length, characteristic length | m |
| m | slope | - |
| M | 1/n (Inverse of the flow behaviour index) | - |
| n | Flow behaviour index | - |
| N | Number of data points | - |
| n' | Apparent flow behaviour index | - |
| n^* | Kozicki and Tiu flow behaviour index which is equal to n | - |
| n_s' | Apparent sheet flow behaviour index | - |
| NAF | Normalised Adherence Function | - |
| n_{Manning} | Manning constant | s/m ^{1/3} |
| p | Pressure | Pa |
| Q | Volumetric flow rate | m ³ /s |
| R | Radius (at r=R) | m |
| r | Radius | m |
| Re | Reynolds number | - |
| Re* | Roughness Reynolds number defined by Eqn. 2.79 | - |
| Re_p^* | Power law Reynolds number defined by Eqn. 2.55 | - |
| Re _B | Bingham Reynolds number | - |
| (Re _B) _c | Naik's critical Bingham Reynolds number defined by Eqn. 2.82 | - |
| Re _{c (turb)} | Critical Reynolds number at onset of full turbulence | - |
| Re _H | Haldenwang <i>et al.</i> (2002) Reynolds number | - |
| Re _{Naik} | Naik's Reynolds number | - |
| Re _{Zheng} | Zhengai's Reynolds number | - |
| R _h | Hydraulic radius | m |
| S | Relative density | - |

| | | |
|-----------------|-------------------------------------|-----|
| V | Velocity | m/s |
| V_* | Shear velocity defined by Eqn. 2.60 | m/s |
| V_c | Critical velocity | m/s |
| V_z | Slip velocity | m/s |
| $x_i - \bar{x}$ | Deviation from mean | - |

Greek letters

| Symbol | Definition | S.I. Units |
|----------------|---|------------|
| α | Shape factor | - |
| $\dot{\gamma}$ | Shear rate | s^{-1} |
| Δp | Pressure drop | Pa |
| η_B | Bingham viscosity | Pa.s |
| θ | Slope angle (Angle of inclination) | degrees |
| λ_h | Half width to depth ratio of channel | - |
| λ | Friction factor defined by Zhang and Ren (1982) as $96/Re_{\text{Zhang and Ren}}$ | - |
| μ | Dynamic viscosity | Pa.s |
| μ_B | Bingham plastic viscosity | Pa.s |
| ρ | Density | kg/m^3 |
| σ | Standard deviation | - |
| τ | Shear stress | Pa |
| τ_w | Wall shear stress | Pa |
| τ_y | Yield stress | Pa |
| τ_{yHB} | Herschel Bulkley yield stress | Pa |
| τ_{yB} | Bingham yield stress | Pa |
| ϕ | Kozicki and Tiu shape factor function defined by Eqn. 2.35 | - |
| ϕ_c | Ratio of Bingham yield stress to critical wall shear stress | - |
| χ | Von Karman constant | - |

Subscripts/superscripts

| Symbol | Definition |
|---------------|--|
| B | pertaining to Bingham fluid model |
| c | critical |
| calc | calculated |
| HB | Herschel Bulkley |
| i | inside |
| l | loss |
| L | laminar flow |
| obs | observed (experimental) |
| s | solids |
| w | water |
| x | horizontal displacement |
| xx,yy,zz | normal stress components |
| r | radial coordinate |
| 0 | at the wall of the pipe or flume |
| 90 | 90 th percentile of particles passing |

CHAPTER 1

Chapter 1: Introduction

1.1 Introduction

Some research has been done on the flow of homogeneous non-Newtonian fluids in open channels. This particular field has received attention by authors such as Kozicki and Tiu (1967), Wilson (1991), Coussot (1994 and 1997), Haldenwang (2003), Haldenwang and Slatter (2006), Haldenwang *et al.* (2002 and 2010), Burger *et al.* (2010a) and Slatter (2013a & 2013b).

Open channels find their applications in the sewage sludge transport, in the polymer processing and textile fibre industries (Kozicki and Tiu, 1988) as well as in the mining industries where homogeneous non-Newtonian slurries have to be transported around plants and to tailings dams (Sanders *et al.*, 2002). As water becomes scarcer and more costly due to legislative limitations and rationing, higher concentrations of slurries have to be transported. The main objectives in the transport of tailings slurries are to achieve stable flow conditions throughout the conduit (pipe or open channel) and control or eliminate the conduit's internal corrosion and/or erosion to extend the life of the design (Abulnaga, 2002). Transitional flow is often characterised by its unstable nature. Therefore it is important to predict the transition region so that it can be avoided.

A systematic study on the effect of open channel shape on transitional flow for different non-Newtonian fluids has as far as can be ascertained not been done to date.

This research problem requires attention because the understanding of transitional flow of non-Newtonian fluids through open-channels of various cross-sectional shapes will help to improve the design of open channels.

There are three classes of slurries flowing through open-channels:

Homogeneous slurries: relatively small particles are kept in suspension by the carrier fluid, which is generally water. In the absence of flow, eventually the particles will settle at least partially. These slurries are characterised as non-Newtonian and can be rheologically characterised.

Coarse particle mineral slurries: characterised as settling slurries, the velocity of the carrier fluid is critical, as the particles have to be suspended for a better transportation.

Mixed regime slurries: a mixture of the slow and rapid settling slurries (Wilson, 1991)

This work focuses on the flow of non-Newtonian slurries in smooth rectangular, triangular, trapezoidal and semi-circular open channels in the transition region.

1.2 Problem statement

Critical flows may be associated with a degree of instability and wavy motion, leading to working problems and overflows. As for pipe flow the transition zone for open channels is difficult to predict. However, there is a lack of conclusive guidelines in the literature to predict the transitional flow for different shapes, as well as a need for comparison between different predictive models of transitional flow in various flume shapes.

1.3 Objective

The aim of this work is to evaluate whether it is necessary or not to include the effect of shape of the channel when predicting transition while designing open channels by critically evaluating the models presented and to commend and optimise the best model.

1.4 Methodology

In order to meet the objectives, the following research methodology was followed:

Databases published by Haldenwang (2003) and Haldenwang and Slatter (2006) for rectangular channels and by Burger *et al.* (2010b) for trapezoidal, semi-circular and triangular channels were used in this work to evaluate transition models.

Viscous fluids tested include materials that can be characterised using different flow curve models:

- Carboxymethyl cellulose solutions: Power-law model
- Bentonite in water suspensions: Bingham model
- Kaolin in water suspensions: Herschel-Bulkley model

In order to evaluate the models available in literature for the prediction of transitional non-Newtonian flow, a comparison of actual velocities with models velocities was conducted.

In this work, the following models were evaluated:

- Hao and Zhenghai's (1980) approach which is applicable to Bingham plastic fluids in rectangular, trapezoidal and U-shaped channels.
- Naik's (1983) approach will be incorporated in the flow of a Bingham plastic fluid in a rectangular flume.

-
- Coussot's (1997) adaptation of the Hanks criterion will assist with the yield-shear thinning fluids in wide channels.
 - Haldenwang's (2003) and Haldenwang *et al.*'s (2010) model, based on the Froude number and the apparent viscosity of the fluid, developed for rectangular channels will be tested for the different shapes. The model was developed to be used for all the fluids investigated.
 - Fitton's (2008) model which is based on the Hagen-Poiseuille and the Colebrook-White equations to predict the transition point by changing the depth of flow.
 - Slatter's (2013a & 2013b) model applicable to sheet flow will be evaluated for power law and yield-pseudoplastic fluids in rectangular channels.

1.5 Delineation

The following topics fall outside the scope of this thesis:

- The effect of channel shape in laminar and turbulent flow regimes
- The effect of surface roughness in open channel flow of non-Newtonian fluids
- Time-dependent fluids

1.6 Summary

This thesis is concerned with the prediction of transitional flow in open channels of various shapes. It is therefore subdivided as follows:

- A summary of the relevant literature on pipe and open channel flow of fluids is presented in Chapter 2.
- The methodology used to analyse the data published by Haldenwang and Slatter (2006) and Burger *et al.* (2010b) is covered in Chapter 3.
- The results and discussions obtained after data analysis are presented in Chapters 4 and 5.
- The main conclusions drawn from the discussion of results are summarised in Chapter 6.

CHAPTER 2

Chapter 2: Literature Review

2.1 Introduction

This chapter provides a review of flow of fluids in open channels with the emphasis on transitional flow of non-Newtonian fluids in flumes of different shapes. It will review the literature and theory that is relevant to the understanding of the prediction of the transitional flow in open channels of various geometries at different slopes.

The flow phenomena in open channels will be presented from laminar to turbulent regime. The relevant literature on the flow of fluids in pipes is reviewed since some models and theories on open channels were developed from pipe flow models.

The rheology of non-Newtonian fluids and corresponding models will be discussed. The Herschel-Bulkley or yield shear-thinning model will be reviewed since it accommodates Bingham and power law fluids and reverts in its most basic form to Newtonian fluid flow.

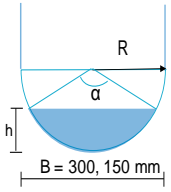
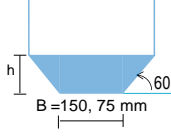
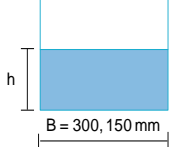
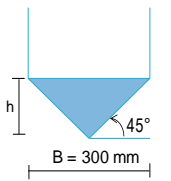
Different flow regimes will be covered as they describe the flow behaviour in closed pipes and open channels. However, greater attention will be paid to the transitional flow behaviour in open channels as it is the focus of this research. Non-Newtonian Reynolds numbers for open channel flow relevant to this work will also be discussed and evaluated.

2.2 Geometry of open channels

By definition, an open channel is a duct in which the fluid has a continuous free surface. This may either be natural such as streams or rivers or artificial such as flumes. These flumes differ according to their cross-sectional shapes.

Frequently used shapes for open channels include semi-circular, rectangular, trapezoidal and triangular. The aforementioned channel shapes are summarised in Table 2.1.

Table 2.1: Various channel shapes characteristics

| Flume shape | Cross sectional area | Wetted perimeter | Surface width | Hydraulic radius |
|--|---|--|--|--|
| Semi-circular  | $\frac{D^2}{8}(\alpha - \sin\alpha)$ where $\alpha = 2\cos^{-1}\left(1 - \frac{2h}{D}\right)$ | $D\left(\frac{1}{2}\alpha\right)$ where $\alpha = 2\cos^{-1}\left(1 - \frac{2h}{D}\right)$ | $D\left(\sin\frac{1}{2}\alpha\right)$ where $\alpha = 2\cos^{-1}\left(1 - \frac{2h}{D}\right)$ | $\frac{D}{4\alpha}(\alpha - \sin\alpha)$ |
| Trapezoidal  | $h(B+xh)$ where $x=1/\tan 60^\circ$ | $B+2h(1+x^2)^{0.5}$ where $x=1/\tan 60^\circ$ | $B+2xh$ where $x=1/\tan 60^\circ$ | $\frac{h(B+xh)}{B+2h\sqrt{1+x^2}}$ |
| Rectangular  | Bh | $B+2h$ | B | $Bh/B+2h$ |
| Triangular  | h^2 | $2h\sqrt{2}$ | $2h$ | $\frac{h}{2\sqrt{2}}$ |

The trapezoidal shape is widely used for many reasons. It is an efficient shape due to its large flow area relative to its wetted perimeter. The sloped sides are convenient for channels made in the earth, because the slopes can be set at an angle at which construction materials are stable (Mott, 2000).

The rectangular shape is a special case of the trapezoidal shape with a side slope of 90° . Formed concrete channels are often made in this shape. The triangular channel is also a special case of the trapezoidal shaped channel with a bottom width of zero. Simple ditches in earth are often made in this shape (Mott, 2000).

Importance of open channels

Flume design for homogeneous non-Newtonian fluids is problematic and not much research has been conducted in this field until recently. This application is industrially important in the sewage sludge transport, in the polymer processing, in the textile fibre industries and in mining industries where slurries have to be transported to processing or disposal sites at higher concentrations because water is becoming a scarce and expensive commodity (Haldenwang *et al.*, 2004).

2.3 Flow regimes

The different flow regimes encountered in pipe and open channel flow will be defined and examined in the following sections. Fluid flow in a closed pipe or an open channel can be categorised as laminar, transitional or turbulent.

2.3.1 Reynolds number

Osborne Reynolds was the first to publish work on fluid flow patterns in tubes and observed the flow patterns of fluid by injecting a dye into the moving stream. Reynolds modelled his data by using a dimensionless group Re , which later became known as the Reynolds number (Holland, 1973). The Reynolds number is proportional to the ratio between inertial and viscous forces and is defined as follows:

$$Re = \frac{\rho V D}{\mu}$$

2.1

For all fluids, the state of the flow is determined by the ratio between the inertial and the viscous forces. For Newtonian fluids, the relative importance between these forces is determined by the value of the Reynolds number. Stable laminar flow ceases to occur at a generally accepted Reynolds number of 2100 for Newtonian fluids (Chhabra & Richardson, 2008). Turbulent flow occurs at Reynolds numbers of about 4000 (Griskey, 2002). Transitional flow is observed at Reynolds numbers of 2100 to about 4000 (Griskey, 2002). In open channel flow, the corresponding transitional flow ranges from Reynolds numbers of 500 to 1000 since the hydraulic radius is a quarter of the pipe diameter (Chow, 1959).

For time-independent fluids, the critical Reynolds number value depends on the type and the degree of non-Newtonian behaviour (Chhabra & Richardson, 2008). In practice, however, transitional flow arises over a range of conditions rather than abruptly (Abulnaga, 2002; Chhabra & Richardson, 2008).

2.3.2 Laminar flow

In laminar flow, fluid layers move relative to each other without any macroscopic intermixing (Holland, 1973). Chaudhry (2008) defined laminar flow as the region where liquid particles are displaced in definite smooth paths and the flow appears as a movement of superimposed thin layers.

2.3.3 Transitional flow

The transition from a laminar to a turbulent flow is difficult to describe (Abulnaga, 2002). Many authors describe the transitional flow regime as the region between laminar and turbulent flow regimes (Coulson & Richardson, 1999; Griskey, 2002). Transitional flow can be defined as an unstable region where the laminar and turbulent flow regimes are mixed (Chow, 1959).

2.3.4 Turbulent flow

In turbulent flow, fluid particles move in an irregular random movement in directions transverse to the main flow (Holland, 1973). Chaudhry (2008) stated that in turbulent flow, the liquid particles move in irregular paths which are fixed irrespective of neither time nor space.

2.3.5 Froude number

The Froude number, named after William Froude, is a dimensionless number, defined as the ratio of inertial forces to gravitational forces and is defined as follows (Chanson, 2004):

$$Fr = \frac{V}{\sqrt{g \frac{A}{B}}} \propto \sqrt{\frac{\text{inertial force}}{\text{weight}}} \quad 2.2$$

where A is the cross-sectional area and B the top width of the channel.

The Froude number for a rectangular open channel is defined as follows (Chaudhry, 2008):

$$Fr = \frac{V}{\sqrt{gh}} \quad 2.3$$

Chanson (2004) defined the Froude numbers for triangular channels as:

$$Fr = \frac{V}{\sqrt{g \frac{h}{2}}} \quad 2.4$$

for semi-circular channels as:

$$Fr = \frac{V}{\sqrt{g \frac{D(\alpha - \sin \alpha)}{8(\sin 0.5\alpha)}}} \quad 2.5$$

and for trapezoidal channels as:

$$Fr = \frac{V}{\sqrt{g \frac{h(B + x h)}{B + 2 x h}}} \quad 2.6$$

The flow is denoted as sub-critical when the Froude number is less than one ($Fr < 1$) and in such a flow, the gravitational forces are greater than inertial forces (Chaudhry, 2008). It is important to avoid subcritical flows when dealing with slurries as they often cause settling problems (Abulnaga, 2002).

The Froude number is called super-critical when its value is greater than one ($Fr > 1$), and in this flow, inertial forces are dominant and there is usually a high velocity (Chaudhry, 2008). Supercritical flows are recommended in order to avoid regimes of instabilities (Abulnaga, 2002).

In the case where the Froude number is equal to unity ($Fr = 1$), the flow is classified as critical and occurs in an unstable region (Chaudhry, 2008). When using slurries, critical flows may be linked to a degree of instability and wavy motion, resulting in some cases in working problems and overflows (Abulnaga, 2002).

2.3.6 Types of flow in open channels

There are several classes of open channel flow as shown in Figure 2.1.

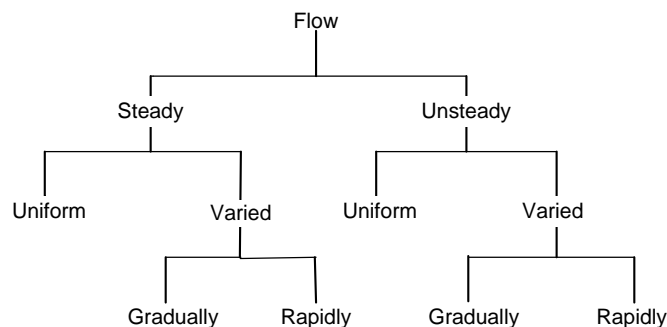


Figure 2.1: Types of flow (Chaudhry, 2008)

The two categories relevant to this work are as follows:

2.3.6.1 Uniform and varied flow

The flow is said to be uniform in an open channel when the flow depth remains the same at every section of the channel. The flow is varied when the flow depth changes over the section of the channel considered (Chow, 1959).

2.3.6.2 Steady and unsteady flow

In an open channel, the flow is steady when the depth h of the liquid is uniform and does not change over time; the slope of the channel bed and the hydraulic slope of the free liquid surface are parallel to each other. Unsteady flow occurs when the depth h of the liquid changes with time (Holland, 1973).

2.3.7 The most efficient shape for open channels

The carrying capacity of open channels is known as conveyance and its value can be obtained from Manning's equation which is defined as (Mott, 2000):

$$V = \frac{1}{n_{\text{Manning}}} (R_h)^{\frac{2}{3}} \sqrt{\sin\theta} \quad 2.7$$

where n_{Manning} is the Manning constant. The conveyance of a channel would be maximum when the wetted perimeter is the least for a given area. Using this criterion, it was found that the most efficient shape is the semi-circle, that is, the circular section running half full (Massey, 1998 & Mott, 2000). The semi-circular, trapezoidal, rectangular and triangular channel shapes are shown in Table 2.1.

Open channel flow is sometimes referred to as free surface flow over a plane in which fluids are transported as a result of a hydraulic gradient due to gravity. The flow can occur either in an open or closed conduit where in both cases the fluid has a free surface. Open channel flow can thus be distinguished from pipe flow which usually flows full and where there is an absence of the free surface and the pressure gradient is usually provided by a pump (Alderman & Haldenwang, 2004).

A summary of the differences between pipe and open channel flows are presented in Table 2.2.

Table 2.2: Differences between pipe and open channel flow of an incompressible fluid (Chanson, 2004)

| | Pipe flow | Open channel flow |
|--------------------------------|---|---|
| Flow driven by | Pressure | Gravity |
| Flow cross-section | Known (fixed by pipe geometry) | Unknown because it changes with flow depth |
| Characteristic flow parameters | Velocity deduced from continuity equation | Flow depth and velocity deduced by solving simultaneously the continuity and momentum equations |
| Specific boundary conditions | | Atmospheric pressure at the free surface |

In order to design efficient open channel flow, it is important to understand the rheology of the fluids used.

2.4 Fluid rheology

Rheology is the branch of science which deals with the deformation and flow of matter (Coulson & Richardson, 1999). There are two types of fluid flow behaviour namely Newtonian and non-Newtonian. This section provides a description of the flow behaviour of Newtonian and non-Newtonian fluids. The flow characterisation techniques are briefly covered.

2.4.1 Newtonian fluid behaviour

Considering two parallel plates as shown in Figure 2.2 with a thin fluid layer in between, separated by a distance y , with a fixed lower plate and a shearing force F applied to the upper plate, knowing that fluids can be deformed continuously under shear, the movable plate moves at a fixed velocity V_x relative to the fixed lower plate. Under steady-state conditions, the force F is balanced by the fluid's internal frictional force due to its viscosity and the shear force per unit area which is proportional to the fluid's velocity gradient, (Coulson & Richardson, 1999):

$$\frac{F}{A} = \tau \propto \frac{V_x}{y} \propto \frac{dV_x}{dy} \quad 2.8$$

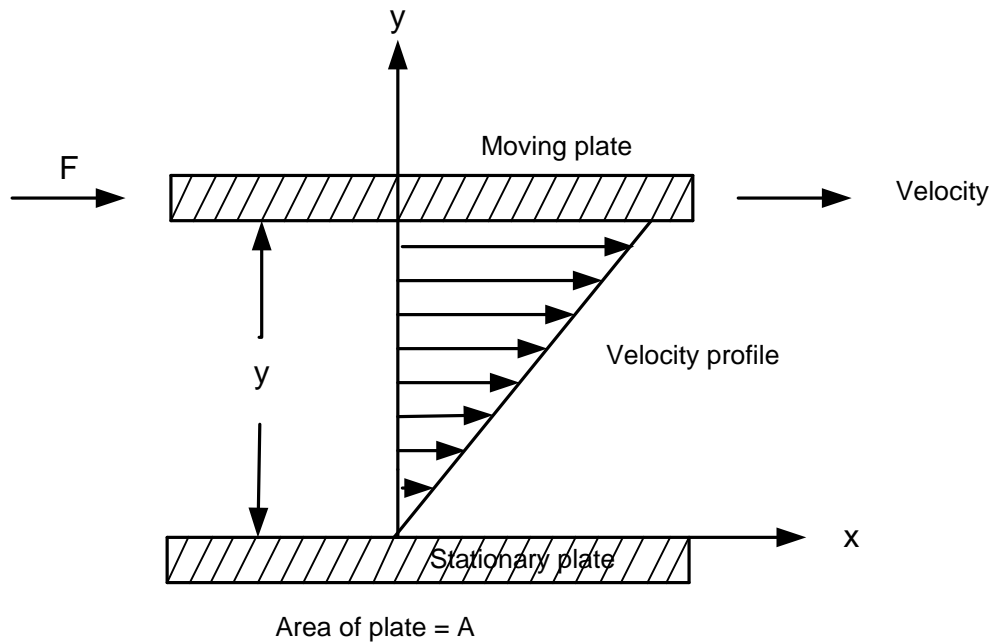


Figure 2.2: Shear stress and velocity gradient in a fluid (Coulson & Richardson, 1999)

where τ is the shear stress in the fluid and dV_x/dy is known as the shear rate or the velocity gradient. The proportionality sign can be replaced by the proportionality factor μ , which is the viscosity, to give (Coulson & Richardson, 1999):

$$\tau = \pm \mu \frac{dV_x}{dy} \quad 2.9$$

A Newtonian fluid has a linear relationship between the shear stress and shear rate with a zero intercept over a wide range of shear rates at constant temperature and pressure (Coulson & Richardson, 1999). Furthermore, a Newtonian fluid satisfies the condition of Equation (2.10) or the complete Navier-Stokes equations.

$$\tau_{xx} = \tau_{yy} = \tau_{zz} = 0 \quad 2.10$$

2.4.2 Non-Newtonian fluid behaviour

A non-Newtonian fluid is a fluid which does not have a linear relationship between the shear stress and the shear rate. This also includes relationships where the flow curve does not go through the origin, which indicates a yield stress. The relationship between shear stress and shear rate is known as a flow curve and is usually graphically represented on a Rheogram as illustrated in Figure 2.3. The proportionality constant, μ for non-Newtonian fluids is dependent on the flow geometry, the shear rate, the kinematic history, etc. Non-Newtonian fluids may be divided in three general classes (Chhabra & Richardson, 2008):

- Time independent or purely viscous fluids: the shear rate at any point is solely determined by the shear stress value at that instant at that point.
- Time dependent fluids: more complex fluids for which the shear stress and shear rate relationship is dependent, in addition, on the duration of shearing and their kinematic history.
- Viscoelastic fluids: exhibit viscous and solid-like characteristics as well as a full, partial or zero elastic recovery after deformation is observed.

In this study, only time independent fluids are considered.

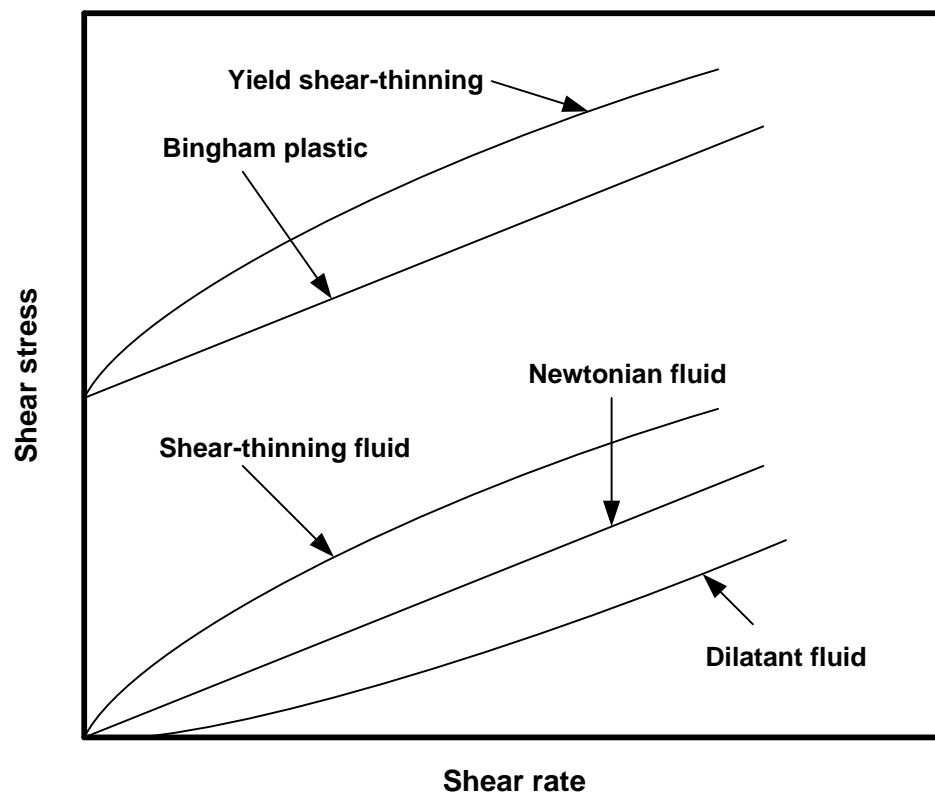


Figure 2.3: Flow curve models

2.4.3 Time independent models

Time independent fluids may be further divided into three classes, namely shear-thinning, viscoplastic and shear-thickening or dilatant fluids. The slurries used in this work are characterised by their rheological behaviour, namely shear-thinning, Bingham and yield shear-thinning.

2.4.3.1 *Shear-thinning model*

Shear-thinning fluids are characterised by a decreasing apparent viscosity with an increasing shear rate (Barnes, 2000).

The power law or Ostwald de Waele model can be used to characterise a fluid with shear-thinning properties and is defined as follows:

$$\tau = k \dot{\gamma}^n \quad 2.11$$

The rheological parameters, k and n are simply curve fitting parameters where k is the fluid consistency and n the flow behaviour index.

If $n < 1$, the fluid is shear-thinning.

If $n > 1$, the fluid is shear-thickening or dilatant.

If $n = 1$, the fluid is Newtonian with $k = \mu$ (de Nevers, 2005).

2.4.3.2 *Viscoplastic flow behaviour*

When an external stress is applied to a viscoplastic fluid which is characterised by the presence of a yield stress, it will deform elastically if the external force is smaller than the yield stress. Otherwise, the flow curve may be linear or non-linear and will not pass through the origin if the magnitude of the external force or stress exceeds the yield stress (Chhabra & Richardson, 2008).

The following two models characterise fluids with a yield stress τ_y .

2.4.3.3 *Bingham plastic model*

The Bingham model is used to describe a fluid with a yield stress as follows:

$$\tau = \tau_y + k \dot{\gamma} \quad 2.12$$

The Bingham equation is linear and has the yield stress as the intercept (Abulnaga, 2002).

2.4.3.4 *Herschel Bulkley or yield-shear thinning model*

The Herschel Bulkley model or the generalised Bingham plastic model, which embraces the non-linear flow curve, is written as follows (Chhabra & Richardson, 2008):

$$\tau = \tau_y + k \dot{\gamma}^n \quad 2.13$$

The yield shear-thinning model can be reduced to the shear-thinning and the Bingham plastic models:

When $\tau_y=0$, the model reverts to the power law model given by Eqn. (2.11).

When $n=1$ and k becomes the plastic viscosity, the model reverts to the Bingham plastic model

When $n=1$, k becomes the Newtonian viscosity and $\tau_y=0$, the model reverts to the Newtonian model.

Barnes and Walters (1985) argued that the yield stress does not exist and it is only an idealisation. The yield stress is however a reality for engineering design since at low enough shear rates, there will be no flow.

2.4.4 Rheometry for non-Newtonian fluids

It is widely accepted that the characterisation of non-Newtonian fluids is complex (Chhabra & Richardson, 2008).

It is a challenge to determine even the seemingly simple relationship between the shear rate and the shear stress and vice versa of non-Newtonian fluids, as the shear rate can only be determined directly if it remains constant throughout the measuring system employed. In order to overcome this difficulty when using a rotary viscometer, the shearing gap of the cone and plate and cup and bob systems are often kept small (Chhabra & Richardson, 2008).

The rheological parameters k , τ_y and n are established by measuring the flow curve using tube, capillary or rotational viscometers.

2.4.4.1 Rotary viscometer

Various geometries of rotational viscometers are used to characterise rheologically the flow behaviour of non-Newtonian fluids.

The controlled shear rate and controlled shear stress instruments are the two types of rotational viscometers used. The concentric cylinder, cone-and-plate and parallel plate systems are the main measuring geometries which come with the above-mentioned types of rheometers (Chhabra & Richardson, 2008).

2.4.4.2 Tube viscometer

The use of rotational viscometers has its advantages. Certain authors have a preference for tube viscometers when dealing with non-Newtonian slurries (Slatter, 1994). Lower shear

rates can be attained with the use of rotational viscometers. The geometric similarity of tube viscometers to a pipeline is an advantage. Another advantage is the flume setup with inline tube viscometer which is essential since the changes in the fluid rheology can be detected during the flume test (Haldenwang, 2003). Large volumes of fluid, the use of various capillary tubes for fluids with different viscosities, difficulties in cleaning the capillary tubes, are some of the disadvantages of tube viscometers (Chhabra & Richardson, 2008).

Ideally, a tube viscometer has a fluid flowing steadily in laminar flow at constant temperature and with a pressure drop Δp caused by laminar friction between the inlet and the outlet.

The relationship between the volumetric flow rate Q and the wall shear stress τ_0 and the shear stress τ is as follows:

$$\frac{Q}{\pi R^3} = \frac{1}{\tau_0^3} \int_0^{\tau_0} \tau^2 f(\tau) d\tau \quad 2.14$$

where

$\tau_0 = \frac{R}{2} \left(-\frac{\Delta p}{L} \right)$ and $\left(-\frac{\Delta p}{L} \right)$ is the pressure drop per unit length of tube.

At any radius r , the shear stress is defined as follows:

$$\tau = \frac{r}{2} \left(-\frac{\Delta p}{L} \right) \quad 2.15$$

A plot of $\frac{Q}{\pi R^3}$ vs. τ_0 gives a single line for a given material for all values of R and $\left(-\frac{\Delta p}{L} \right)$

(Chhabra & Richardson, 2008).

In tube viscometry $8V/D$ is the wall shear rate for a Newtonian fluid and not the true shear rate for a non-Newtonian fluid, thus the $8V/D$ has to be transformed to the true shear rate $\dot{\gamma}$ (Chhabra & Richardson, 2008).

For a rheogram which has an unknown form, Equation (2.13), after some manipulation, will yield the following (Chhabra & Richardson, 2008):

$$\left(-\frac{du}{dr}\right)_0 = \frac{8V}{D} \left(\frac{3}{4} + \frac{1}{4} \frac{d \log\left(\frac{8V}{D}\right)}{d \log \tau_0} \right) \quad 2.16$$

Equation (2.16) is a general relationship for the wall shear rate which is known as the Rabinowitsch-Mooney equation and can be simplified as:

$$\dot{\gamma}_0 = \left(-\frac{du}{dr}\right)_0 = \frac{8V}{D} \left(\frac{3n'+1}{4n'} \right) \quad 2.17$$

where

$$n' = \frac{d(\log \tau_0)}{d\left(\log\left(\frac{8V}{D}\right)\right)} \quad 2.18$$

When τ_0 versus $8V/D$ is plotted on logarithmic coordinates in the laminar flow region, n' is the slope of the tangent of the graph. If it is a power-law fluid, the slope will be constant (Chhabra & Richardson, 2008).

The Rabinowitsch-Mooney transformation procedure for pipe data is used to obtain the rheological parameters τ_y , k and n of a fluid. Lazarus and Slatter (1988) developed a method to optimise these rheological parameters by minimising the sum of the mean error square of the N data points as follows:

$$E = \sum_{i=1}^N \left(\frac{\frac{8V}{D_{i\text{obs}}} - \frac{8V}{D_{i\text{calc}}}}{\frac{8V}{D_{i\text{obs}}}} \right)^2 \quad 2.19$$

For a yield shear-thinning fluid, τ_y , k and n will be optimised, for a Bingham plastic fluid, n will be 1, and for a shear-thinning fluid, τ_y will be 0.

2.5 Newtonian open channel flow

The flow of Newtonian fluids in open channels is covered in several textbooks including Chow (1959), Chadwick and Morfett (1999) and Chanson (2004).

It is crucial to determine whether the flow regime in open channels is laminar, transitional or turbulent. These flow regimes may be illustrated on a Moody diagram which is a double

logarithmic plot of the Fanning friction factor against the Reynolds number. The Fanning friction factor is written as follows:

$$f = \frac{2 \tau_0}{\rho V^2} \quad 2.20$$

where τ_0 the average wall shear stress is defined as:

$$\tau_0 = \rho g R_h \sin \theta \quad 2.21$$

2.5.1 Laminar flow

The laminar flow of Newtonian fluids in open channels is not often encountered. Water can flow in the laminar region only when the flow depth is very small in comparison to the flow width, i.e., it is sheet flow (Chow, 1959).

Flow in a pipe varies with the pipe wall shear stress τ_0 , the viscosity μ and the diameter D which can be derived from the pipe shear stress distribution as follows:

$$\tau_0 = \mu \left(\frac{8V}{D} \right) \quad 2.22$$

For a pipe running full, the correlation between the pipe diameter D and the hydraulic radius R_h is expressed as follows:

$$D = 4 R_h \quad 2.23$$

Then, the Fanning friction factor can be rewritten from equations (2.20) and (2.21) as follows:

$$f = \frac{2 R_h g \sin \theta}{V^2} \quad 2.24$$

Therefore, the corresponding Reynolds number for Newtonian open channel flow is defined as:

$$Re = \frac{\rho V 4 R_h}{\mu} \quad 2.25$$

Thus, the relationship between the Fanning friction factor and the Reynolds number in Newtonian laminar open channel flow is defined as:

$$f = \frac{16}{\text{Re}}$$

2.26

On a Moody diagram, this gives a straight line with a slope of -1. This is similar to pipe flow (Douglas *et al.*, 2001).

2.5.2 Turbulent flow

Many mathematical expressions are available for the turbulent flow regime of Newtonian fluids in open channels. The Chézy (Chow, 1959), Manning (1890), Blasius (1913) and Colebrook and White (Colebrook, 1939) expressions are detailed in this section.

2.5.2.1 Chézy

Chézy introduced the Chézy equation in 1769 after his design work for a water supply in Paris (Chow, 1959). The application of the Chézy equation is limited to turbulent flow of water in open channels, and can be written as follows:

$$V = C_{\text{Chézy}} \sqrt{R_h \sin\theta}$$

2.27

where $C_{\text{Chézy}}$ is known as the Chézy coefficient expressed in $\text{m}^{1/2}\text{s}^{-1}$. The values of the Chézy coefficient have a typical range from $30 \text{ m}^{1/2}\text{s}^{-1}$ (small rough channel) up to $90 \text{ m}^{1/2}\text{s}^{-1}$ (large smooth channel).

Chézy presented various values for the Chézy coefficient. Several researchers have made the assumption that this constant did not depend on flow conditions, but research has proved the assumption false (Chanson, 1999). There are several empirical expressions available for the calculation of the Chézy coefficient such as the G-K expression (Ganguillet & Kutter, 1869), the Bazin (1865) expression, the Keulegan (1938) expression and the Powell (1950) expression.

2.5.2.2 Manning or Gauckler-Manning

Derived from the Chézy equation, the Manning equation defined in Equation (2.7) (Manning, 1890) is applicable to both uniform and non-uniform (gradually varied) flow of water. Dooge (1991) suggested that the Manning equation be renamed as the Gauckler-Manning equation because it was primarily introduced by Gauckler (1867) from his reanalysis of the data obtained by Darcy and Bazin (1865).

Typical values of the Manning constant can be found in Chow (1959).

2.5.2.3 Blasius

The correlation between friction factor and Reynolds number was introduced by Blasius (1913), for Newtonian fluids through smooth pipes in the turbulent flow regime and is defined as:

$$f = 0.0791\text{Re}^{-0.25} \quad 2.28$$

The Blasius equation can be used to predict the flow of Newtonian fluids in smooth open channels in the turbulent regime by replacing D with D_h in the Reynolds number (Chow, 1959). The Blasius equation is valid for Reynolds numbers ranging from 3000 to 10^5 (Chanson, 1999).

2.5.2.4 Colebrook-White

Colebrook and White (Colebrook, 1939) combined the von Karmán-Prandtl (von Karman, 1930 & Prandtl, 1935) expressions for smooth and rough pipe flow into one single equation as follows:

$$\frac{1}{\sqrt{4f}} = -2 \log \left(\frac{e}{3.71D} + \frac{2.51}{\text{Re} \sqrt{4f}} \right) \quad 2.29$$

This equation can be adapted to open channel flow by replacing the pipe diameter with the hydraulic diameter which is four times the hydraulic radius (Chanson, 1999). Applicable to turbulent flow of Newtonian fluids in smooth and rough channels, equation (2.29) can be rewritten as:

$$\frac{1}{\sqrt{4f}} = -2 \log \left(\frac{e}{14.84R_h} + \frac{2.51}{\text{Re} \sqrt{4f}} \right) \quad 2.30$$

where e is the equivalent roughness height given in

Table 2.3.

Table 2.3: The equivalent roughness height (Chanson, 2004)

| Material | e, the equivalent roughness height (mm) |
|--------------------------------|---|
| PVC (plastic) | 0.01 to 0.02 |
| Painted pipe | 0.02 |
| Riveted steel | 1 to 10 |
| Cast iron (new) | 0.25 |
| Cast iron (rusted) | 1 to 1.5 |
| Concrete | 0.3 to 3 |
| Untreated shot-concrete | 3 to 10 |
| Planed wood | 0.6 to 2 |
| Rubble masonry | 5 to 10 |
| Straight uniform earth channel | 3 |

Featherstone and Nalluri (2009) expressed Equation (2.30) in an explicit form by writing in terms of the mean fluid velocity:

$$V = \sqrt{32 R_h \sin \theta} \log \left(\frac{e}{14.84 R_h} + \frac{1.255 \mu}{R_h \rho \sqrt{32 g R_h \sin \theta}} \right) \quad 2.31$$

2.5.3 Laminar-Turbulent Transition

The laminar-turbulent transition in pipe flow occurs over a range of Reynolds numbers. Straub *et al.* (1958) presented a summary of experimental studies of the critical Reynolds number Re_c for Newtonian flow conducted in channels of rectangular, triangular and semi-circular shapes. They found the Re_c to vary from 2000 to more than 3000 for flow depth to channel width h/B ratios from 1.35 to 3.70. Straub *et al.* (1958) concluded that the critical Reynolds number values for open channel flow are dependent on the channel shape to a certain extent and these values are generally larger than those for closed conduit flow.

The Darcy friction factor–Reynolds number relationship shown in Figure 2.4 was based on the data developed at the University of Illinois and the University of Minnesota.

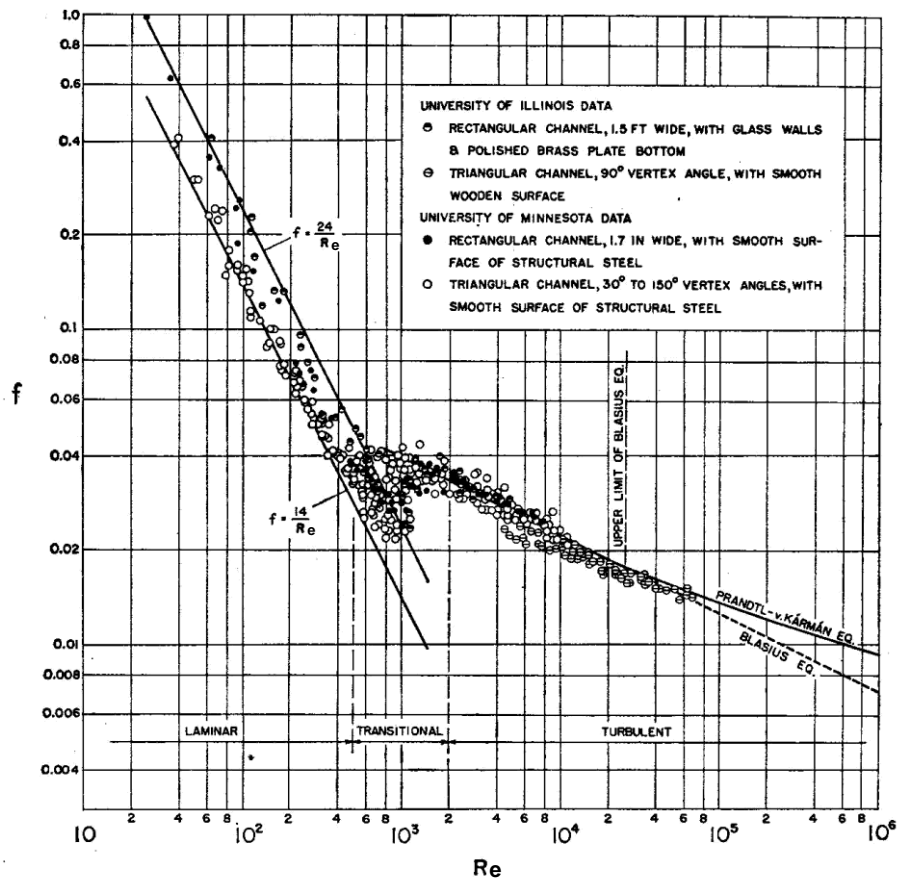


Figure 2.4: The f - Re relationship for flow in smooth channels (Chow, 1959)

The lower critical Reynolds number is dependent on channel shape to some extent. In practice, the transitional flow regime for open-channel flow is assumed to vary between Reynolds numbers of 500 to 2000. It should be noted that the upper critical Reynolds number value is arbitrary, since there is no definite upper limit for all flow conditions (Chow, 1959).

For laminar flow in smooth channels, the value of the channel shape constant K can be determined theoretically and Figure 2.4 shows that K is approximately 14 for triangular channels and 24 for rectangular channels (Chow, 1959).

In turbulent flow, the channel shape does not influence friction significantly as it does in laminar flow. However for turbulent flow in rough channels, the channel shape has a pronounced effect on the friction factor. It is believed that, when the degree of roughness remains constant, the friction factor decreases in the order of rectangular, triangular, trapezoidal and circular channels (Chow, 1959).

At Prandtl's suggestion, Kirschmer (1949a & 1949b) stated that the channel shape effect may be a result of the development of secondary flow, which is apparently more pronounced in rectangular channels than it is in triangular channels (Chow, 1959). The secondary flow is defined as the movement of fluid particles on a cross section normal to the longitudinal

direction of the channel. A high secondary flow involves high energy loss and thus accounts for high channel resistance (Chow, 1959).

2.6 Non-Newtonian open channel flow

This section focuses on the research conducted on the flow of non-Newtonian fluids in open channels.

2.6.1 Laminar flow

2.6.1.1 Work done by Kozicki and Tiu

Kozicki and Tiu (1967) conducted analytical work on the effect of shape of open channels in laminar flow region.

Effect of channel shape

The effect of shape was first established by Straub *et al.* (1958) during their open channel flow study using Newtonian fluids. Kozicki and Tiu (1967) extended Straub's work to open channels using non-Newtonian fluids by proposing shape factors defined as:

$$a = 0.5 \left(\frac{\lambda_h}{1 + \lambda_h} \right)^2 \left(1 - \frac{32}{\pi^3} \sum_0^{\infty} \left(\frac{(-1)^n}{(2n+1)^3} \right) \left(\frac{1}{\cosh \left(\frac{(2n+1)}{2} \pi \lambda_h \right)} \right) \right)^{-1} \quad 2.32$$

with

$$\lambda_h = \frac{B}{h} \quad 2.33$$

$$b = a(3\phi - 1) \quad 2.34$$

with

$$\phi = \frac{\left(1 - \frac{32}{\pi^3} \sum_0^{\infty} \left(\frac{(-1)^n}{(2n+1)^3} \right) \left(\frac{1}{\cosh \left(\frac{(2n+1)}{2} \pi \lambda_h \right)} \right) \right)}{\left(1 - \frac{192}{\pi^5} \frac{1}{\lambda} \sum_0^{\infty} \left(\frac{1}{(2n+1)^5} \right) \tanh \left(\frac{(2n+1)}{2} \pi \lambda_h \right) \right)} \quad 2.35$$

Kozicki & Tiu (1967) used these shape factors to derive different Reynolds numbers for various non-newtonian models such as the power law, Bingham plastic, Ellis, Meter, and Reiner-Rivlin models.

➤ **Kozicki and Tiu's Reynolds number for power law fluids**

This Reynolds number encompassed the shape factors as follows:

$$Re = \frac{\rho V^{(2-n)} R_h^n}{2^{n-3} k \left(\frac{a + bn}{n} \right)^n} \quad 2.36$$

The geometric coefficients, 'a' and 'b', incorporated the changes in aspect ratio as the depth increases as shown in Equations 2.32 and 2.34.

➤ **Kozicki and Tiu's Reynolds number for Bingham plastic fluids**

The Reynolds number for Bingham plastic fluids is written as follows:

$$Re = \frac{4R_h V \rho}{k} \left[\frac{1}{a+b} - \frac{1}{b} \left(\frac{\tau_y}{\tau_0} \right) + \frac{a}{b(a+b)} \left(\frac{\tau_y}{\tau_0} \right)^{\left(1 - \frac{b}{a} \right)} \right] \quad 2.37$$

with the wall shear stress defined by Equation 2.21.

2.6.1.2 Work done by Hao and Zhenghai

Hao and Zhenghai (1980) investigated the flow of the Yellow river in China. Sediment particles of $d_{90}=0.063$ mm, $d_{50}=0.042$ mm, and $d_{10}=0.01$ mm were mixed with water to make up a slurry or a mud. The rheological characteristics of the mud were measured using a capillary viscometer and the mud was characterised as a Bingham plastic fluid. Their flume tests were conducted in a 43 m long concrete rectangular channel with only one slope and width.

The Reynolds number developed for laminar flow is only applicable to Bingham plastic fluids and it is defined as follows:

$$Re = \frac{4 R_h \rho V}{k + \left(\frac{\tau_y R_h}{2 V} \right)} \quad 2.38$$

The friction factor was defined by Equation (2.24).

2.6.1.3 Work done by Coussot

Coussot (1994) investigated the flow of concentrated mud suspensions in open channels. He used kaolin suspensions which he characterised as a Herschel-Bulkley fluid and tested various concentrations for which he fixed the value of n to 0.333.

Coussot defined the Herschel-Bulkley number as follows:

$$H_b = \frac{\tau_y}{k} \left(\frac{h}{V} \right)^n \quad 2.39$$

From this, he was able to establish the empirical expressions of the average wall shear stress for both rectangular and trapezoidal channel shapes as follows:

$$\tau_0 = \tau_y \left(1 + a (H_b)^{-0.9} \right) \quad 2.40$$

with 'a' being a shape factor which varies for each channel shape.

For a rectangular channel shape, the shape factor 'a' was defined as follows:

$$a = 1.93 - 0.43 \left(\arctan \left(\left(\frac{10h}{B} \right)^{20} \right) \right) \quad 2.41$$

This shape factor was applicable only for (h/B) ratio less than 1 ($h/B < 1$). Coussot (1994) stated that this equation could predict his experimental results to within an error range of 30%.

For the trapezoidal channel shape, Coussot established the factor "a" to be:

$$a = 1.93 - 0.6 \left(\arctan \left(\left(\frac{0.4h}{B} \right)^{20} \right) \right) \quad 2.42$$

He claimed this geometric coefficient to be valid for $h/B < 4$ and was able to predict all his experimental results within an error range of 35%.

Equation (2.40) can be expressed in terms of H_b as follows:

$$H_b = \left(\frac{\tau_0 - 1}{\tau_y} \right)^{\frac{1}{0.9}} \frac{1}{a} \quad 2.43$$

Cousot (1994) stated that these empirical expressions are only applicable to Herschel-Bulkley fluids and the value of n should be fixed to 0.333. With these limitations, these expressions can be used to calculate the normal depth of any flow in the trapezoidal and rectangular channels by equating Equations (2.24) and (2.36), with the wall shear stress defined by Equation (2.21).

2.6.1.4 Abulnaga's approach

The design method presented by Abulnaga (2002) was for transporting slurries through rectangular flumes which behave as Bingham plastic fluids. He adapted the Buckingham equation for pipe flow to open channel flow by expressing both Reynolds and Hedström numbers in terms of the hydraulic radius.

The dimensionless form of the Buckingham equation for pipe flow is expressed as follows (Chhabra & Richardson, 2008):

$$\frac{1}{\text{Re}_B} = \frac{f}{16} - \frac{\text{He}}{6 \text{Re}_B^2} + \frac{\text{He}^4}{4 f \text{Re}_B^8} \quad 2.44$$

where Re_B is the Bingham Reynolds number and He is the Hedström number.

The Bingham Reynolds number and the Hedström number modified by Abulnaga (2002) for open channel flow are expressed respectively as follows:

$$\text{Re}_B = \frac{4 R_h V \rho}{\eta_B} \quad 2.45$$

and

$$\text{He} = \frac{16 R_h^2 \rho \tau_{yB}}{\eta_B^2} \quad 2.46$$

Ignoring the third term of the RHS of Equation (2.44) and substituting Re_B and He with Equations (2.45) and (2.46) respectively, the following equation was obtained (Abulnaga, 2002):

$$\frac{\eta_B}{4 R_h V \rho} \approx \frac{f}{16} - \frac{\tau_{yB}}{6 V^2 \rho} \quad 2.47$$

which can be written after rearrangement as:

$$f = \frac{16}{\text{Re}_B} \left(1 + \frac{\text{He}}{6 \text{Re}_B} \right) \quad 2.48$$

In case the flow is fully developed and uniform, the slope or energy gradient of an open channel in terms of head loss per unit length is (Henderson, 1990):

$$S = \frac{h}{L} = \frac{f V^2}{2 g R_h} \quad 2.49$$

By choosing a velocity and flow rate, the Hedström and Reynolds numbers can be determined provided the Bingham plastic viscosity and Bingham yield stress of the fluid are known. For laminar flow, the friction can be obtained using Equation (2.48) and the slope can then be determined by using Equation (2.49).

This method was successfully used to design a tailings open channel in 1997 for a Peruvian copper mine in order to transport tailings containing soft clay (Abulnaga, 2002). Paterson *et al.* (2004) also used this approach to analyse the capacity of existing channels from two Andean mines in southern Peru. They stated that Abulnaga's approach provided a good approximation of the flow behaviour of the copper tailings in the channels.

2.6.1.5 De Kee *et al.*'s thin film approach

De Kee *et al.* (1990) developed correlations for flow of viscoplastic fluids on an inclined plane. These equations are only applicable to flow on an infinitely wide plane (i.e. sheet flow).

The average wall shear is defined by Equation (2.21) whereas the average velocity based on the Herschel-Bulkley model is expressed as:

$$V = \frac{n k}{(2n + 1) \rho g \sin \theta} \left(\frac{\tau_0}{k} \right)^{\left(\frac{n+1}{n} \right)} \left(1 - \frac{\tau_{yHB}}{\tau_0} \right)^{\left(\frac{n+1}{n} \right)} \left(1 + \left(\frac{n}{n+1} \right) \frac{\tau_{yHB}}{\tau_0} \right) \quad 2.50$$

This correlation was used in the test work conducted by De Kee *et al.* (1990) with two industrial suspensions, of which one was a milk of lime suspension with a density of 1164 kg/m³ and the other a ketchup sample with a density of 1140 kg/m³, on an inclined plane (0.058 m wide and 0.615 m long) with a polished plastic surface. The angle of inclination was changed by adjusting the vertical position of the feed tank, allowing the plane to turn on its pivot.

Haldenwang *et al.* (2004) tested this approach and used the criteria for thin film in a channel as proposed by Coussot (1994). He proposed that for a width to depth ratio of 10:1 the side wall effect would be negligible.

2.6.1.6 Work done by Haldenwang

Haldenwang (2003) investigated the flow of non-Newtonian fluids through rectangular open channels. He tested various concentrations of different materials such as CMC solutions, bentonite and kaolin suspensions. Haldenwang characterised the CMC solution as a power law fluid, the bentonite suspension as a Bingham plastic fluid and the kaolin suspension as a Herschel-Bulkley fluid. He tested these non-Newtonian fluids in three different sizes of rectangular shaped flumes, which were 75 mm, 150 mm, and 300 mm wide. The 75 mm flume was 4.5 m long and the 150 mm and the 300 mm flumes were 10 m long. The flumes could be tilted up to 5° from the horizontal.

Haldenwang *et al.* (2002) modified the Slatter Reynolds number for non-Newtonian pipe flow to open channel flow by substituting the pipe diameter with the hydraulic radius as follows:

$$\text{Re}_H = \frac{8 \rho V^2}{\tau_y + k \left(\frac{2V}{R_h} \right)^n} \quad 2.51$$

For power law fluids, equation (2.51) reduces to:

$$\text{Re}_H = \frac{8 \rho V^2}{k \left(\frac{2V}{R_h} \right)^n} \quad 2.52$$

For Bingham fluids, equation (2.51) reduces to:

$$\text{Re}_H = \frac{8 \rho V^2}{\tau_y + k \left(\frac{2V}{R_h} \right)^n} \quad 2.53$$

This Reynolds number in its most basic form reduces to the Newtonian Reynolds number. This Reynolds number (equation (2.51)) adequately predicted the laminar flow of non-Newtonian fluids he used in his study to within an average deviation of +/- 30%. The friction factor was obtained by using equation (2.24).

Haldenwang *et al.* (2004) published work on the effect of shape on rectangular, semi-circular and trapezoidal flumes using kaolin and bentonite suspensions as well as CMC solutions of

different concentrations. They concluded for the fluids and flume shapes tested that the use of friction factor given by Equation 2.20 with the appropriate Reynolds number for power-law (Equation 2.52), Bingham plastic (Equation 2.53) or yield-shear thinning fluids (Equation 2.51) predicted their experimental data in the laminar flow regime with an average deviation of +/- 30%, provided the correct equation is used to account for the rheology of the test fluid used. Furthermore, they found the more complex Reynolds number defined by Kozicki and Tiu (1967, 1988) consisting of two shape factors did not give a good prediction of their experimental data in the laminar flow regime. This was due to the yield stress having a significant effect which was not accounted for by Kozicki and Tiu (1967, 1988) and that the hydraulic radius used in the Reynolds number presented by Haldenwang *et al.* (2002) is sufficient to account for the flume shape effect. Haldenwang (2003) used the flow paradigm of $f=16/Re$ to describe the laminar flow data in rectangular channels.

2.6.1.7 Work done by Burger

Burger *et al.* (2010a & 2010b) conducted experiments on the flow of non-Newtonian fluids in triangular, semi-circular and trapezoidal shaped channels in order to extend the database published by Haldenwang and Slatter (2006) for rectangular open channels.

Using the Haldenwang *et al.* (2002) definition of Reynolds number (Re), the shape effect of the friction factor f vs. Re relationship for laminar flow of non-Newtonian fluids in open channels, was investigated in some depth. Furthermore, the validity of the pipe flow paradigm of $f = 16/Re$ (where $K=16$) used by Haldenwang *et al.* (2002, 2004), and Haldenwang (2003) for open rectangular channels was tested in other shaped channels by Burger *et al.* (2010a).

Burger *et al.* (2010a) found the pipe flow paradigm of $f = 16/Re$ used by Haldenwang *et al.* (2002, 2004) to be incorrect for the various shapes. Burger *et al.* (2010a) described the laminar flow data of triangular, semi-circular, rectangular and trapezoidal channels by $f = K/Re$. They determined that the overall average K value for triangular channels with a vertex angle of 90° to be 14.6, for semi-circular channels 16.2, for rectangular channels 16.4 and 17.6 for trapezoidal channels with 60° sides. These K values were similar to those published by Straub *et al.* (1958) and Chow (1959) for open channel flow of Newtonian fluids.

2.6.1.8 Experimental procedure used by Haldenwang and Burger

The flume tests were carried out in a 10 m long tilting flume (shown in Figure 2.5), in the Flow Process and Rheology Center at the Cape Peninsula University of Technology. The flume can be tilted from 1 to 5° from the horizontal. The width of the flume can be varied from

300 mm to 150 mm by inserting a partition mid-section lengthways down the flume. The rectangular flume shape can be changed by inserting an appropriate cross-sectional insert to achieve a triangular, trapezoidal or semi-circular flume shape (Burger *et al.*, 2010b). The same fluids were also tested in a 5 m by 75 mm wide tilting flume by Haldenwang (2003). A 100 mm progressive cavity, positive displacement pump and a Warman 4x3 centrifugal slurry pump were used to regulate the flow with a maximum flow rate of 45 l/s (Haldenwang, 2003).

Digital depth gauges placed at 5 m and 6 m from the entrance of the 10 m long tilting flume were used to measure the flow depths. The depth gauge positions were shown to be the optimum ones in a study by Haldenwang (2003) since the difference between the two positions was minimum. The flow depth measurements had an error of less than 5% and the flow in the measuring section was deemed to be steady and uniform (Haldenwang, 2003).

The flumes were linked to an inline tube viscometer (shown in Figure 2.6) consisting of three pipes of various diameters (13, 28 and 80 mm). Each pipe was fitted with a magnetic flow meter and differential pressure gauges were used to measure a pressure drop over a fixed length. The pseudo shear rate $8V/D$ and the average wall shear stress data can be obtained from these measurements. The combined error for the pipe wall shear stress was found to be less than 5% and the pseudo shear rate error no more than 0.5% (Haldenwang, 2003). The true shear rate was evaluated after transformation of the data using the Rabinowitsch-Mooney method. Various rheological models were used to fit the flow data (Haldenwang, 2003).

Aqueous suspensions of bentonite and kaolin clays as well as aqueous solutions of carboxymethyl cellulose were used as test fluids. The bentonite, kaolin and CMC solutions (fluids) were prepared by a gradual addition of the appropriate amount of dry solids to the measured quantity of water by gentle agitation using paddles in an open tank. There was no settling of the solid particles over the wide range of concentrations under different flow conditions. This showed the stability of different suspensions over a long period of time and thus all fluids used were treated as homogeneous continua. A constant-volume density bottle was used to measure the fluids densities (Haldenwang, 2003). The physical characteristics of the test fluids used are presented in the appendix section.

The flume tests were conducted by taking measurements of the flow rate using the magnetic flow meters and the flow depth using the depth gauges, at various slopes varying from 1° to 5°. A data logger was used to connect these instruments to a PC. The calibrated data inputs were recorded on a spreadsheet and plotted as a Moody diagram in order to enable one to

make instant observations and make the necessary corrections (Haldenwang *et al.*, 2010). For each flume shape, flume size, sets of flow data were collected for different concentrations, slopes, and flow rate. Tube viscometer data was also obtained before and after each set. This large database was then used to investigate the accuracy of various open channel flow models.

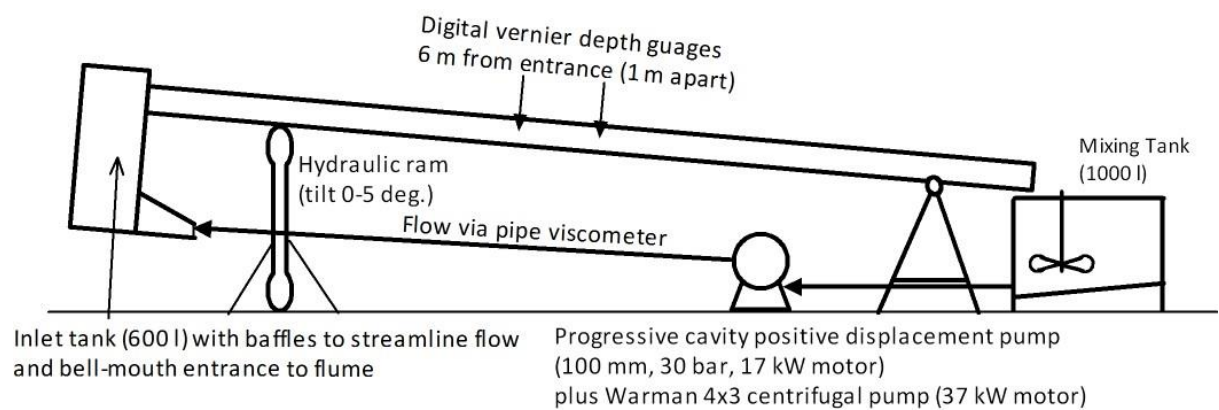


Figure 2.5: 10 m flume rig (Haldenwang, 2003)

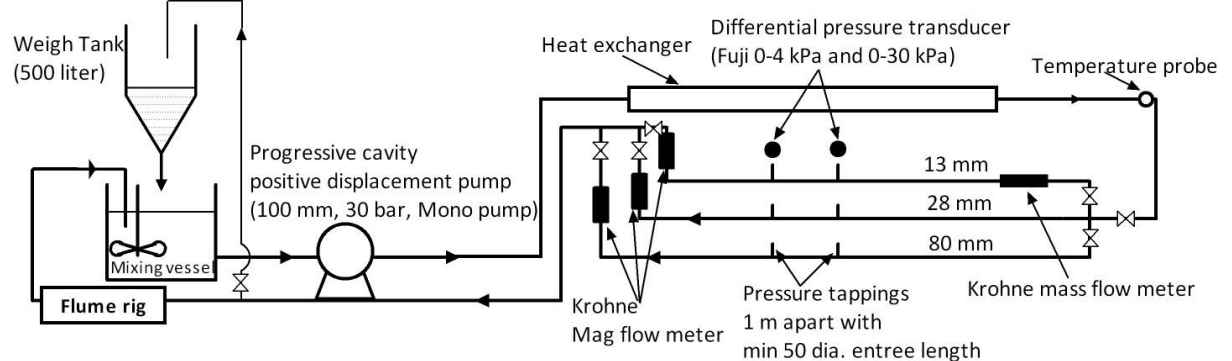


Figure 2.6: In-line pipe viscometer (Haldenwang, 2003)

2.6.2 Turbulent flow

In this section, different models available in literature to predict the mean flow velocity of non-Newtonian fluids in turbulent open channel flow are presented.

2.6.2.1 Kozicki and Tiu approach

At low Reynolds numbers, the friction factor correlation in turbulent flow of Newtonian fluids in smooth open channels was found to be similar to closed conduits (Straub *et al.*, 1958). Kozicki and Tiu's (1967) reasoning was that the same would also apply to non-Newtonian

fluids. However, unlike the Manning equation for turbulent Newtonian equation flow in open channels, the wall roughness was not accounted for in the following equations.

➤ **Power law model**

Kozicki and Tiu (1967) suggested that the friction factor for turbulent flow of a power-law fluid in open channels of arbitrary cross-section may be examined using the Dodge and Metzner (1959) equation for circular pipes written in terms of n^* , Re_p^* and the geometric parameters, a and b . This is expressed as follows:

$$\frac{1}{\sqrt{f}} = \frac{40}{n^{*0.75}} \log \left[Re_p^* f^{\left(1-\frac{n^*}{2}\right)} \right] - \frac{0.40}{n^{*1.2}} + 4.0 n^{*0.25} \log \left[\frac{4(a + b n^*)}{(1 + 3 n^*)} \right] \quad 2.54$$

where n^* is equal to n and Re_p^* is given by:

$$Re_p^* = \frac{R_h^n V^{2-n} \rho}{2^{n-3} k \left(\frac{a + b n}{n} \right)^n} \quad 2.55$$

➤ **Bingham plastic model**

No correlations were presented by Kozicki and Tiu (1967) for estimating the friction factor for turbulent flow of a Bingham plastic fluid in open channels of arbitrary cross-section. However, it is reasonable to use a similar approach to that of Kozicki and Tiu (1967) for power law fluids. Hence, rewriting the Darby and Melson (1981) approach equation for circular pipes in terms of Re_B^* and the geometric parameters, a and b gives

$$f = 10^{c^*} \left(\frac{Re_B^*}{\frac{1}{a+b} - \frac{\chi}{b} + \frac{a}{b(a+b)} \chi^{\frac{b}{a+1}}} \right)^{-0.193} \quad 2.56$$

in which c^* is given by

$$c^* = -1.378 \left(1 + 0.146 \exp \left[-2.9 \times 10^{-5} \left(\frac{Re_B^*}{\frac{1}{a+b} - \frac{\chi}{b} + \frac{a}{b(a+b)} \chi^{\frac{b}{a+1}}} \right) \right] \right) \quad 2.57$$

and χ is τ_{yB}/τ_0 .

It should be noted that Equation (2.56) is not applicable when the Hedström number, expressed as:

$$\text{He}^* = \frac{64 V^2 \chi \rho}{\tau_0 \left(\frac{1}{a+b} - \frac{\chi}{b} + \frac{a}{b(a+b)} \chi^{\frac{b}{a+1}} \right)} \quad 2.58$$

is less than 1000.

2.6.2.2 Torrance pipe flow model adapted

Torrance (1963) established a turbulent flow correlation for non-Newtonian slurries exhibiting yield-pseudoplastic behaviour in smooth pipes. Using the Herschel-Bulkley model, this is expressed as:

$$\frac{V}{V_*} = \frac{3.8}{n} + \frac{2.78}{n} \ln \left(1 - \frac{\tau_y}{\tau_0} \right) + \frac{2.78}{n} \ln \left(\frac{V_*^{2-n} \rho R^n}{K} \right) - 4.17 \quad 2.59$$

where V_* is defined by

$$V_* = \sqrt{\frac{\tau_0}{\rho}} \quad 2.60$$

For open channel flow, Equation (2.59) may be used by replacing R with $2R_h$. Hence Equation (2.59) becomes:

$$\frac{V}{V_*} = \frac{3.8}{n} + \frac{2.78}{n} \ln \left(1 - \frac{\tau_y}{\tau_0} \right) + \frac{2.78}{n} \ln \left(\frac{V_*^{2-n} \rho (2R_h)^n}{k} \right) - 4.17 \quad 2.61$$

This model was not experimentally verified against any data set by the author. However, Haldenwang (2003) attempted to verify this model with his experimental data and found that it did not give a good approximation.

2.6.2.3 Slatter's pipe flow model adapted

Slatter (1994) established a turbulent flow model for non-Newtonian slurries displaying yield-pseudoplastic behaviour in smooth and rough wall pipes. For smooth wall pipe flow, this is expressed as follows:

$$V = V_* \left(2.5 \ln \left(\frac{R}{d_x} \right) + 2.5 \ln \text{Re}_r + 1.75 \right) \quad 2.62$$

where V_* is given by Equation 2.60, d_x is the representative particle size of the solids and Re_r is the roughness Reynolds number proposed by Slatter (1994) as:

$$Re_r = \frac{8 \rho (V_*)^2}{\tau_y + k \left(\frac{8 V_*}{d_x} \right)^n} \quad 2.63$$

For fully developed rough wall pipe flow, this is expressed as:

$$V = V_* \left(2.5 \ln \left(\frac{R}{d_x} \right) + 4.75 \right) \quad 2.64$$

For the slurries used to build the database (kaolin, CMC and bentonite), Slatter (1994) found d_x was best represented by d_{85} .

For open channel flow, the pipe radius can be substituted by the equivalent hydraulic radius. Hence Equation (2.62) and Equation (2.64) become for smooth wall open channel flow

$$V = V_* \left(2.5 \ln \left(\frac{2R_h}{d_{85}} \right) + 2.5 \ln Re_r + 1.75 \right) \quad 2.65$$

and for rough wall open channel flow.

$$V = V_* \left(2.5 \ln \left(\frac{2R_h}{d_{85}} \right) + 4.75 \right) \quad 2.66$$

Haldenwang (2003) attempted to verify this model with his experimental data. He found that Slatter's model predicted open channel turbulent flow better than the Torrance model.

2.6.2.4 Naik's model

By using the criteria for turbulent flow of a Newtonian fluid in a rough wall open channel of semi-circular cross-section (Chow, 1959), Naik (1983) expressed the mean velocity of a Bingham plastic fluid flowing in a rough open channel of a rectangular cross-section as follows:

$$V = 2.5 V_* \left(1 - \frac{\tau_y}{\tau_0} \right)^{0.5} \left(A_0 + \ln \left(\frac{R_h}{e} \right) \right) \quad 2.67$$

where:

$$A_0 = \ln \left(\left(\frac{30h}{R_h} \right)^{-1 - \left(\frac{\left(\frac{B+2}{h} \right) h^2}{4A} \right)} \right) \quad 2.68$$

He also expressed the friction factor for fully-developed turbulent flow of a Bingham plastic fluid in a rough open channel as follows:

$$\left(\frac{2}{f} \right)^2 = 2.5 \left(1 - \frac{\tau_y}{\tau_0} \right)^{0.5} \left(A_0 + \ln \left(\frac{R_h}{e} \right) \right) \quad 2.69$$

Equation (2.69) can be written in a dimensionless form as follows:

$$\left(\frac{2}{f} \right)^2 = 2.5 \left(1 - \frac{2He}{f Re_B^2} \right)^{0.5} \left(A_0 + \ln \left(\frac{R_h}{e} \right) \right) \quad 2.70$$

Naik (1983) used kaolin slurries in a 12.2 m steel flume (with a roughness of 3.048 mm) of a 300 × 300 mm rectangular cross-section tilted at various slopes up to a maximum slope of 2.29°, and found a reasonably good agreement between the experimental data and his model for fully-developed turbulent flow of a Bingham plastic fluid in a rough wall open channel.

2.6.2.5 Abulnaga's approach

Darby and Melson (1981) adapted the semi-empirical correlation proposed by Hanks and Dadia (1971) for turbulent pipe flow of Bingham plastic slurries in closed conduits. The friction factor they established for the turbulent regime is:

$$f_T = 10^a Re_B^b \quad 2.71$$

where

$$a = -1.47 \left(1 + 0.146 \exp \left(-2.9 \times 10^{-5} He \right) \right) \quad 2.72$$

and $b = -0.193$

Abulnaga's Reynolds number and the Hedström number were defined in equations (2.45) and (2.46) respectively.

Abulnaga (2002) proposed that Equation 2.71 and Equation 2.72 may be tentatively adapted to open channels to give:

$$f_T = 10^a \left(\frac{4R_h V \rho}{\eta} \right)^b \quad 2.73$$

where

$$a = -1.47 \left(1 + 0.146 \exp \left(-2.9 \times 10^{-5} \left(\frac{16R_h^2 \rho \tau_0}{\eta^2} \right) \right) \right) \quad 2.74$$

and $b = -0.193$

However, the empirical parameters 'a' and 'b' have yet to be experimentally confirmed for open channels.

Darby and Melson (1981) combined the Buckingham equation for f_L for laminar pipe flow with Equation (2.71) for turbulent pipe flow to obtain a single friction factor expression valid for all flow regimes:

$$f = \left(f_L^m + f_T^m \right)^{\left(\frac{1}{m} \right)} \quad 2.75$$

where

$$m = 1.7 + \frac{40000}{Re_B} \quad 2.76$$

Abulnaga (2002) suggested the use of Equation (2.75) for open channels provided Equation (2.76) is changed to:

$$m = 1.7 + \frac{10000\eta}{R_h V \rho} \quad 2.77$$

He used this method to design a tailings channel to transport tailings rich in soft clay for a Peruvian copper mine.

2.6.2.6 Yang and Zhao's model

Wan and Wang (1994) referred to the work conducted by Yang and Zhao (1983) on hyperconcentrated flow over a rough flume surface. The roughness was created by glueing small concrete blocks of 20×20×20 mm on the flume bottom. Based on their experimental results, Yang and Zhao (1983) proposed the following correlation for the friction factor

$$\frac{1}{\sqrt{f}} - 2 \log \frac{R_h}{e} = 13.81 - 4.71 \log Re^* \quad 2.78$$

where Re^* is the roughness Reynolds number given by:

$$Re^* = \frac{\rho V^* e}{\eta} \quad 2.79$$

and e is the size of the roughness element ($e=20$ mm).

Yang and Zhao (1983) also suggested that for smooth boundary hyper-concentrated flow in open channels, the Blasius model defined by Equation (2.28) can be used. It seems that the materials used all possessed a low yield stress together with the sediment concentration being less than 270 kg/m^3 .

2.6.2.7 Haldenwang's turbulent model

Haldenwang (2003) stated that before the onset of full turbulence can be established, the turbulent flow region must be established. He established the velocity model for turbulent flow as follows:

$$V = \sqrt{gh \sin \alpha} \left(2.5 \ln \frac{2R_h}{k} - 76.86 \mu_{app500} - 9.45 \right) \quad 2.80$$

The Fanning friction factor is given by:

$$f_{turb} = 0.66 \left(\frac{2gh \sin \alpha}{V^2} \right) \quad 2.81$$

2.7 Previous work done in the laminar-turbulent transition region

This region has received a limited attention by a few researchers for non-Newtonian fluids in open-channels. Some authors suggested that the transitional flow behaviour in pipes is applicable to open-channels (Wilson, 1991).

2.7.1 Work done by Hao and Zhengai

During their measurements of flow pulsations, Hao and Zhengai (1980) discovered with a pressure micro-transducer that the pulsations in the transitional flow region originate in the lower region of the flume and weaken towards the free surface. In full turbulence, the pulsations reach a maximum over the full depth of the flume.

They observed that the laminar-turbulent transition occurs between Reynolds number 3000 and 5000 for different channel roughnesses and the friction factor varies between 0.005 and 0.01.

2.7.2 Work done by Naik

Using the Hanks criterion for pipe flow, Naik (1983) derived the following criterion for the onset of the laminar-turbulent transition for flow of a Bingham plastic fluid in a rectangular flume as follows:

$$(\text{Re}_B)_c = \frac{\rho V 4h}{\mu_B} = \left(\frac{\text{He}}{12\phi_c} \right) (1 - 1.5\phi_c + 0.5\phi_c^3) \quad 2.82$$

where h is the flow depth and ϕ_c is the ratio of the Bingham yield stress to the critical wall

shear stress given by $\phi = \frac{\tau_y}{\tau_0}$ and is expressed as:

$$\frac{\phi_c}{(1 - \phi_c)^3} = \frac{\text{He}}{48000} \quad 2.83$$

The Hanks criterion is used to predict the transitional pipe flow of Bingham plastic fluids (Chhabra and Richardson, 2008).

The critical Reynolds number for pipe flow is expressed in terms of the Hedström number (Chhabra and Richardson, 2008).

$$(\text{Re}_B)_c = \frac{\rho V D}{\mu_B} = \frac{1 - \frac{4}{3}\phi_c + \frac{\phi_c^4}{3}}{8\phi_c} \text{He} \quad 2.84$$

with

$$\frac{\phi_c}{(1 - \phi_c)^3} = \frac{\text{He}}{16800} \quad 2.85$$

For open channel flow, $4R_h$ is used in place of D in Equation (2.84) with $4R_h$ being the characteristic length.

According to Naik (1983), the value of the constant in Equation (2.83) may vary between 24000 and 96000 depending upon the value of the critical Newtonian Reynolds number used in the derivation, which may vary between 2000 and 8000.

Hence, for a given Hedström number, the critical Bingham Reynolds number at the onset of transition in open channels can be calculated by first establishing the value for ϕ_c using Equation (2.83) and then using this value in Equation (2.82). For pipe flow, the value for ϕ_c can be established by using Equation (2.85) and then using this value in Equation (2.84).

2.7.3 Wilson's work

Wilson (1991) suggested the following method to predict transition flow in pipes. He stated that pipe viscometer data be used to plot wall shear stress, τ_0 against nominal wall shear rate, $8V/D$. In the laminar flow regime, the data from all pipe diameters for any given fluid must collapse on a single line when the wall slip is absent. On a double logarithmic plot of τ_0 against $8V/D$, this single line which represents laminar flow data is a straight line of slope less than one. Turbulent flow, however, is depicted as a series of parallel lines, one for each pipe diameter, with a slope of approximately 1.75 to 2 which is pipe wall roughness dependent.

Wilson's method is based on the assumption that the pipe flow behaviour in the transition region is exactly the same as for open-channel flow and that the transition will occur at a Reynolds number having a certain value. However, no evidence has been found in order to determine whether any experimental research was done to ascertain the assumption.

2.7.4 Work done by Coussot

Coussot (1997) based his work on the Hanks criteria to develop a model that can be used to predict the onset of turbulence of mudflow which he characterised as a Herschel-Bulkley fluid. His model is applicable for infinitely wide channels.

He suggests that the flow reaches turbulence when the depth of flow is larger than:

$$h = \frac{1}{\rho g \sin \alpha} \tau_y + k \left(\frac{404 (M+1) \rho (g \sin \alpha)^2}{kv} \right)^{\left(\frac{1}{2M+1} \right)} \quad 2.86$$

with

$$M = \frac{1}{n}$$

and

$$v = \left[\left(\frac{M}{2M+1} \right)^{\left(\frac{M}{M-1} \right)} - \left(\frac{M}{2M+1} \right)^{\left(\frac{2M-1}{M+1} \right)} \right] \quad 2.87$$

2.7.5 Work by Slatter and Wasp

Slatter and Wasp (2000) investigated the flow of the transition region in large pipes where a simple criterion, for practical design use was developed based on a comparative approach between the “most accurate theories”. This criterion needs a prediction of the critical velocity or the transition velocity.

The critical velocity is determined by normalising the theoretical calculated laminar flow Reynolds number with the actual Reynolds number. This method is known as the normalised adherence function (NAF) and is defined as:

$$NAF = \frac{Re_{\text{actual}}}{Re_{\text{calculated}}} \quad 2.88$$

The answer to this equation must be equal to unity (Slatter, 1999) since laminar flow ceases to exist at NAF values greater than one. Transition flow occurs when the NAF value starts to deviate from unity. Therefore the critical velocity is determined by finding the corresponding velocity value in the experimental data. The accuracy of the theoretical approaches or models is compared by using the critical velocity.

2.7.6 Work done by Haldenwang

Haldenwang (2003) established a new model for predicting the onset of transition and the onset of turbulence or end of transition for rectangular channels, and stated that the flow behaviour could be characterised by both the Froude number for rectangular channels and the Reynolds number.

He used primarily the Moody diagram to try to establish a relationship between the Reynolds number and the rheological parameters of the different fluids tested. Due to the complex nature of many rheological parameters, a relationship that encompassed all the parameters could not be established.

Secondly, Haldenwang tried to establish a rheological parameter which could characterise the fluids tested, which was the apparent viscosity. This was done at shear rates of 50, 100, 200, and 500 s⁻¹. The apparent viscosity of the fluids tested exhibited some similarity at a shear rate of 100 s⁻¹.

He then plotted the Reynolds number against the Froude number to establish a relationship between the two, and established a power law relation for every slope from 1 to 5 degrees which was slope sensitive.

Therefore the relationship between the two dimensionless numbers was plotted for 1 to 5 degree slopes on the same set of axes. On the resulting graph, a straight line named the transition locus was established for all the slopes. Figure 3.4 is an example plot.

The linear relationship (transition locus) was then plotted against the apparent viscosity. From there a critical Reynolds number predicting the onset of transition was determined using the Froude number. There was a linear relationship between the Froude and the Reynolds numbers for an apparent viscosity at a shear rate of 100 s⁻¹.

The critical Reynolds number developed by Haldenwang (2003) is written as:

$$Re_c = 853.1 \left(\frac{\mu}{\mu_w} \mid \dot{\gamma} = 100s^{-1} \right)^{-0.21} Fr + 12\,630 \left(\frac{\mu}{\mu_w} \mid \dot{\gamma} = 100s^{-1} \right)^{-0.75} \quad 2.89$$

To predict the onset of turbulence, Haldenwang (2003) followed a similar procedure as for predicting the onset of transition with the only difference being that the linear relationship was at an apparent viscosity of 500 s⁻¹. The new critical Reynolds number to predict the end of transition or the onset of turbulence is:

$$Re_{c(turb)} = 3812 \left(\frac{\mu}{\mu_w} \mid \dot{\gamma} = 500s^{-1} \right)^{-0.52} Fr + 9626 \left(\frac{\mu}{\mu_w} \mid \dot{\gamma} = 500s^{-1} \right)^{-0.65} \quad 2.90$$

2.7.7 Work done by Fitton

Fitton (2008) presented a method for the prediction of laminar/turbulent transition for a given non-Newtonian open channel flow scenario, and the subsequent prediction of the friction loss for that same scenario. Fitton (2008) stated that his method could be used as a practical basis for the design of flumes and launders.

The point of laminar/turbulent transition can be calculated by changing the depth of flow until the Hagen-Poiseuille equation for laminar Newtonian flow calculates the same Darcy friction factor as the Colebrook-White equation for turbulent flow. The “solver” or “goal seek”

functions of the spreadsheet program will make this iterative process virtually instant (Fitton, 2008). Once the two equations are calculating the same f_D value, the transition point can be expressed in terms of the corresponding Reynolds number value. The Darcy friction is four times the Fanning friction factor and is given by:

$$f_D = \frac{64}{\text{Re}} \quad 2.91$$

The Colebrook-White equation (2.29) for pipe flow can be applied to open channel flow by replacing D with $4R_h$ as expressed in Equation (2.30).

This version of Equation (2.30) has also been used to generate Moody diagrams that are applicable to open channel flow (Chow, 1959 & Yen, 2002).

2.7.8 Slatter's work

Slatter *et al.* (2011) developed and evaluated a criterion for determining the laminar-turbulent transition for the sheet flow analysis using a power law fluid.

They defined the apparent sheet flow behaviour index n'_* in terms of a power law relationship between the bulk shear rate and the wall shear stress. After the Metzner and Reed (1955) method, the apparent sheet flow fluid consistency index K'_* was expressed as follows:

$$K'_* = \frac{\tau_0}{\left(\frac{3V}{H}\right)^{n'_*}} \quad 2.92$$

which led to the laminar sheet flow design equation as:

$$\tau_0 = K'_* \left(\frac{3V}{H}\right)^{n'_*} \quad 2.93$$

The height H was replaced by the hydraulic radius R_h in order to accommodate the fact that actual channels may approach sheet flow, but will always have side edges at some point so that

$$\tau_0 = K'_* \left(\frac{3V}{R_h}\right)^{n'_*} \quad 2.94$$

A new Reynolds number (Re_4) for sheet flow after the “Newtonian paradigm” was defined as:

$$Re_4 = \frac{8 \rho V^2}{K_* \left(\frac{3V}{R_h} \right)^{n_*}} \quad 2.95$$

Slatter established the transitional flow criterion as $Re_4=700$ by using a normalised adherence function which was defined as the wall shear stress ratio as follows:

$$\tau_{0Ratio} = \frac{\tau_{0Actual}}{\tau_{0Laminar}} \quad 2.96$$

Slatter (2013a) evaluated his new criterion ($Re_4=700$) against the experimental data published by Haldenwang and Slatter (2006) using one concentration from 1 to 5 degrees slope. He stated that the transitions predictions obtained worked generally well even though he only used one data set.

Slatter (2013a) extended the sheet flow analysis from a power law fluid to viscoplastic paste material.

For viscoplastic paste material, the Herschel Bulkley constitutive relation defined by Equation (2.13) is appropriate.

The bulk shear rate $3V/H$ for Herschel Bulkley sheet flow was defined as:

$$\frac{3V}{H} = \frac{3nk}{\tau_0(2n+1)} \left(\frac{\tau_0}{k} \right)^{\left(\frac{n+1}{n} \right)} \left(1 - \frac{\tau_y}{\tau_0} \right)^{\left(\frac{n+1}{n} \right)} \left(1 + \left(\frac{n}{n+1} \right) \frac{\tau_y}{\tau_0} \right) \quad 2.97$$

In order to solve for the Reynolds number Re_4 , Equation (2.97) will yield different values for the apparent sheet flow behaviour index and the apparent sheet flow fluid consistency index. Thus the required sheet flow rheological parameters will need to be evaluated at each requisite τ_0 value. This is similar to the approach used by Metzner and Reed (1955).

Slatter (2013b) introduced another criterion to predict transitional flow which was defined as:

$$V_c = 26 \sqrt{\frac{\tau_y}{\rho}} \quad 2.98$$

2.7.9 Wan and Wang's model

Wan and Wang (1994) reported the experimental work carried out by Wang *et al.* (1990) in a recirculating flume which was 8.7 m long and 10 cm wide. The sediment used was composed of calcite, kaolinite, montmorillonite, quartz and mica. The sediment suspension was characterised as a Bingham plastic fluid with concentration higher than 50 kg/m³. Wang *et al.* (1990) found the onset of transition to occur at a Reynolds number of 2000. They defined the Reynolds number as:

$$Re = \frac{4 \rho h V}{\eta \left(1 + \frac{1}{2} \frac{\tau_y h}{\eta V} \right)} \quad 2.99$$

where h is the flow depth.

Initial turbulent velocity fluctuations were observed by Wan and Wang (1990) to start near the bed whilst it was still laminar flow at the surface.

2.7.10 Yang and Zhao's model

Yang and Zhao (1983) concluded from their experimental work with hyperconcentrated flow with rough open channels that the roughness Reynolds number Re^* (defined in Equation (2.79)) is between 2.3 and 2.6 in the transition zone.

The models reviewed to predict the laminar-turbulent transition of non-Newtonian fluids in open channels are presented in Table 2.4.

Table 2.4: Summary of laminar-turbulent transition open channel models

| Author | Rheological model | | | Shape |
|---|-------------------|-----------------|------------------|--|
| | Power law | Bingham plastic | Herschel-Bulkley | |
| Hao and Zhengai (1980) | | • | | Rectangular Semi-circular Trapezoidal |
| Zhang and Ren (1982) | | • | | Rectangular |
| Naik (1983) | | • | | Rectangular |
| Wilson (1991) | | | | Sheet flow |
| Wan and Wang (1994) | | • | | Not known |
| Coussot (1997) | | | • | Rectangular and Trapezoidal Applicable to wide channels |
| Haldenwang (2003), Haldenwang <i>et al.</i> (2010) | • | • | • | Rectangular |
| Fitton (2008) | | | • | Semi-circular |
| Slatter (2011, 2013a and 2013b) | • | | • | Rectangular |

2.8 Non-Newtonian open channel flow experimental studies

Different experimental studies performed on non-Newtonian fluids in open channels are briefly described in this section.

Zhang and Ren (1982) conducted studies on the simulated flow of Yellow river mud which was classified as a Bingham plastic fluid using a home-made capillary viscometer. The mud particles had dimensions of $d_{90}=0.063\text{mm}$, $d_{50}=0.042\text{ mm}$ and $d_{10}=0.010\text{ mm}$. The preparation of the mud was done by mixing the mud particles together with some sediment to water. The tests were conducted in a rectangular flume at a fixed slope.

Zhang and Ren (1982) studied the effect of roughness on the friction factor as illustrated in Figure 2.7. The roughness was expressed as the ratio of the depth of the fluid to the projected bed surface H/Δ . The friction factor was denoted as λ and was defined as $96/Re_{\text{Zhang and Ren}}$.

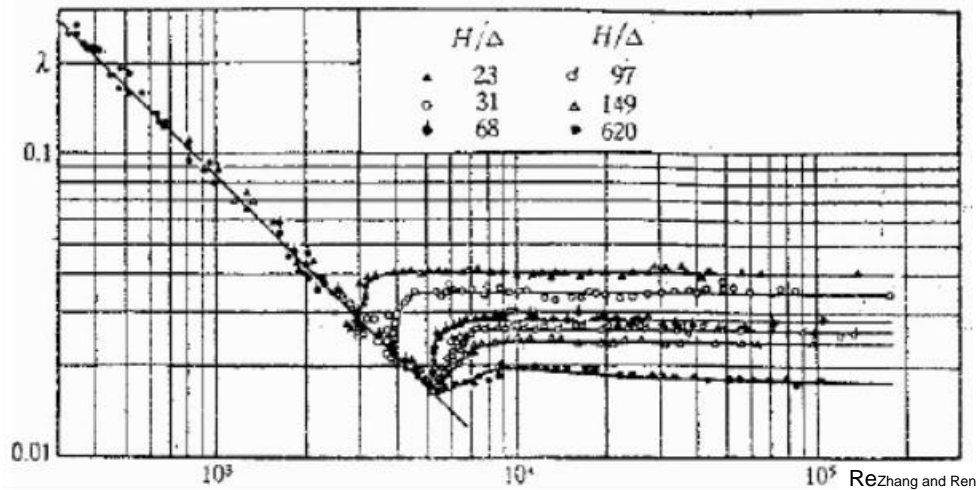


Figure 2.7: Friction factor vs. $Re_{\text{Zhang and Ren}}$ plot for a rectangular channel showing the effect of roughness upon laminar, transitional and turbulent flow (Zhang and Ren, 1982)

Naik (1983) performed tests on kaolin slurries of different concentrations in a rectangular tilting flume with a length of 12.2m and a 300 mm × 300 mm cross-section. The kaolin slurries did exhibit a Bingham plastic behaviour over concentrations of 8.6 to 22.2% by volume. The yield stress and the plastic viscosity of the slurries tested was measured and checked on a daily basis by means of a Fann coaxial cylinder viscometer. The tests flow rates varied from 0.3 to 12.5 l/s, the flow depths from 12 to 122 mm and the flume slopes from 0.38 to 2.29°.

Cousot (1994) tested clay-water suspensions of different concentrations in trapezoidal and rectangular shaped flumes which could be tilted at angles from the horizontal up to a maximum slope of 65%. The width of the rectangular flume could be varied up to 0.6 m with a fixed length of 8 m. The walls of the channel were either smooth (plywood) or rough (metal with a roughness height of 6 mm).

Sanders *et al.* (2002) conducted their research at the Saskatchewan Research Council (SRC) in Saskatoon on the laminar open channel flow of non-Newtonian fine particles slurries containing coarse solids. These idealised thickened tailings slurries consisted of kaolin clay, polymer flocculant and coarse solids. The former were tested to determine whether these so-called non-segragating slurries could continue to be characterised as such in laminar open channel flow.

The friction factors obtained from tests conducted with clay slurry and the flocculant-based slurry were found to be in reasonable agreement with the friction factors predicted using the

laminar flow equation of $f=16/Re_{Zhang}$ and Re_n . This is shown in Figure 2.8 with a maximum error of $\pm 30\%$.

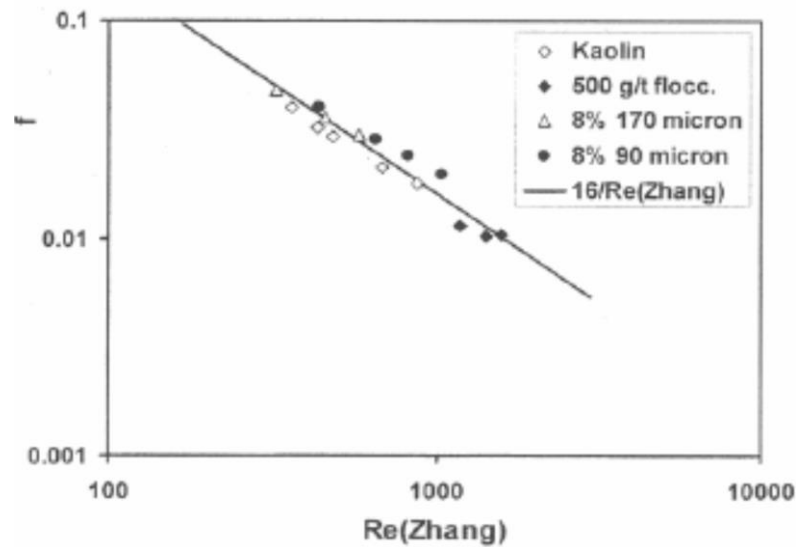


Figure 2.8: Friction factors for idealised tailings slurries flowing in the SRC 150 mm flume

Fitton (2008) established a method to predict the transitional flow in semi-circular channels at a single point rather than over a range of Reynolds numbers. The experiments were run in 5.4 m length pipe with a 50 mm internal diameter. The data obtained from his experiments is presented in Figure 2.9 on a f vs. Re_H plot.

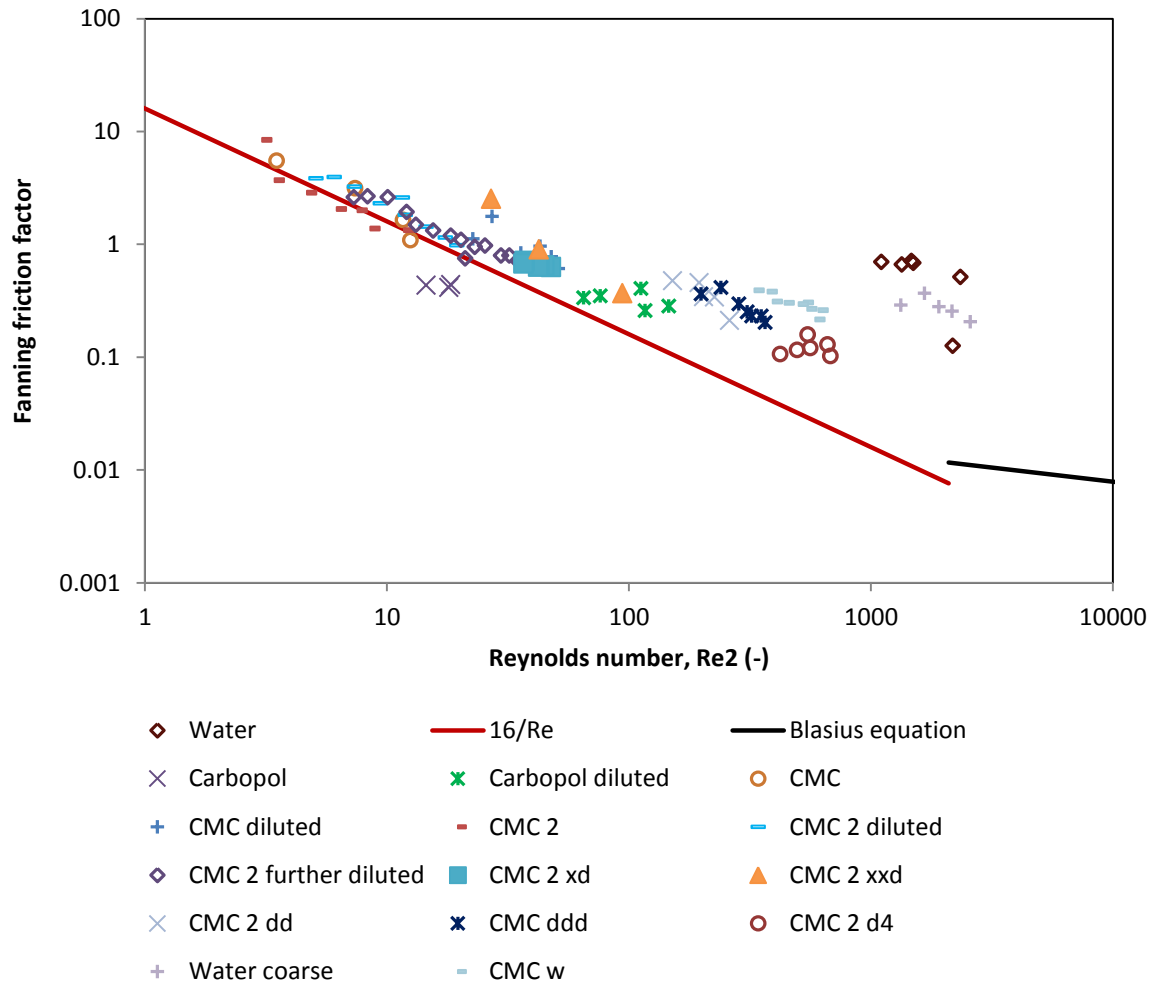


Figure 2.9: Fitton's small flume experimental data

The experimental data obtained by Haldenwang (2003) and Burger *et al.* (2010) are presented in Chapter 3 from Figure 3.7 to 3.10.

2.9 Availability of data in the literature

- Coussot (1994) conducted experiments using kaolin suspensions as his test material, which he characterised as a Herschel-Bulkley fluid. For the concentrations used, he fitted all his data by fixing the value of n to 0.333. The experimental data set published by Coussot (1994) lies in the laminar flow regime since he used very viscous materials. Therefore his data cannot be used in this work to predict the onset of transitional flow.
- Haldenwang (2003) and Haldenwang and Slatter (2006) published a large experimental database for non-Newtonian open channel flow. The experiments were conducted in three rectangular tilting flumes of various widths varying from 75 to 300

mm. The test materials used were kaolin and bentonite suspensions as well as carboxymethyl cellulose solutions, all at different concentrations. The rheological characterisation of the fluids was done in an inline tube viscometer with three different tube diameters.

- Seckin *et al.* (2006) collected experimental data by using a 22 m long tilting rectangular flume with a width of 398 mm. Water was used as the testing material. The flume was set at a fixed slope of 2.024×10^{-3} .
- Fitton (2008) used a 10 m tilting flume with two semi-circular cross-sections of diameters 340 and 415 mm to collect his experimental data containing 49 points. He tested thickened slurries at two separate mine sites, with concentrations ranging between 25 and 68% by weight. The inclination of the flume was varied from 0.0075 to 0.06. The rheological characterisation was done using a cup and bob rheometer (Fitton *et al.*, 2006). He referred to this set of data as “field flume data”.
- Fitton (2008) also used experimental data published by Haldenwang *et al.* (2006) consisting of 623 points as well as the data published by Seckin *et al.* (2006) consisting of 9 points. Fitton (2008) used another set of his own data containing 95 points published by Fitton (2007). This data set was collected in a 5.4 m long glass flume of circular cross-section, with an internal cross-section of 50 mm. Fluids tested included water, Carbopol solutions of two different concentrations and Carboxymethyl cellulose (CMC) solutions of 11 concentrations. The flume slopes were varied between 0.2 and 7.7%. He referred to this set of data as “small flume data”.
- Burger *et al.*, (2010) extended the database published by Haldenwang and Slatter (2006) for the flow on non-Newtonian flow in rectangular open channels to include the test work on kaolin and bentonite in water slurries as well as CMC solutions in flumes of trapezoidal, semi-circular and triangular cross-sections.
- Guang (2011) conducted his experimental studies in a 4 m long pipe with an internal diameter of 50 mm. The flume could be tilted up to 6° from the horizontal. The test material consisted of Carboxymethyl cellulose (CMC) solution at various concentrations. Guang (2011) obtained a limited range of experimental data which cannot be included in this work as it does not fully cover the laminar, transition and turbulent flow regimes. Guang (2011) also used experimental data published by Fitton (2007) as well as the data published by Haldenwang (2003).

There are a number of models in the literature which can be used to predict transitional flow in open channels of different shapes. However, there is limited experimental data which covers the transitional flow regime.

2.10 Conclusion

The flow behaviour in open channels for both Newtonian and non-Newtonian fluids has been described as it plays an important role in the analysis of predicting laminar-turbulent transition. The various criteria used for predicting the onset of transitional and turbulent flow for Newtonian and non-Newtonian fluids were introduced and described. A summary of various models available in literature for the prediction of the laminar-turbulent transition of non-Newtonian fluids in open channels are presented in Table 2.4.

Haldenwang (2003) established a new model for predicting the onset of transition and the onset of turbulence (or end of transition). He stated that the flow behaviour could be characterised by the Froude number and the Reynolds number.

Slatter (2013a, 2013b) established the transitional flow criterion as $Re_4 = 700$ by using a normalised adherence function which was defined as the wall shear stress ratio.

Hao and Zhengai (1980) and Haldenwang (2003) proposed a similar model for the prediction of Bingham plastic fluids in open channels.

Coussot (1997) based his work on the Hanks criteria (1963) and developed a model that can be used to predict the onset of turbulence for mudflow, which he characterised as a Herschel Bulkley fluid with a fixed n value of $1/3$.

Haldenwang (2003) developed a model for the prediction of the onset and end of laminar turbulent transition for the rectangular open channel shape. His methodology was used here to develop other models for transitional flow through open channels of trapezoidal, semi-circular and triangular shape.

From the literature review, it can be seen that very few researchers conducted open channel work on the transitional flow regime. Much of their research tended to be confined to one material, one flume shape and slope with the exception of Haldenwang (2003) who used three different materials, five slopes but only one flume shape and Burger *et al.* (2010b) who produced experimental data covering all the flow regimes in triangular, trapezoidal and semi-circular flumes. It is therefore necessary to evaluate all the models and to modify/develop a model that can predict transitional velocities for all channel shapes.

CHAPTER 3

Chapter 3: Methodology used for data analysis

This chapter describes the procedure used to analyse the data. Experimental data obtained from two sources; one published by Haldenwang (2003) and Haldenwang and Slatter (2006) for a rectangular shaped channel and the other by Burger *et al.* (2010) for trapezoidal, semi-circular and triangular shaped channels was used. No experimental work was conducted by the author as the existing experimental work offered sufficient experimental data that was not specifically analysed to determine the effect of the shape of the channel when designing open channels.

3.1. Flow behaviour

The data depicting the non-Newtonian open channel flow was presented by Chow (1959) in the form of a Moody chart where the Fanning friction factor is plotted against the Newtonian Reynolds number, allowing laminar, transitional or turbulent flow regimes to be identified.

For the laminar flow, the K/Re line was used to predict the flow. The K -values empirically derived for various channel shapes by Burger *et al.* (2010) were used. The Blasius equation, as used by (Haldenwang, 2003) was used for the turbulent flow regime. The appropriate Reynolds number for non-Newtonian fluids was used throughout. The laminar-turbulent transition regime is depicted from where the data deviates from the K/Re line (-1 slope) to the start of the Blasius line (-0.25 slope). For Newtonian fluids, the laminar-turbulent transition occurs between $2000 < Re < 3000$. For non-Newtonian fluids, transitional flow occurs at much lower Reynolds numbers which depend on the flume slope and the viscous properties. In the laminar-turbulent transition region, the flow regimes are mixed, which indicates the end of laminar flow behaviour and the onset of turbulent flow. However, the point where the onset of turbulent flow occurs is not easily depicted on the Moody diagram.

These flow regions are analysed separately for each channel shape for various materials at different slopes as illustrated in Figure 3.1.

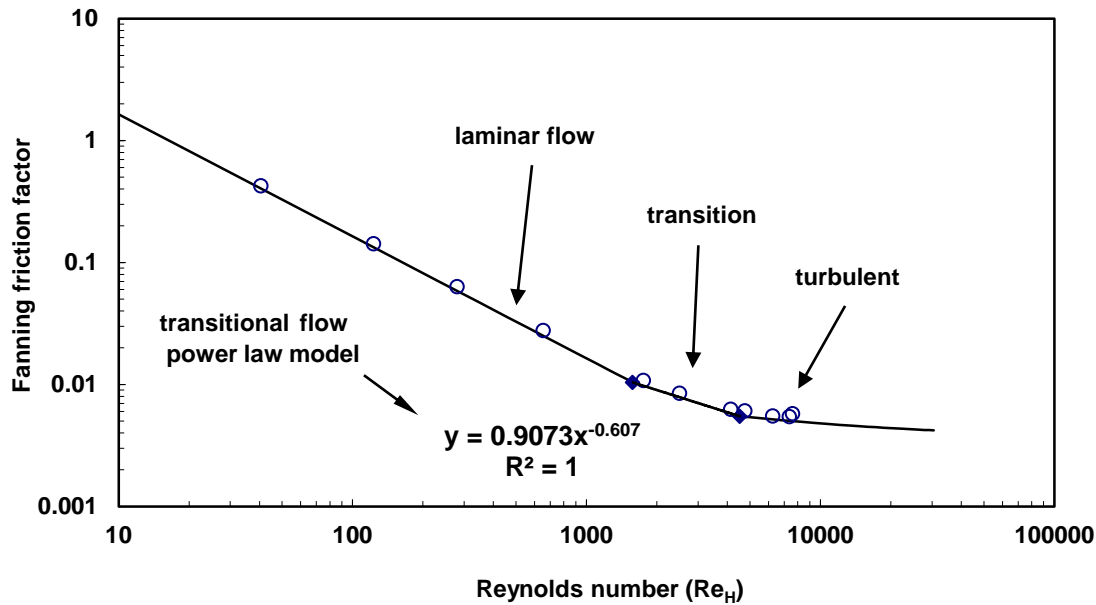


Figure 3.1: 6% kaolin suspension flowing in a rectangular channel set at 3 degrees slope

The models evaluated in this work are applicable to power law, Bingham plastic and yield shear-thinning (Herschel-Bulkley) fluids in the laminar-turbulent transition regime. A summary of various models available in literature for the prediction of the laminar turbulent transition of non-Newtonian fluids in open channels was presented in Table 2.4.

3.2. Critical velocity

The critical velocity was evaluated by plotting the Normalised Adherence Function (NAF) against the Froude number.

The NAF is the ratio of the experimental Reynolds number to the theoretical one for laminar flow. This ratio should be one (Slatter & Wasp, 2000). Transitional flow occurs when the NAF value starts to deviate from unity. Therefore the critical velocity is determined by finding the corresponding velocity value in the experimental data. The critical velocity is used to compare the accuracy of the theoretical approaches or models.

Figure 3.2 illustrates how the critical velocity is established by plotting the NAF against the Froude number. This value is also checked on the Moody diagram to see if this point also starts to deviate from the laminar flow line.

In order to evaluate the models available in literature for the prediction of transitional non-Newtonian flow, a comparison of actual velocities with models' velocities was conducted.

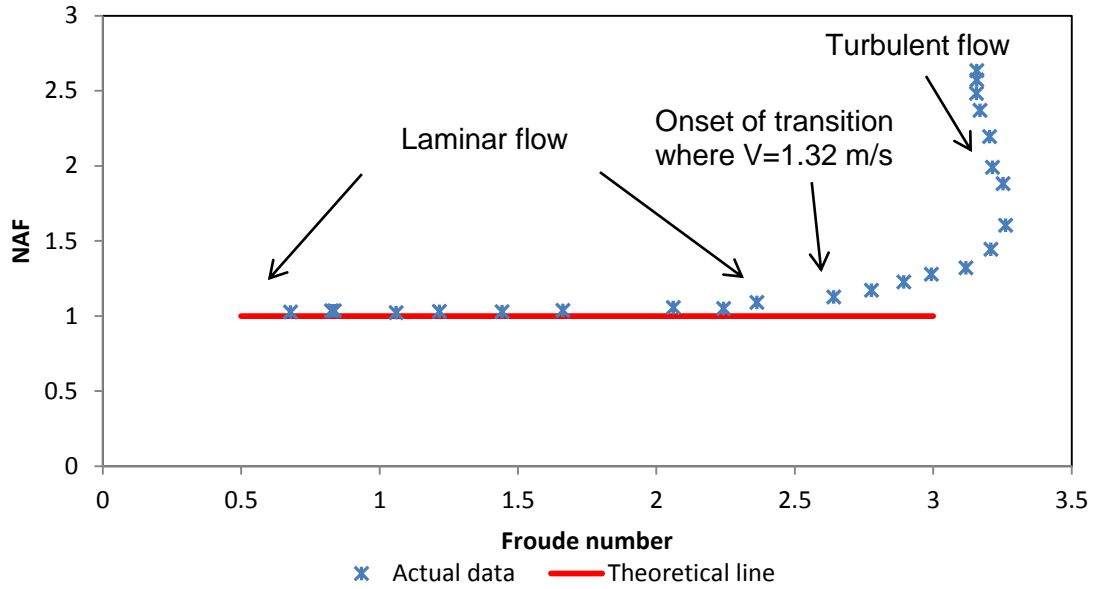


Figure 3.2: 7.1% kaolin suspension flowing in a 150 mm trapezoidal channel set at 4 degrees slope

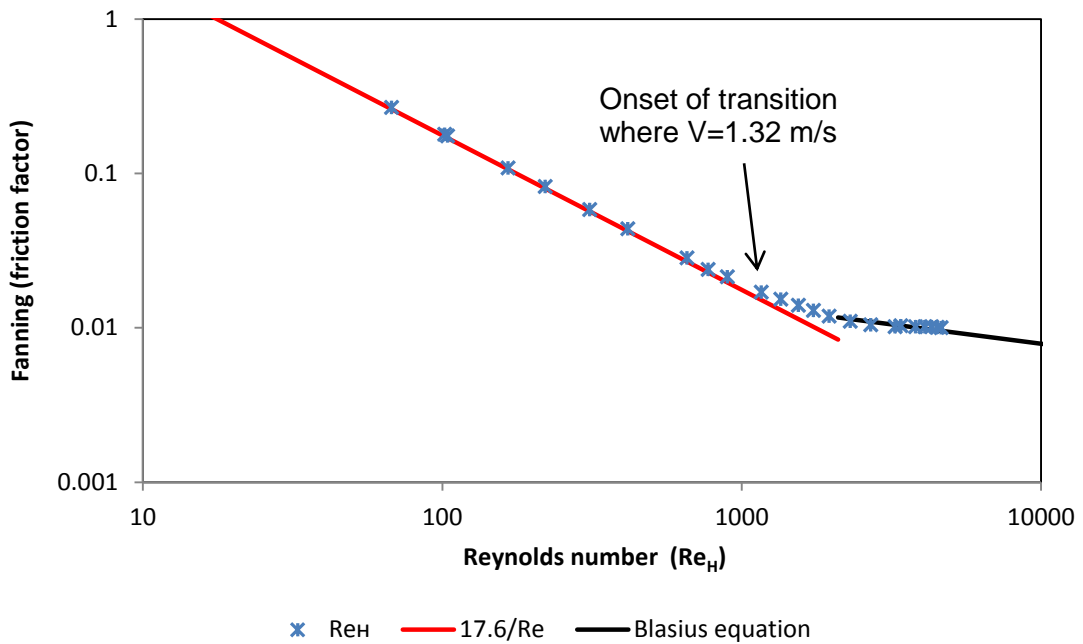


Figure 3.3: 7.1% kaolin suspension flowing in a 150 mm trapezoidal channel set at 4 degrees slope

It can be seen from both Figure 3.2 and Figure 3.3, that the deviation from the laminar flow region is similar on both graphs. This indicates that the onset of transition can be seen from both graphs.

The onset of turbulence is not easily identified on a Moody diagram; hence the NAF vs. Fr number plot was used and the onset of turbulent flow was found to occur at a point where the Fr was maximum.

The critical velocity which was found experimentally is compared with the transition velocity found using different predictions to check the accuracy of the approaches in predicting the transition for the various flume shapes evaluated in this thesis. Consequently, a statistical analysis has to be performed to determine the best critical velocity model.

3.3. Statistical analysis

The log standard error (LSE) method was used to perform a statistical analysis in this study.

The log standard error (Lazarus and Nielson, 1978) is defined as:

$$\text{LSE} = \frac{\sqrt{\sum (\log(V_{\text{obs}}) - \log(V_{\text{calc}}))^2}}{N - 1} \quad 3.1$$

The LSE in this study is based on the difference between the observed critical velocity and the calculated critical velocity using different critical Reynolds number models. The smaller the LSE values, the more accurate the model is.

The standard deviation σ is a measure of the amount of variation from the mean. A low value of standard deviation means that the data points are close to the average value and a high value of standard deviation is an indication of how large the spread of the data points is over the mean (Weiss, 2012).

The standard deviation is expressed as:

$$\sigma = \sqrt{\frac{1}{N - 1} \sum_{i=1}^N (x_i - \bar{x})^2} \quad 3.2$$

After comparison of various models, Haldenwang's model will be adapted as described in the next section to other shapes and a statistical analysis will be performed for the new models developed.

3.4. Adaptation of Haldenwang's (2003) model to other channel shapes

Haldenwang developed a model for the prediction of the onset and end of laminar-turbulent transition for the rectangular open channel shape. His methodology was used to develop other models for transitional flow through open channels of trapezoidal, semi-circular and triangular shapes.

He primarily used the Moody diagram to try to establish a relationship between the Reynolds number and the rheological parameters of the different fluids tested. Due to the complex nature of many rheological parameters, it was difficult to establish a relationship that encompassed all the parameters (Haldenwang, 2003).

Secondly, Haldenwang tried to establish a rheological parameter with the ability to characterise the fluids tested, which is known as the apparent viscosity (ratio of shear stress to shear rate at a given shear rate). This was done at shear rates of 50, 100, 200 and 500 s⁻¹. The apparent viscosity of the fluids tested exhibited some similarity at a shear rate of 100 s⁻¹.

He then plotted the Reynolds number against the Froude number to establish a relationship between the two, and found the relationship to be slope sensitive. Therefore the relationship between the two dimensionless numbers was plotted for 1° to 5° slopes and a linear relationship was found between the slopes as shown in Figure 3.4 at a shear rate of 100 s⁻¹ and in Figure 3.5 at a shear rate of 500 s⁻¹ (Haldenwang, 2003).

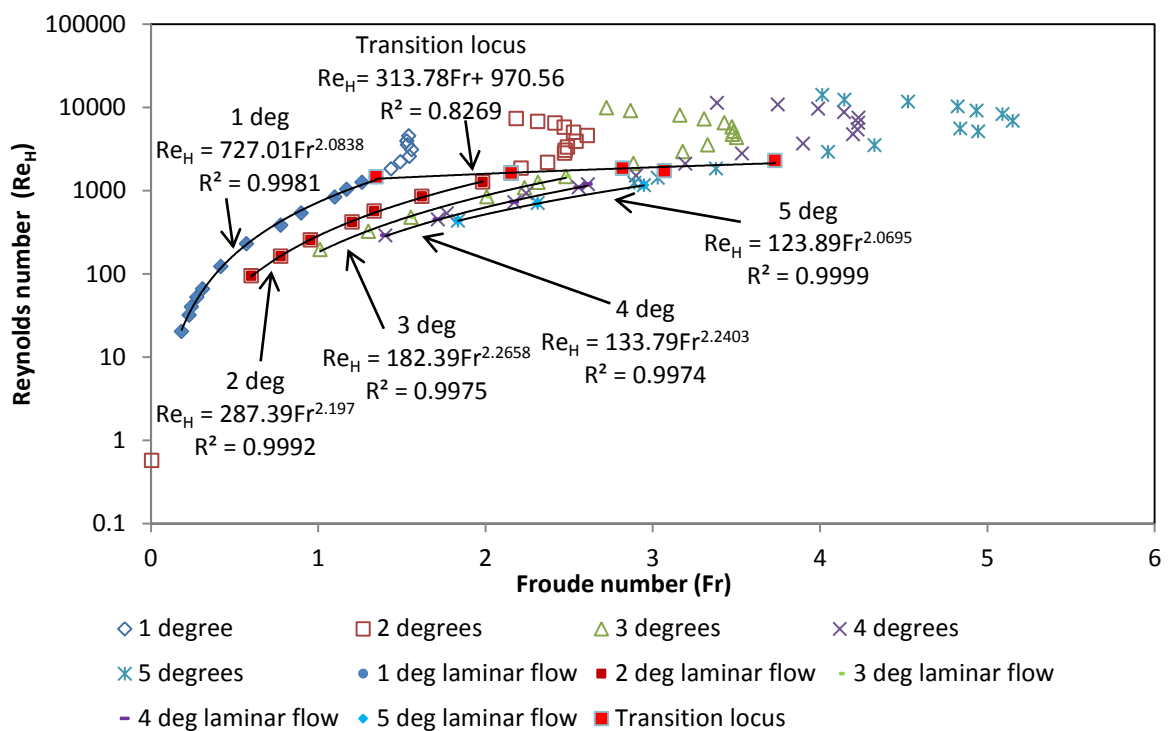


Figure 3.4: Onset of transition locus for 4.6% bentonite slurry in a 150 mm trapezoidal flume

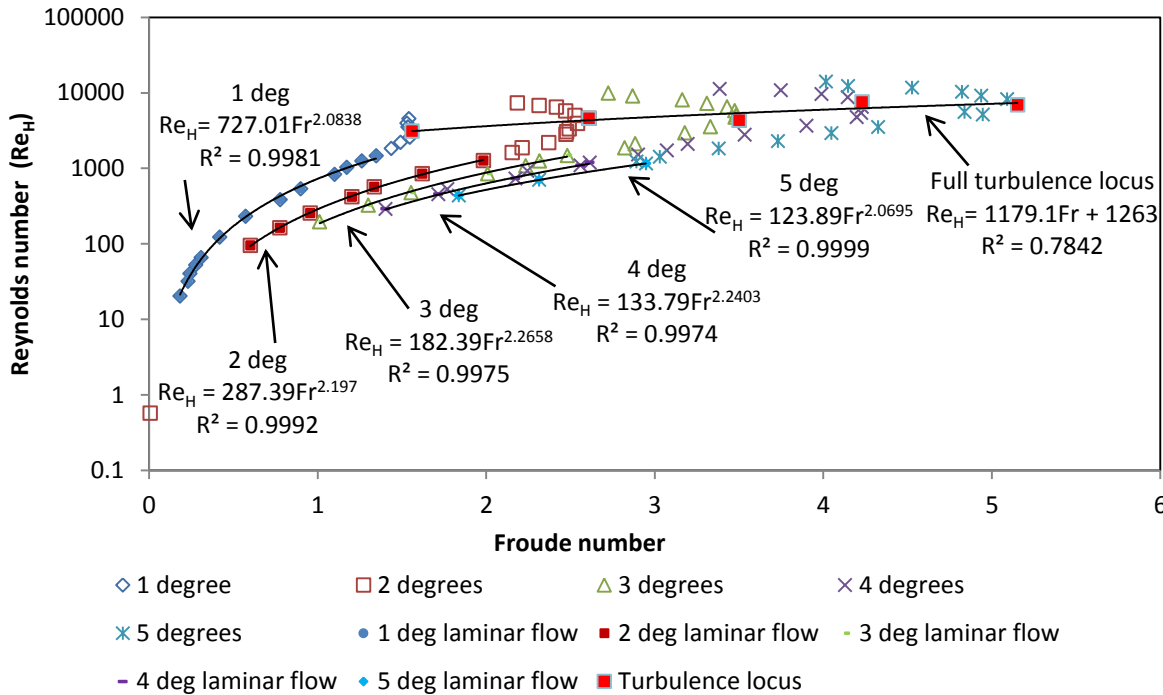


Figure 3.5: Onset of “full turbulence” for 4.6 % bentonite slurry in a 150 mm trapezoidal flume

The linear relationship was then plotted against the apparent viscosity. From there a critical Reynolds number predicting the onset of transition was determined using the Froude number. There was a linear relationship between the Froude and the Reynolds numbers for an apparent viscosity at a shear rate of 100 s^{-1} . The linear relationships and the new critical Reynolds number correlations are shown in Chapter 4.

Haldenwang's (2003) critical velocity model

The method used to obtain the critical velocities was described by Haldenwang (2003) and the numerical process is briefly described.

The material used to illustrate the procedure is a 5.3% CMC suspension flowing in a 150 mm semi-circular flume at a 5 degrees slope with the following properties:

| | |
|--------------------------------------|----------|
| Fluid consistency index (K) | 0.92 |
| Flow behaviour index (n) | 0.678 |
| Yield stress (τ_y) | 0 |
| Density (ρ) | 1028 |
| Apparent dynamic viscosity (100 1/s) | 0.209 |
| Apparent dynamic viscosity (500 1/s) | 0.124 |
| Slope (degrees) | 5 |
| Channel width (m) | 0.15 |
| Hydraulic roughness (m) | 0.000001 |
| Slope in radians (calculated) | 11.47 |

The Reynolds number used to describe laminar flow was defined by Equation (2.53). The Fanning friction factor was obtained by using Equation (2.24).

A Reynolds number (Re selected) was chosen first. Then, the friction factor in the laminar region was calculated using the relationship $f = K/Re$, where $K=16.2$ for semi-circular channels and Re is the chosen Reynolds number. The velocity V was calculated using Equation (2.24) with V as the subject of the equation. The friction factor obtained was also used in Equation (2.24) to calculate the velocity. The velocity obtained was used to compute the Haldenwang's Reynolds number $Re_{H\text{ calc}}$ (Equation (2.53)) as well as the Froude number. At this point, the Haldenwang's Reynolds number $Re_{H\text{ calc}}$ was different from the selected Reynolds number. Thus, the flow depth value was estimated and optimised until the selected Reynolds number was equal to the calculated Reynolds number. Then, the Froude number for semi-circular channels was calculated using Equation (2.5). From that, the critical Reynolds number Re_c (Equation (4.9)) was computed and this was different from the selected and calculated Reynolds numbers. Finally, the selected Reynolds number was optimized until the critical Reynolds number Re_c was equal to the Haldenwang's Reynolds number $Re_{H\text{ calc}}$ as shown in Table 3.1.

The onset of transition occurred at Reynolds number 439. At this point, lower Reynolds numbers can be chosen until the required velocities or depths are obtained. The corresponding critical velocity was 1.02 m/s.

Table 3.1: Determination of laminar flow in semi-circular flumes

| Depth m | V m/s | R_h m | Q l/s | Optimize Re | | Interval | Optimize Depth | |
|------------|--------------|------------|----------|----------------------|-------------|------------------------------|----------------|------------------|
| | | | | $Re_{H\text{ Calc}}$ | Re selected | f (fanning) $16.2/Re =$ | Froude number | Rec (transition) |
| 0.0135 | 0.095 | 0.0086 | 0.19 | 10 | 10 | 1.62 | 0.32 | 167 |
| 0.0198 | 0.231 | 0.0123 | 0.68 | 41 | 41 | 0.395 | 0.63 | 219 |
| 0.0230 | 0.329 | 0.0142 | 1.14 | 72 | 72 | 0.225 | 0.83 | 252 |
| 0.0254 | 0.412 | 0.0156 | 1.57 | 103 | 103 | 0.157 | 0.99 | 278 |
| 0.0274 | 0.485 | 0.0167 | 1.99 | 134 | 134 | 0.121 | 1.12 | 299 |
| 0.0290 | 0.553 | 0.0176 | 2.41 | 165 | 165 | 0.0982 | 1.24 | 319 |
| 0.0305 | 0.616 | 0.0183 | 2.82 | 196 | 196 | 0.0827 | 1.35 | 336 |
| 0.0318 | 0.675 | 0.0190 | 3.22 | 227 | 227 | 0.0714 | 1.44 | 352 |
| 0.0330 | 0.732 | 0.0197 | 3.62 | 258 | 258 | 0.0628 | 1.53 | 367 |
| 0.0341 | 0.786 | 0.0202 | 4.02 | 289 | 289 | 0.0561 | 1.62 | 381 |
| 0.0351 | 0.838 | 0.0208 | 4.41 | 320 | 320 | 0.0506 | 1.70 | 394 |
| 0.0361 | 0.888 | 0.0213 | 4.80 | 351 | 351 | 0.0462 | 1.77 | 407 |
| 0.0370 | 0.936 | 0.0217 | 5.19 | 382 | 382 | 0.0424 | 1.85 | 418 |
| 0.0378 | 0.983 | 0.0222 | 5.57 | 413 | 413 | 0.0392 | 1.92 | 430 |
| 0.0385 | 1.021 | 0.0225 | 5.89 | 439 | 439 | 0.0369 | 1.97 | 439 |

The turbulent flow region was first established before the end of transitional flow could be established.

To determine turbulent flow, a deeper depth than the depth at the onset of transitional flow was chosen. The hydraulic radius (given in Table 2.1 for the semi-circular flume shape) was calculated. The velocity was calculated using Equation (2.80). From this velocity, the friction factor (Equation (2.81)) as well as the Reynolds numbers (Equation (2.53)) were calculated.

Before the final step was performed, the onset of “full turbulence” was established and was given by Equation (4.11). To determine the onset of “full turbulence”, the Froude number (Equation (2.5)) and the critical Reynolds number at the end of transitional flow (Equation (4.11)) were calculated.

Table 3.2: Determination of turbulent flow in semi-circular flumes

| Depth (selected) m | V m/s | R _h m | Q l/s | Optimize | | Calculate Interval | |
|--------------------------|----------|---------------------|----------|-----------------|-------------|--------------------|-----------------------|
| | | | | Re _H | f (Fanning) | Froude number | Re Full Turbulence |
| 0.0571 | 1.90 | 0.0310 | 16.26 | 1237 | 0.01789 | 2.94 | 1237 |
| 0.0617 | 2.01 | 0.0328 | 18.59 | 1386 | 0.01730 | 2.97 | 1247 |
| 0.0664 | 2.11 | 0.0346 | 21.03 | 1535 | 0.01680 | 3.00 | 1255 |
| 0.0710 | 2.21 | 0.0362 | 23.58 | 1685 | 0.01637 | 3.01 | 1260 |
| 0.0757 | 2.31 | 0.0377 | 26.23 | 1834 | 0.01600 | 3.02 | 1263 |
| 0.0803 | 2.40 | 0.0391 | 28.97 | 1982 | 0.01568 | 3.03 | 1265 |
| 0.0850 | 2.50 | 0.0404 | 31.80 | 2128 | 0.01540 | 3.04 | 1267 |
| 0.0896 | 2.58 | 0.0416 | 34.72 | 2273 | 0.01516 | 3.04 | 1269 |
| 0.0943 | 2.67 | 0.0428 | 37.72 | 2416 | 0.01495 | 3.05 | 1271 |
| 0.0989 | 2.75 | 0.0438 | 40.81 | 2557 | 0.01475 | 3.05 | 1272 |
| 0.1036 | 2.83 | 0.0448 | 43.97 | 2697 | 0.01458 | 3.06 | 1274 |
| 0.1082 | 2.91 | 0.0457 | 47.22 | 2835 | 0.01443 | 3.06 | 1275 |
| 0.1128 | 2.99 | 0.0466 | 50.54 | 2972 | 0.01428 | 3.06 | 1277 |
| 0.1175 | 3.06 | 0.0474 | 53.94 | 3108 | 0.01415 | 3.07 | 1278 |
| 0.1221 | 3.13 | 0.0482 | 57.41 | 3241 | 0.01404 | 3.07 | 1279 |
| 0.1268 | 3.21 | 0.0489 | 60.95 | 3374 | 0.01393 | 3.08 | 1280 |
| 0.1314 | 3.28 | 0.0496 | 64.56 | 3505 | 0.01383 | 3.08 | 1281 |
| 0.1361 | 3.34 | 0.0503 | 68.24 | 3635 | 0.01373 | 3.08 | 1282 |
| 0.1407 | 3.41 | 0.0509 | 71.99 | 3763 | 0.01365 | 3.09 | 1283 |
| 0.1454 | 3.48 | 0.0515 | 75.81 | 3890 | 0.01357 | 3.09 | 1284 |
| 0.1500 | 3.54 | 0.0521 | 79.69 | 4016 | 0.01349 | 3.09 | 1285 |

The end of transitional flow was found by optimising the depth until the Reynolds number was similar to the full turbulence Reynolds number as indicated in Table 3.2.

Once the Reynolds number and the friction factor were obtained at the onset and end of transitional flow, a power law relationship was established between the two points as shown in Figure 3.6.

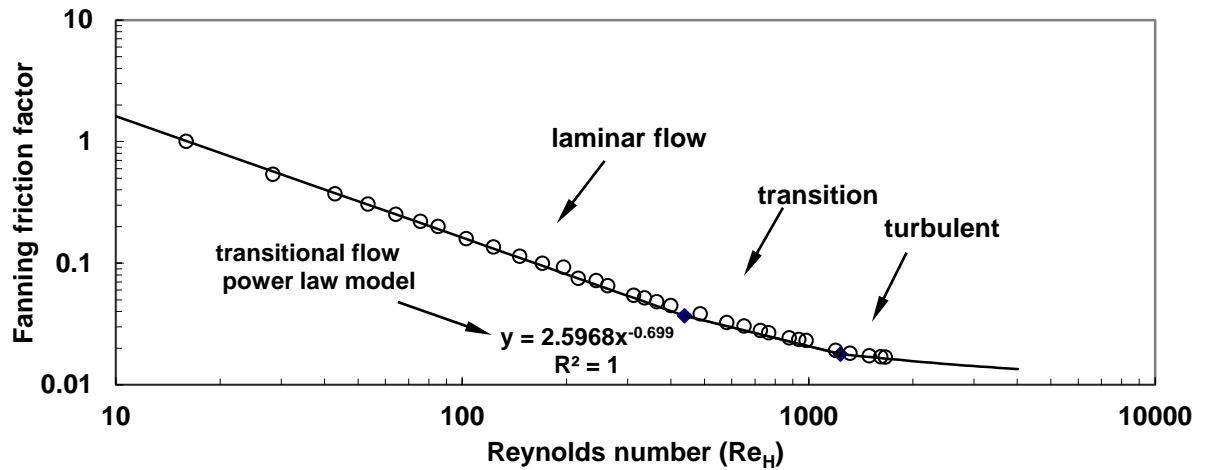


Figure 3.6: Moody diagram for 5.3% CMC in water solution flowing in a 150 mm semi-circular flume at 5 degrees slope

In the transition region, the relationship between the Reynolds number and the Fanning friction factor is defined by a power law model as follows:

$$f = \frac{2.5968}{Re^{0.70}} \quad 3.3$$

This relationship is valid between $Re=439$ and $Re=1237$.

Table 3.3: Determination of transitional flow in semi-circular flumes

| Depth m | V m/s | Rh m | Q l/s | Re = Calc | Re = selected | $f=2.5968 * Re^{-0.69}$ |
|------------|----------|---------|----------|-----------|---------------|-------------------------|
| 0.0385 | 1.02 | 0.0225 | 5.89 | 439 | 439 | 0.0369 |
| 0.0452 | 1.23 | 0.0257 | 8.31 | 612 | 612 | 0.0293 |
| 0.0518 | 1.43 | 0.0287 | 11.1 | 806 | 806 | 0.0242 |
| 0.0585 | 1.62 | 0.0315 | 14.2 | 1017 | 1017 | 0.0205 |
| 0.0652 | 1.81 | 0.0341 | 17.7 | 1237 | 1237 | 0.0179 |

Reynolds numbers can be manipulated in this region to obtain the required flow rates, velocities or flow depths as shown in Table 3.3.

Haldenwang (2003) and Burger *et al.* (2010) conducted experiments on the same flume rig in the Flow Process and Rheology Center at the Cape Peninsula University of Technology. An extract of the experimental studies carried out by Haldenwang (2003) and Burger *et al.*

(2010) in the field of non-Newtonian flow in open channels is presented next. This is done to illustrate the range of Reynolds numbers covered by the data in the laminar, transitional and turbulent flow regimes.

Haldenwang (2003) conducted his research in smooth rectangular channels of various sizes and covered the laminar, transitional and turbulent flow regions. An extract of the data obtained by Haldenwang (2003) for 3° slope is represented in Figure 3.7 for clarity.

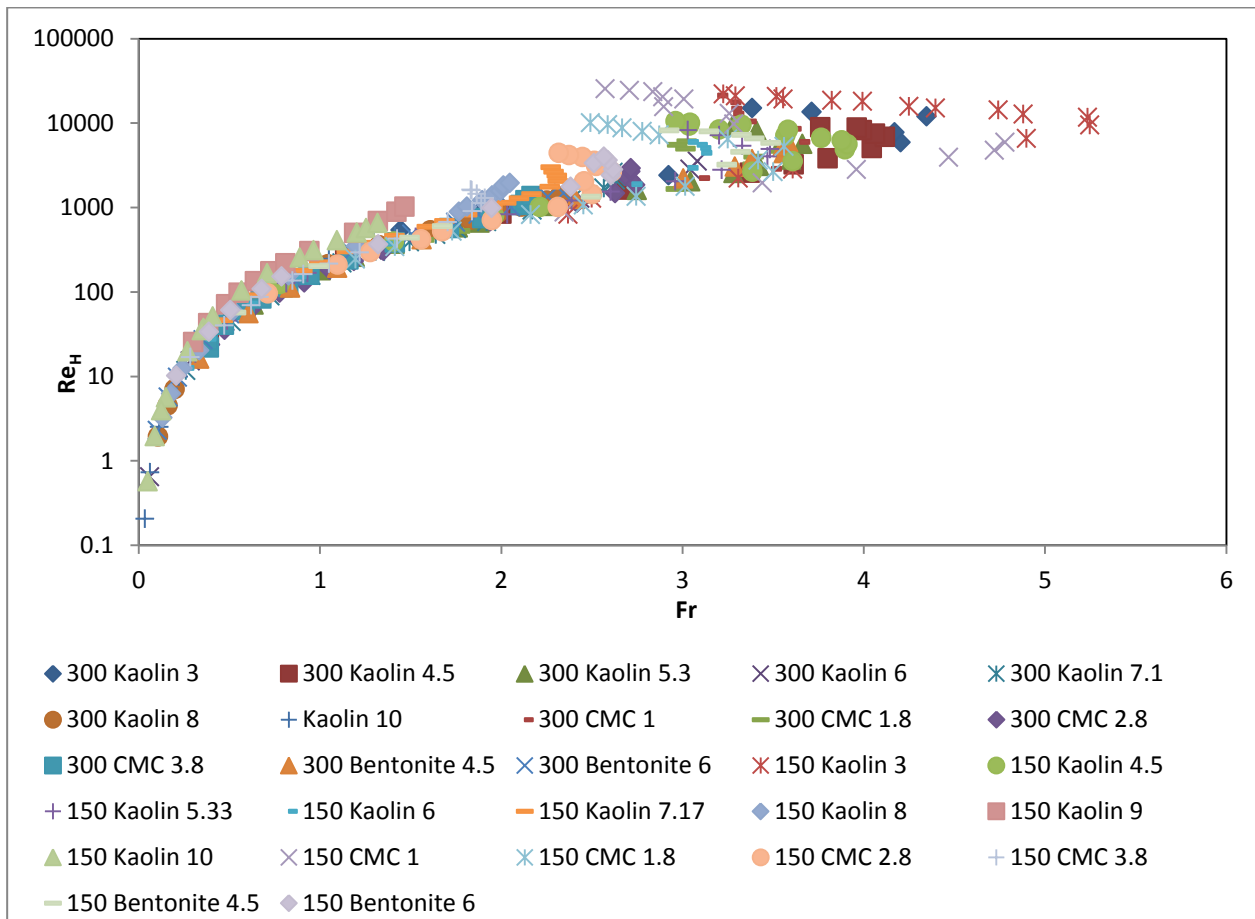


Figure 3.7: Rectangular flume experimental data at 3 degree slope

Burger *et al.* (2010) carried out experiments in smooth channels of triangular, semi-circular and trapezoidal shapes and the data for each respective shape for 3° slope are here presented from Figure 3.8 to Figure 3.10.

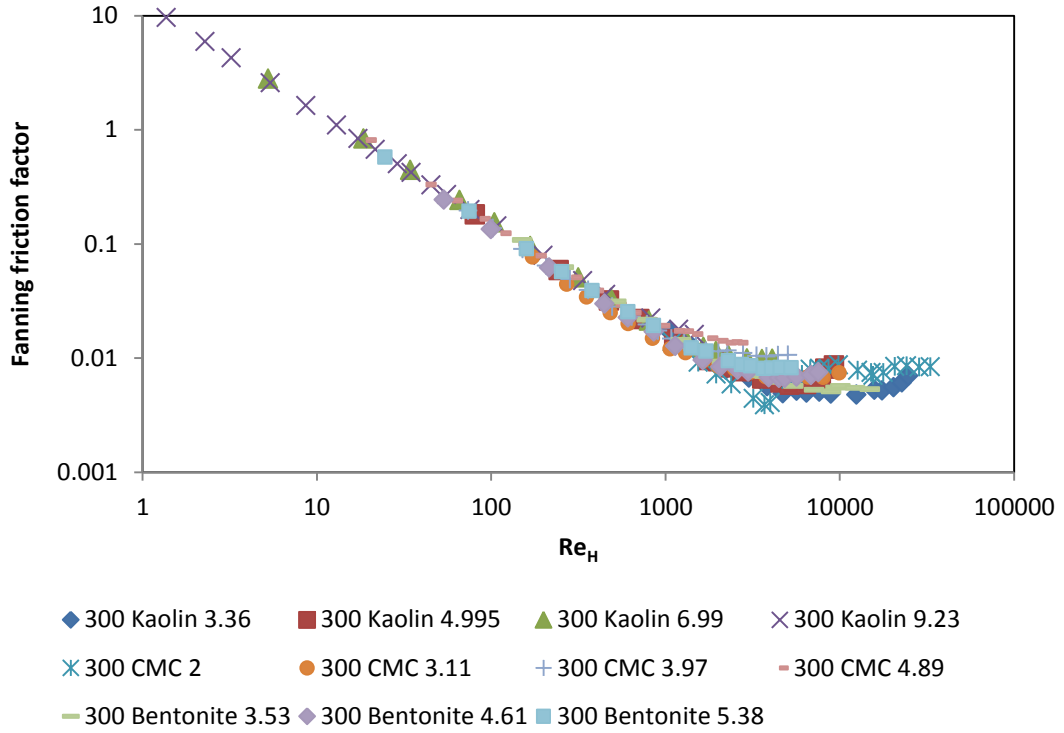


Figure 3.8: $A f$ vs. Re_H plot for experimental data in a triangular flume at a 3 degree slope

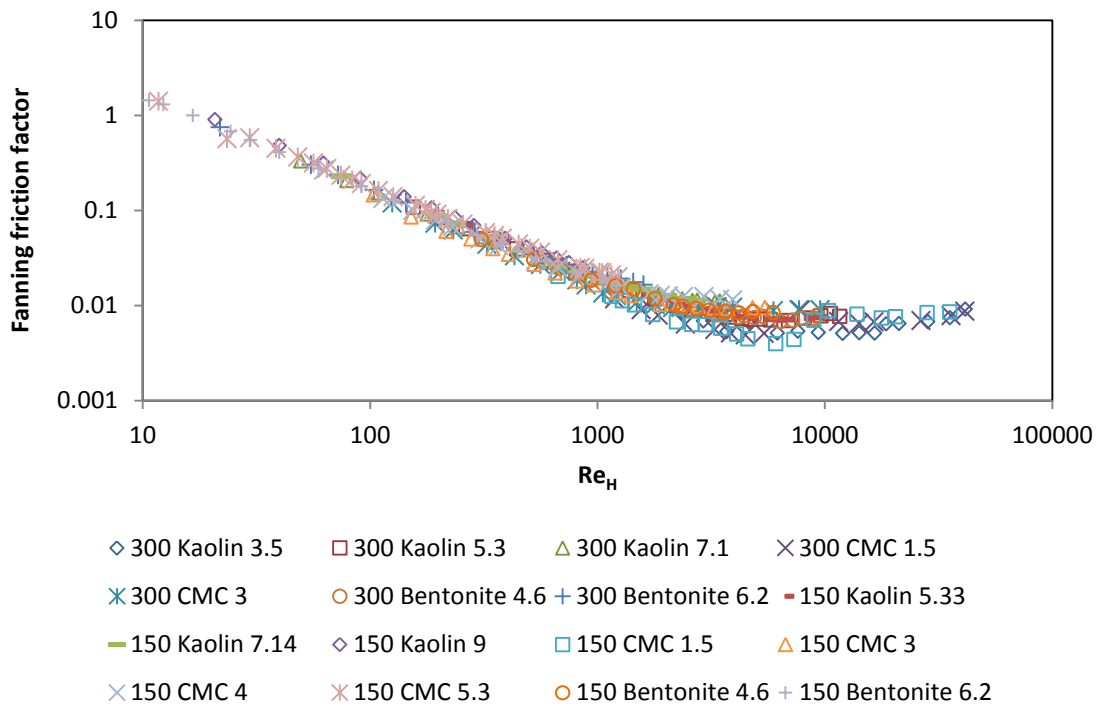


Figure 3.9: $A f$ vs. Re_H plot for experimental data in a semi-circular flume at a 3 degree slope

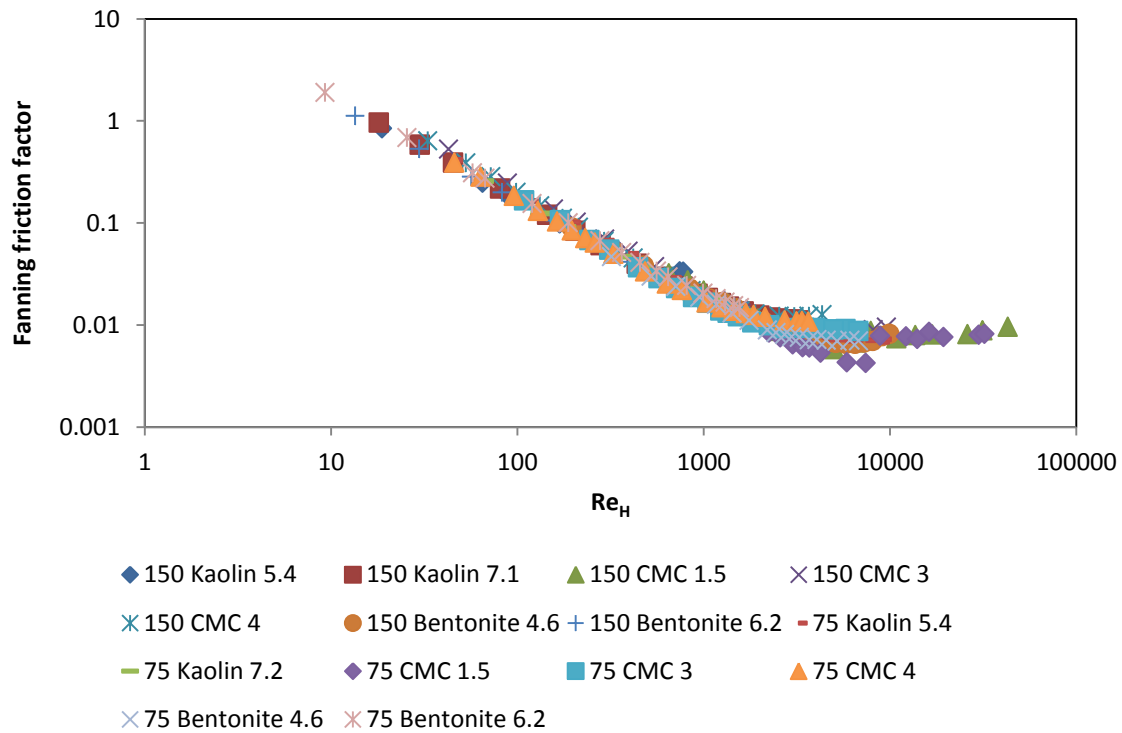


Figure 3.10: Af vs. Re_H plot for experimental data in a trapezoidal flume at a 3 degree slope

A matrix of the published work by various authors in terms of channel shapes, slopes, fluids and transitional flow models used is presented in Table 3.4.

Table 3.4: Summary of published work by various authors (transitional flow)

| Models | Fluids | | | Rectangular | Semi-circular | Trapezoidal | Triangular |
|--|--------|-----------|--------|-------------|---------------|-------------|------------|
| | CMC | Bentonite | Kaolin | | | | |
| Hao and Zhenghai (1980) | | • | | • | • | • | |
| Naik (1983) | | • | | • | | | |
| Cousot (1994) | | | • | • | | • | |
| Fitton (2008) use of Haldenwang's (2003) data | • | • | • | • | • | • | • |
| Re _H Rectangular Haldenwang et al. (2010) | • | • | • | • | • | • | • |
| Slatter (2013) | • | | • | • | | | |
| Re _H Semi-circular (This work) | • | • | • | | • | | |
| Re _H Trapezoid (This work) | • | • | • | | | • | |
| Re _H Triangular (This work) | • | • | • | | | | • |
| Re _H Combined (This work) | • | • | • | • | • | • | • |

In the next chapter, the analysis of the data published by Haldenwang (2003); Haldenwang and Slatter (2006) and Burger *et al.* (2010) given in Appendices A to D depending on the channel shape will be evaluated using different models, presented and discussed.

CHAPTER 4

Chapter 4: Haldenwang (2003) transitional flow models adapted for shape effect

4.1 Introduction

This chapter presents the Haldenwang (2003) critical Reynolds number for the onset and end of transition adapted for triangular, trapezoidal and semi-circular shapes. A combined model applicable to channels of rectangular, triangular, trapezoidal and semi-circular channels is also presented.

4.2 Triangular flume

The methodology used by Haldenwang (2003) for rectangular channels as described in Section 3.4 was used. A straight line relationship between the Reynolds and Froude numbers giving the slope and intercept for the viscosities at 100 s^{-1} and 500 s^{-1} was established from 1° to 5° slopes. To obtain the adapted critical Reynolds numbers, the slope (m) and the y-intercept (c) values were plotted against the apparent viscosities at a shear rate of 100 s^{-1} for the onset of transition and a shear rate of 500 s^{-1} for the end of transition. A shear rate of 100 s^{-1} was chosen since at that value the apparent viscosity was similar for various fluids in the region of the onset of transitional flow and a similar observation was noted at a shear rate of 500 s^{-1} for the onset of turbulent flow. Figure 4.1 shows the slope (m) against the apparent viscosity and the y-intercept (c) vs. the apparent viscosity is illustrated in Figure 4.2 for the onset of transition.

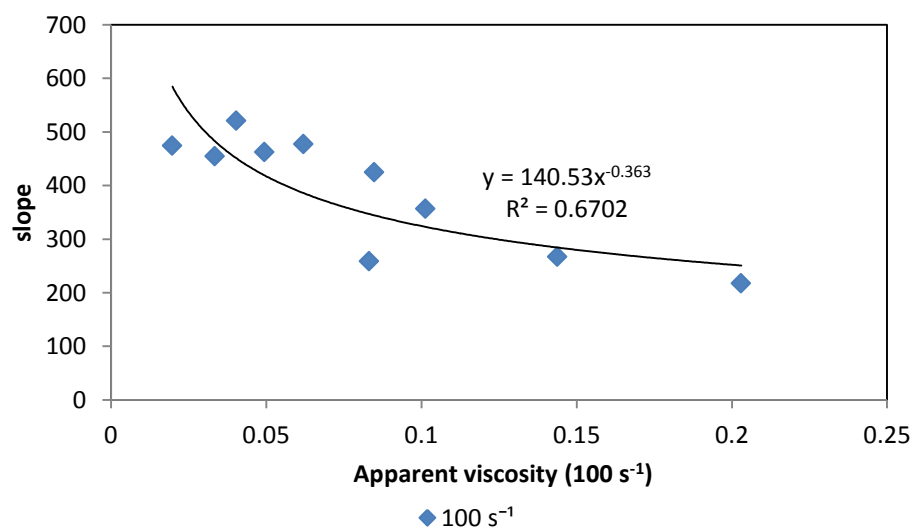


Figure 4.1: Onset of transition locus – relationship of m -values with apparent viscosity at 100 s^{-1} for all fluids flowing in a 300 mm triangular flume

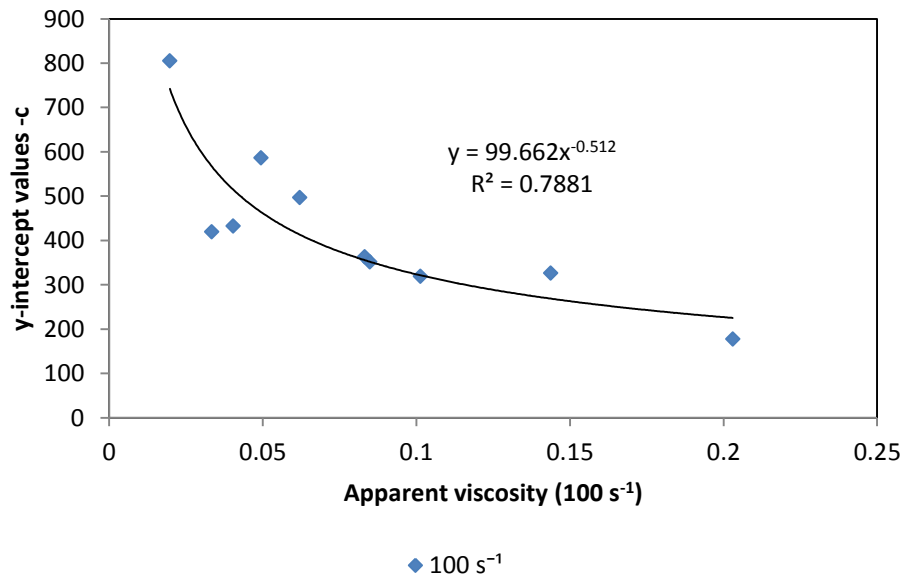


Figure 4.2: Onset of transition locus – relationship of y-intercept values with apparent viscosity at 100 s⁻¹ for all fluids flowing in a 300 mm triangular flume

From the relationships given in Figures 4.1 and 4.2 a critical Reynolds number for predicting the onset of transitional flow in triangular channels was established using the Froude number as the dependent variable, the power law equation in Figure 4.1 as the slope and the power law equation in Figure 4.2 as the intercept of Equation (4.1). The same procedure was used for the equations developed for the other shapes.

The adapted critical Reynolds number for the onset of transitional flow in a triangular flume is expressed as:

$$Re_c = 141(\mu | \dot{\gamma} = 100s^{-1})^{-0.36} Fr + 100(\mu | \dot{\gamma} = 100s^{-1})^{-0.51} \quad 4.1$$

The constant 141 has a unit of Pa.s^{0.36} and the constant 100, a unit of Pa.s^{0.51}.

The dimensionless form was obtained by dividing Equation (4.1) by the viscosity of water (10⁻³ Pa.s) at a shear rate of 100 s⁻¹ and is expressed as:

$$Re_c = 1695 \left(\frac{\mu}{\mu_w} | \dot{\gamma} = 100s^{-1} \right)^{-0.36} Fr + 3388 \left(\frac{\mu}{\mu_w} | \dot{\gamma} = 100s^{-1} \right)^{-0.51} \quad 4.2$$

where μ_w is the viscosity of water.

The critical Reynolds number for the onset of turbulent flow was obtained at a shear rate of 500 s^{-1} from the power-law relationships illustrated in Figures 4.3 and 4.4.

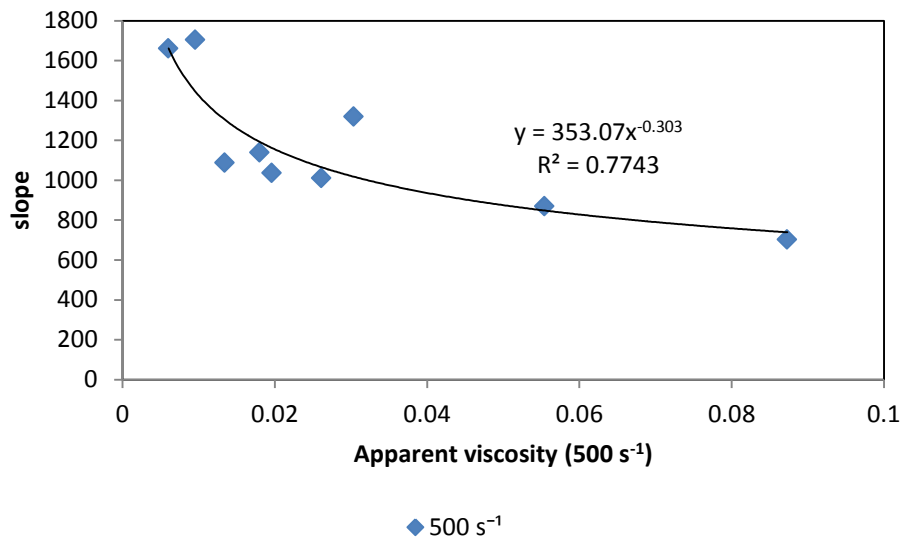


Figure 4.3: Onset of 'Full turbulence' locus – relationship of m-values with apparent viscosity at 500 s^{-1} for all fluids flowing in a 300 mm triangular flume

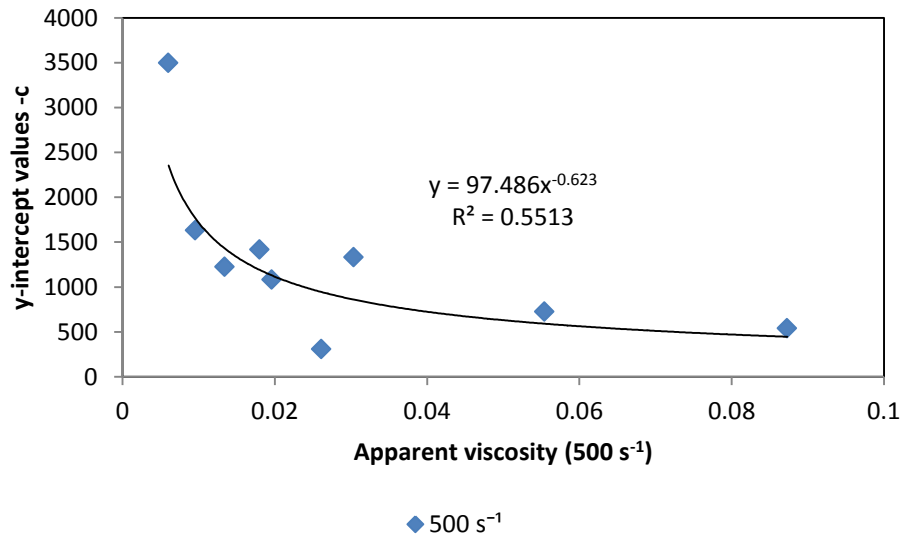


Figure 4.4: Onset of 'Full turbulence' locus – relationship of c-values with apparent viscosity at 500 s^{-1} for all fluids flowing in a 300 mm triangular flume

The adapted critical Reynolds number for the end of transitional flow in the triangular flume is as follows:

$$\text{Re}_c = 353 \left(\mu | \dot{\gamma} = 500 \text{s}^{-1} \right)^{-0.4} \text{Fr} + 97 \left(\mu | \dot{\gamma} = 500 \text{s}^{-1} \right)^{-0.62} \quad 4.3$$

The constant 353 has a unit of $\text{Pa}\cdot\text{s}^{0.4}$ and the constant 97, a unit of $\text{Pa}\cdot\text{s}^{0.62}$.

The dimensionless form of Equation (4.3) is written as:

$$\text{Re}_{c(\text{turb})} = 5595 \left(\frac{\mu}{\mu_w} | \dot{\gamma} = 500 \text{s}^{-1} \right)^{-0.4} \text{Fr} + 7027 \left(\frac{\mu}{\mu_w} | \dot{\gamma} = 500 \text{s}^{-1} \right)^{-0.62} \quad 4.4$$

The adapted triangular models for the onset and end of transitional flow were evaluated for a 3% CMC suspension flowing in a 300 mm triangular flume as shown in Figure 4.5.

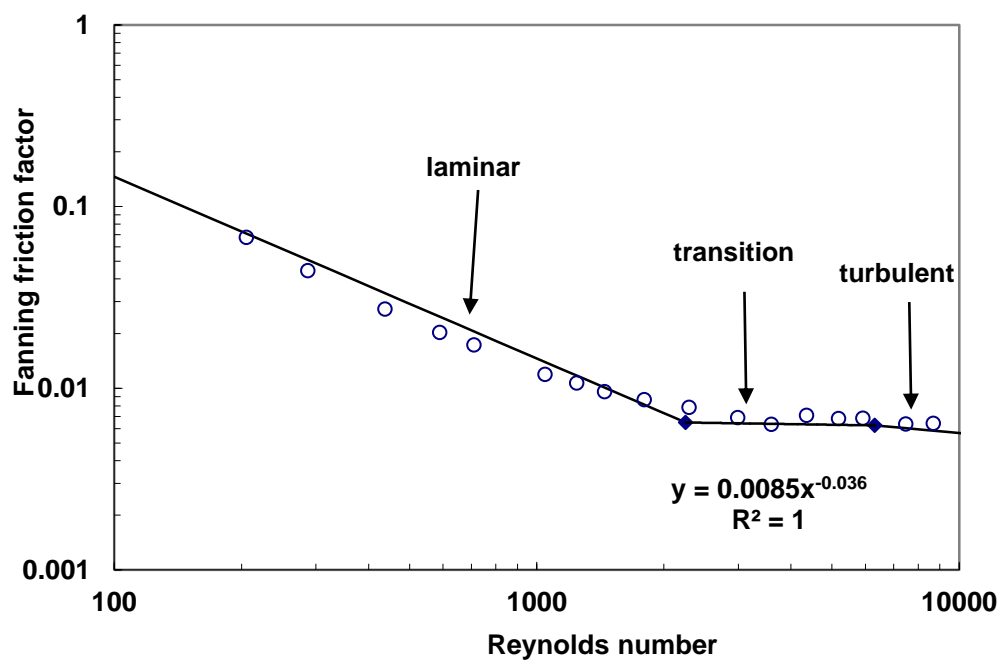


Figure 4.5: Evaluation of the adapted triangular models at the onset and end of transition

4.3 Trapezoidal flume

Figures 4.6 and 4.7 show the two relationships used to obtain the critical Reynolds number for the onset of transition in the trapezoidal flume.

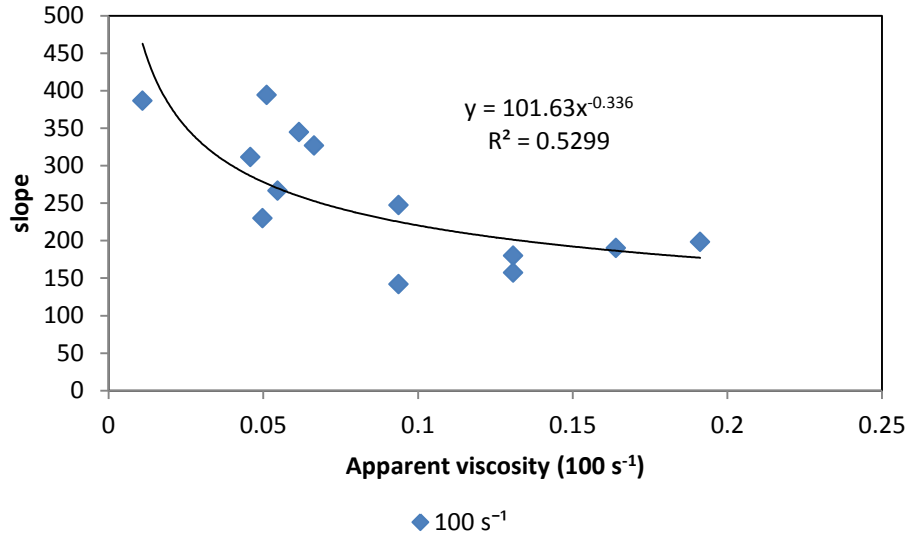


Figure 4.6: Onset of transition locus – relationship of m-values with apparent viscosity at 100 s⁻¹ for all fluids flowing in 75 and 150 mm trapezoidal flumes

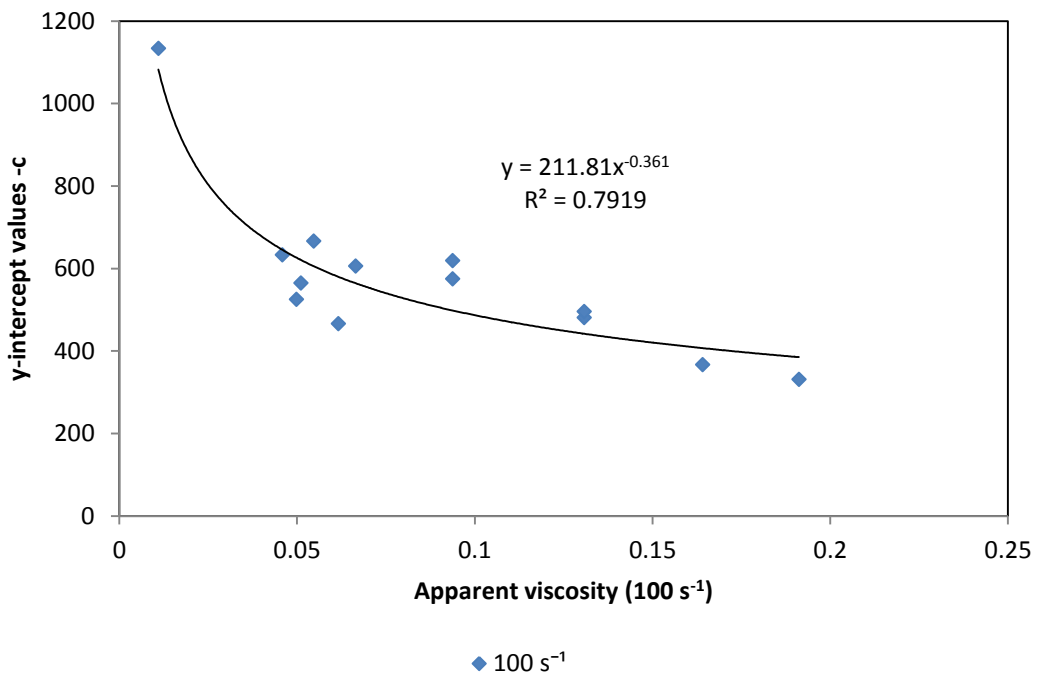


Figure 4.7: Onset of transition locus – relationship of y-intercept values with apparent viscosity at 100 s⁻¹ for all fluids flowing in 75 and 150 mm trapezoidal flumes

The critical Reynolds number for the onset of transition is expressed as:

$$Re_c = 102(\mu | \dot{\gamma} = 100s^{-1})^{-0.34} Fr + 212(\mu | \dot{\gamma} = 100s^{-1})^{-0.36}$$

4.5

The constant 1068 has a unit of $\text{Pa}\cdot\text{s}^{0.34}$ and the constant 212, a unit of $\text{Pa}\cdot\text{s}^{0.36}$.

Equation (4.5) is rewritten in a dimensionless form as:

$$\text{Re}_c = 1068 \left(\frac{\mu}{\mu_w} \mid \dot{\gamma} = 100\text{s}^{-1} \right)^{-0.34} \text{Fr} + 2545 \left(\frac{\mu}{\mu_w} \mid \dot{\gamma} = 100\text{s}^{-1} \right)^{-0.36} \quad 4.6$$

The two relationships obtained for the critical Reynolds number for the end of transition are shown in Figures 4.8 and 4.9.

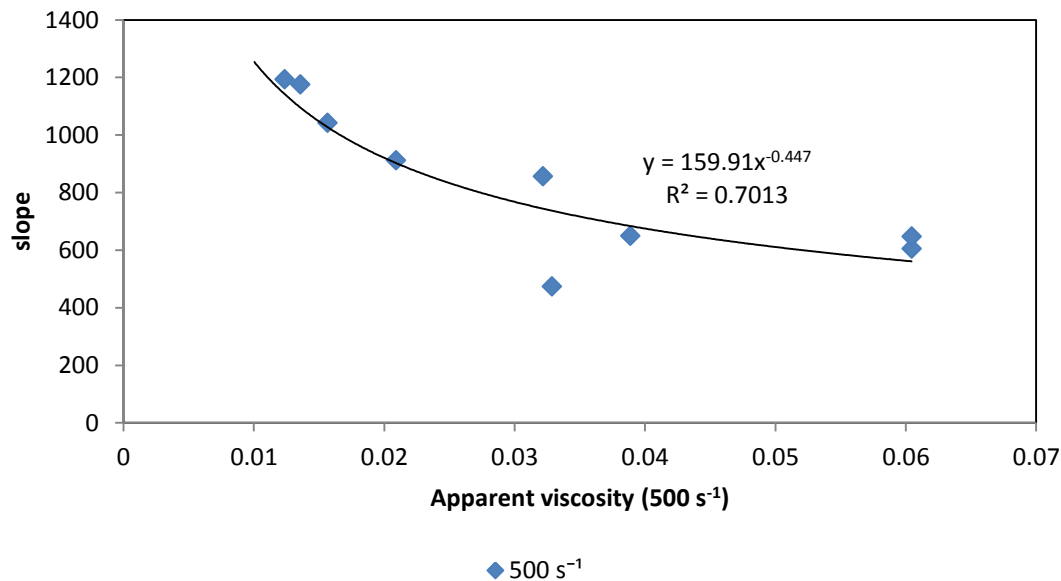


Figure 4.8: Onset of ‘Full turbulence’ locus – relationship of m-values with apparent viscosity at 500 s^{-1} for all fluids flowing in 75 and 150 mm trapezoidal flumes

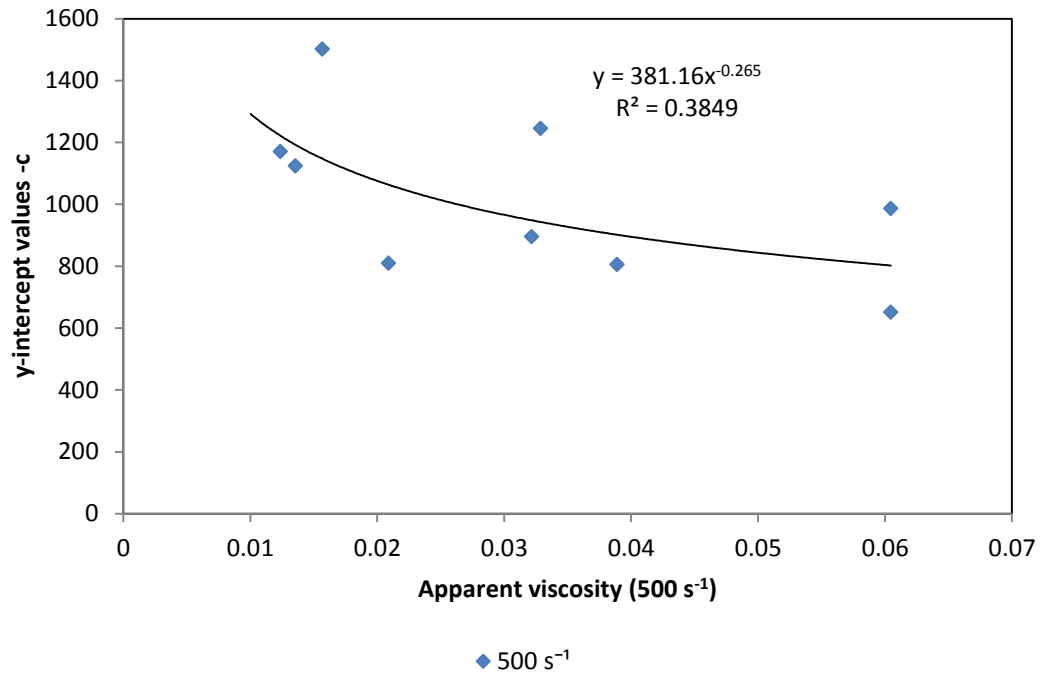


Figure 4.9: Onset of ‘Full turbulence’ locus – relationship of y-intercept values with apparent viscosity at 500 s⁻¹ for all fluids flowing in 75 and 150 mm trapezoidal flumes

The critical Reynolds number for the end of transition is expressed as:

$$Re_c = 160 (\mu | \dot{\gamma} = 500s^{-1})^{-0.45} Fr + 381 (\mu | \dot{\gamma} = 500s^{-1})^{-0.27} \quad 4.7$$

The constant 160 has a unit of Pa.s^{0.45} and the constant 381, a unit of Pa.s^{0.27}.

The dimensionless form of Equation (4.7) is defined as:

$$Re_{c(turb)} = 3582 \left(\frac{\mu}{\mu_w} | \dot{\gamma} = 500s^{-1} \right)^{-0.45} Fr + 2460 \left(\frac{\mu}{\mu_w} | \dot{\gamma} = 500s^{-1} \right)^{-0.27} \quad 4.8$$

An evaluation of the adapted trapezoidal models for the onset and end of transitional flow is illustrated in Figure 4.10 for a 4.6% bentonite slurry flowing in a 150 mm channel of trapezoidal shape.

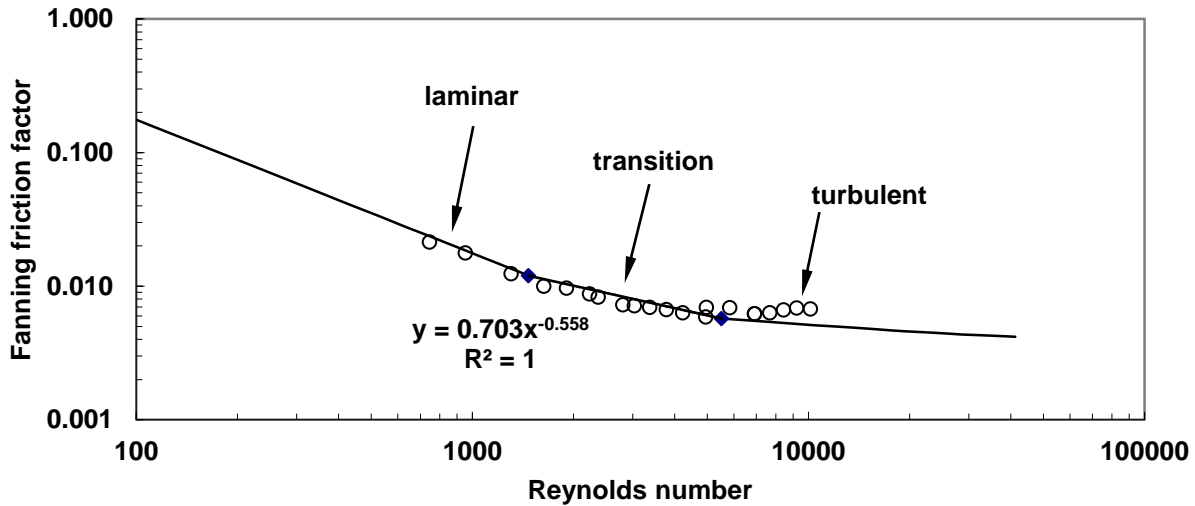


Figure 4.10: Evaluation of the adapted transition models for trapezoidal flume at the onset and end of transition

4.4 Semi-circular flume

The critical Reynolds number correlations on a semi-circular shaped flume were obtained from Figures 4.11 and 4.12.

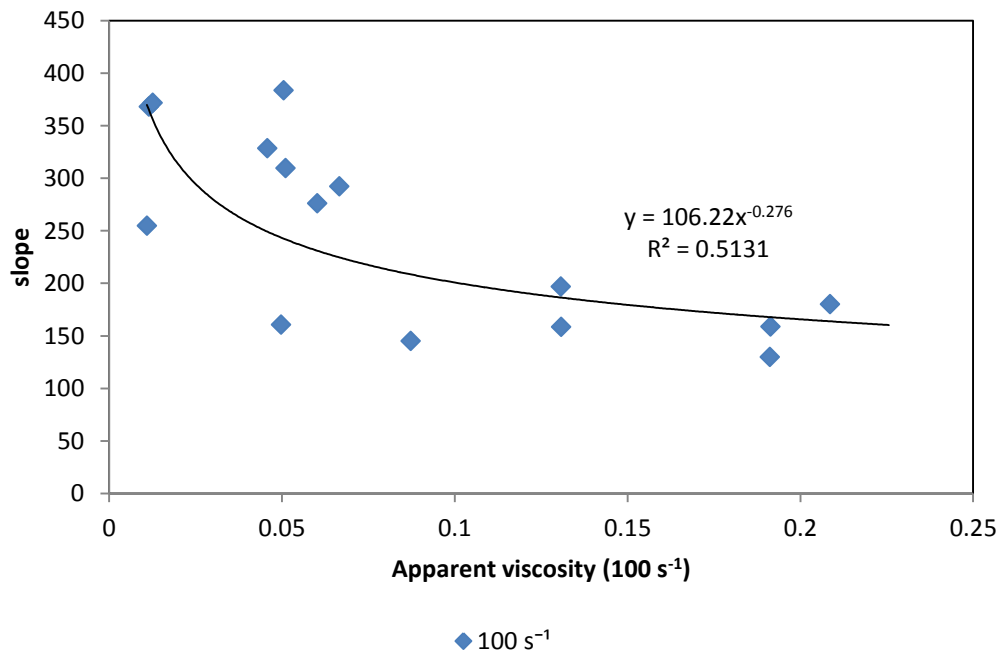


Figure 4.11: Onset of transition locus – relationship of m-values with apparent viscosity at 100 s^{-1} for all fluids flowing in 150 and 300 mm semi-circular flumes

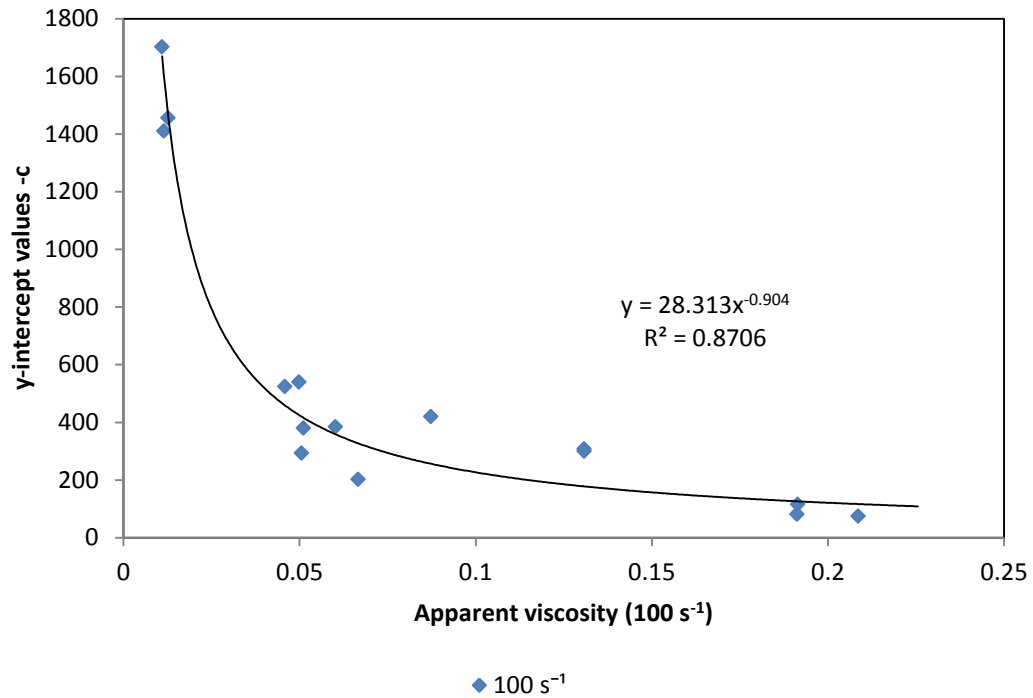


Figure 4.12: Onset of transition locus – relationship of c-values with apparent viscosity at 100 s⁻¹ for all fluids flowing in 150 and 300 mm semi-circular flumes

Thus, the adapted critical Reynolds number for the semi-circular flume is written as:

$$Re_c = 106 (\mu | \dot{\gamma} = 100s^{-1})^{-0.28} Fr + 28 (\mu | \dot{\gamma} = 100s^{-1})^{-0.9} \quad 4.9$$

The constant 106 has a unit of Pa.s^{0.28} and the constant 28, a unit of Pa.s^{0.9}.

The dimensionless form of the critical Reynolds number for the onset of transition in a semi-circular flume (Equation (4.9)) is expressed as:

$$Re_c = 733 \left(\frac{\mu}{\mu_w} | \dot{\gamma} = 100s^{-1} \right)^{-0.28} Fr + 14\,033 \left(\frac{\mu}{\mu_w} | \dot{\gamma} = 100s^{-1} \right)^{-0.9} \quad 4.10$$

Similarly, the critical Reynolds number for the onset of turbulent flow in the semi-circular flume was obtained from Figures 4.13 and 4.14.

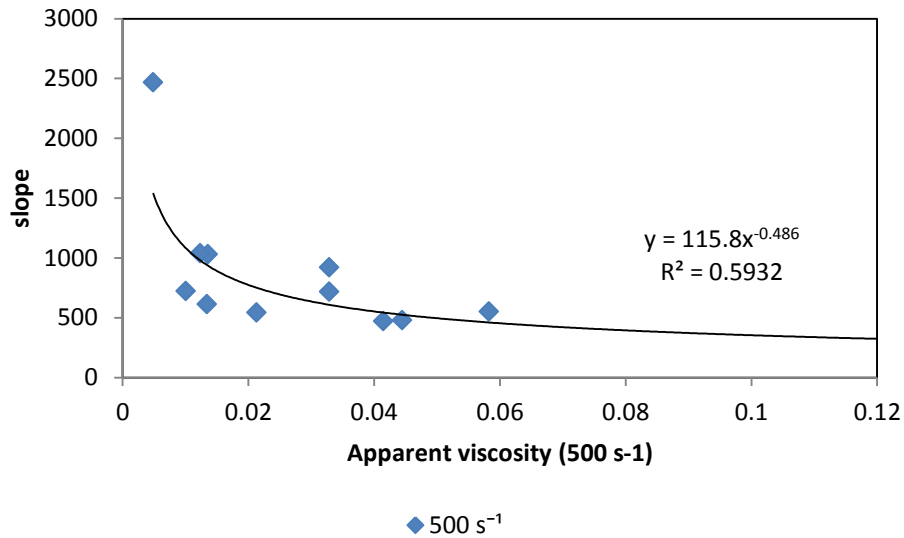


Figure 4.13: Onset of 'Full turbulence' locus – relationship of m-values with apparent viscosity at 500 s⁻¹ for all fluids flowing in 150 and 300 mm semi-circular flumes

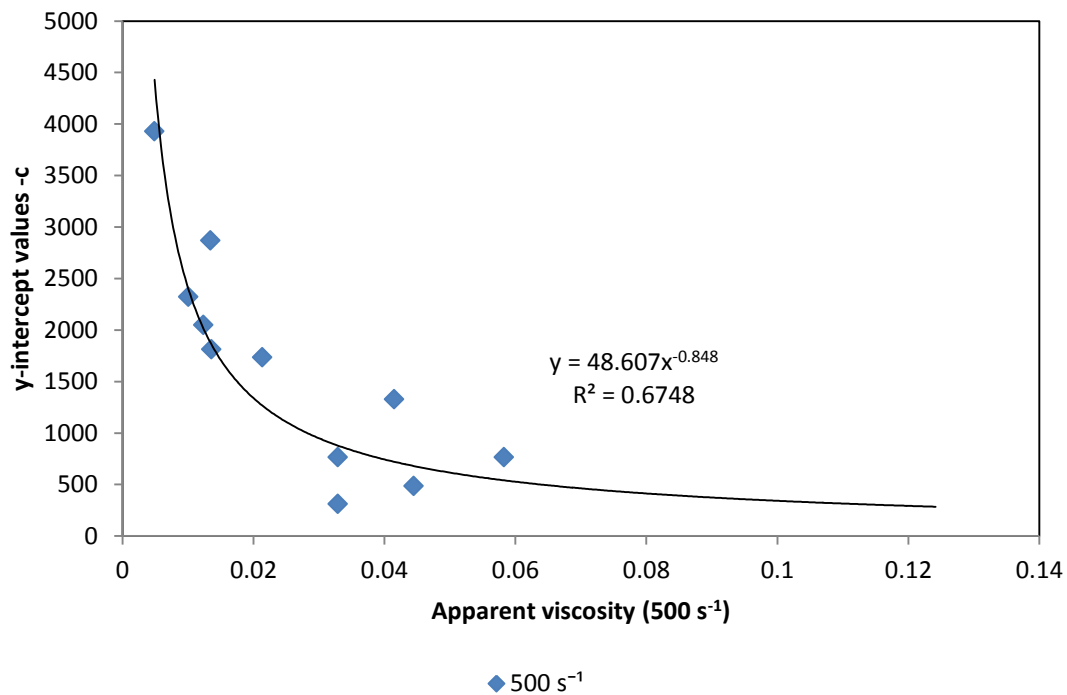


Figure 4.14: Onset of 'Full turbulence' locus – relationship of y-intercept values with apparent viscosity at 500 s⁻¹ for all fluids flowing in 150 and 300 mm semi-circular flumes

The semi-circular flume upper critical Reynolds number is written as:

$$\text{Re}_c = 116 \left(\mu | \dot{\gamma} = 500 \text{s}^{-1} \right)^{-0.49} \text{Fr} + 49 \left(\mu | \dot{\gamma} = 500 \text{s}^{-1} \right)^{-0.85} \quad 4.11$$

The constant 116 has a unit of $\text{Pa}\cdot\text{s}^{0.49}$ and the constant 49, a unit of $\text{Pa}\cdot\text{s}^{0.85}$.

The dimensionless form of Equation (4.11) is expressed as:

$$\text{Re}_{c(\text{turb})} = 3423 \left(\frac{\mu}{\mu_w} | \dot{\gamma} = 500 \text{s}^{-1} \right)^{-0.49} \text{Fr} + 17\,386 \left(\frac{\mu}{\mu_w} | \dot{\gamma} = 500 \text{s}^{-1} \right)^{-0.85} \quad 4.12$$

The semi-circular models for transition were evaluated for a 4.6% bentonite slurry flowing in a 300 mm semi-circular flume as shown in Figure 4.15.

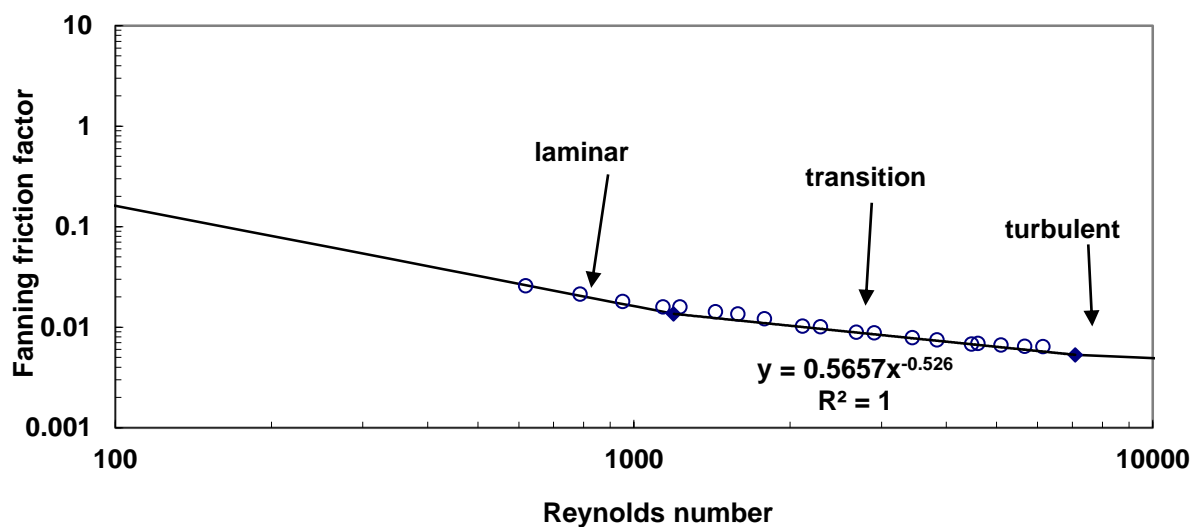


Figure 4.15: Evaluation of the transition models at the onset and end of transition in the semi-circular flume

4.5 Combined model

The data used in the four different flumes were put together to obtain the combined model. Figures 4.16 and 4.17 show the two relationships used to obtain the lower critical Reynolds number for all flumes data used.

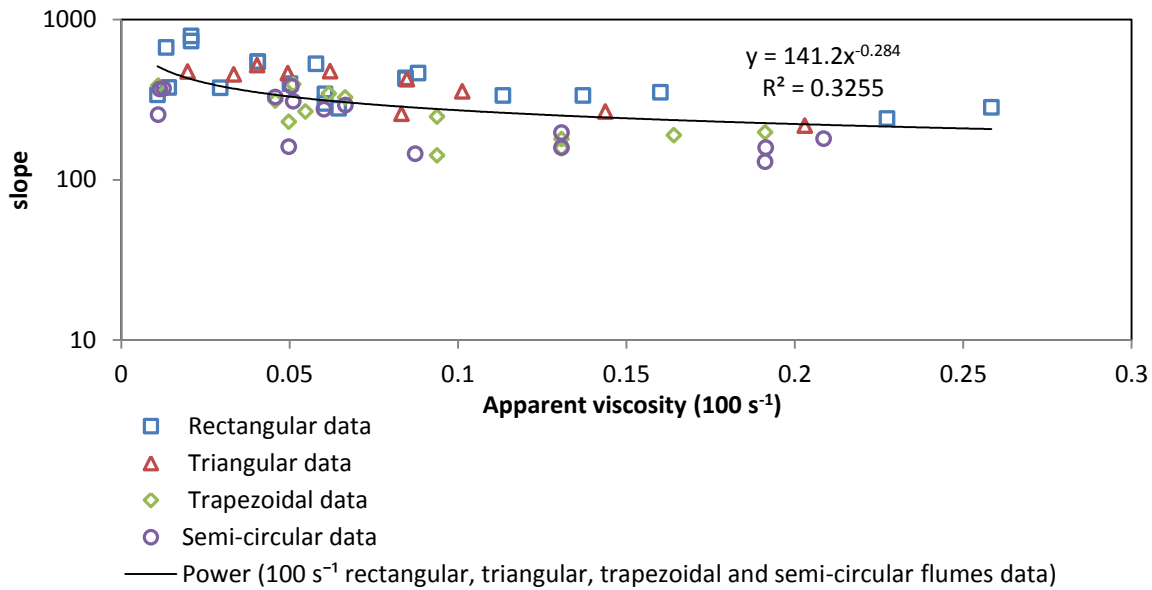


Figure 4.16: Onset of transition locus – relationship of m-values with apparent viscosity at 100 s^{-1} for all fluids in all flumes used

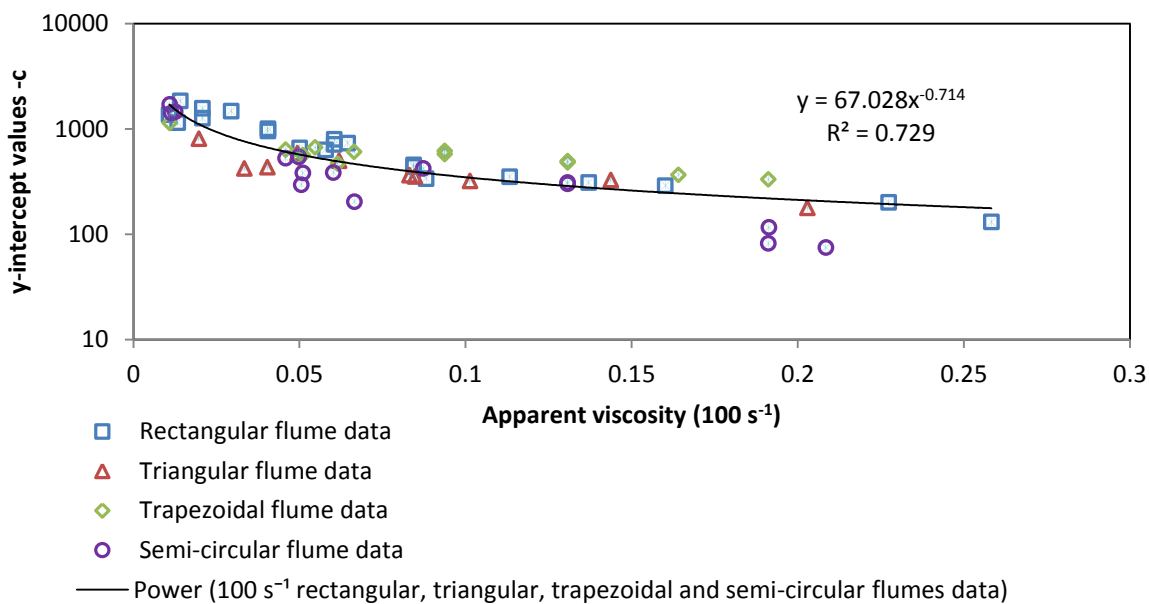


Figure 4.17: Onset of transition locus – relationship of y-intercept values with apparent viscosity at 100 s^{-1} for all fluids in all flumes used

The critical Reynolds number at the onset of transitional flow is expressed as:

$$Re_c = 141 (\mu | \dot{\gamma} = 100 \text{ s}^{-1})^{-0.28} Fr + 67 (\mu | \dot{\gamma} = 100 \text{ s}^{-1})^{-0.71} \quad 4.13$$

The constant 141 has a unit of $\text{Pa} \cdot \text{s}^{0.28}$ and the constant 67, a unit of $\text{Pa} \cdot \text{s}^{0.71}$.

The dimensionless form of Equation (4.13) is as follows:

$$Re_c = 975 \left(\frac{\mu}{\mu_w} \Big| \dot{\gamma} = 100s^{-1} \right)^{-0.28} Fr + 9038 \left(\frac{\mu}{\mu_w} \Big| \dot{\gamma} = 100s^{-1} \right)^{-0.71} \quad 4.14$$

The two relationships obtained for the upper critical Reynolds number are shown in Figures 4.18 and 4.19.

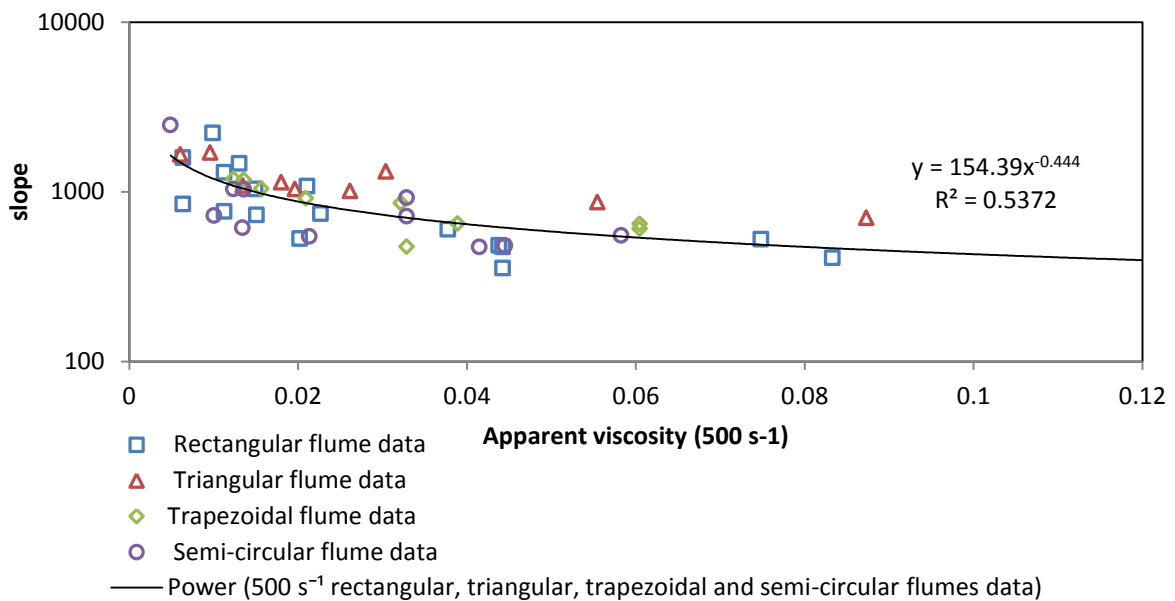


Figure 4.18: Onset of 'Full turbulence' locus – relationship of m-values with apparent viscosity at 500 s⁻¹ for all fluids in all flumes used

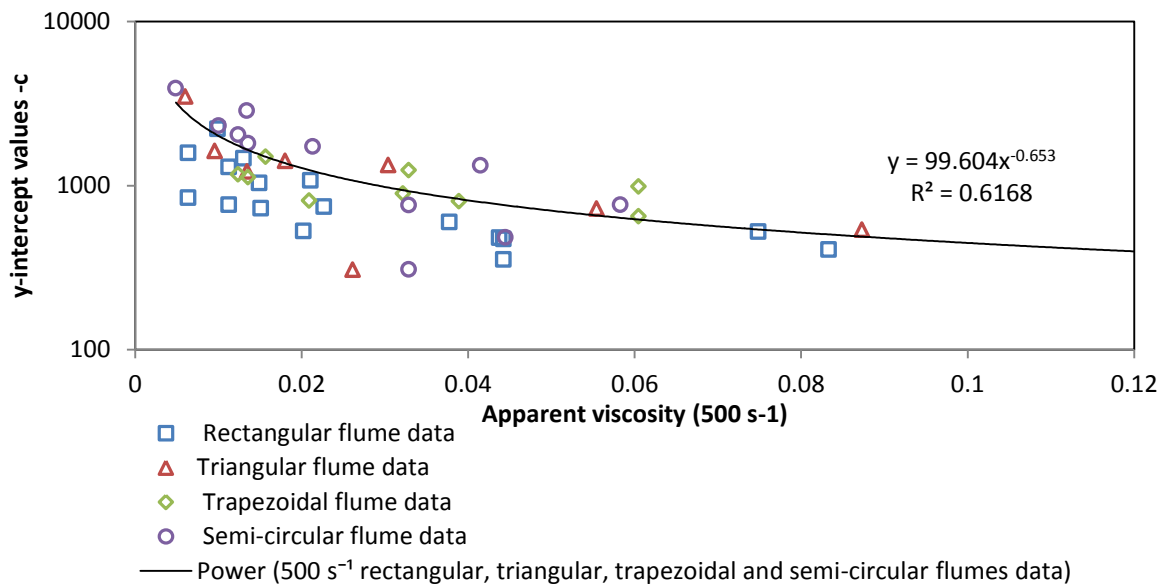


Figure 4.19: Onset of 'Full turbulence' locus – relationship of y-intercept values with apparent viscosity at 500 s⁻¹ for all fluids in all flumes used

The critical Reynolds number at the end of transitional flow is expressed as:

$$\text{Re}_c = 154 \left(\mu \mid \dot{\gamma} = 500 \text{s}^{-1} \right)^{-0.44} \text{Fr} + 100 \left(\mu \mid \dot{\gamma} = 500 \text{s}^{-1} \right)^{-0.65} \quad 4.15$$

The constant 154 has a unit of $\text{Pa}\cdot\text{s}^{0.44}$ and the constant 100, a unit of $\text{Pa}\cdot\text{s}^{0.65}$.

The dimensionless form of Equation (4.15) is written as follows:

$$\text{Re}_{c(\text{turb})} = 3218 \left(\frac{\mu}{\mu_w} \mid \dot{\gamma} = 500 \text{s}^{-1} \right)^{-0.44} \text{Fr} + 8913 \left(\frac{\mu}{\mu_w} \mid \dot{\gamma} = 500 \text{s}^{-1} \right)^{-0.65} \quad 4.16$$

The combined models for transition were evaluated for a 6% kaolin slurry flowing in a 150 mm rectangular channel as illustrated in Figure 4.20.

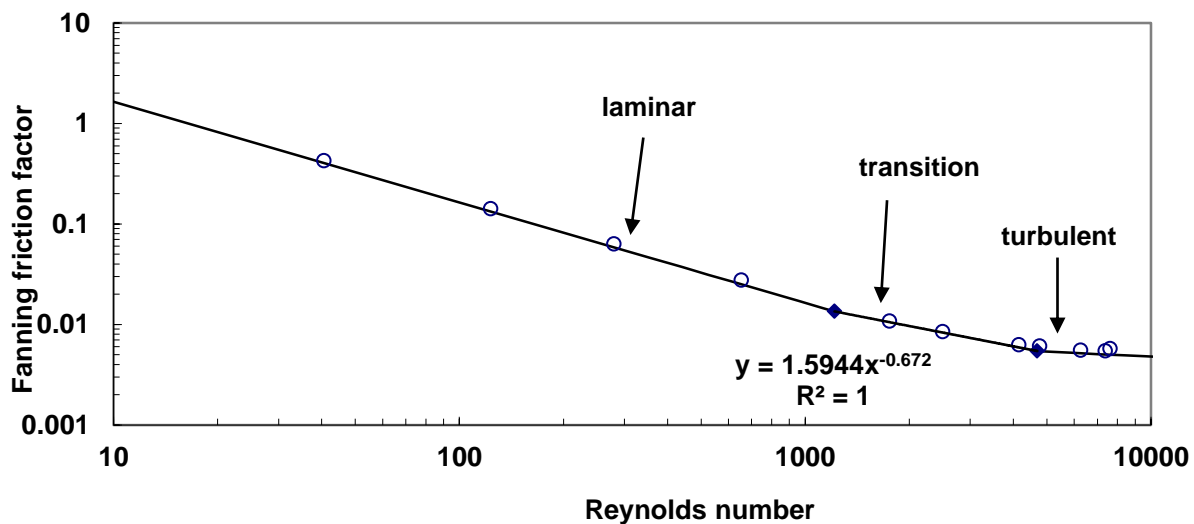


Figure 4.20: Evaluation of the combined transition models at the onset and end of transition in a 150 mm rectangular flume

4.6 Conclusion

Critical Reynolds number correlations for the onset and end of transitional flow for triangular, trapezoidal and semi-circular channels as well as a combined model were established. The methodology was based on Haldenwang's (2003) procedure for rectangular channels.

The adapted models will be evaluated and compared in Chapter 5 with the models for appropriate channel shapes found in the literature.

CHAPTER 5

Chapter 5: Comparison of the adapted models with those found in the literature

5.1. Introduction

The aim of this work was to evaluate the cross-sectional shape effect of open channels by critically evaluating the models presented by Naik (1983), Coussot (1997), Fitton (2008), Haldenwang (2003), Haldenwang *et al.* (2010) and Slatter (2013a & 2013b) and to commend and optimise the best model. The appropriate models presented in the literature were evaluated using the database compiled by Haldenwang (2003) and Burger *et al.* (2010b).

Thus, this chapter evaluates the models found in literature which can be used to predict transitional flow in open channels of various cross-sectional shapes. Different models are evaluated and compared for power law, Bingham plastic and yield shear-thinning fluids. The models found in literature will also be compared with the correlations established in Chapter 4 for triangular, semi-circular and trapezoidal channels.

5.2. Transitional flow

The flow of non-Newtonian fluids in open channels is divided in three flow regimes, namely: laminar, transitional and turbulent. The main focus of this work is the transitional flow region.

For laminar-turbulent transition prediction of slurries in pipes, there are a number of methods described in the literature. The same cannot be said about open channel flow. The complexity of transitional open channel flow is due to the presence of the free surface which presents an additional variable as opposed to pipe flow where the diameter is fixed.

The onset of transition is described as the point which deviates from the linear laminar flow regime, but predicting the onset point is still a challenge.

For some authors (Thomas & Wilson, 1991 & Fitton, 2007), transitional flow occurs at a single point whereas for others (Straub *et al.* 1958, Haldenwang, 2003 & Slatter, 2013b) it occurs over a range of Reynolds numbers.

The Froude and the Reynolds numbers will be used to describe transitional flow of non-Newtonian fluids in channels of different shapes.

To be able to predict transition accurately is essential when open channels are designed. The non-Newtonian nature of the fluid must be taken into account as transition will occur at lower Reynolds numbers. This will increase the friction factor at transition (Haldenwang, 2003).

5.2.1 Work done by Straub *et al.* (1958) for Newtonian fluids

Straub *et al.* (1958) conducted measurements of the critical Reynolds number Re_c for Newtonian flow in rectangular channels and found Re_c to vary from 2000 to more than 3000 for h/B ratios from 1.35 to 3.70. They also found that the Re_c (critical Reynolds number) values for open channel flow, which are dependent on the channel shape to a certain extent, are generally larger than those for closed conduit flow. The authors did not clarify this.

5.2.2 Evaluation of power law fluids

This section uses the Haldenwang (2003), Fitton (2008) and Slatter (2013) models to evaluate the transitional flow of a power law fluid.

5.2.2.1 Work done by Haldenwang

Haldenwang (2003) established a new model for predicting the onset of transition and the onset of turbulence (or end of transition). He stated that the flow behaviour could be characterised by the Froude number and the Reynolds number.

Haldenwang's model for a rectangular channel is evaluated for 3.8% and 2.8% CMC solutions flowing in 150 mm rectangular channel and is illustrated in Figures 5.1 and 5.2.

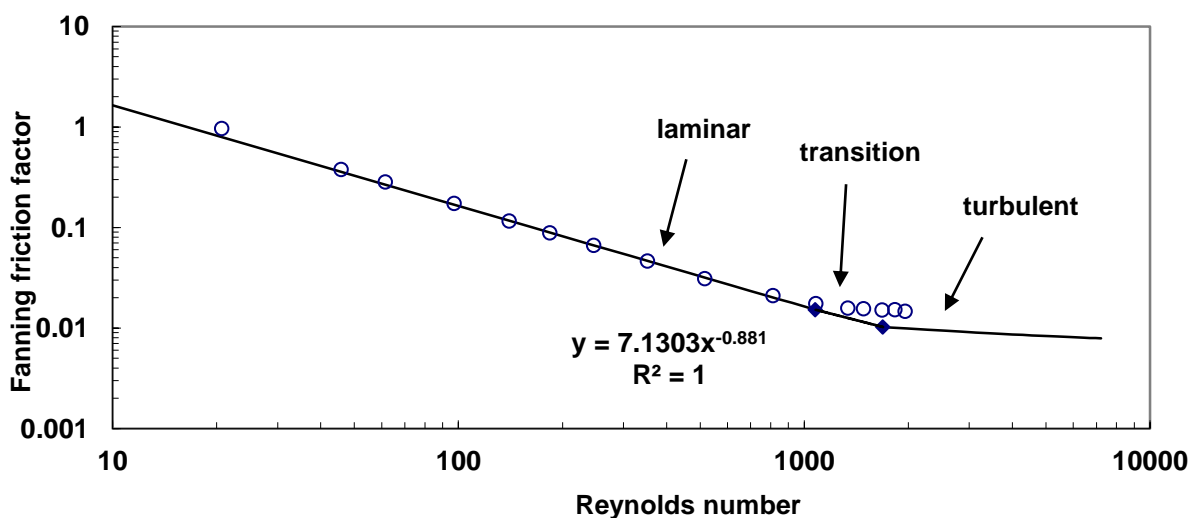


Figure 5.1: Prediction of transition. 3.8% CMC suspension flowing in a 150 mm rectangular shape at 4° slope

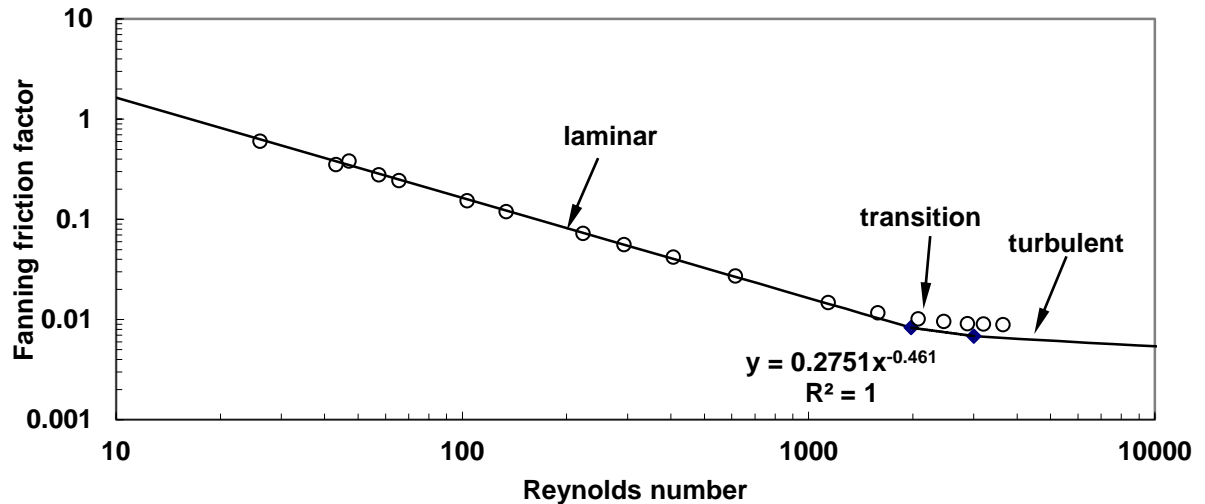


Figure 5.2: Prediction of transition. 2.8% CMC suspension flowing in a 150 mm rectangular shape at 5° slope

Figures 5.1 and 5.2 show that Haldenwang's (2003) model gives a good prediction of the onset of transition of power law fluids for the rectangular flume shape used in this work. This is shown by the onset of transition points which collapse on the theoretical transition line represented by the power law model. However, the end of transitional flow is not well predicted by Haldenwang's (2003) model. It can be seen that transition occurs earlier in open channel flow than in pipe flow. At Reynolds numbers less than 1000, the viscous forces are dominant over the inertial forces. In the vicinity of Reynolds numbers equal to 1000, the data points start to deviate from laminar flow and the Fanning friction factor becomes independent of Reynolds number. However, in Figure 5.2 transition occurs at Reynolds number close to 2000 for 2.8% CMC suspension. This shows that the onset of transitional flow is dependent on the concentration of the material flowing in a flume.

The percentage deviation is a measure of the difference between the predicted and the critical value. The percentage deviation between Haldenwang's prediction and the critical velocities are tabulated in Tables 5.1 and 5.2. The deviation sign (positive or negative), indicates the direction of that difference (the percentage deviation is positive when the predicted velocity value is greater than the critical velocity value).

Table 5.1: Haldenwang's transition model for 3.8% CMC solution flowing in a 150 mm rectangular channel

| Slope (°) | Critical velocity (m/s) | V_c Haldenwang (m/s) | % Deviation |
|------------------|--------------------------------|---------------------------------------|--------------------|
| 1 | 0.79 | 0.66 | -16 |
| 2 | 0.95 | 0.95 | 1 |
| 3 | 1.00 | 1.21 | 21 |
| 4 | 1.20 | 1.45 | 21 |
| 5 | 1.39 | 1.68 | 21 |

Table 5.2: Haldenwang's transition model for 2.8% CMC solution flowing in a 150 mm rectangular channel

| Slope (°) | Critical velocity (m/s) | V_c Haldenwang (m/s) | % Deviation |
|------------------|--------------------------------|---------------------------------------|--------------------|
| 1 | 0.73 | 0.71 | -3 |
| 2 | 0.83 | 1.02 | 22 |
| 3 | 1.20 | 1.28 | 7 |
| 4 | 1.39 | 1.53 | 10 |
| 5 | 1.51 | 1.77 | 17 |

It can also be seen in Figure 5.3 that 60% of transition predictions by the Haldenwang model fall within the +/- 20% deviation range.

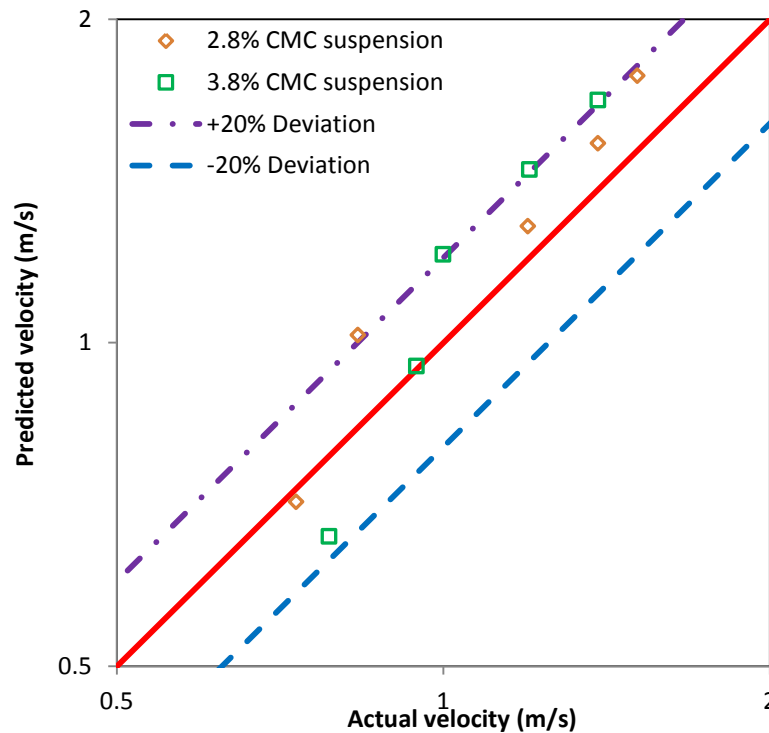


Figure 5.3: Haldenwang's transition model for 2.8% and 3.8% CMC solutions flowing in a 150 mm rectangular flume

5.2.2.2 Work done by Fitton

Fitton's (2008) model was developed to predict the transitional flow in open channels of various shapes for yield shear-thinning fluids. Since it uses the Haldenwang Reynolds number which takes into account the shape effect, it was evaluated for power law and Bingham plastic fluids in all shapes used in this study.

The Darcy friction factor obtained from Equation (2.91) was divided by four to obtain the corresponding Fanning friction factor for the laminar region represented in Figure 5.4. However, the Fanning friction factor obtained from Equation (2.30) was used for turbulent flow and is shown in Figure 5.4. The intersection between the Fanning friction factors for laminar flow and turbulent flow is deemed to be the point of transition. Figure 5.4 shows that the point of transition occurs at a Fanning friction factor of 0.01592 with a corresponding critical velocity of 1.22 m/s for 3.8% CMC solution flowing in a 150 mm semi-circular channel.

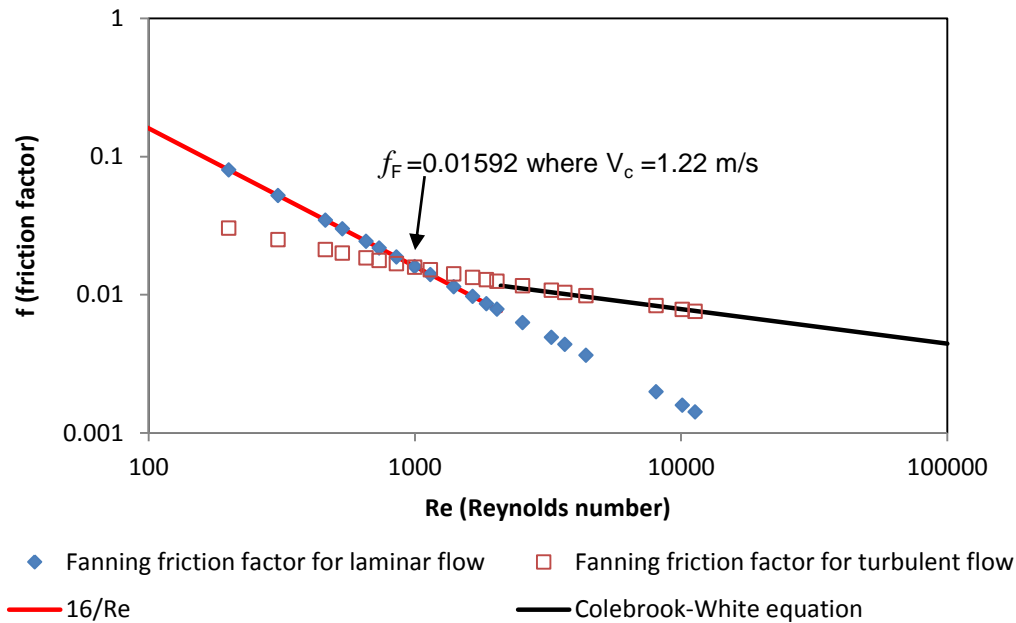


Figure 5.4: Prediction of transition showing the intersection between the laminar flow and the turbulent flow Fanning friction factors. 3.8% CMC solution flowing in a 300 mm semi-circular channel at 4° slope

Fitton's (2008) prediction does not give a range of transitional flow but a single point. The same procedure was used to determine transition points for the power law fluid used in all the different shapes available in this study. The effect of shape is included in the Reynolds number and friction factor and that is why the Fitton (2008) prediction can be applied.

Table 5.3: 3.8% CMC solution flowing in a 150 mm rectangular channel shape

| Slope (°) | Critical velocity (m/s) | V_c Fitton (m/s) | % Deviation |
|-----------|-------------------------|--------------------|-------------|
| 1 | 0.79 | 0.94 | 19 |
| 2 | 0.95 | 1.15 | 22 |
| 3 | 1.00 | 1.32 | 32 |
| 4 | 1.20 | 1.40 | 17 |
| 5 | 1.39 | 1.39 | 0 |

Table 5.4: 3.8% CMC solution flowing in a 150 mm semi-circular channel shape

| Slope (°) | Critical velocity (m/s) | V _c Fitton (m/s) | % Deviation |
|-----------|-------------------------|-----------------------------|-------------|
| 1 | 0.65 | 0.77 | 18 |
| 2 | 0.85 | 0.99 | 17 |
| 3 | 0.96 | 1.12 | 17 |
| 4 | 1.14 | 1.22 | 7 |
| 5 | 1.35 | 1.35 | 0 |

Table 5.5: 3.8% CMC solution flowing in a 150 mm trapezoidal channel shape

| Slope (°) | Critical velocity (m/s) | V _c Fitton (m/s) | % Deviation |
|-----------|-------------------------|-----------------------------|-------------|
| 1 | 0.68 | 0.85 | 25 |
| 2 | 0.84 | 1.05 | 24 |
| 3 | 0.98 | 1.19 | 22 |
| 4 | 1.07 | 1.20 | 12 |
| 5 | 1.17 | 1.17 | 0 |

Table 5.6: 3.8% CMC solution flowing in a 300 mm triangular channel shape

| Slope (°) | Critical velocity (m/s) | V _c Fitton (m/s) | % Deviation |
|-----------|-------------------------|-----------------------------|-------------|
| 1 | 0.82 | 0.82 | 0 |
| 2 | 0.83 | 1.00 | 20 |
| 3 | 0.93 | 1.13 | 21 |
| 4 | 1.11 | 1.22 | 10 |
| 5 | 1.25 | 1.25 | 0 |

From Table 5.3 to 5.6, it can be seen that Fitton (2008) predicts the transition point with a deviation of less than 30% for 3.8% CMC solution in the various shapes studied. It is illustrated in Figure 5.5 that 70% of the data falls inside the +/- 20% deviation range.

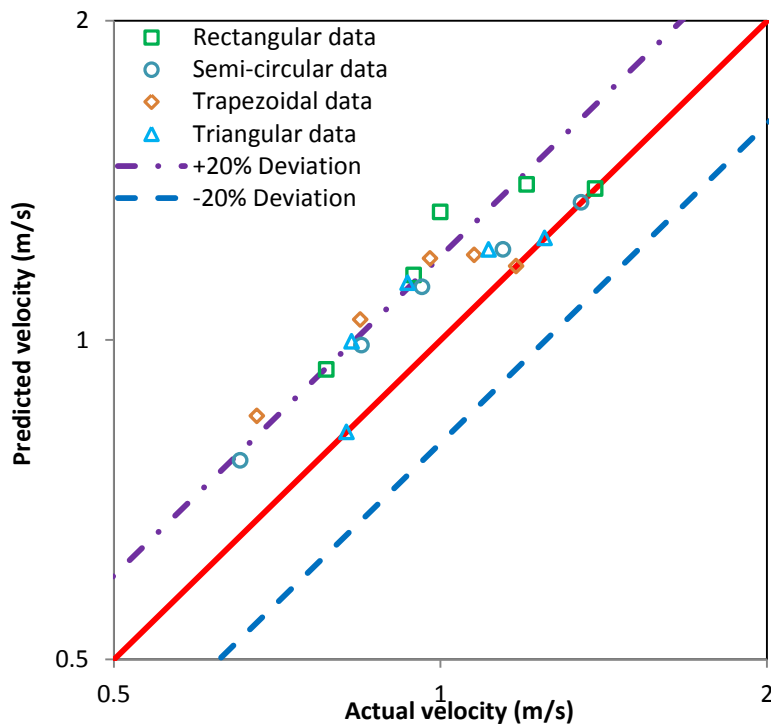


Figure 5.5: Fitton's transition model for 3.8% CMC solution

5.2.2.3 Work done by Slatter (2013)

Slatter *et al.* (2011) developed and evaluated a criterion for determining the laminar-turbulent transition for the sheet flow analysis using a power law fluid.

Slatter (2013a) evaluated his new criterion ($Re_4=700$) against the experimental data published by Haldenwang (2003) using one concentration from 1 to 5 degrees slope. He stated that the transition predictions obtained worked generally well.

In this study, Slatter's evaluation is extended to more than a single concentration as shown from Figure 5.6 to 5.13. The points considered meet the sheet flow criteria established by Coussot (1994) where the flow depth to flume width (h/B) ratio is less than 0.1.

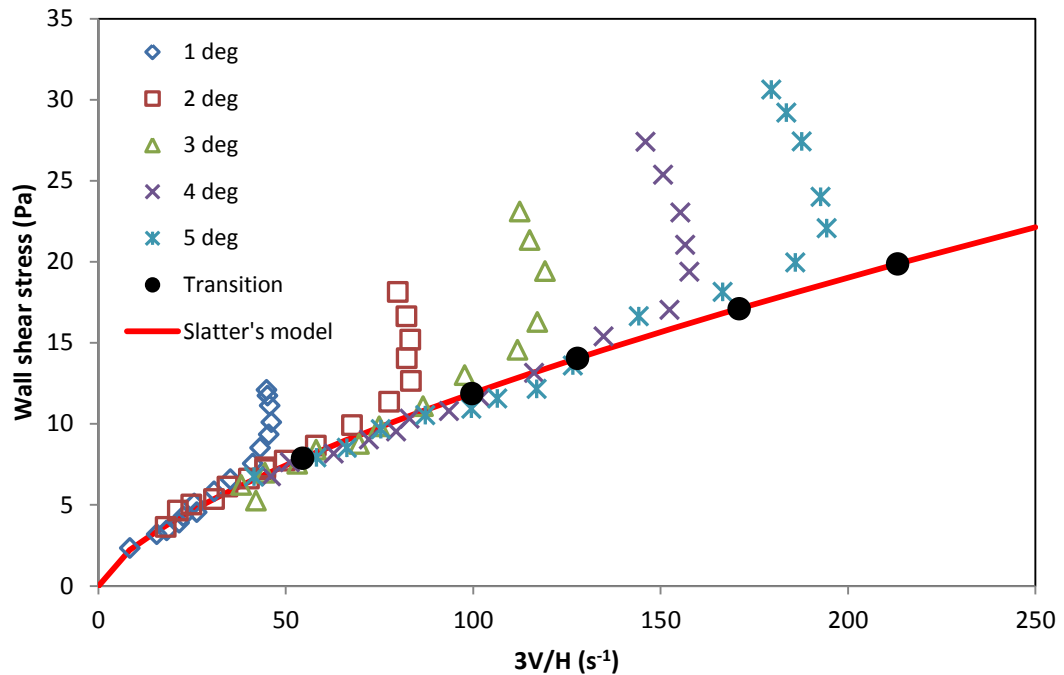


Figure 5.6: Slatter's transition model for 3.8% CMC solution

Figure 5.6 shows graphically the change in behaviour between the laminar and turbulent regimes. The viscous state in the laminar flow regime is superimposed for the various slopes but the rheological parameters were obtained from a tube viscometer. Figure 5.6 also shows a plot of the bulk shear rate versus the wall shear stress with the onset of transition points obtained by using the criterion $Re_4=700$. Slatter's prediction of transition occurs generally late as can be seen from Figure 5.7 to 5.9. For brevity, only three slopes are separately shown. The same behaviour was observed for the other slopes.

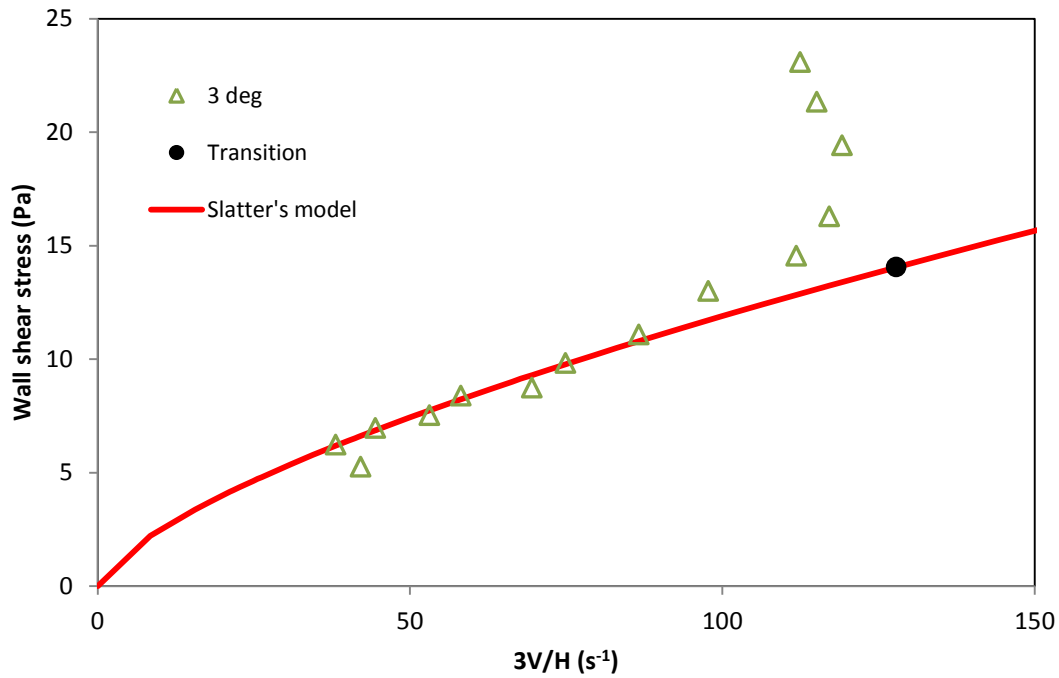


Figure 5.7: Slatter's transition model for 3.8% CMC solution flowing in a 300 mm rectangular flume at 3 degrees slope

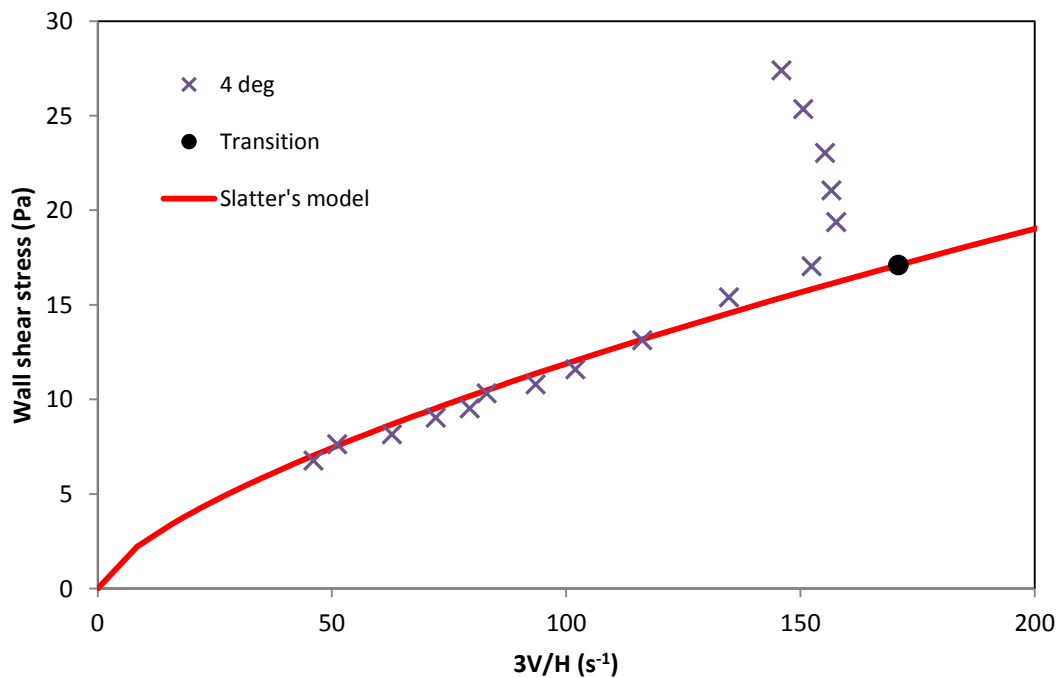


Figure 5.8: Slatter's transition model for 3.8% CMC solution flowing in a 300 mm rectangular flume at 4 degrees slope

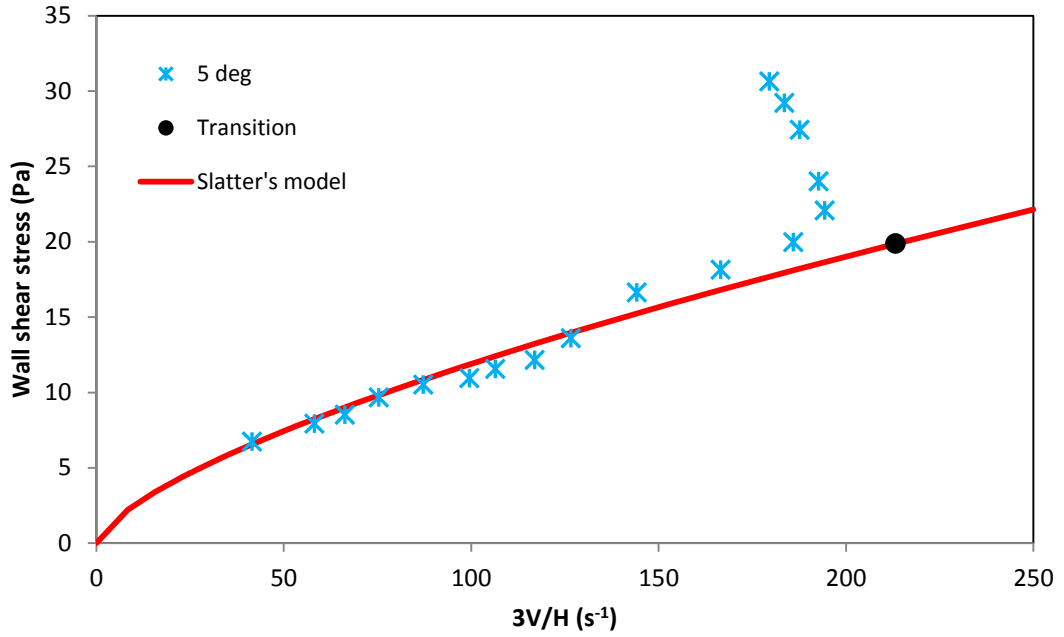


Figure 5.9: Slatter’s transition model for 3.8% CMC solution flowing in a 300 mm rectangular flume at 5 degrees slope

Figure 5.10 shows the evaluation of Slatter’s predictive model of transition for 2.8% CMC solution flowing in a 300 mm rectangular flume. It can be seen that Slatter’s predictive model of transition for 2.8% CMC solution works better with less deviation at the 5 degree slope as is illustrated from Figure 5.11 to 5.13. For brevity reasons, only three slopes are presented.

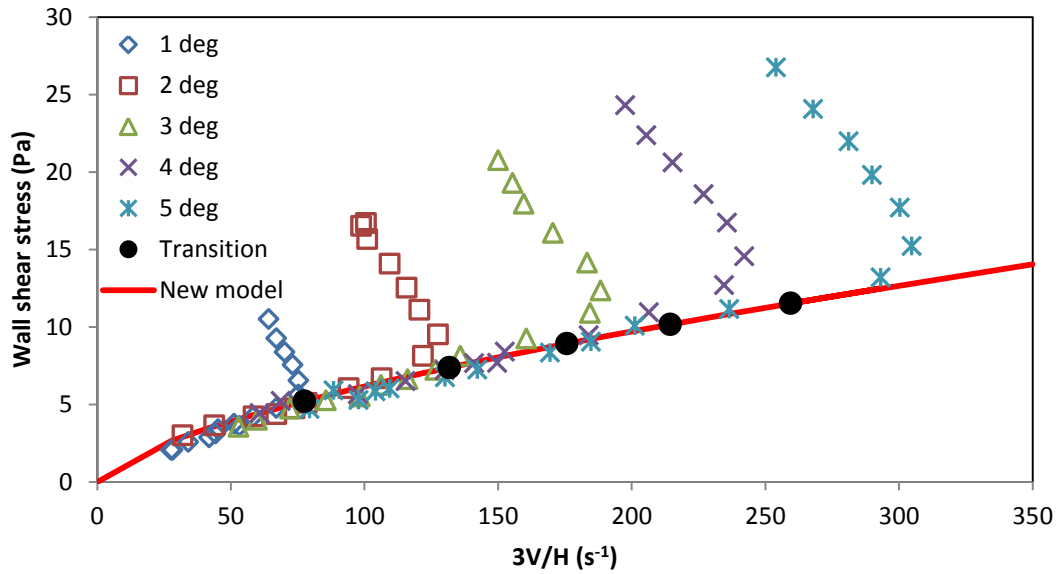


Figure 5.10: Slatter’s transition model for 2.8% CMC solution flowing in a 300 mm rectangular flume

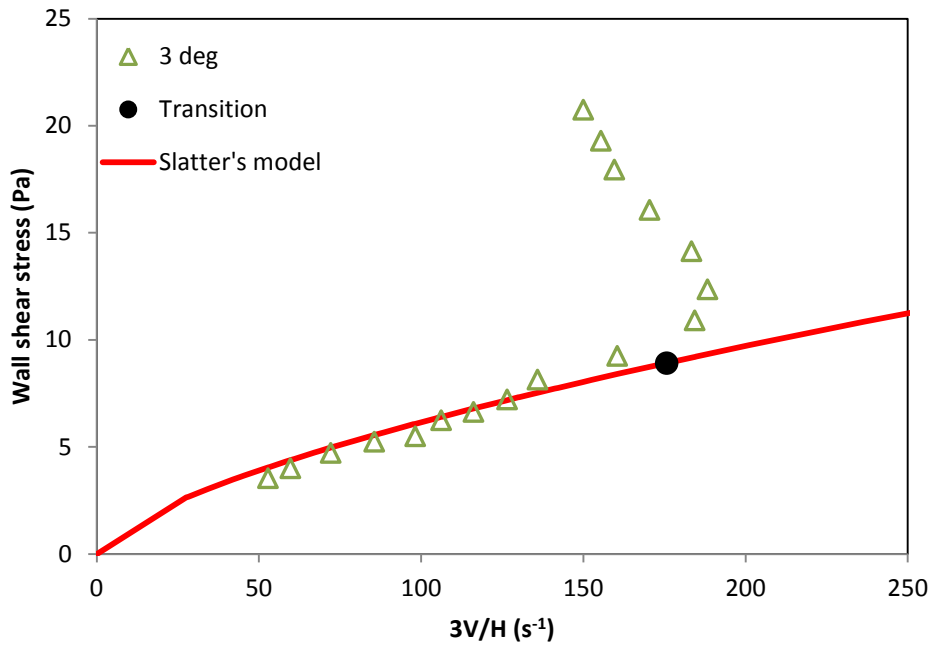


Figure 5.11: Slatter's transition model for 2.8% CMC solution flowing in a 300 mm rectangular flume at 3 degrees slope

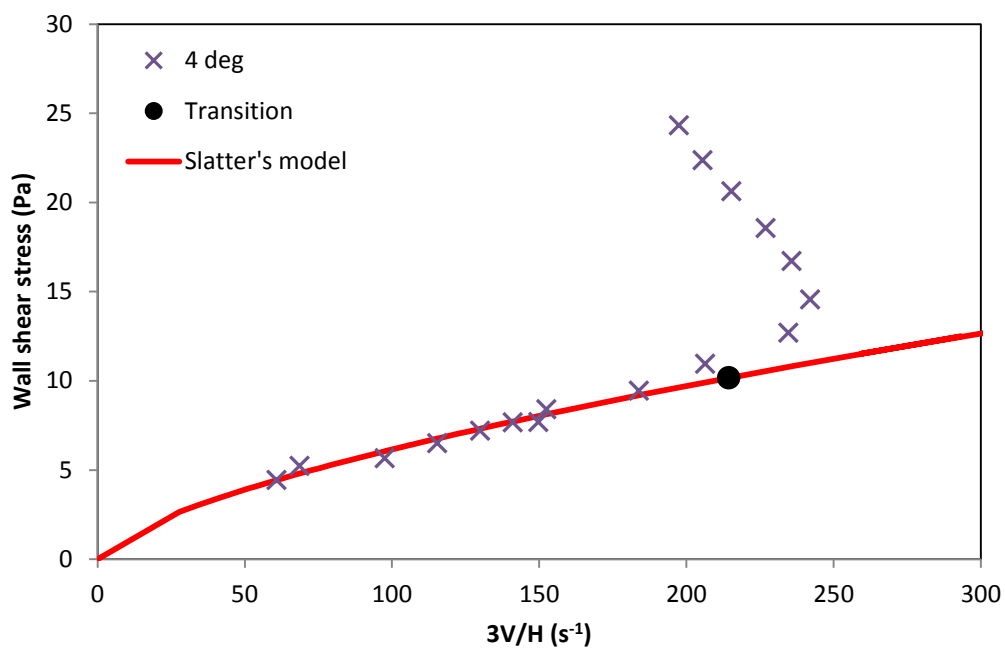


Figure 5.12: Slatter's transition model for 2.8% CMC solution flowing in a 300 mm rectangular flume at 4 degrees slope

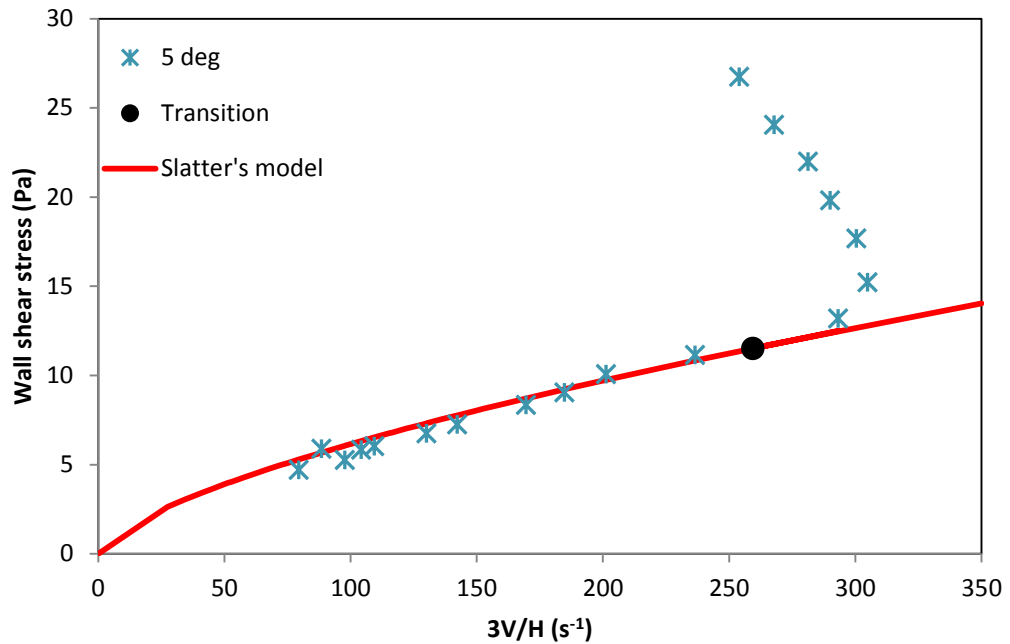


Figure 5.13: Slatter's transition model for 2.8% CMC solution flowing in a 300 mm rectangular flume at 5 degrees slope

When Slatter's prediction is evaluated at two different concentrations, it can be seen that the onset of transition varies with concentration. This may be due to the fact that the criterion for the onset of transition was fixed to a value of 700. However, it has been shown by Haldenwang (2003) that the onset of transitional flow cannot be fixed to a single value since it varies with the flume slope and the fluid concentration.

Figure 5.14 shows that 40% of the transition points obtained using Slatter's prediction fall within the $\pm 20\%$ deviation range.

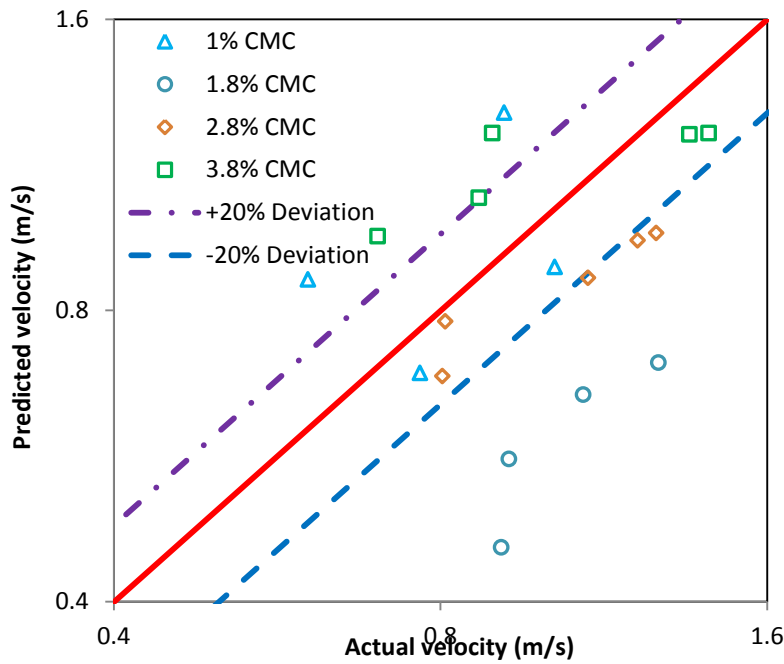


Figure 5.14: Slatter's transition model for 1%, 1.8%, 2.8% and 3.8% CMC solutions flowing in a 300 mm rectangular flume

5.2.3 Evaluation of Bingham plastic fluids

Bingham plastic fluids are characterised by a yield stress which has to be overcome to initiate the flow as well as a Bingham viscosity. Hao and Zenghai (1980), Naik (1983), Haldenwang (2003) as well as Fitton (2008) models were used for the evaluation of Bingham plastic fluids.

5.2.3.1 Work done by Hao and Zenghai

Hao and Zenghai's model for Bingham plastic fluid is similar to the Reynolds number developed by Haldenwang *et al.* (2002). Haldenwang's model (Equation (2.53)) is not only applicable to Bingham plastic fluids but also to power-law and yield shear-thinning fluids. Hao and Zenghai's model is written as:

$$Re_{\text{Zheng}} = \frac{4 \rho R_h V}{K + \frac{\tau_y R_h}{2V}} \quad 2.38$$

Hao and Zenghai and Haldenwang models for Bingham plastic fluids are mathematically identical, although they are expressed in a different format. Hence, Hao and Zenghai's model will not be evaluated in this thesis.

5.2.3.2 Work done by Naik

The Bingham Reynolds number used by Naik is a Newtonian Reynolds number. It does not account for the presence of a yield stress.

The Naik Reynolds number is expressed as follows:

$$Re_{(\text{Naik})} = \frac{\rho V 4 R_h}{k} \quad 2.82$$

The friction factor used was adapted for open channels and is written as follows:

$$f = \frac{2 \rho g R_h}{V^2} \quad 2.24$$

Naik classified kaolin in water slurries in his work as a Bingham plastic fluid. The bentonite in water slurries used in this work was used to compare the Reynolds number proposed by Naik with the one developed by Haldenwang to predict transitional flow. Figure 5.15 shows that Naik's (1983) model does not predict well the flow of bentonite in water slurries in open channels as it is slope sensitive.

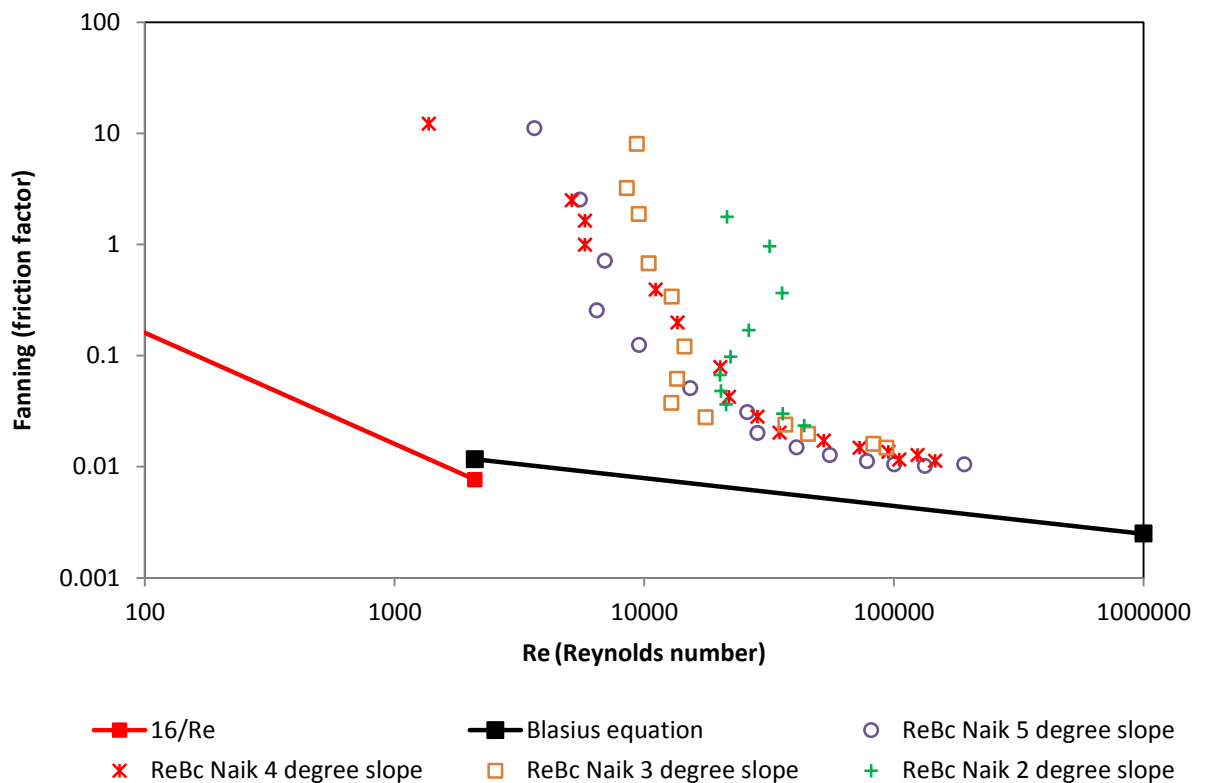


Figure 5.15: 6% bentonite slurry flowing in a 300 mm rectangular flume at slopes 2-5 degrees

5.2.3.3 Work done by Haldenwang

The evaluation of Bingham plastic fluid for this study uses Haldenwang's (2003) model for the rectangular flume shape.

Figures 5.16 and 5.17 show that Haldenwang's transition prediction model for Bingham plastic fluids works well in the rectangular flume shape used in this work since the actual data points fall on the transition line.

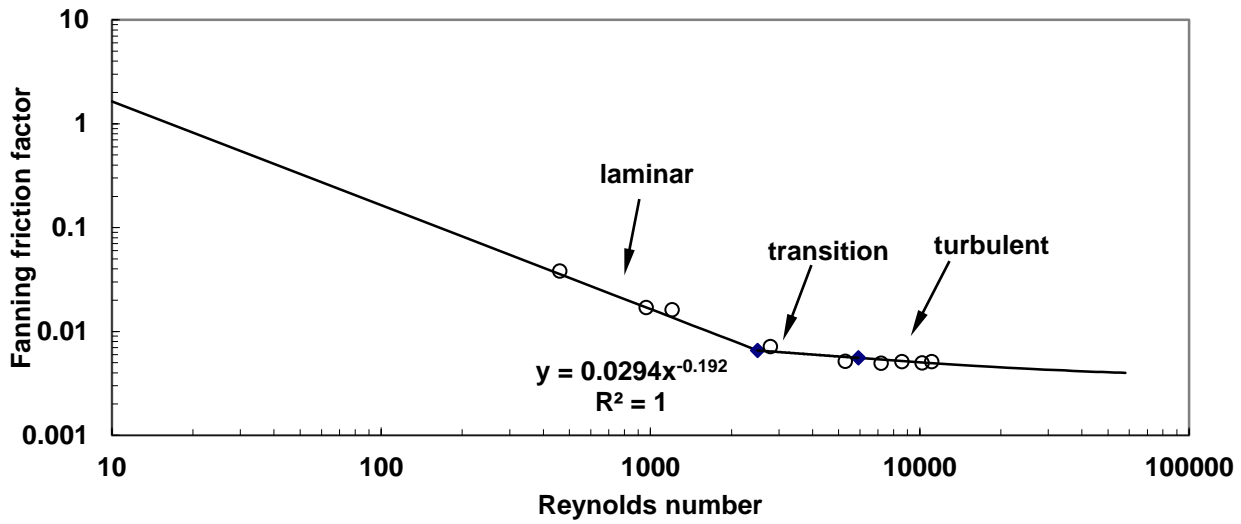


Figure 5.16: Prediction of transition. 4.5% bentonite in water slurry flowing in a 150 mm rectangular flume at 5° slope

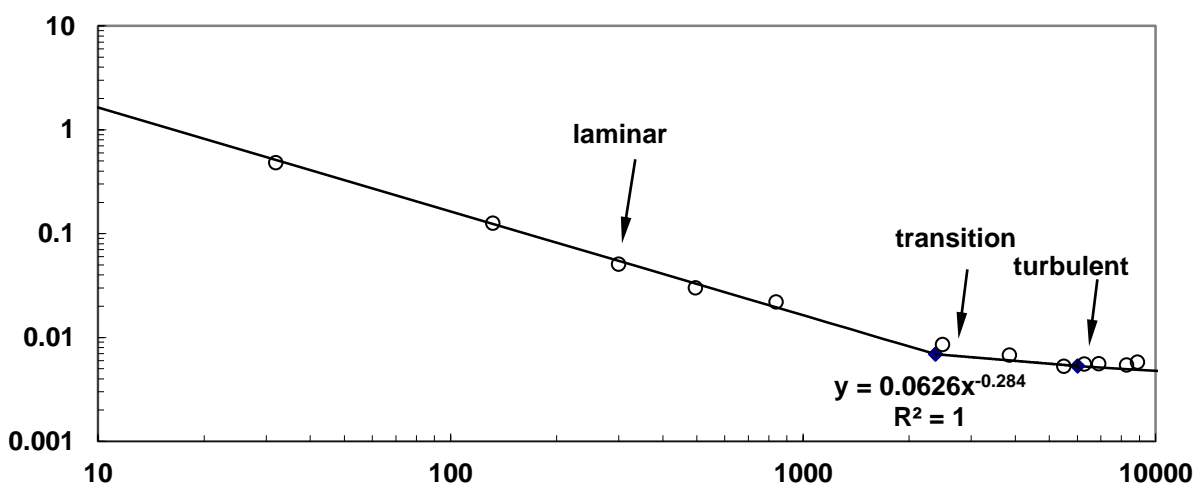


Figure 5.17: Prediction of transition. 4.5% bentonite in water slurry flowing in a 300 mm rectangular flume at 5° slope

The deviation ranges of the predictions of Haldenwang's critical velocities are tabulated in Tables 5.7 and 5.8.

Table 5.7: Haldenwang's transition model for 4.5% bentonite in water slurry flowing in 150 mm rectangular channel

| Slope | Critical velocity | V_c Haldenwang | % Deviation |
|-------|-------------------|------------------|-------------|
| 1 | 0.61 | 0.81 | 33 |
| 2 | 0.79 | 0.98 | 25 |
| 3 | 0.93 | 1.13 | 21 |
| 4 | 1.14 | 1.28 | 12 |
| 5 | 1.47 | 1.42 | -3 |

Table 5.8: Haldenwang's transition model for 4.5% bentonite in water slurry flowing in 300 mm rectangular channel

| Slope | Critical velocity | V_c Haldenwang | % Deviation |
|-------|-------------------|------------------|-------------|
| 1 | 0.76 | 0.86 | 14 |
| 2 | 0.95 | 1.02 | 7 |
| 3 | 0.96 | 1.16 | 21 |
| 4 | 1.19 | 1.29 | 8 |
| 5 | 1.41 | 1.41 | 0 |

Figure 5.18 also shows that 60% of the transition points obtained using Haldenwang (2010) prediction are between the +/- 20% deviation range.

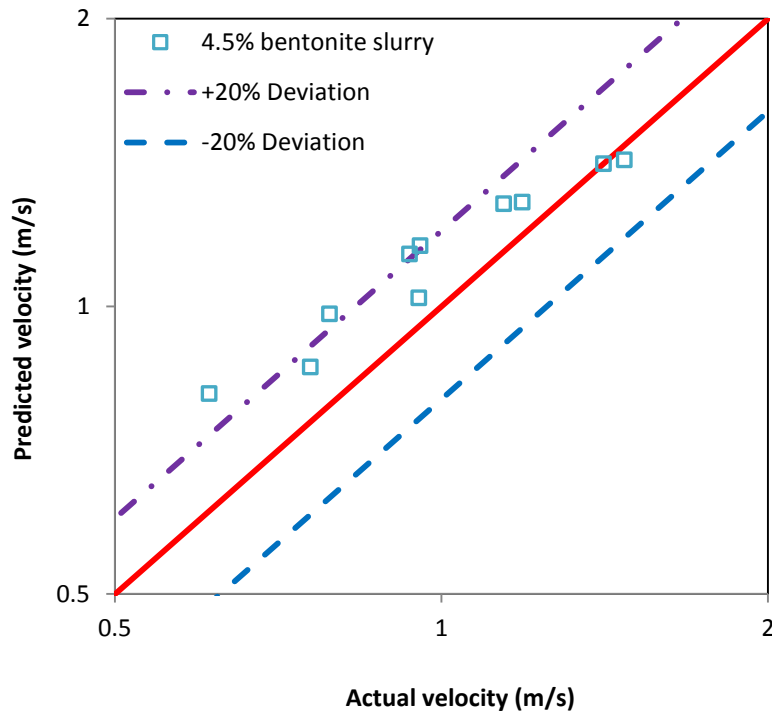


Figure 5.18: Haldenwang's transition model for 4.5% bentonite in water slurry flowing in a 150 mm and 300 mm rectangular channel

5.2.3.4 Work done by Fitton

Fitton's (2008) prediction of transition for 4.5% bentonite in water slurry is evaluated from Table 5.9 to 5.12.

Table 5.9: 4.5% bentonite in water slurry in a 300 mm rectangular channel shape

| Slope | Critical velocity | V_c Fitton | % Deviation |
|-------|-------------------|--------------|-------------|
| 1 | 0.76 | 0.87 | 15 |
| 2 | 0.95 | 0.95 | 0 |
| 3 | 0.96 | 0.96 | 0 |
| 4 | 1.19 | 0.69 | -42 |
| 5 | 1.41 | 0.80 | -44 |

Table 5.10: 4.5% bentonite in water slurry in a 300 mm semi-circular channel shape

| Slope | Critical velocity | V _c Fitton | % Deviation |
|-------|-------------------|-----------------------|-------------|
| 1 | 0.49 | 0.80 | 62 |
| 2 | 0.66 | 0.80 | 20 |
| 3 | 0.76 | 0.84 | 10 |
| 4 | 0.86 | 0.78 | -9 |
| 5 | - | - | - |

Table 5.11: 4.5% bentonite in water slurry in a 150 mm trapezoidal channel shape

| Slope | Critical velocity | V _c Fitton | % Deviation |
|-------|-------------------|-----------------------|-------------|
| 1 | 0.70 | 0.78 | 11 |
| 2 | 0.88 | 0.88 | 0 |
| 3 | 0.96 | 0.82 | -15 |
| 4 | 1.05 | 0.83 | -21 |
| 5 | 1.23 | 0.87 | -30 |

Table 5.12: 4.5% bentonite in water slurry in a 300 mm triangular channel shape

| Slope | Critical velocity | V _c Fitton | % Deviation |
|-------|-------------------|-----------------------|-------------|
| 1 | 0.77 | 0.87 | 13 |
| 2 | 0.86 | 0.86 | 0 |
| 3 | 1.16 | 0.96 | -17 |
| 4 | 1.25 | 0.95 | -24 |
| 5 | 1.36 | 0.95 | -30 |

The critical and Fitton velocities tabulated from Table 5.9 to 5.12 were plotted in Figure 5.19. It can be seen that 63% of the data points fall within the +/- 20% deviation region.

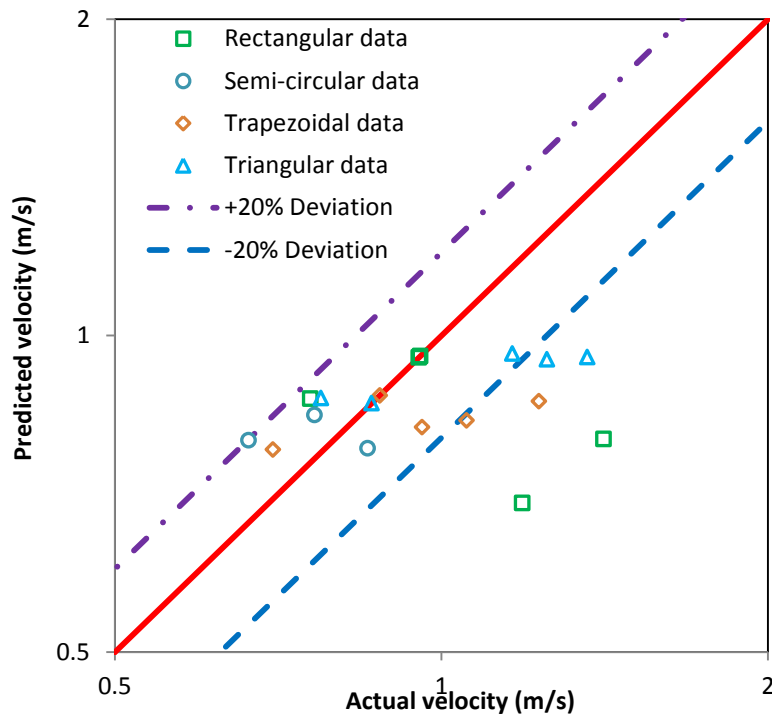


Figure 5.19: Fitton's transition model for 4.5% bentonite in water slurry

5.2.4 Evaluation of yield shear-thinning fluids

Yield shear-thinning fluids are characterised by a yield stress and an apparent viscosity which decreases with an increasing shear rate. Coussot (1997), Haldenwang (2003), Fitton (2008) as well as Slatter (2013) models were used for the evaluation of yield shear-thinning fluids.

5.2.4.1 Work done by Coussot

Coussot (1997) based his work on the Hanks criteria and developed a model that can be used to predict the onset of turbulence of mudflow, which he characterised as a Herschel-Bulkley fluid. His model is applicable for infinitely wide channels or thin film flow. Coussot's (1997) model can be applied to rectangular and trapezoidal channels. Coussot stated that the flow reaches turbulence when the flow depth becomes larger than h defined by Equation 2.86.

Coussot's prediction is evaluated for 5.3% kaolin in water slurries since it is characterised as a Herschel-Bulkley fluid. Tables 5.13 and 5.14 show that Coussot's prediction of transition improves with an increase of the flume slope.

Table 5.13: 5.3% kaolin in water slurry flowing in a 300 mm rectangular channel shape

| Slope | Critical velocity | V_c Coussot | % Deviation |
|--------------|--------------------------|------------------------------|--------------------|
| 1 | 0.83 | 0.35 | -57 |
| 2 | 0.88 | 0.64 | -27 |
| 3 | 1.06 | 0.79 | -25 |
| 4 | 1.03 | 0.90 | -13 |
| 5 | 1.16 | 0.89 | -23 |

Table 5.14: 5.3% kaolin in water slurry flowing in a 150 mm trapezoidal channel shape

| Slope | Critical velocity | V_c Coussot | % Deviation |
|--------------|--------------------------|------------------------------|--------------------|
| 1 | 1.20 | 0.19 | -84.2 |
| 2 | 1.24 | 0.63 | -48.8 |
| 3 | 1.31 | 0.70 | -46.8 |
| 4 | 1.63 | 0.91 | -44.3 |
| 5 | 1.69 | 1.02 | -39.8 |

Coussot's prediction works better in a rectangular channel shape compared to the trapezoidal shape considered in this work since the error is quite significant. Coussot's prediction model of transition does not give in general a good prediction as shown in Figure 5.20 where only 10% of the data are within the +/- 20% deviation range.

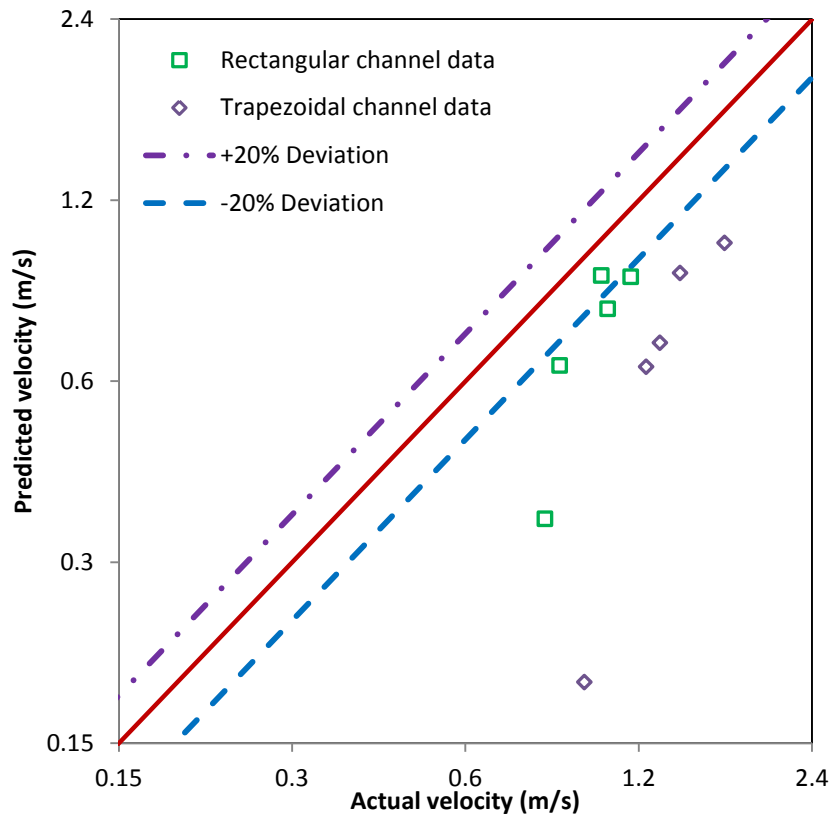


Figure 5.20: Coussot's transition model for kaolin in water slurries

5.2.4.2 Work done by Haldenwang

Haldenwang established a model to predict the onset of transition as well as the onset of turbulence for a rectangular open channel. Figures 5.21 and 5.22 show the evaluation of Haldenwang's (2003) prediction model of transition for kaolin in water slurries in four different shapes.

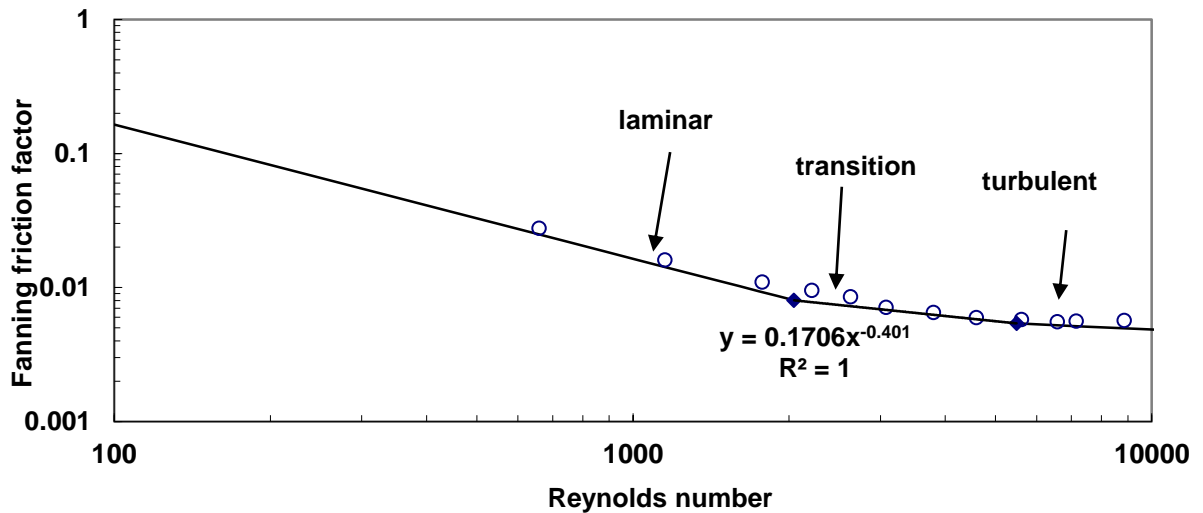


Figure 5.21: Prediction of transition. 5.3% kaolin in water slurry flowing in a 150 mm rectangular flume at 3° slope

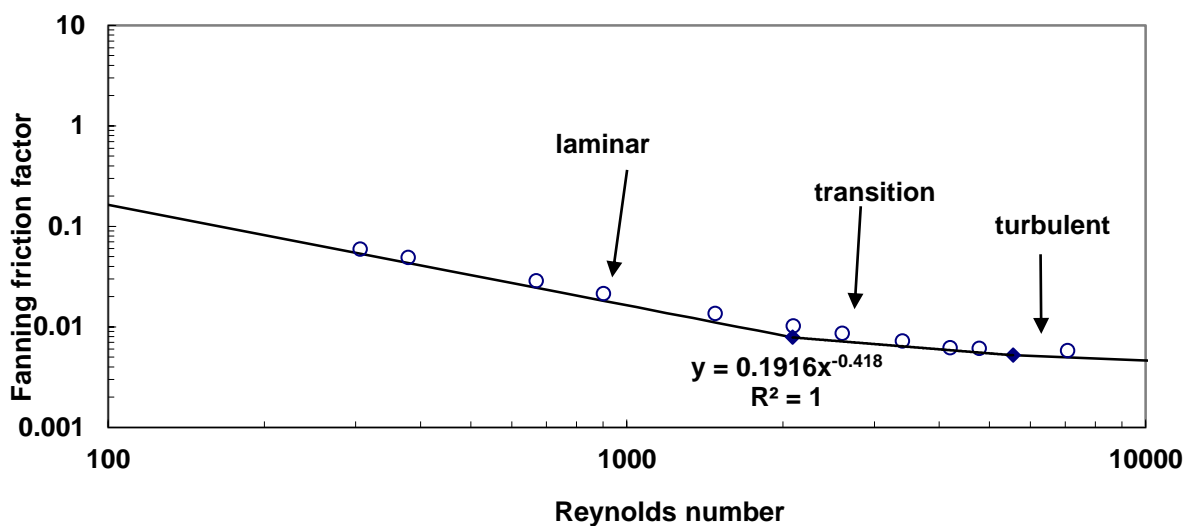


Figure 5.22: Prediction of transition. 5.3% kaolin in water slurry flowing in a 300 mm rectangular shape at 3° slope

Figures 5.21 and 5.22 show that Haldenwang's (2010) prediction is acceptable for the onset as well as the end of transitional flow in the rectangular flume shape considered in this study. The deviation ranges of Haldenwang's critical model of transition are presented in Tables 5.15 and 5.16.

Table 5.15: Haldenwang's transition model for 5.3% kaolin in water slurry flowing in a 150 mm rectangular channel

| Slope (°) | Critical velocity (m/s) | V_c Haldenwang (m/s) | % Deviation |
|------------------|--------------------------------|---------------------------------------|--------------------|
| 1 | 0.75 | 0.79 | 6 |
| 2 | 0.77 | 0.97 | 26 |
| 3 | 0.91 | 1.11 | 22 |
| 4 | 1.27 | 1.25 | -2 |
| 5 | 1.33 | 1.37 | 3 |

Table 5.16: Haldenwang's transition model for 5.3% kaolin in water slurry flowing in a 300 mm rectangular channel

| Slope (°) | Critical velocity (m/s) | V_c Haldenwang (m/s) | % Deviation |
|------------------|--------------------------------|---------------------------------------|--------------------|
| 1 | 0.83 | 0.83 | 1 |
| 2 | 0.88 | 1.00 | 14 |
| 3 | 1.06 | 1.14 | 7 |
| 4 | 1.03 | 1.26 | 22 |
| 5 | 1.16 | 1.39 | 19 |

Figure 5.23 shows that Haldenwang's transition model works well as 70% of the data points lie within the +/- 20% deviation region.

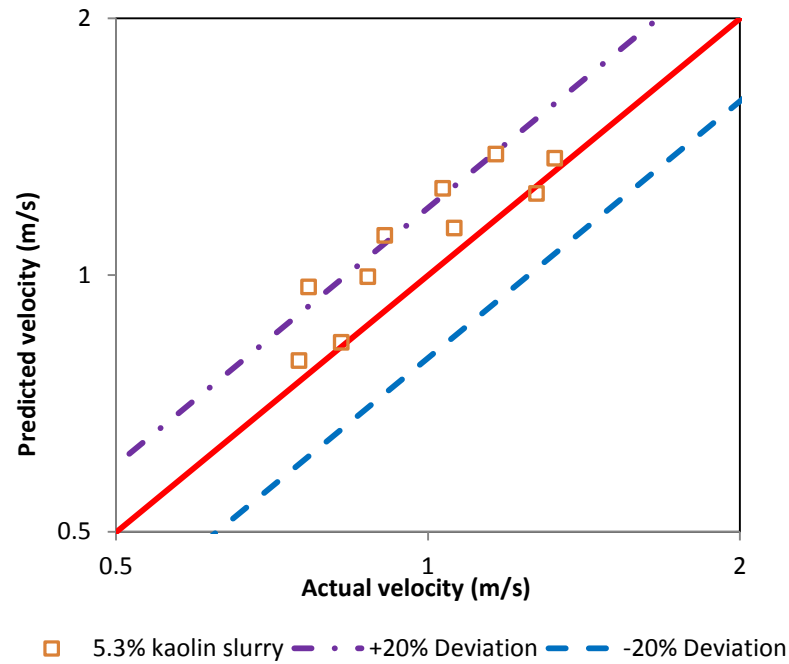


Figure 5.23: Haldenwang’s transition model for kaolin in water slurries

5.2.4.3 Work done by Fitton

Figure 5.24 shows the evaluation of Fitton’s (2008) prediction of transition for various channels geometries. Although Fitton (2008) conducted experiments in semi-circular channels, he stated that his laminar-turbulent transition prediction model could be applied to other geometries of open channels. Furthermore, he tested his model using rectangular flume data.

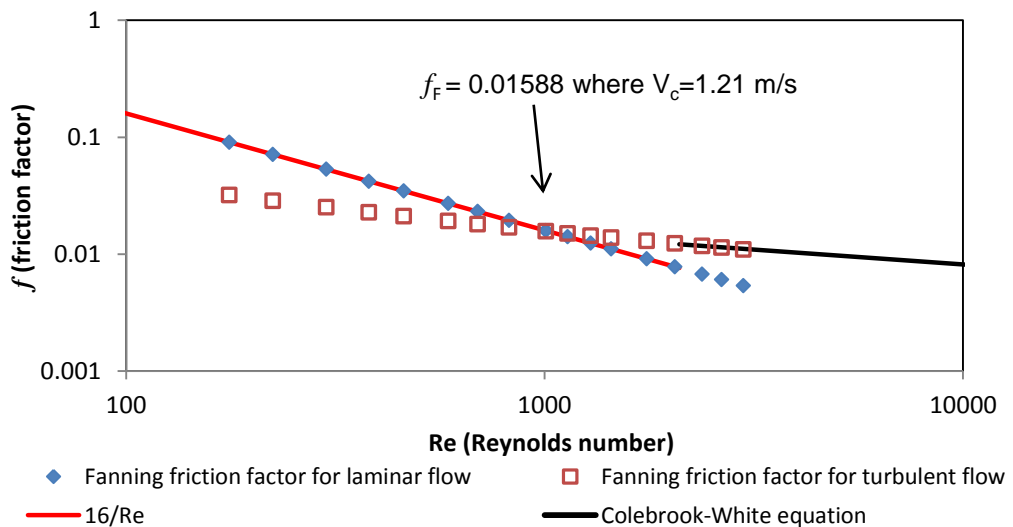


Figure 5.24: Prediction of transition. 7.2% kaolin in water slurry flowing in a 150 mm rectangular channel

It can be seen in Figure 5.24 that the point of transition occurs at a Fanning friction factor of 0.016 for 7.2% kaolin in water slurry flowing in a 150 mm rectangular channel. The same procedure was used to determine transition points for all fluids used in all the different shapes available in this study.

The corresponding critical velocities determined using Fitton's (2008) prediction was compared to the critical velocities obtained using Haldenwang (2003) as well as Slatter and Wasp (2000) models and the values are tabulated from Table 5.17 to 5.20.

Table 5.17: 5.3% kaolin in water slurry flowing in a 300 mm rectangular channel shape

| Slope (°) | Critical velocity (m/s) | V_c Fitton (m/s) | % Deviation |
|------------------|--------------------------------|-----------------------------------|--------------------|
| 1 | 0.83 | 0.83 | 0 |
| 2 | 0.88 | 0.80 | -9 |
| 3 | 1.06 | 0.85 | -20 |
| 4 | 1.03 | 0.80 | -23 |
| 5 | 1.16 | 0.89 | -23 |

Table 5.18: 5.3% kaolin in water slurry flowing in a 300 mm semi-circular channel shape

| Slope (°) | Critical velocity (m/s) | V_c Fitton (m/s) | % Deviation |
|------------------|--------------------------------|-----------------------------------|--------------------|
| 1 | 0.54 | 0.72 | 34 |
| 2 | 0.84 | 0.74 | -12 |
| 3 | 0.84 | 0.70 | -16 |
| 4 | 1.10 | 0.98 | -10 |
| 5 | 1.26 | 1.11 | -12 |

Table 5.19: 5.3% kaolin in water slurry flowing in a 150 mm trapezoidal channel shape

| Slope (°) | Critical velocity (m/s) | V_c Fitton (m/s) | % Deviation |
|------------------|--------------------------------|-----------------------------------|--------------------|
| 1 | 0.97 | 0.89 | -7 |
| 2 | 1.24 | 0.85 | -32 |
| 3 | 1.31 | 0.88 | -33 |
| 4 | 1.42 | 0.86 | -49 |
| 5 | 1.69 | 1.02 | -40 |

Table 5.20: 5.3% kaolin in water slurry flowing in a 300 mm triangular channel shape

| Slope (°) | Critical velocity (m/s) | V_c Fitton (m/s) | % Deviation |
|------------------|--------------------------------|-----------------------------------|--------------------|
| 1 | 0.92 | 0.81 | -12 |
| 2 | 0.93 | 0.82 | -12 |
| 3 | 1.12 | 0.83 | -26 |
| 4 | 1.23 | 0.87 | -29 |
| 5 | 1.24 | 0.86 | -30 |

From Table 5.17 to 5.20, it can be seen that for Fitton's (2008) prediction of transition in all channel shapes, 45% of the data is within the +/- 20% deviation range as illustrated in Figure 5.25.

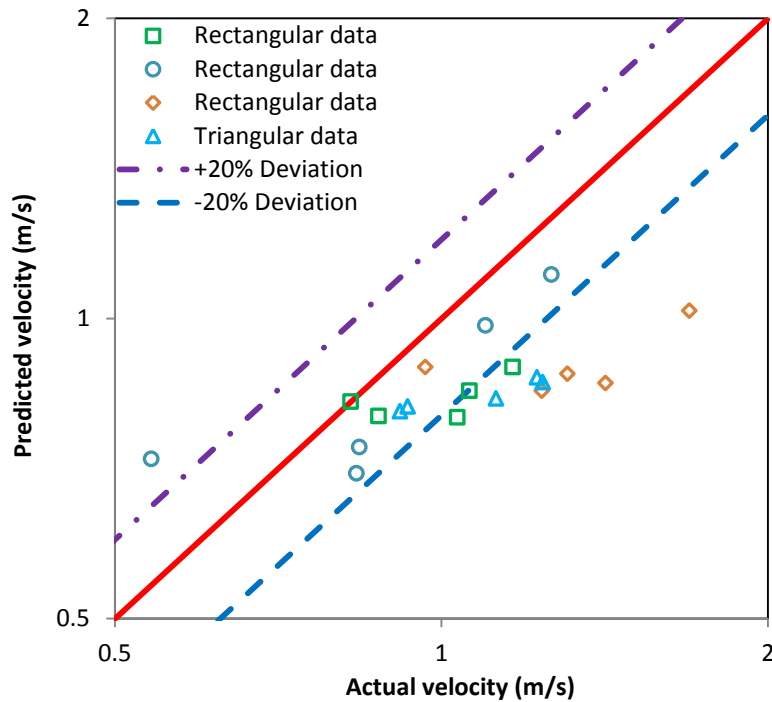


Figure 5.25: Fitton's transition model for kaolin in water slurries

5.2.4.4 Work done by Slatter

Slatter (2013a) extended the sheet flow analysis from a power law fluid to viscoplastic materials. Slatter (2013a) validated his model for sheet flow using rectangular flume data published by Haldenwang (2003). Thus Slatter's (2013a) model is used in this work, but only flow depths of less than 30 mm in the 300 mm flume ($h/B < 0.1$) were considered (Cousot, 1994).

Slatter (2013b) introduced another criterion to predict transitional flow velocity which was defined by Equation (2.98).

Figure 5.26 shows a plot of the wall shear stress versus the bulk shear rate with transition points obtained by using the criterion $Re_4=700$ as well as the critical velocity V_c as an alternative criterion (Slatter, 2013a). He set his $Re_4=700$ criterion by using a normalised adherence function defined in equation 2.96) since below Re_4 of 700, the flow was laminar and approached unity. In the vicinity of $Re_4=700$, he observed that laminar flow ceased to exist since in this region, the NAF started to deviate from one. Slatter (2013b) stated that V_c defined in Equation 2.98 was independent of the hydraulic diameter and at that velocity occurs transitional flow.

Slatter (2013a) used a concentration of 6% kaolin flowing in a 300 mm rectangular flume. To apply his model, concentrations of 4.5% and 5.3% kaolin in water slurries were used as they cover the laminar, transition and turbulent flow regimes. The one degree slope data for the 5.3% kaolin in water slurry was omitted in Figure 5.26 since it does not meet the sheet flow criteria established by Coussot (1994). It can be seen from Figure 5.26 to 5.29 that Slatter's predictive model of transition for 5.3% kaolin in water slurry is slope sensitive with a greater deviation at the 5 degree slope. For a better distinction of the two criteria proposed by Slatter (2013), three slopes are separately plotted from Figure 5.27 to 5.29.

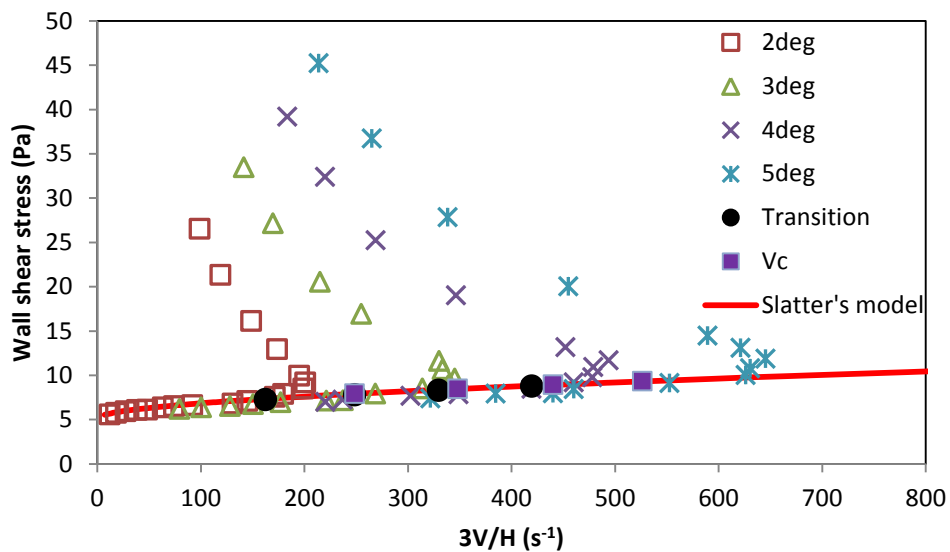


Figure 5.26: 5.3% kaolin in water slurry flowing in a 300 mm rectangular flume

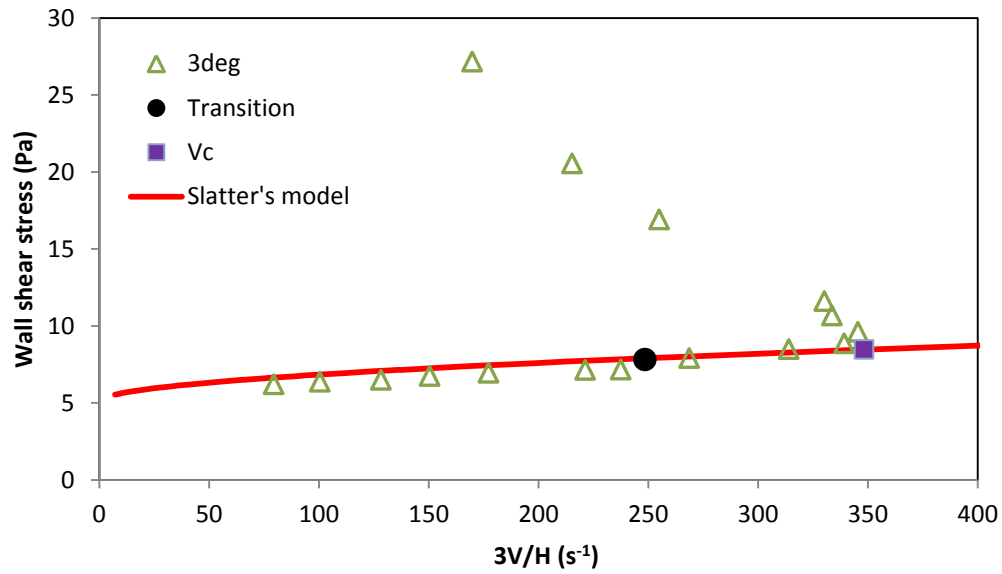


Figure 5.27: Slatter's transition model for 5.3% kaolin in water slurry flowing in a 300 mm rectangular flume at 3 degrees slope

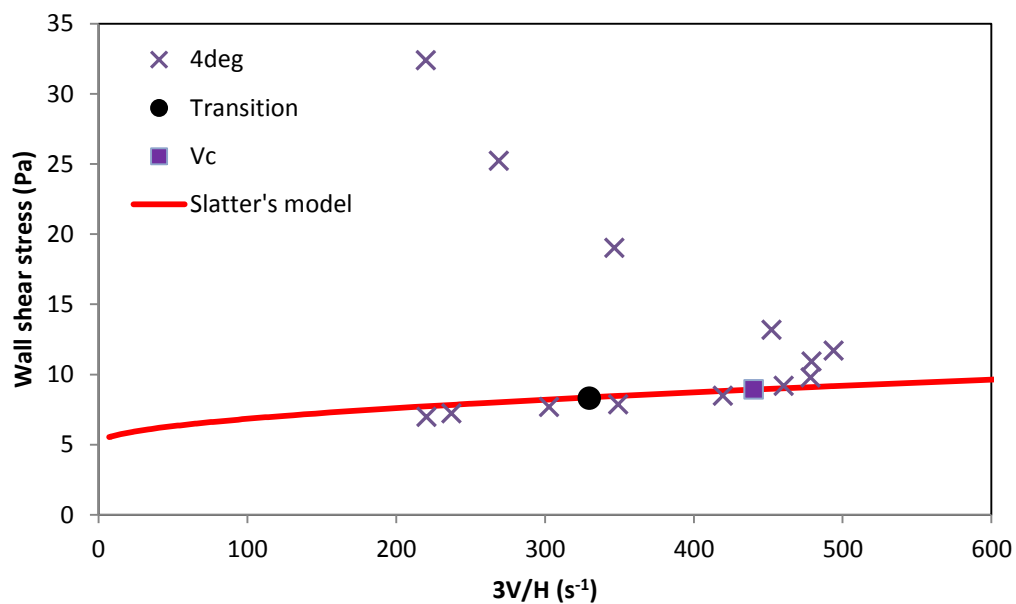


Figure 5.28: Slatter's transition model for 5.3% kaolin in water slurry flowing in a 300 mm rectangular flume at 4 degrees slope

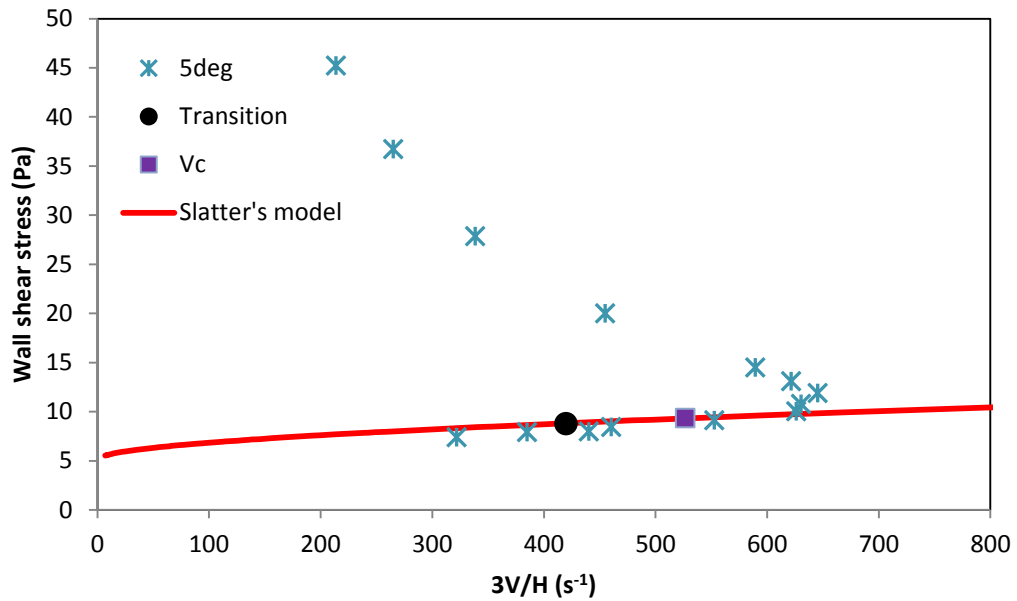


Figure 5.29: Slatter's transition model for 5.3% kaolin in water slurry flowing in a 300 mm rectangular flume at 5 degrees slope

Slatter's predictive model of transition was also evaluated for 4.5% kaolin. It can be seen that Slatter's predictive model of transition for 4.5% kaolin did not predict transition well with a greater deviation at the 5 degree slope as is illustrated from Figure 5.30 to 5.33.

Slatter's criterion model ($Re_4=700$) does not perform well as the onset of transition is not fixed at a single value. This is due to the fact that there are many parameters such as the flume slope and the fluid concentration which influence the onset of transitional flow.

The same goes for the critical velocity criterion which gives a single value of velocity at different slopes. Transitional flow is slope sensitive and thus cannot occur at the same velocity value at different flume slopes (Haldenwang, 2003).

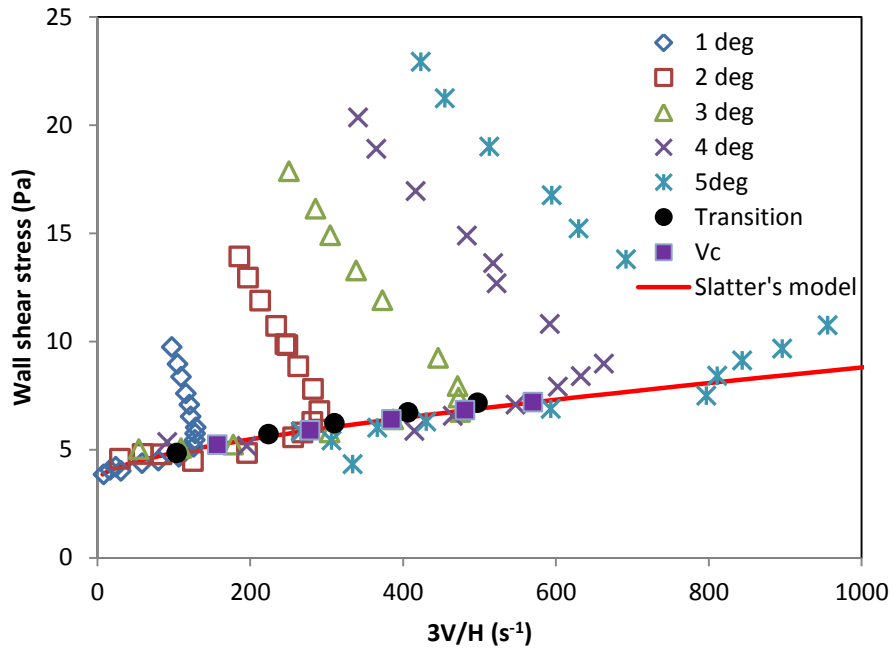


Figure 5.30: 4.5% kaolin in water slurry flowing in 300 mm rectangular flume

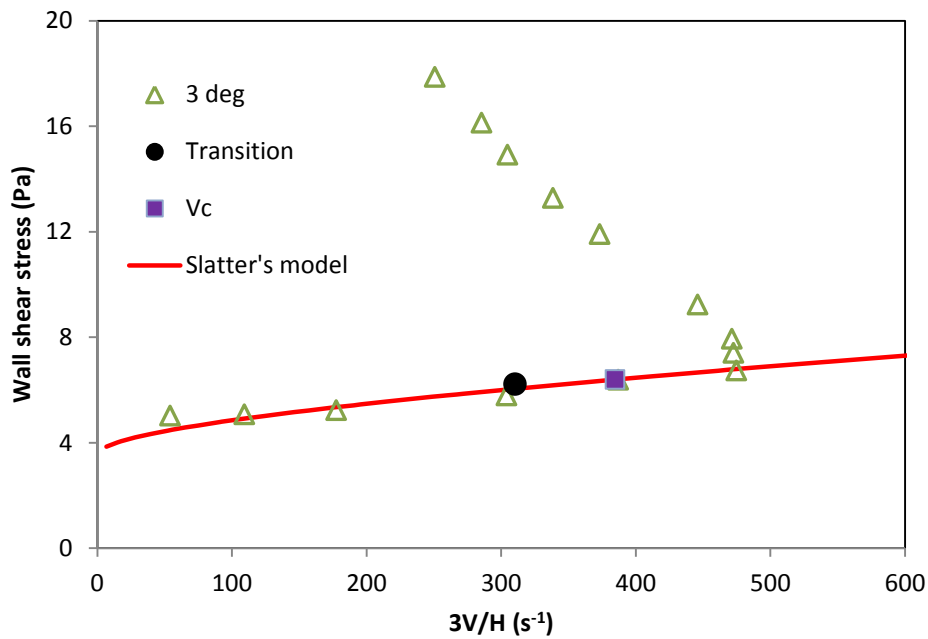


Figure 5.31: Slatter's transition model for 4.5% kaolin in water slurry flowing in a 300 mm rectangular flume at 3 degrees slope

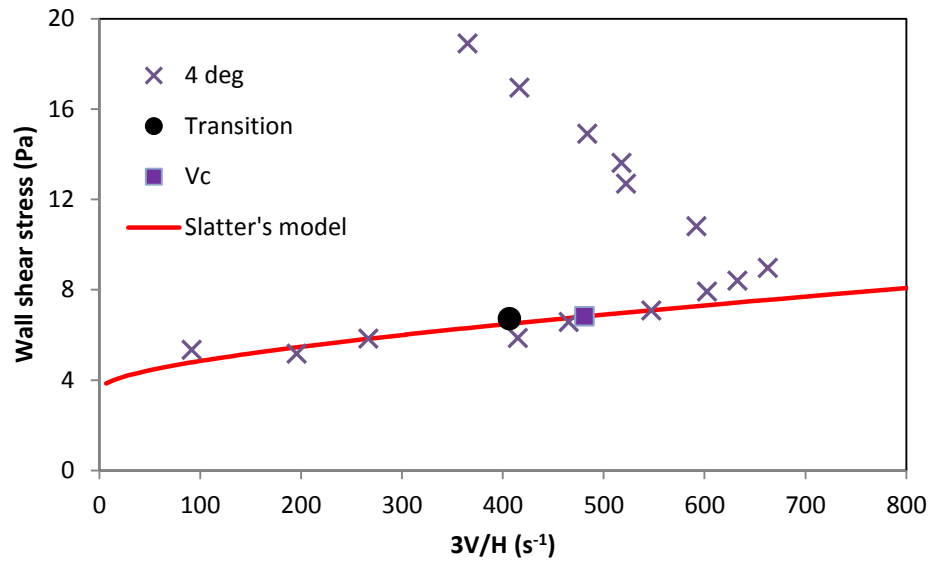


Figure 5.32: Slatter's transition model for 4.5% kaolin in water slurry flowing in a 300 mm rectangular flume at 4 degrees slope

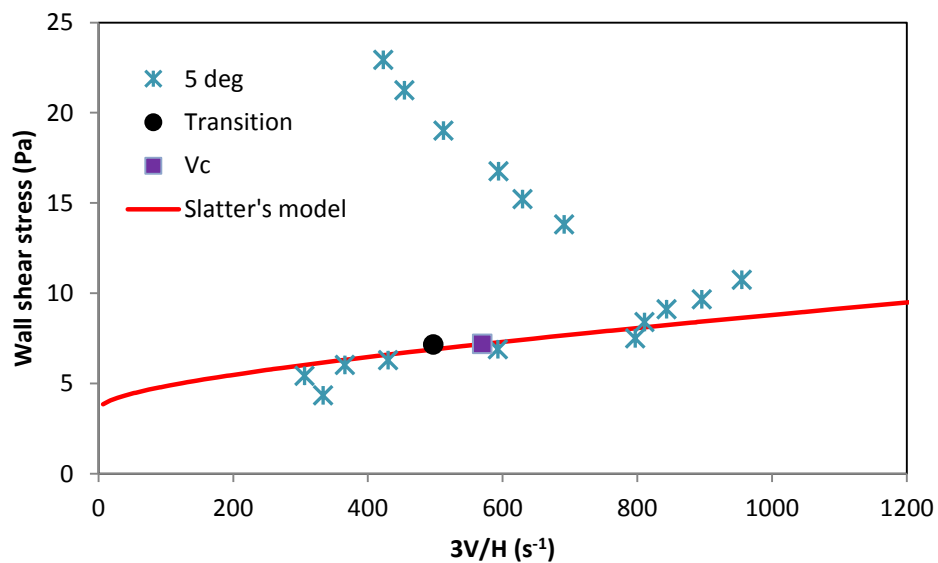


Figure 5.33: Slatter's transition model for 4.5% kaolin in water slurry flowing in a 300 mm rectangular flume at 5 degrees slope

Figure 5.34 shows Slatter's critical velocities ($Re_4=700$ and V_c) criteria used to predict transitional flow. It is shown that Slatter's Re_4 criterion works better than the V_c criterion since 22% of the data fall within the $\pm 20\%$ deviation range for the $Re_4=700$ criterion compared to 10% of the transition data for the V_c criterion. However, both predictions are poor.

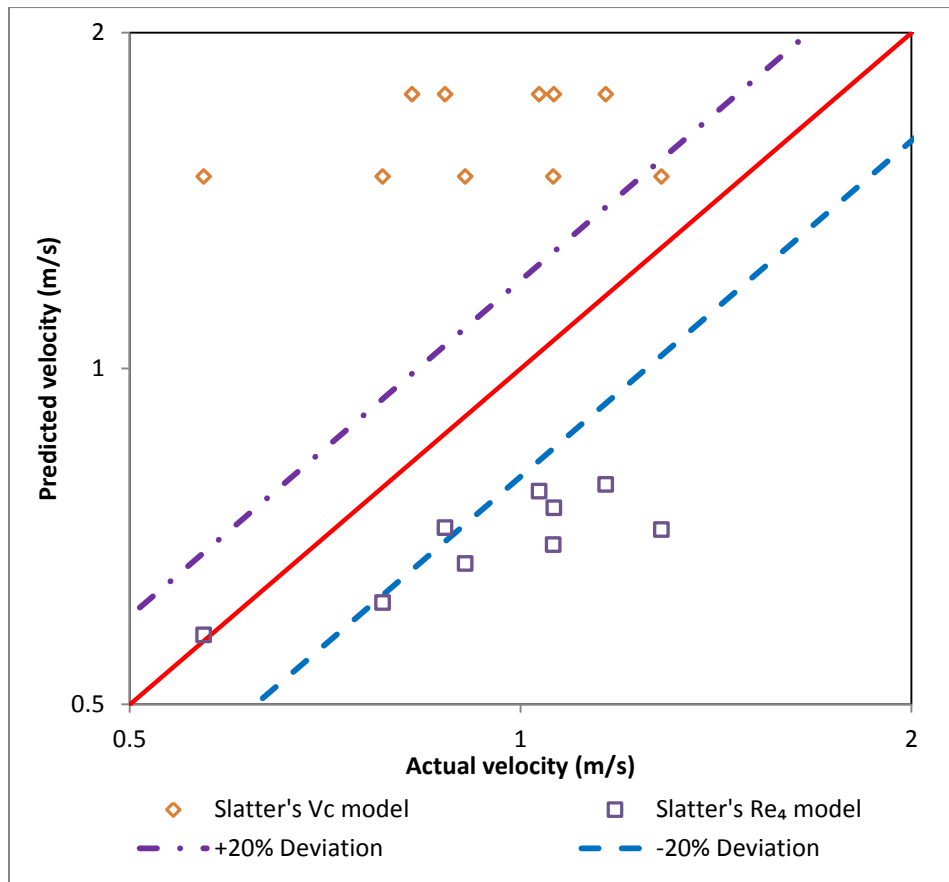


Figure 5.34: Slatter's transition models ($Re_4=700$ and V_c criteria) for 4.5% & 5.3% kaolin in water slurries in a 300 mm rectangular flume

5.2.5 Comparison between models

In this section, comparisons between the various models used to predict transition for power law, Bingham plastic and yield shear-thinning fluids are made. These comparisons are made to determine the optimum model for each type of fluid.

5.2.5.1 Comparison between Haldenwang and Fitton's models for power law fluids

Haldenwang (2003), Fitton (2008) and Slatter (2013) models were used to predict transition for power law fluids. In this section, the Re_H rectangular model shown in graphs and tables refers to the Haldenwang's critical Reynolds number model for rectangular channels. Figure 5.35 shows how well are the predicted critical velocity values against the actual experimental values. Figure 5.36 is a histogram on which the frequency indicates the number of critical velocities of different models and the % deviation within which these values lie. It can be seen in Figures 5.35 and 5.36 that the Haldenwang and Fitton predictive models give better predictions compared to the Slatter's prediction. However, Fitton model only gives a single point of transition whereas Haldenwang model gives a range of transition points depending

on the flume slope. It can also be seen in Table 5.21 that 52% of the data predicted by Haldenwang's model fall within the $\pm 20\%$ deviation range. However, Fitton's and Slatter's predictions have a lower standard deviation and a wide spread of data points.

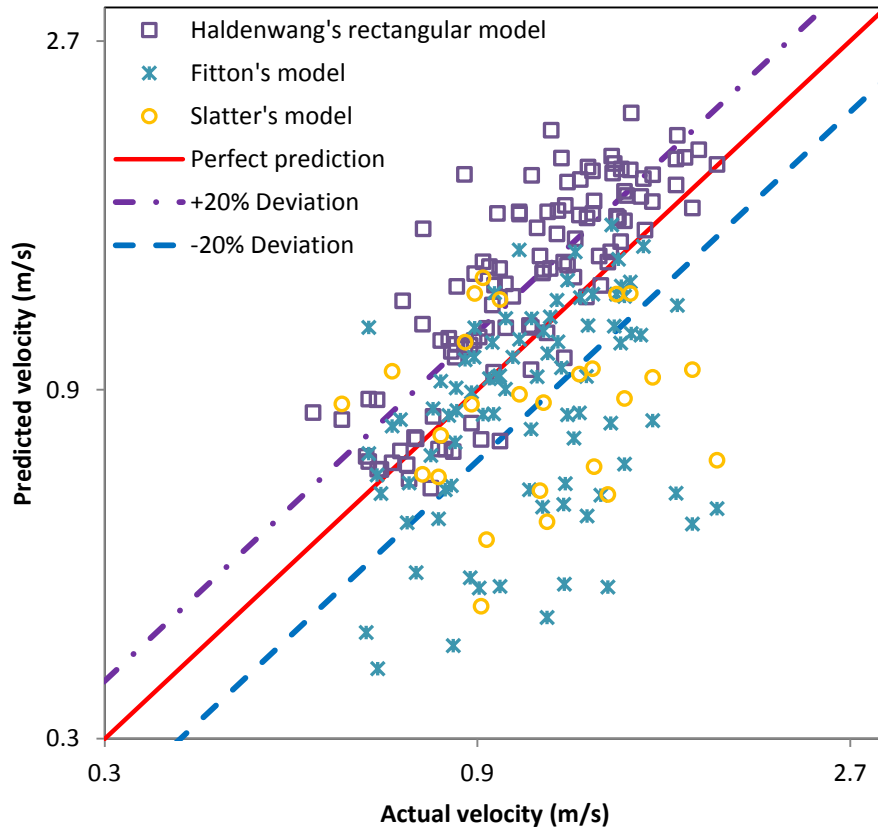


Figure 5.35: Comparison between Haldenwang, Fitton and Slatter models for transition for power law fluids

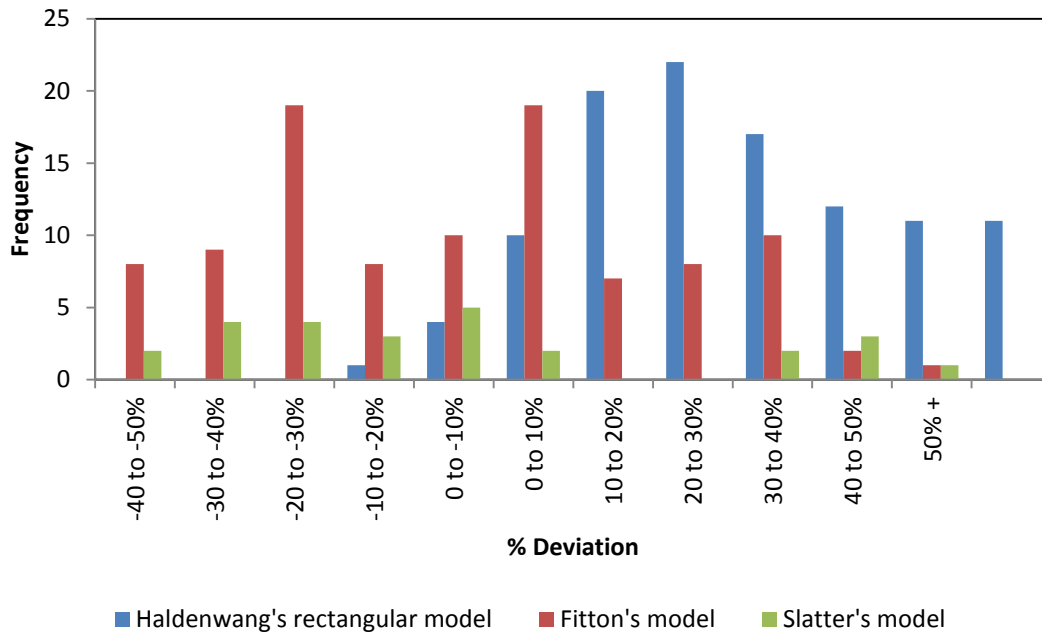


Figure 5.36: Comparison between critical models for power law fluids

Table 5.21: Statistical analysis for power law models

| | LSE | Min% Dev | Max % Dev | Standard deviation | % Data falling within +/- 20% region |
|-----------------------------------|--------|----------|-----------|--------------------|--------------------------------------|
| Re_H Rectangular | 0.0108 | -20 | 105 | 0.45 | 52 |
| Fitton's model | 0.0164 | -59 | 42 | 0.33 | 44 |
| Slatter's model | 0.037 | -60 | 43 | 0.32 | 27 |

5.2.5.2 Comparison between Haldenwang and Fitton's models for Bingham plastic fluids

Fitton (2008) and Haldenwang (2010) models were used to predict the transition velocities for Bingham plastic fluids. It is shown in Figures 5.37 and 5.38 that Haldenwang's model gives a better prediction in comparison with Fitton's model with 42% of data falling within the +/- 20% deviation range as indicated in Table 5.22. However Fitton's prediction is widely distributed whereas Haldenwang's prediction is skewed to the right.

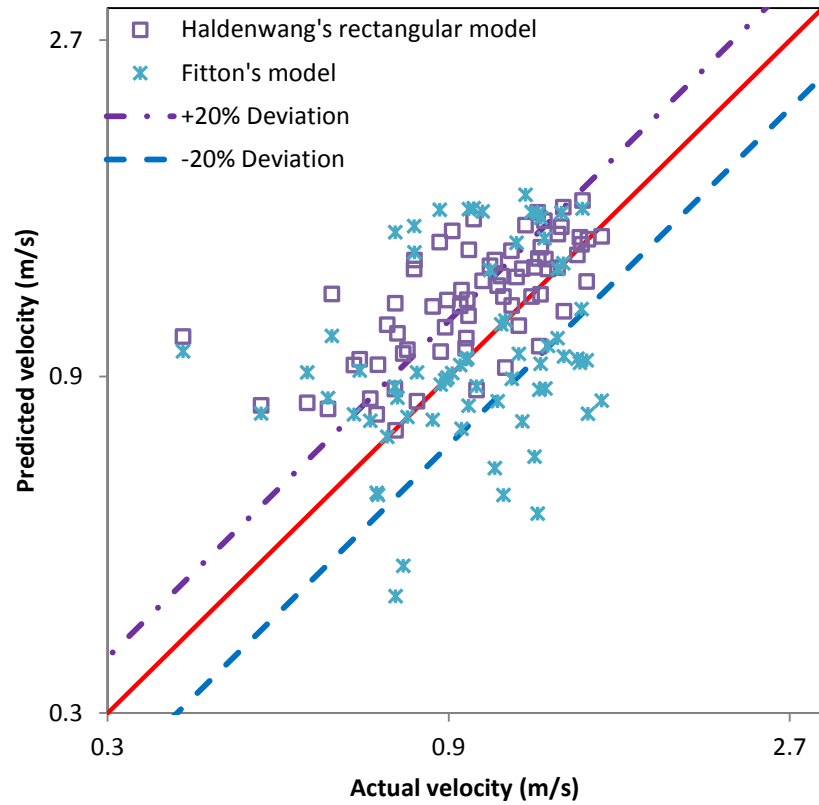


Figure 5.37: Comparison between Fitton and Haldenwang models for transition for Bingham plastic fluids

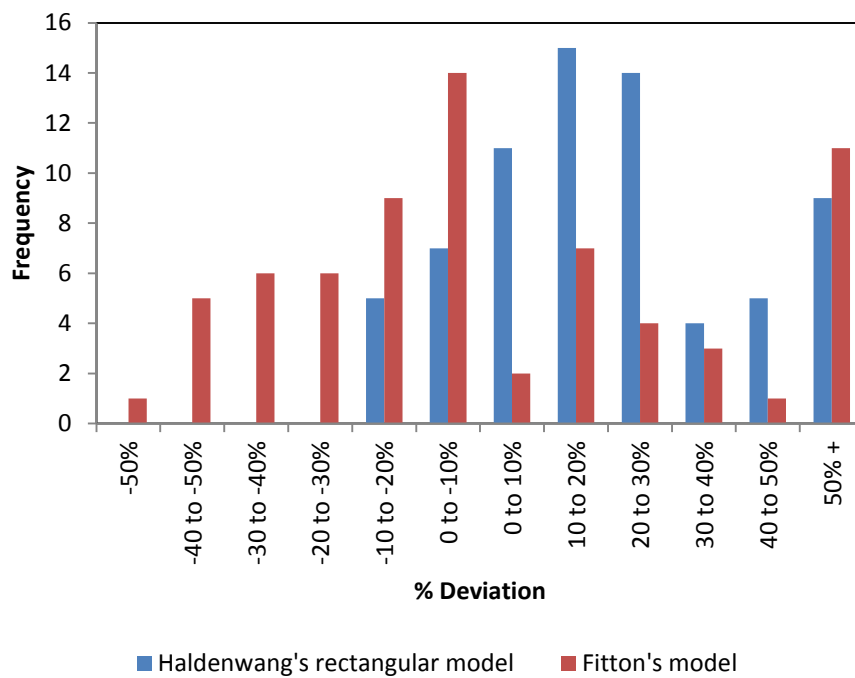


Figure 5.38: Comparison between critical velocity models for Bingham plastic fluids

Table 5.22: Statistical analysis for Bingham plastic models

| | LSE | Min% Dev | Max % Dev | Standard deviation | % Data falling within +/- 20% region |
|--------------------|--------|----------|-----------|--------------------|--------------------------------------|
| Re_H Rectangular | 0.0140 | -18 | 168 | 0.28 | 54 |
| Fitton's model | 0.0183 | -52 | 155 | 0.31 | 42 |

5.2.5.3 Comparison between Coussot, Haldenwang, Fitton and Slatter's models for yield shear-thinning fluids

Coussot (1997), Fitton (2008), Haldenwang (2010) and Slatter (2013) models were used to predict transition velocities for yield shear-thinning fluids. From Figure 5.39, it can be seen that Haldenwang's predictions of transition velocity work best for yield shear-thinning fluids compared to the Slatter, Fitton and Coussot predictions as indicated in Table 5.23 with 61% of the data falling within the +/- 20% deviation range. It can also be seen Haldenwang's prediction gives the smallest standard deviation. Figure 5.40 shows that the Fitton, Coussot and Slatter models give a wide distribution of data. However, Coussot and Fitton predictions are negatively skewed whereas Slatter's prediction is positively skewed.

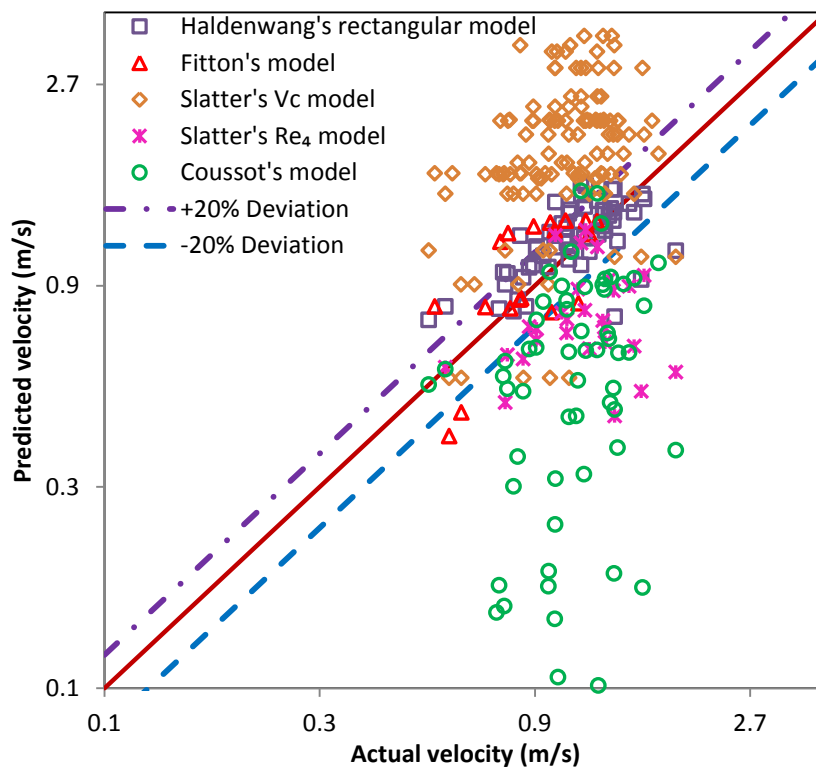


Figure 5.39: Comparison between the Coussot, Fitton, Haldenwang and Slatter models for transition velocity for yield shear-thinning fluids

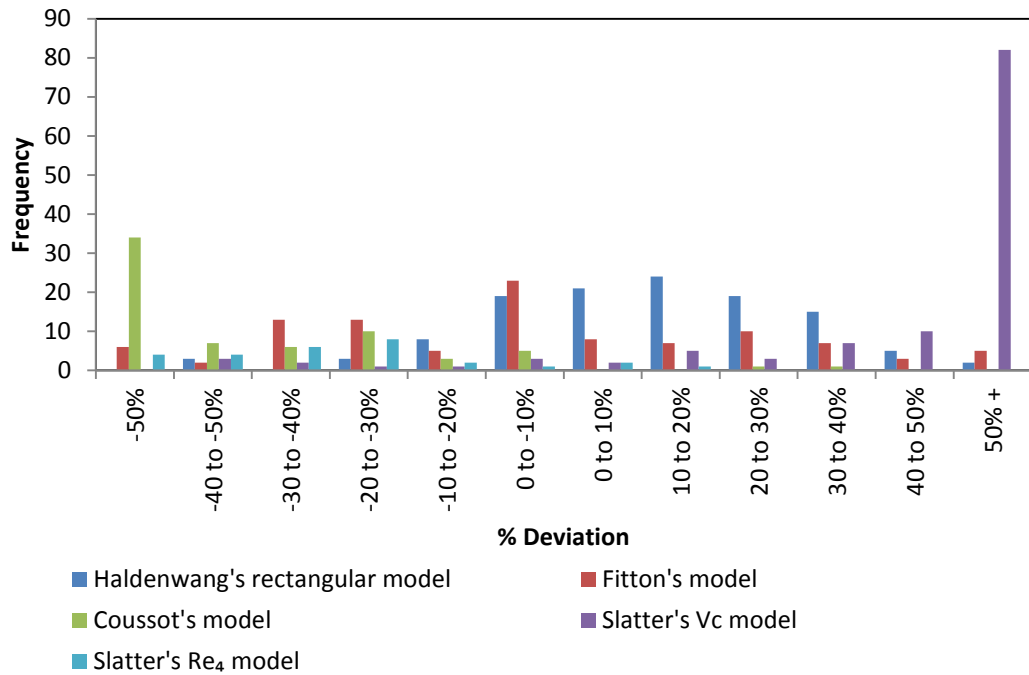


Figure 5.40: Comparison between critical velocity models for yield shear-thinning fluids

Table 5.23: Statistical analysis for yield shear-thinning models

| | LSE | Min% Dev | Max % Dev | Standard deviation | % Data falling within +/- 20% region |
|---------------------------------------|--------|----------|-----------|--------------------|--------------------------------------|
| Re_H Rectangular | 0.0083 | -44 | 57 | 0.24 | 61 |
| Fitton's model | 0.0195 | -90 | 86 | 0.36 | 42 |
| Slatter's Re₄ model | 0.0458 | -70 | 18 | 0.38 | 21 |
| Coussot's model | 0.0689 | -97 | 32 | 0.65 | 12 |
| Slatter's V_c model | 0.0276 | -49 | 300 | 1.13 | 9 |

5.3. End of transitional flow (Onset of turbulent flow)

The model developed by Haldenwang (2010) to predict the end of transitional flow is evaluated in this section for power law, Bingham plastic and yield shear-thinning fluids.

5.3.1 Power law fluids

The data points presented in Section 5.3 are from the rectangular channel. Figures 5.41 and 5.42 show that Haldenwang's (2010) critical Reynolds number model for end of transition in rectangular channels gives a good prediction for the onset of turbulence since 69% of the data points lie within the $\pm 20\%$ deviation range as indicated in Table 5.24. It can also be seen in Figure 5.42 that Haldenwang's prediction is positively skewed. Haldenwang's (2010) model is the only model available in the literature that gives a prediction for the end of transition for power law fluids in open channels. Thus, no comparison with other models can be made.

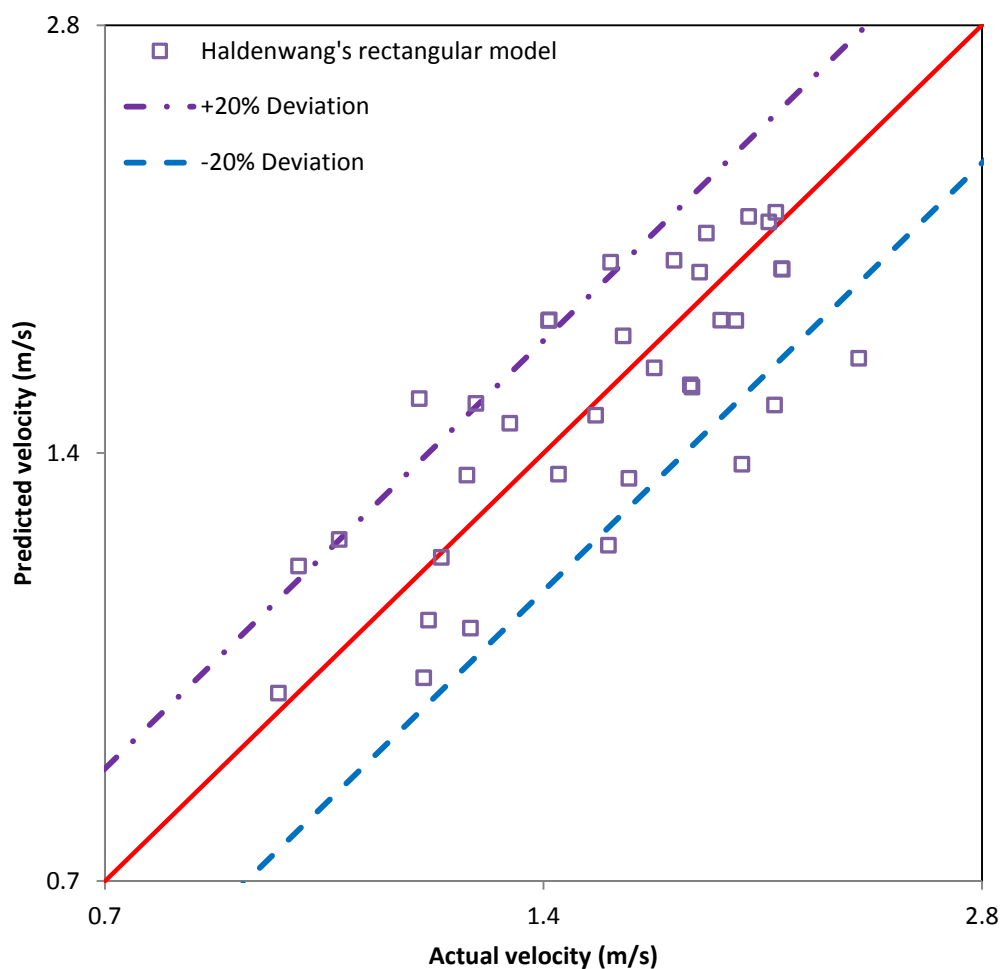


Figure 5.41: Haldenwang (2010) model for end of transition

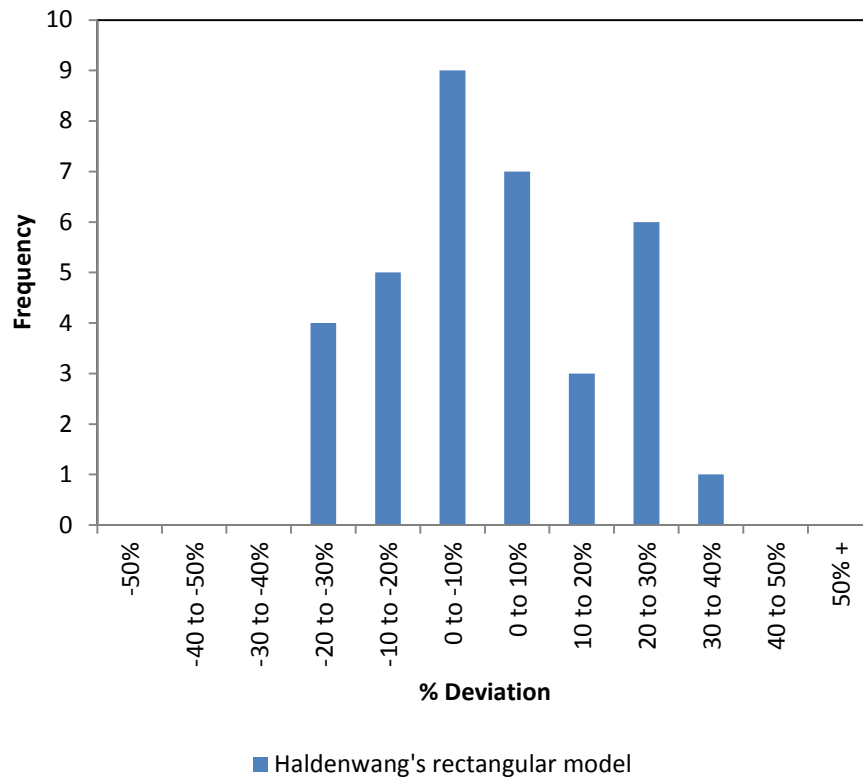


Figure 5.42: Haldenwang's prediction for end of transitional flow of a power law fluid

Table 5.24: Statistical analysis for Haldenwang's upper critical velocity model for a power law fluid

| | LSE | Min% Dev | Max % Dev | Standard deviation | % Data falling within +/- 20% region |
|--------------------|--------|----------|-----------|--------------------|--------------------------------------|
| Re_H Rectangular | 0.0121 | -29 | 33 | 0.32 | 69 |

5.3.2 Bingham plastic fluids

Figures 5.43 and 5.44 illustrate that Haldenwang's (2010) critical Reynolds number model for end of transition gives a good prediction for the onset of turbulence for Bingham plastic fluids since 80% of the data points lie within the +/- 20% deviation range as shown in Table 5.25. It is also shown in Figure 5.44 that Haldenwang's prediction is narrowly distributed.

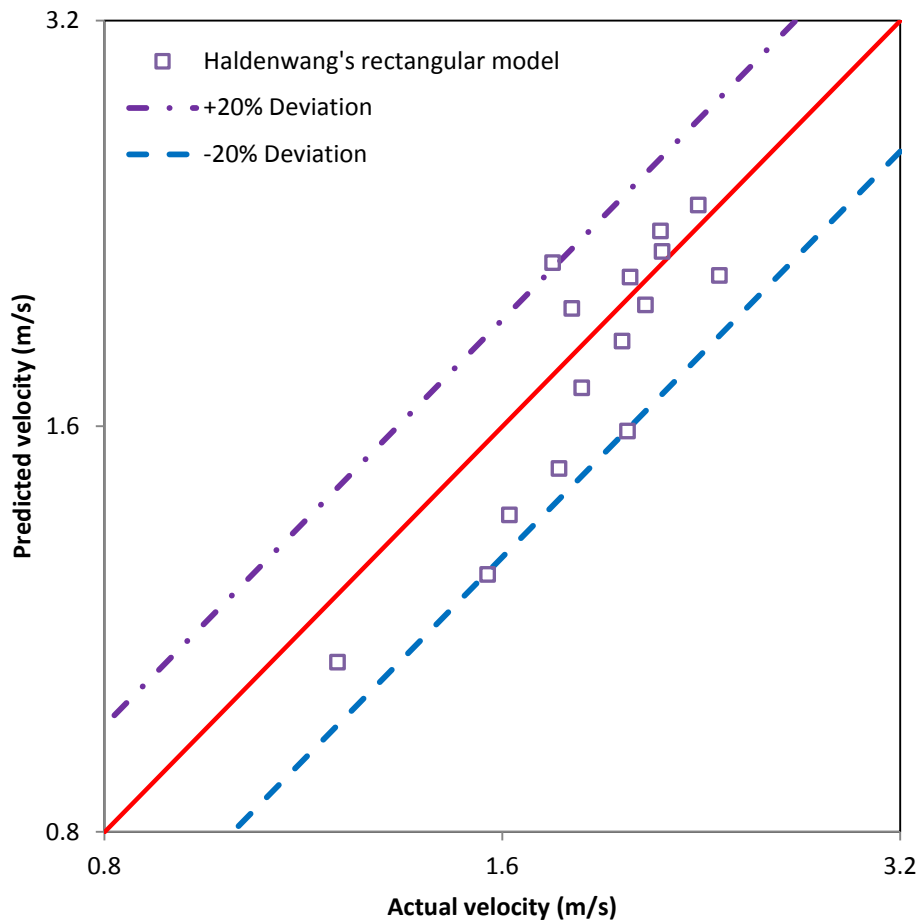


Figure 5.43: Haldenwang (2010) model for end transition

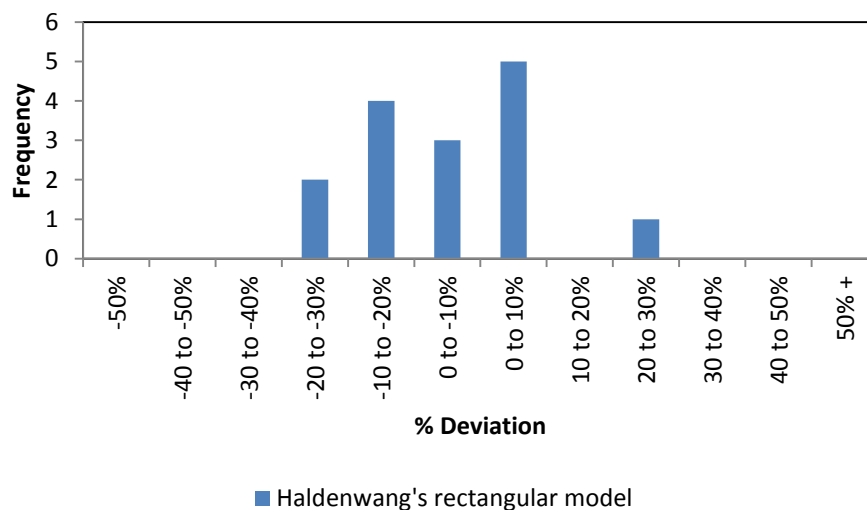


Figure 5.44: Haldenwang's prediction for end of transitional flow of a Bingham plastic fluid

Table 5.25: Statistical analysis for Haldenwang's upper critical model for a Bingham plastic fluid

| | LSE | Min% Dev | Max % Dev | Standard deviation | % Data falling within +/- 20% region |
|--------------------|--------|----------|-----------|--------------------|--------------------------------------|
| Re_H Rectangular | 0.0154 | -20 | 21 | 0.43 | 80 |

5.3.3 Yield shear-thinning fluids

It can be seen in Figures 5.45 and 5.46 that Haldenwang's (2010) model for end of transition gives a good prediction for the onset of turbulence for yield shear-thinning fluids since 89% of the data points lie within the +/- 20% deviation range as shown in Table 5.26. It is also illustrated in Figure 5.46 that Haldenwang's prediction is skewed to the right.

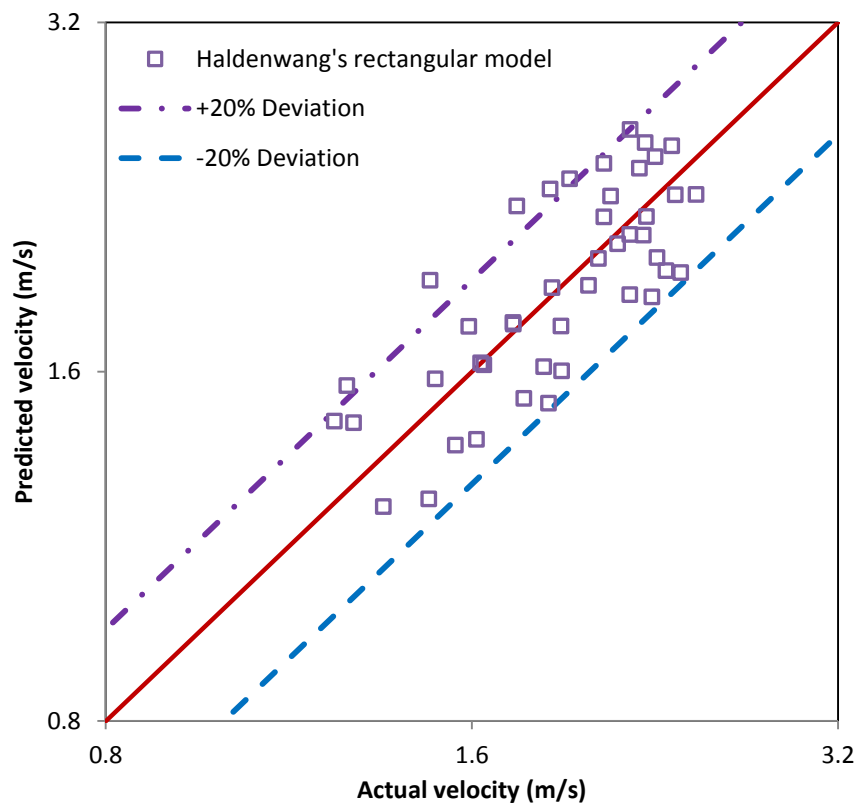


Figure 5.45: Haldenwang (2010) model for end of transition

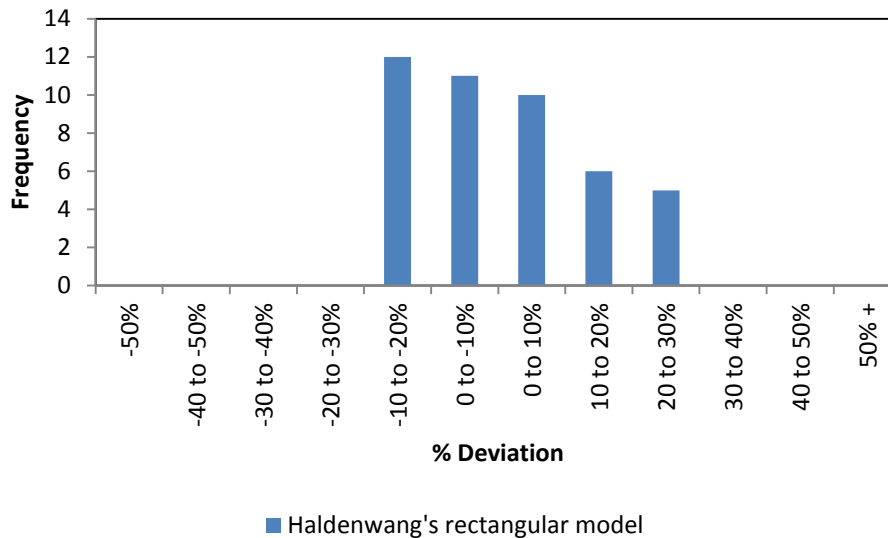


Figure 5.46: Haldenwang's prediction for end of transitional flow of a yield shear-thinning fluid

Table 5.26: Statistical analysis for Haldenwang's upper critical model for a yield shear-thinning fluid

| | LSE | Min% Dev | Max % Dev | Standard deviation | % Data falling within +/- 20% region |
|--------------------|--------|----------|-----------|--------------------|--------------------------------------|
| Re_H Rectangular | 0.0088 | -19 | 30 | 0.37 | 89 |

5.4. Comparison of the adapted transitional models

The adapted critical Reynolds numbers models were evaluated and compared to other models as shown from Figure 5.47 to 5.62. The onset and end of transitional flow in rectangular, triangular, semi-circular and trapezoidal flumes are evaluated respectively.

5.4.1 Onset of transitional flow: Rectangular flume

The critical Reynolds number developed by Haldenwang for a rectangular flume is compared against the combined model, Fitton's model and Coussot's model. The combined model was developed using data for all four different flume shapes. From Figures 5.47 and 5.48, it can be seen that the combined model gives the best prediction of transitional flow followed by Haldenwang's model. Coussot's predictive model gives the worst prediction with a greater standard deviation of 0.62 as presented in Table 5.27. From Figure 5.48, it is shown that Coussot's prediction is negatively skewed. The rectangular and combined models are

positively skewed. Fitton's model give a poor prediction with a wide distribution of data over the +/- 20% deviation range.

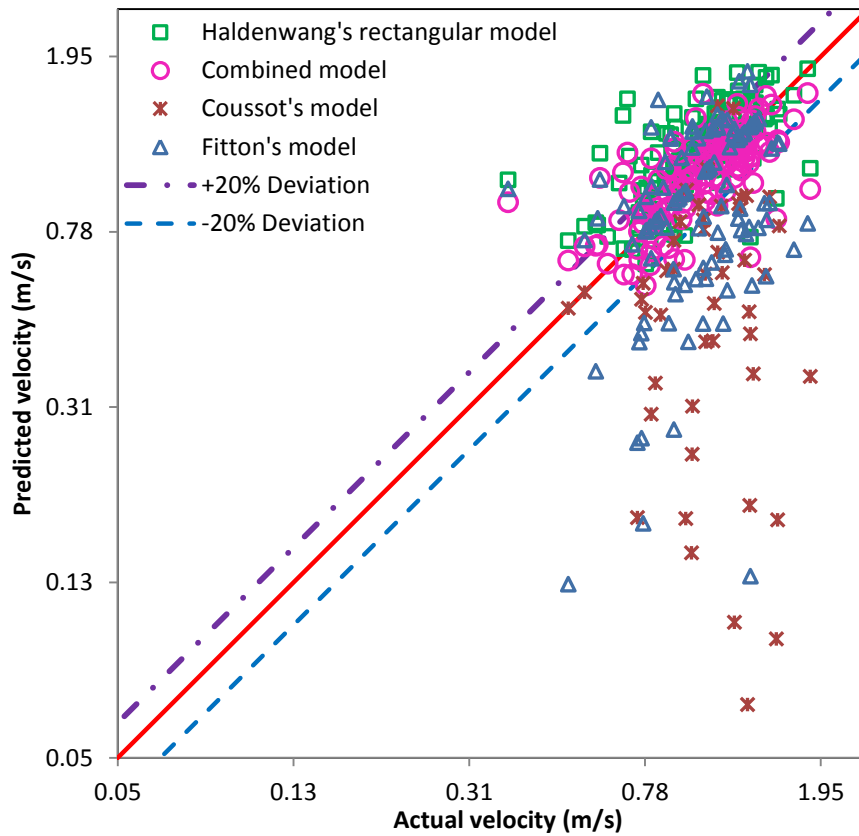


Figure 5.47: Model comparison for the onset of transition in a rectangular flume

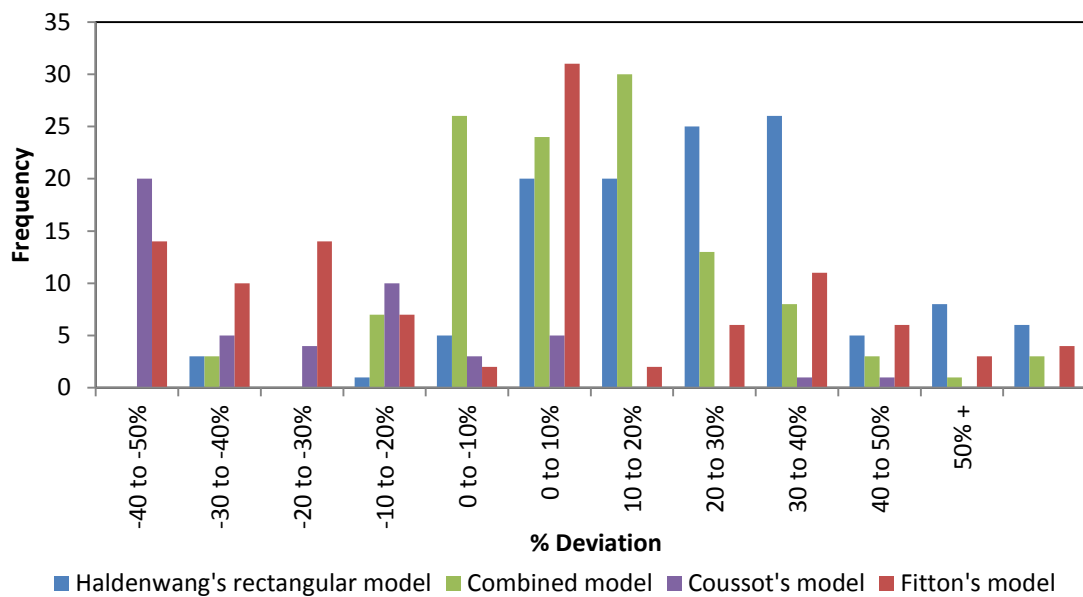


Figure 5.48: Onset of transitional flow in rectangular flume: model comparison

Table 5.27: Statistical analysis for the onset of transition in a rectangular flume

| | LSE | Min% Dev | Max % Dev | Standard deviation | % Data falling within the 20% margin |
|--------------------|--------|----------|-----------|--------------------|--------------------------------------|
| Re_H Rectangular | 0.0131 | -44 | 168 | 0.31 | 59 |
| Re_H Combined | 0.0121 | -49 | 138 | 0.24 | 79 |
| Re Fitton | 0.0238 | -90 | 155 | 0.38 | 37 |
| Re Coussot | 0.0694 | -95 | 32 | 0.62 | 16 |

5.4.2 End of transitional flow: Rectangular flume

Figures 5.49 and 5.50 present a comparison between the rectangular and the combined models for the prediction of the onset of turbulent flow. It can be seen that the rectangular model gives a better prediction than the combined model with 80% of the data points falling within the $\pm 20\%$ deviation range as suggested in Table 5.28. However, both models are positively skewed as shown in Figure 5.50.

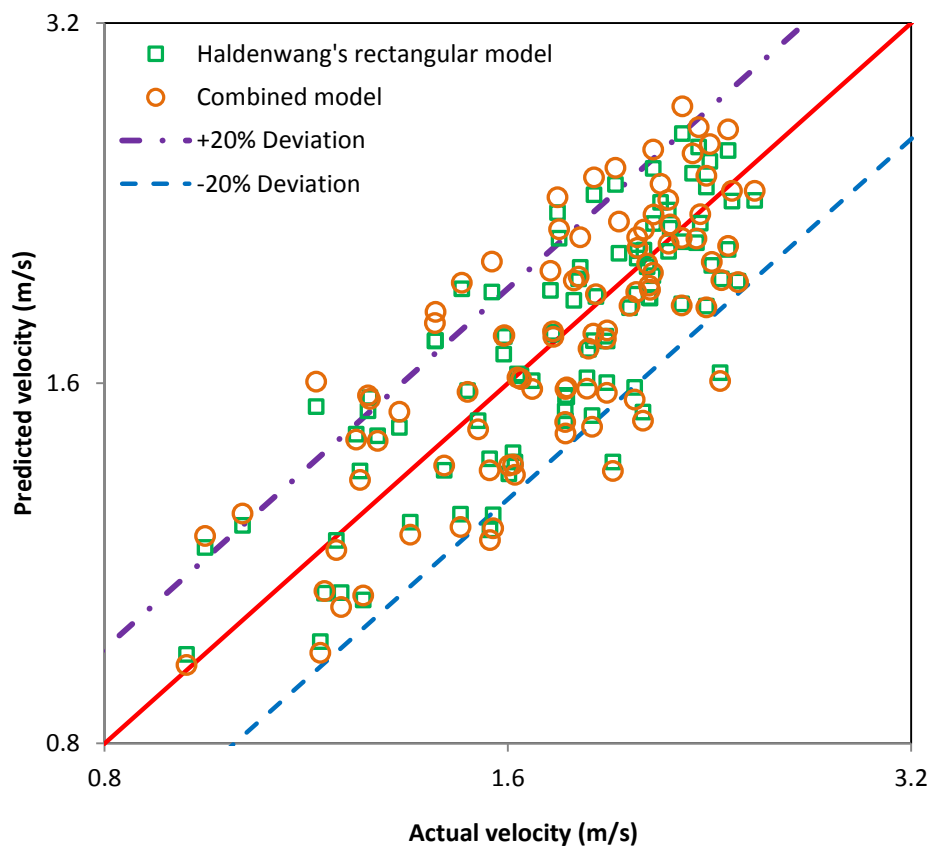


Figure 5.49: Model comparison for the end of transition in a rectangular flume

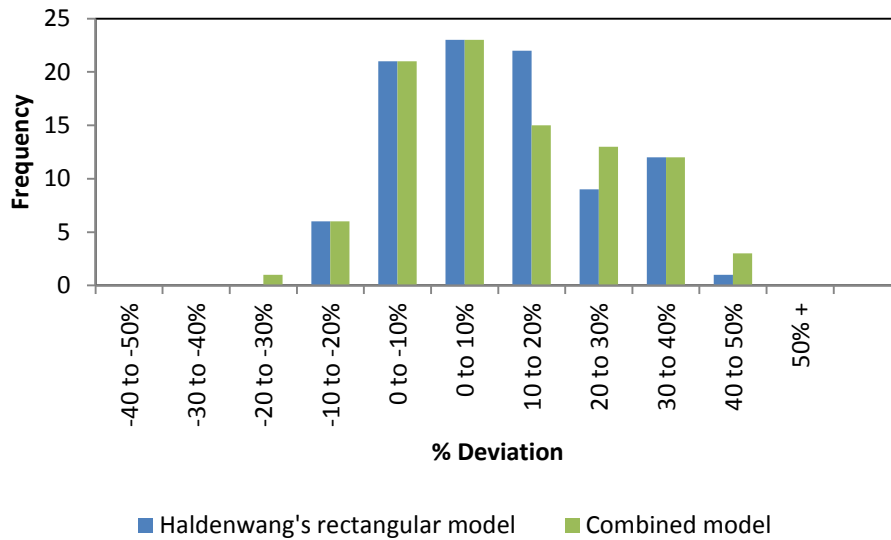


Figure 5.50: End of transitional flow in rectangular flume: model comparison

Table 5.28: Statistical analysis for the end of transition in a rectangular flume

| | LSE | Min% Dev | Max % Dev | Standard deviation | % Data falling within the 20% margin |
|-----------------------------------|--------|----------|-----------|--------------------|--------------------------------------|
| Re_H Rectangular | 0.0065 | -29 | 33 | 0.33 | 80 |
| Re_H Combined | 0.0072 | -30 | 39 | 0.36 | 77 |

5.4.3 Onset of transitional flow: Triangular flume

The adapted critical Reynolds number for triangular channels is compared against the combined model and the Fitton's model. From Figure 5.51, it can be seen that all models give a good prediction of transitional flow with the best ones being the triangular and the combined models as presented in Table 5.29. Figure 5.52 shows the data distribution on a % deviation basis. It is shown that the triangular model is skewed to the right with a narrow distribution of data whereas Fitton's model gives a wide distribution of data.

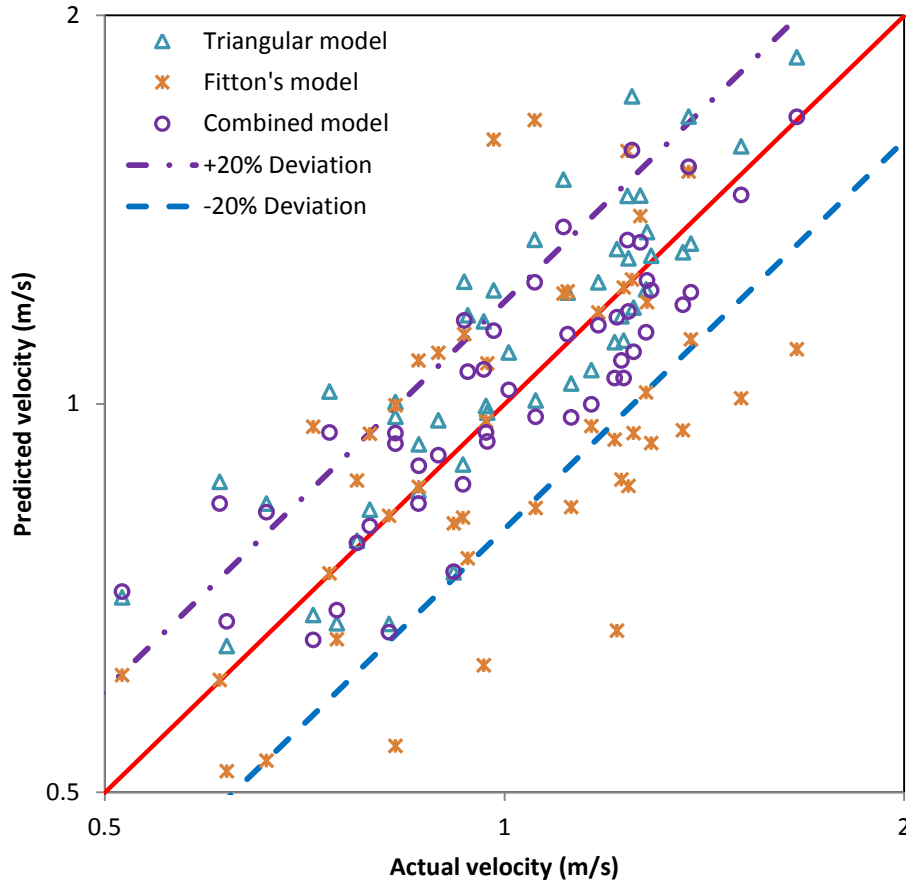


Figure 5.51: Model comparison for the onset of transition in a triangular flume

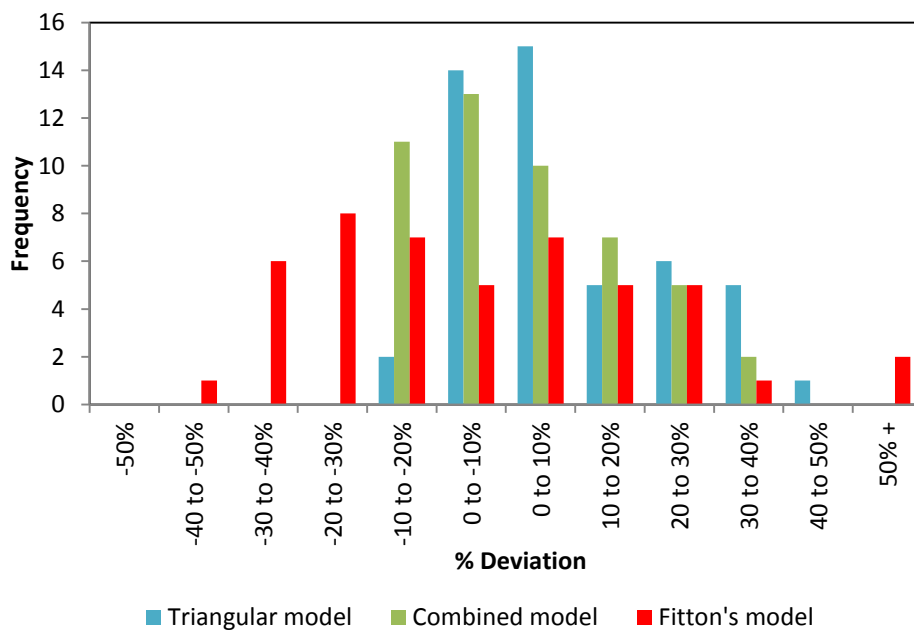


Figure 5.52: Onset of transitional flow in triangular flume: model comparison

Table 5.29: Statistical analysis for the onset of transition in a triangular flume

| | LSE | Min% Dev | Max % Dev | Standard deviation | % Data falling within the 20% margin |
|----------------------------------|------------|---------------------|----------------------|-------------------------------|---|
| Re_H Triangular | 0.0101 | -19 | 42 | 0.3 | 75 |
| Re_H Combined | 0.0087 | -19 | 39 | 0.24 | 85 |
| Re Fitton | 0.0164 | -45 | 63 | 0.28 | 51 |

5.4.4 End of transitional flow: Triangular flume

Figure 5.53 shows a comparison between the triangular and combined models for the prediction of the onset of turbulent flow. It can be seen that the triangular model was less favourable since 33% of the data points were within the +/- 20% deviation range. Various attempts were made to improve the triangular model but there was no significant difference of the result. Table 5.30 suggests that the combined model predicts better the end of transitional flow in a triangular flume. This is clearly shown in Figure 5.54. It is also shown in Figure 5.54 that the prediction of the triangular model is positively skewed with the highest standard deviation.

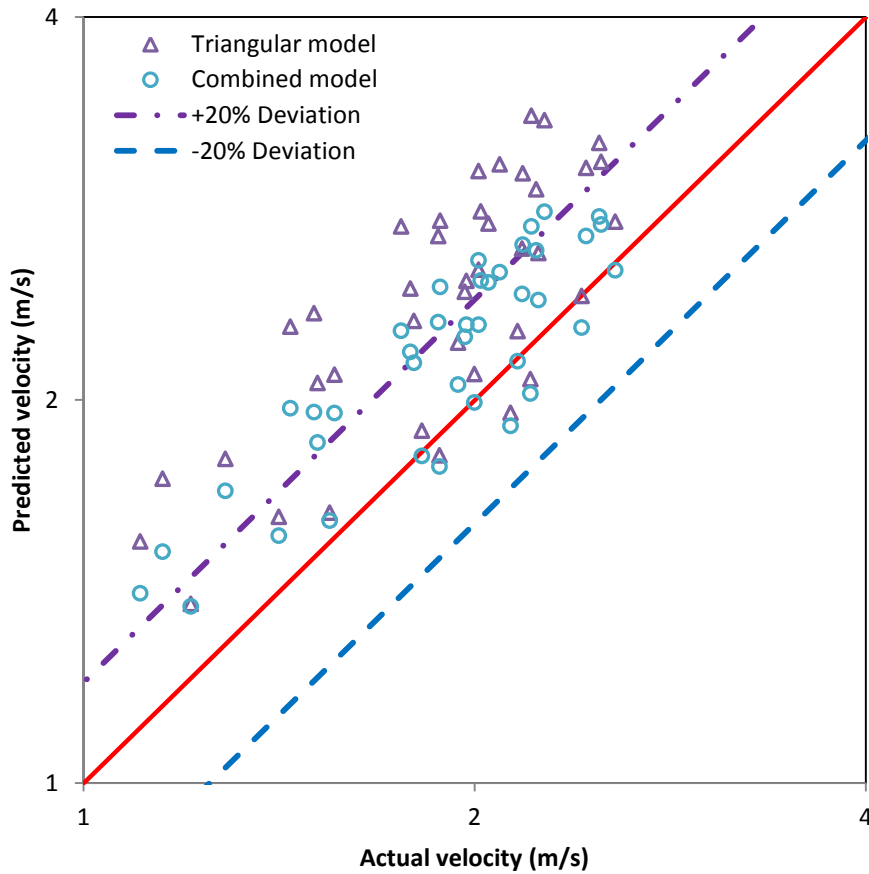


Figure 5.53: Model comparison for the end of transition in a triangular flume

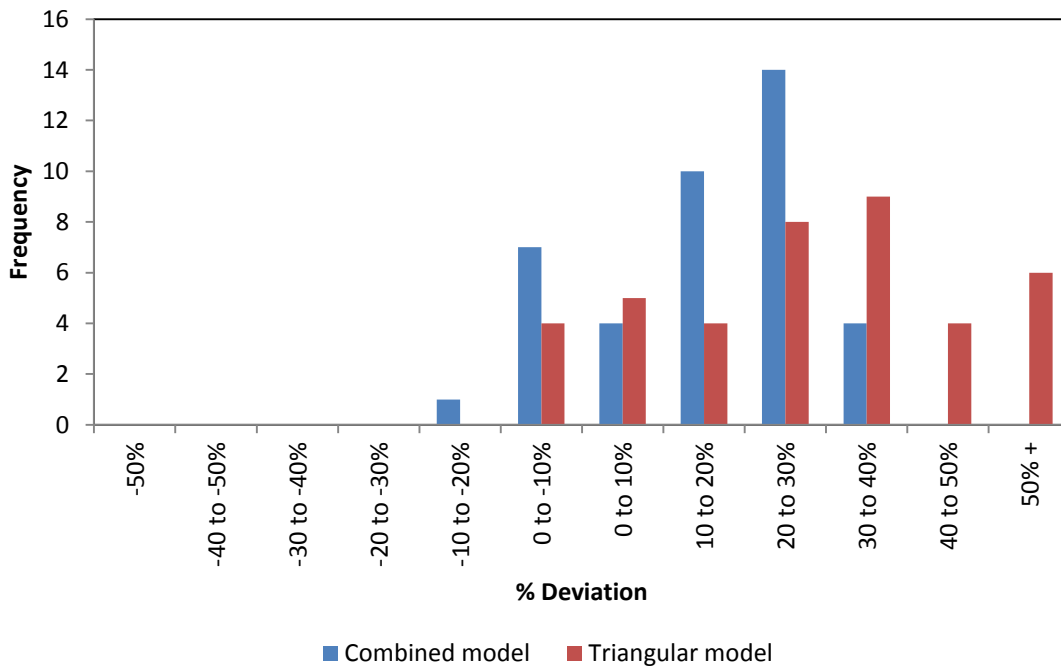


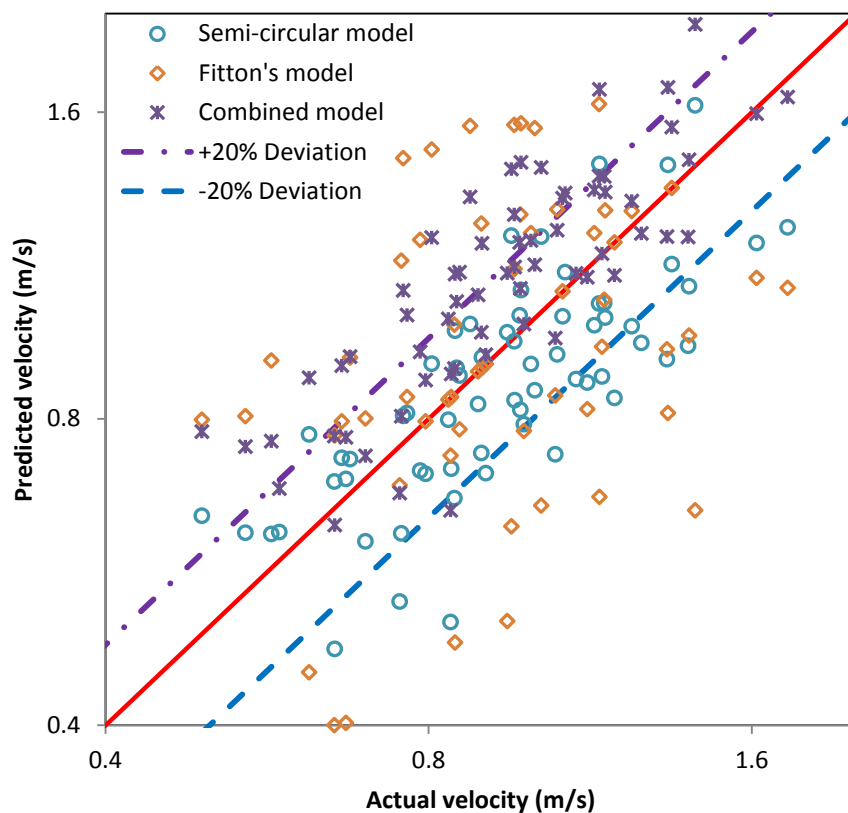
Figure 5.54: End of transitional flow in triangular flume: model comparison

Table 5.30: Statistical analysis for the end of transition in a triangular flume

| | LSE | Min% Dev | Max % Dev | Standard deviation | % Data falling within the 20% margin |
|-------------------|--------|----------|-----------|--------------------|--------------------------------------|
| Re_H Triangular | 0.0195 | -8 | 58 | 0.73 | 33 |
| Re_H Combined | 0.0122 | -11 | 37 | 0.48 | 55 |

5.4.5 Onset of transitional flow: Semi-circular flume

The adapted critical Reynolds number for semi-circular channels is compared against the combined model and Fitton's model. From Figure 5.55 and Table 5.31, it can be seen that the semi-circular model gives the best prediction. It is shown in Figure 5.56 that the combined and Fitton models are positively skewed. Fitton's model gives the worst prediction of transitional flow with 41% data points falling within the +/-20% deviation range as presented in Table 5.31.

**Figure 5.55: Model comparison for the onset of transition in a semi-circular flume**

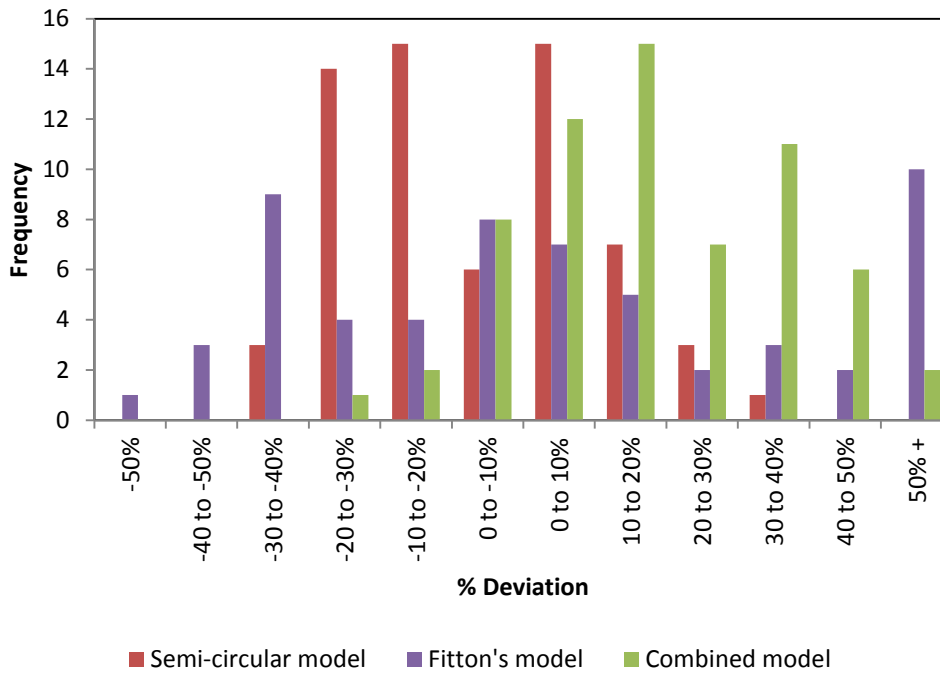


Figure 5.56: Onset of transitional flow in semi-circular flume: model comparison

Table 5.31: Statistical analysis for the onset of transition in a semi-circular flume

| | LSE | Min% Dev | Max % Dev | Standard deviation | % Data falling within the 20% margin |
|-------------------------------------|--------|----------|-----------|--------------------|--------------------------------------|
| Re_H Semi-circular | 0.0110 | -40 | 30 | 0.24 | 67 |
| Re_H Combined | 0.0119 | -23 | 58 | 0.32 | 58 |
| Re Fitton | 0.0205 | -54 | 90 | 0.32 | 41 |

5.4.6 End of transitional flow: Semi-circular flume

Figure 5.57 shows a comparison between the semi-circular and combined models for the prediction of the onset of turbulent flow. It can be seen that both models give a good prediction of transition since three quarters of the data points were within the +/- 20% deviation range as suggested in Table 5.32. Figure 5.58 and Table 5.32 suggest that the semi-circular model gives the best prediction. It is also shown in Figure 5.58 that both models are positively skewed.

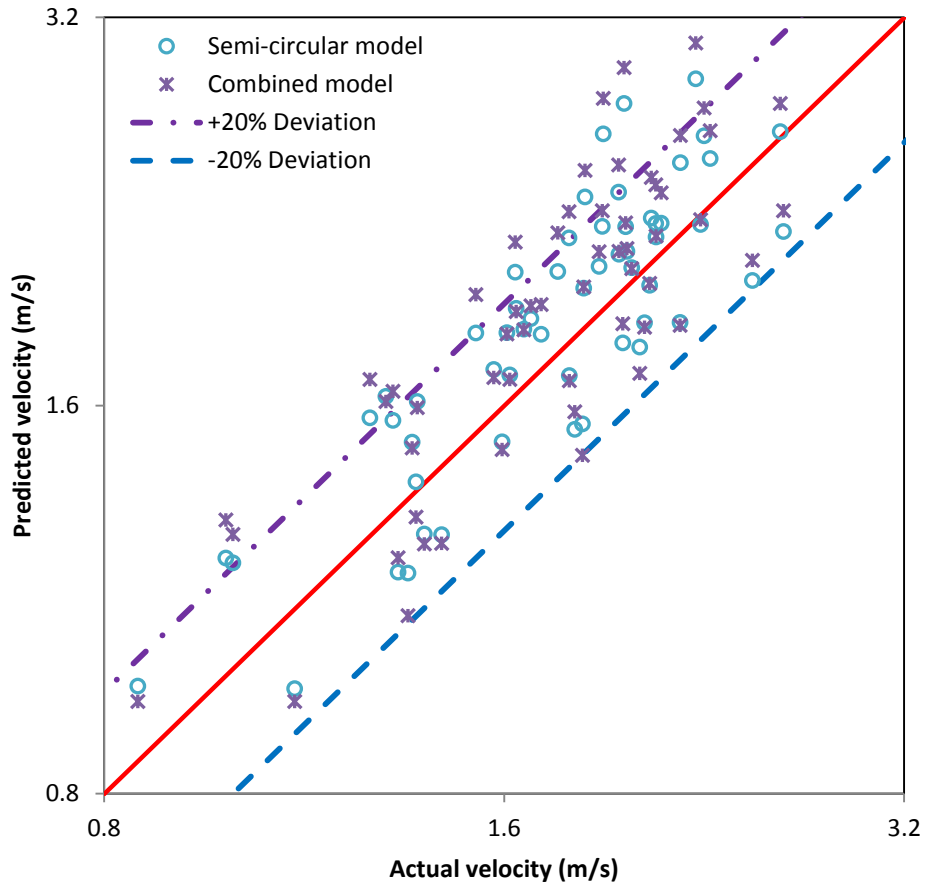


Figure 5.57: Model comparison for the end of transition in a semi-circular flume

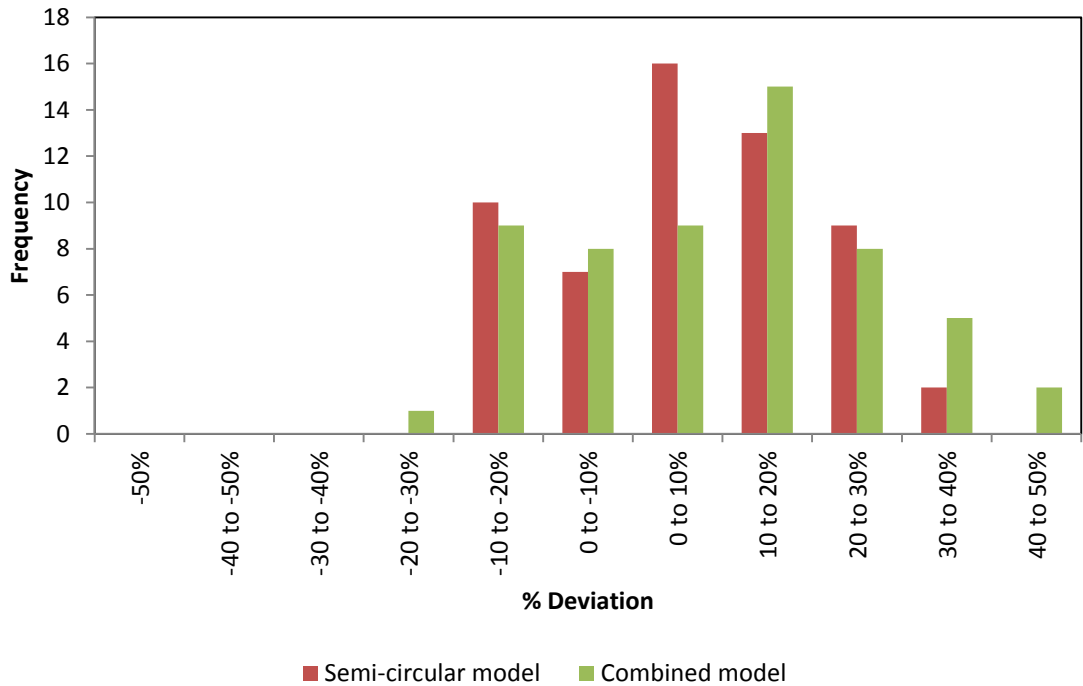


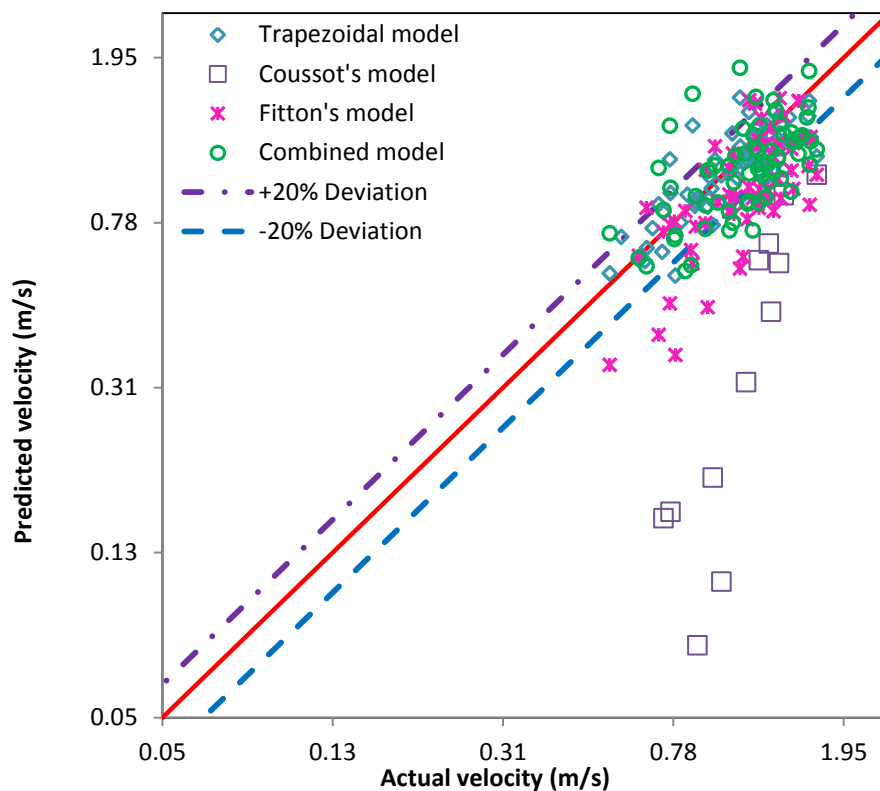
Figure 5.58: End of transitional flow in semi-circular flume: model comparison

Table 5.32: Statistical analysis for the end of transition in a semi-circular flume

| | LSE | Min% Dev | Max % Dev | Standard deviation | % Data falling within the 20% margin |
|----------------------|--------|----------|-----------|--------------------|--------------------------------------|
| Re_H Semi-circular | 0.0085 | -19 | 39 | 0.46 | 81 |
| Re_H Combined | 0.0102 | -20 | 48 | 0.52 | 72 |

5.4.7 Onset of transitional flow: Trapezoidal flume

The adapted critical Reynolds number applicable to trapezoidal channels is compared against the combined, Fitton's and Coussot's models. From Figures 5.59 and 5.60, it can be seen that all models give a good prediction of transitional flow except for Coussot's prediction as presented in Table 5.33. It is also shown in Table 5.33 that the adapted critical Reynolds number for trapezoidal flumes gives the best prediction of the laminar-turbulent transition. It can also be seen in Figure 5.60 that the trapezoidal and combined models predictions are positively skewed whereas Coussot's and Fitton's models are negatively skewed.

**Figure 5.59: Model comparison for the onset of transition in a trapezoidal flume**

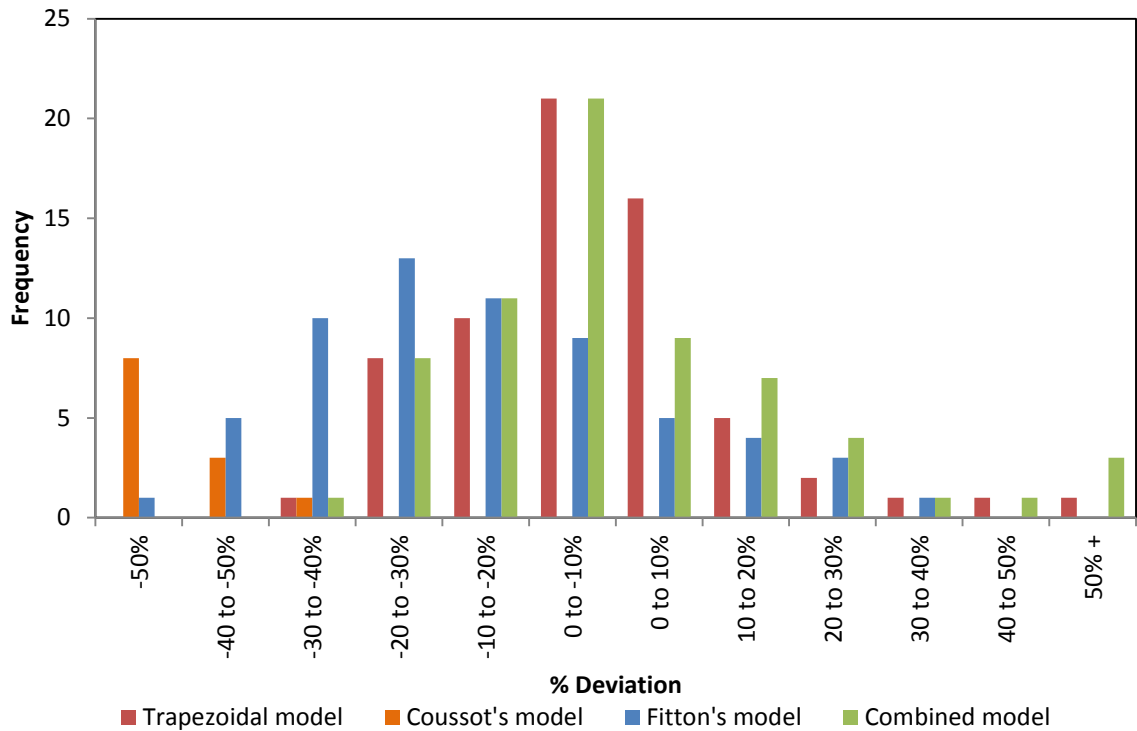


Figure 5.60: Onset of transitional flow in trapezoidal flume: model comparison

Table 5.33: Statistical analysis for the onset of transition in a trapezoidal flume

| | LSE | Min% Dev | Max % Dev | Standard deviation | % Data falling within the 20% margin |
|-----------------------------------|--------|----------|-----------|--------------------|--------------------------------------|
| Re_H Trapezoidal | 0.0091 | -33 | 55 | 0.25 | 79 |
| Re_H Combined | 0.011 | -31 | 84 | 0.28 | 73 |
| Re Fitton | 0.0166 | -53 | 31 | 1.07 | 47 |
| Re Coussot | 0.2076 | -93 | -40 | 0.92 | 0 |

5.4.8 End of transitional flow: Trapezoidal flume

Figures 5.61 and 5.62 show a comparison between the trapezoidal and combined models for the prediction of the onset of turbulent flow. It can be seen that both models give a good prediction of transition since the data points were within the +/- 20% deviation range as suggested in Table 5.34. However, the combined model gives the best prediction with 76%

of the data points falling within the $\pm 20\%$ deviation range. It can also be seen that both models are positively skewed.

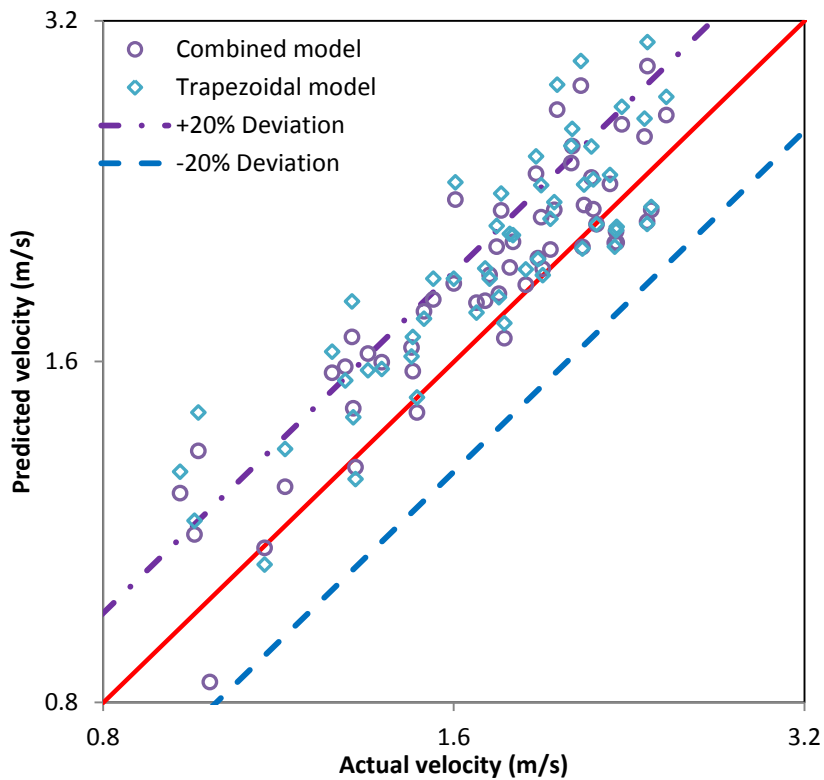


Figure 5.61: Model comparison for the end of transition in a trapezoidal flume

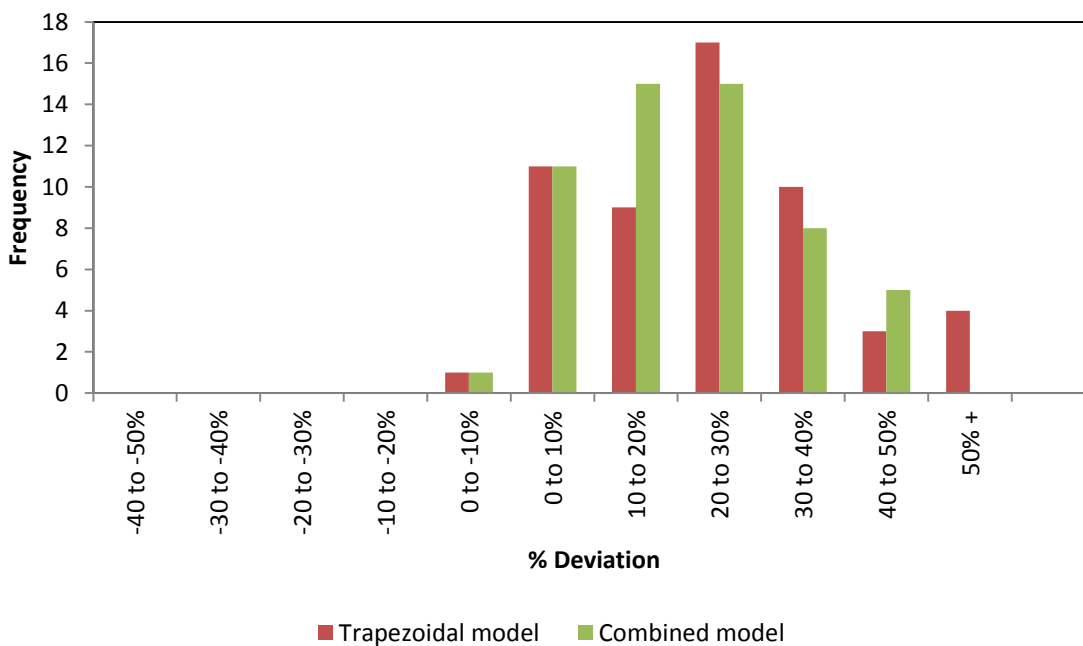


Figure 5.62: End of transitional flow in trapezoidal flume: model comparison

Table 5.34: Statistical analysis for the end of transition in a trapezoidal flume

| | LSE | Min% Dev | Max % Dev | Standard deviation | % Data falling within the 20% margin |
|-----------------------------------|------------|---------------------|----------------------|-------------------------------|---|
| Re_H Trapezoidal | 0.0106 | -19 | 49 | 0.53 | 69 |
| Re_H Combined | 0.009 | -16 | 39 | 0.48 | 76 |

5.5. Conclusions

The objective of this work was to evaluate the cross-sectional shape effect of open channels by critically evaluating the models presented and to commend and optimise the best model.

Different models were evaluated separately for power law (PL), Bingham plastic (BP) and yield shear-thinning (YST) fluids at the onset and end of transitional flow in the flume shapes studied. Aqueous solutions of CMC were characterised as power law fluids. Bentonite and kaolin in water slurries were characterised as Bingham plastic and yield shear-thinning fluids respectively. The four channels shapes studied were rectangular, triangular, semi-circular and trapezoidal.

A summary of the overall performance of the different models used is presented in Table 5.35.

Table 5.35: Overall performance of transitional flow models used for different flume shapes

| Model | Channel shape | | | | | | | | | | | |
|-----------------------------|---------------|----|-----|------------|----|-----|---------------|----|-----|-------------|----|-----|
| | Rectangular | | | Triangular | | | Semi-circular | | | Trapezoidal | | |
| | PL | BP | YST | PL | BP | YST | PL | BP | YST | PL | BP | YST |
| Haldenwang (2003) | 2 | 2 | 2 | - | - | - | - | - | - | - | - | - |
| Fitton (2008) | 3 | 3 | 3 | 3 | 3 | 3 | 3 | 3 | 3 | 3 | 3 | 3 |
| Coussot (1994) | 6 | 6 | 5 | - | - | - | - | - | - | 4 | 4 | 4 |
| Slatter (2013a) | 4 | - | 4 | - | - | - | - | - | - | - | - | - |
| Slatter (2013b) | 5 | 5 | 6 | - | - | - | - | - | - | - | - | - |
| Adapted triangular model | - | - | - | 2 | | | - | - | - | - | - | - |
| Adapted semi-circular model | - | - | - | - | - | - | 1 | | | - | - | - |
| Adapted trapezoidal model | - | - | - | - | - | - | - | - | - | 1 | | |
| Combined model | 1 | | | 1 | | | 2 | | | 2 | | |

The numbers in Table 5.35 indicate the ranking from the best model (i.e. 1) to the worst (i.e. 6). Thus, from Table 5.35 it can be seen that the combined model can be used to predict transition in the rectangular, triangular, semi-circular and trapezoidal channels. The adapted models can be applied to their specific flume shapes. The combined and adapted models for different shapes are also applicable to power-law, Bingham plastic and yield shear-thinning fluids for the range of solids concentrations studied.

The main outcome of this study was the establishment of new correlations for the onset and end of transitional flow of various fluids in four different channel shapes. A combined model which can be used to predict transitional flow in channels of rectangular, triangular, trapezoidal and semi-circular shape has also been established.

CHAPTER 6

Chapter 6: Conclusions and Recommendations

6.1 Introduction

A significant amount of research has been done on the flow of water in open channels (Sturm, 2001; Chanson, 2004; Chaudhry, 2008), but the same cannot be said about the flow of homogeneous non-Newtonian fluids in open channels.

Open-channels are used in the sewage sludge transport, in the polymer processing and textile fibre industries (Kozicki and Tiu, 1988) as well as in the mining industries where homogeneous non-Newtonian slurries have to be transported around plants and to tailings dams (Sanders *et al.*, 2002). As water becomes scarcer and more costly due to legislative limitations and rationing, higher concentrations of slurries have to be transported. This research problem required attention because the understanding of transitional flow of non-Newtonian fluids through open-channels of various cross-sectional shapes will help to improve the design of open channels.

Critical flows may be associated with a degree of instability and wavy motion, leading to working problems and overflows. As for pipe flow the transition zone for open channels is difficult to predict. However, there is a lack of conclusive guidelines in the literature to predict the transitional flow for different shapes, as well as a need for comparison between different predictive models of transitional flow in various flume shapes.

Thus a summary of the work done on the shape effect of open channels in the transitional flow, the main contribution and recommendations for future research are presented in this chapter.

6.2 Summary

An investigation on the shape effect of the flow of non-Newtonian slurries in smooth rectangular, triangular, trapezoidal and semi-circular open channels in the transition region was conducted in this study.

No experimental work was conducted in this study. The data published by Haldenwang *et al.* (2006) and Burger *et al.* (2010) was used here.

Haldenwang *et al.*'s (2002) Reynolds number (Re_H) was used to predict the flow behaviour of shear-thinning, Bingham plastic and yield shear-thinning fluids in channels of rectangular, semi-circular, trapezoidal and triangular shapes.

Different predictive models for the onset of transitional flow were evaluated for the respective fluids in various channel shapes. This was done to determine and optimise the best model.

Firstly, Fitton's (2008) for semi-circular channels, Haldenwang (2003) for rectangular channels and Slatter (2013) for sheet flow models were evaluated for power law fluids. It was found that Haldenwang's model predicted the onset of transitional flow best. However, for the end of transitional flow, a comparison of models could not be made since Haldenwang's model is the only one in the literature which predicts the onset of "full turbulence".

Secondly, Hao and Zenghai (1980) for rectangular, semi-circular and trapezoidal channels, Naik (1983) for rectangular channels, Haldenwang (2003) for rectangular channels as well as Fitton (2008) for semi-circular channels models were evaluated for Bingham plastic fluids. It was found that Haldenwang's model predicted the onset of transitional flow best and a comparison for the end of transition was not possible since Haldenwang's model only was available. However, Fitton's model was not much worse.

Finally, Coussot (1997) for rectangular and trapezoidal channels, Haldenwang (2003) for rectangular channels, Fitton (2008) for semi-circular channels as well as Slatter (2013) for sheet flow models were evaluated for yield shear-thinning fluids. It was found that Haldenwang's model predicted the onset of transitional flow best and a comparison for the end of transition was not possible since Haldenwang's model only was available in the literature.

In order to apply Haldenwang's predictive model of transitional flow for a rectangular flume in flumes of different cross-sectional shapes, new critical Reynolds number models for each shape as well as a combined model (developed using data for all 4 different flume shapes) for all shapes were developed based on Haldenwang's (2010) method.

For the onset of transitional flow in a triangular flume, the adapted triangular model was compared against the Fitton and the combined models. It was shown that the combined model gave a better prediction. However the adapted triangular and the combined models gave a good prediction of transitional flow. Fitton's model gave a poor prediction.

A comparison was made between the adapted triangular and combined models for the prediction of the onset of turbulent flow in the triangular flume. It was seen that the adapted

triangular model was less favourable since only 33% of data points were within the +/- 20% deviation range. The combined model gave a good prediction for the end of transitional flow.

In the semi-circular flume, the adapted semi-circular model was compared against the combined model and Fitton's (2008) model. It was shown that all models gave a good prediction of transitional flow except for Fitton's (2008) model.

After comparison between the semi-circular and combined models for the prediction of the onset of turbulent flow in a semi-circular flume, it was seen that all models gave a good prediction of transition since 70% of the data points were within the +/- 20% deviation range.

In the trapezoidal flume, the adapted trapezoidal model was compared against the combined model and Coussot's (1997) model. It was seen that all models gave a good prediction of transitional flow except for Coussot's model.

The trapezoidal and combined models for the prediction of the onset of turbulent flow were compared for the end of transitional flow in the trapezoidal flume. It was seen that both models gave a good prediction of transition since more than 60% of the data points were within the +/- 20% deviation range.

A shape effect was studied and, it was shown that there was no significant effect on transitional flow in channels of different shapes. Thus, it seemed that Haldenwang's (2003) method described better the transitional flow of fluids in open channels because it incorporated the Froude number in its critical Reynolds number predictive model.

6.3 Contributions

New correlations for the onset and end of transitional flow in channels of triangular, semi-circular and trapezoidal shapes have been established.

Table 6.1 gives a summary of the model that should be used for the corresponding channel shape. The Re_H rectangular critical Reynolds number model is recommended for the prediction of the onset of transitional flow in rectangular flumes. The adapted Re_H triangular, Re_H semi-circular and Re_H trapezoidal critical Reynolds number models should be used in their respective flume shapes. The combined model can be used to predict the onset and end of transitional in the four flume shapes studied.

Table 6.1: Summary of models to be used

| Rectangular flume | | Semi-circular flume | | Trapezoidal flume | | Triangular flume | |
|-----------------------|-----------------------|-------------------------|-------------------------|-----------------------|-----------------------|----------------------|--------------------|
| Onset of transition | End of transition | Onset of transition | End of transition | Onset of transition | End of transition | Onset of transition | End of transition |
| Re_H Rectangular | Re_H Rectangular | Re_H Semi-circular | Re_H Semi-circular | Re_H Trapezoidal | Re_H Trapezoidal | Re_H Triangular | Re_H Combined |
| Re_H Combined | Re_H Combined | Re_H Combined | Re_H Combined | Re_H Combined | Re_H Combined | Re_H Combined | - |

6.4 Conclusion

By combining all the transition data for the four shapes a new correlation “combined model” was developed for onset of transition and onset of full turbulence which can adequately accommodate the four different channel shapes for all fluids tested.

As far as can be ascertained, it is the first time that a systematic study has been carried out on the effect of open channel shape on transitional flow for different non-Newtonian fluids.

6.5 Recommendations

Recommendations for further research include:

The effect of roughness, as the flumes that were used were nearly smooth which is different from many flumes found in industry. This study needs to be conducted because the flume roughness influences the onset and end of transitional flow.

Velocity profiles and pressure fluctuations in the laminar-turbulent transition region should be conducted to verify the onset and end of transitional flow in open channels. This study will help to improve the predictions of transitional flow in various channels of different shapes.

REFERENCES

References

- Abulnaga, B. 2002. *Slurry systems handbook*. New York: McGraw-Hill.
- Alderman, N.J. & Haldenwang, R. 2004. A review of Newtonian and non-Newtonian flow in rectangular open channels. *The 17th International conference on the hydraulic transport of solids*, Cape Town, 7-11 May. *Hydrotransport 17*: 87-106.
- Barnes, H.A. 2000. *A handbook of elementary rheology*. The University of Wales: Wales.
- Barnes, H.A. & Walters, K. 1985. The yield stress myth?. *Rheologica Acta*. 24: 323-326.
- Bazin, H. 1865. Recherches expérimentale sur l'écoulement de l'eau dans les canaux découverts (Experimental research on water flow in open channels). *Mémoires présentés par divers savants à l'Académie des Sciences*, 19: 1-494 (in French)
- Blasius, P. R. H. 1913. Das Aehnlichkeitsgesetz bei Reibungsvorgängen in Flüssigkeiten. (The law of similitude for frictional motion in fluids). *Forschungsheft des Vereins Deutscher Ingenieure*, (131): 1-41.
- Burger J, Haldenwang R, & Alderman N.J. 2010a. Friction factor-Reynolds number relationship for laminar flow of non-Newtonian fluids in open channels of different cross-sectional shapes. *Chemical Engineering Science*, 6 (11): 3549–3556.
- Burger, J., Haldenwang, R. & Alderman, N. 2010b. Experimental database for non-Newtonian flow in four channel shapes. *Journal of Hydraulic Research*, 48 (3): 363-370.
- Chadwick, A & Morfett, J. 1999. *Hydraulics in civil and environmental engineering*. London: E & FN Spon.
- Chanson, H. 2004. *The hydraulics of open channel flow: an introduction*. 2nd ed. London: Arnold.
- Chaudhry, M.H. 2008. *Open channel flow*. 2nd ed. New York: Springer.
- Chhabra, R.P. & Richardson, J.F. 2008. *Non-Newtonian flow and applied rheology*. 2nd ed. Oxford: Butterworth-Heinemann.
- Chow, V.T. 1959. *Open channel hydraulics*. New York: McGraw-Hill.
- Colebrook, C.F. 1939. Turbulent flow in pipes with particular reference to the transition region between the smooth and rough pipe laws. *Journal of the institution of civil engineers*. London. Paper no. 5204. 11 (4): 133-156.
- Coulson, J.M. & Richardson, J.F. 1999. *Coulson & Richardson's chemical engineering: Fluid flow, Heat transfer and Mass transfer*. 6th ed. Vol 1. Oxford: Butterworth-Heinemann.
- Coussot, P. 1994. Steady laminar flow of concentrated mud suspensions in open channels. *Journal of Hydraulic Research*, 4 (32): 535-558.
- Coussot, P. 1997. *Mudflow rheology and dynamics*. Rotterdam: A.A.Balkema.
- Darby, R. & Melson, J. 1981. How to predict the friction factor for the flow of Bingham plastics. *Chemical Engineering*, 28 Dec, 88 (26), 59-61.

Darcy, H.P.G. & Bazin, H. 1865. *Recherches Hydrauliques*. (Hydraulic Research.) (Imprimerie Impériale: Paris, France), Parties 1ere et 2eme (in French). (Book)

De Kee, D., Chhabra, R. P., Powley, M.B. & Roy, S. 1990. Flow of viscoplastic fluids on an inclined plane: evaluation of yield stress, *Chem. Eng. Comm.* 96, 229-239.

De Nevers, N. *Fluid mechanics for chemical engineers*. 3rd ed. Boston: McGraw-Hill.

Dooge, J.C.I. 1991. The Manning formula in context; In *Channel Flow Resistance: Centennial of Manning's Formula*, B.C. Yen (ed) (Water Resources Publishers, Littleton CO, USA) pp. 136-185.

Douglas, J.F., Gasiorek, J.M. & Swaffield, J.A. 2001. *Fluid mechanics*. 4th ed. Harlow: Prentice-hall.

Featherstone, R.E. & Nalluri, C. 2009. *Nalluri & Featherstone's civil engineering hydraulics: essential theory with worked examples*. 5th ed. Oxford: Wiley-Blackwell.

Fitton, T. G. 2008. *Non-Newtonian open channel flow: a simple method of estimation of laminar/turbulent transition and flow resistance*, by Fourie, A.B., Jewell, R.J., Paterson, A. & Slatter, P.T. Reviewed in: *Paste*, 245-251.

Fitton, T.G. 2007. Tailings beach slope prediction. Unpublished PhD thesis, RMIT University, Melbourne.

Fitton, T.G., Chrissy, A.G. & Battacharya, S.N. 2006. Tailings beach slope prediction: a new rheological method. *International Journal of Surface mining, Reclamation and Environment*. 20 (3): 181-202.

Ganguillet, E. & Kutter, W.R. 1869. An investigation to establish a new general formula for uniform flow of water in canals and rivers. *Zeitschrift des Oesterreichischen Ingenieur un Architekten Vereines*, 21 (1): 6-25; 21(2-3): 46-59.

Gauckler, P. G. 1867. Etudes Theoriques et Pratiques sur l'Ecoulement et le Mouvement des Eaux (Theoretical and Practical Studies of the Flow and Motion of Waters). *Comptes Rendues de l'Academie des Sciences: Paris France*, Tome 64, pp. 818-822 (in French).

Griskey, R.G. 2002. *Transport phenomena and unit operations: a combined approach*. New-York: John-Wiley & Sons.

Guang, R. 2011. Particle transportation in turbulent non-Newtonian suspensions in open channels. Unpublished PhD thesis, RMIT university, Melbourne.

Haldenwang, R., Slatter, P.T. & Chhabra, R.P. 2002. Laminar and transitional flow in open channels for non-Newtonian fluids. *Proceedings of the 15th International conference on the hydraulic transport of solids in pipes*, Banff, Canada, pp. 755-768.

Haldenwang, R. 2003. Flow of non-Newtonian fluids in open channels. Unpublished PhD thesis, Cape Technikon, Cape Town.

Haldenwang R., Slatter P.T., Vanyaza, S. & Chhabra R.P. 2004. The effect of shape on laminar flow in open channels for non-Newtonian fluids. *Proceedings of the 16th International Conference on Hydrotransport*, Santiago, 26-28 April, 2004, pp. 311 - 324.

- Haldenwang, R. & Slatter, P.T. 2006. Experimental procedure and database for non-Newtonian open channel flow. *Journal of the Hydraulic Research*, 44 (2): 283 – 287.
- Haldenwang, R., Slatter, P.T. & Chhabra, R.P. 2010. An experimental study of non-Newtonian fluid flow in rectangular flumes in laminar, transition and turbulent flow regimes. *Journal of the South African Institution of Civil Engineering*, 52 (1): 11-19.
- Hanks, R. 1963. The laminar – turbulent transition in pipes, concentric annuli and parallel plates. *American Institute of Chemical Engineers Journal*, (9): 173–181.
- Hanks, R.W. & Dadia, B.H. 1971. Theoretical analysis of the turbulent flow of non-Newtonian slurries in pipes. *American Journal of Chemical Engineering*. 17, 554-557.
- Hao, Z. & Zhenghai, R. 1980. Settling of sediment and the resistance to flow at hyper-concentration. *Proceedings of the international symposium on river sedimentation*, 1 (Paper B4): 185-194.
- Henderson, F.M. 1990. *Open Channel Flow*. New York: Macmillan.
- Holland, F.A. 1973. *Fluid flow for chemical engineers*. London: Edward Arnold.
- Keulegan, G.H. 1938. Laws of turbulent flow in open channels. *Journal of Research, U.S. National Bureau of Standards*, 21 (Paper RP1151): 707-741, December.
- Kirschmer, O. 1949a. Frictional losses in pipes and channels. *Die Wasserwirtschaft*, 39 (7): 137-142, April; 39 (8): 168-174, May.
- Kirschmer, O. 1949b. Pertes des charges dans les conduites forcées et les canaux découverts (Energy losses in pressure conduits and open channels). *Révue Générale de l'Hydraulique*, 15 (51): 115-138, May-June.
- Kozicki, W. & Tiu, C. 1967. Non-Newtonian flow through open channels. *The Canadian journal of chemical engineering*, 45 (3): 127-134.
- Kozicki, W. & Tiu, C. 1988. Parametric modelling of flow geometries in non-Newtonian flows. Chapter 8. *Encyclopedia of fluid mechanics*. Vol 7. Rheology and non-Newtonian flows. Editor: Cheremisinoff, N.P. Houston: Gulf Publishing Company.
- Lazarus, J.H. & Slatter P.T. 1988. A method for the rheological characterisation of tube viscometer data, *Journal of Pipelines*. 7: 165-176.
- Manning, R. 1890. On the flow of water in open channels and pipes. *Transactions of the Institution of Civil Engineers*, 1(20): 161–207.
- Massey, B. & Ward-Smith, J. 1998. *Mechanics of fluids*. 7th ed. London: Stanley Thornes.
- Mott, R.L. 2000. *Applied fluid mechanics*. 5th ed. London: Prentice-Hall.
- Munson, B.R., Young, D.F., Okiishi, T.H. & Huebsch, W.W. 2010. *Fundamentals of fluid mechanics*. 6th ed. New Jersey: John Wiley & sons, Inc (Asia) Pte Ltd.
- Naik, B. 1983. Mechanics of mudflow treated as the flow of a Bingham fluid. Unpublished PhD thesis, Washington state University, Pullman, WA.
- Paterson, A.J.C., Williamson, J.R.G., and Oliveros Salas, U. 2004. Hydraulic transport considerations for high density thickened copper tailings at Southern Peru Copper Corporation. *Proceedings of the 16th International Conference on the Hydraulic Transport of Solids in Pipes*, Santiago, 26-28 April, pp. 13-24.

-
- Powell, R.W. 1950. Resistance to flow in rough channels. *Transactions American Geophysical Union*, 31 (4): 575-582.
- Prandtl, L. 1935. The mechanics of viscous fluids. In W.F. Durand (ed). *Aerodynamic theory*. Berlin: Springer-Verlag, 3 (Division G):142.
- Sanders, R. S., Schaan, J., Gillies, R. G., McKibben, M. J., Sun, R. & Shook, C.A. 2002. Solids transport in laminar, open-channel flow of non-Newtonian slurries. *Hydrotransport 15*. Canada: Bannf.
- Seckin, G., Seckin, N. and Yurtal, R. 2006. Boundary shear stress analysis in smooth rectangular channels. *Canadian Journal of Civil Engineering*. 33 (3): 336-342.
- Slatter, P.T. 1994. Transitional and Turbulent flow of non-Newtonian slurries in pipes. Unpublished PhD thesis, University of Cape Town, Cape Town.
- Slatter, P. 1999. A new friction factor for yield stress fluids at low Reynolds numbers. BHR Group. *Hydrotransport 14*, Maastricht, Netherlands, pp. 255-265.
- Slatter, P.T. & Wasp, E.J. 2000. The laminar/turbulent transition in large pipes. *Proceedings of the 2000 10th International Conference on Transport and sedimentation of solid particles*, Wroclaw, 4-7 September 2000, pp. 389-399.
- Slatter, P., Haldenwang, R. & Chhabra, R. P. 2011. The laminar/turbulent transition for paste sheet flow. *Proceedings of the 14th international seminar on Paste and Tailings*, R.J. Jewel and A.B. Fourie (ed.), ACG, Perth, Australia, pp. 381-388.
- Slatter, P. 2013a. Analysis and flow behaviour prediction of paste material in sheet flow. *Proceedings of the 15th international seminar on paste and thickened tailings*, R.J. Jewel and A.B. Fourie (ed.), ACG, Perth, Australia. *Paste 2013*, Belo Horizonte, 17-20 June, pp. 473-480.
- Slatter, P. 2013b. Transitional flow behaviour for free surface flow of viscoplastic material. *Proceedings of the 16th international conference on transport and sedimentation of solid particles*, Rostock, 18-20 September, pp. 125-135.
- Straub, L.B., Silberman, E. & Nelson, H.C. 1958. Open-channel flow at small Reynolds numbers. *American society of civil engineers*, 123: 685-714.
- Sturm, T.W. 2001. *Open channel hydraulics*. New York: McGraw-Hill.
- Torrance, B. 1963. Friction factors for turbulent non-Newtonian flow in circular pipes. *S.A. mechanical engineer*. 13, 89-91.
- von-Karman, T. 1930. Mechanical similitude and turbulence. *Proceedings of the 3^d International Congress for Applied Mechanics*, 1: 85-93.
- Wan, Z. and Wang, Z. 1994. *Hyperconcentrated Flow*. Rotterdam: AA Balkema.
- Wang, Z., Lin, B. & Zhang, X. 1990. Instability of non-Newtonian fluid flow (in Chinese). *Mechanica Sinica*, (3): 266-275.
- Weiss, N.A. 2012. *Elementary statistics*. 8th ed. Boston: Pearson Education, Inc.
- Wilson, K. C. 1991. *Slurry transport in flumes*, by Brown, N.P. & Heywood, N.I. Reviewed in: *Slurry handling: design of solid-liquid systems*, 167-180. London: Elsevier Science Publishers.

Wilson, K.C. 1991. Flume design for homogeneous slurry flow. *Particulate Science and Technology*, 9: 149-159.

Yang, W. & Zhao, W. 1983. An experimental study of the resistance to flow with hyperconcentration in rough flumes. *Proceedings of 2nd International Symposium on River Sedimentation*, Water Resources and Electric Power, 45-55.

Yen, B.C. 2002. Open channel flow resistance. *Journal of hydraulic engineering*, 128 (1): 20-39.

Zhang, H. & Ren, Z. 1982. Discussion on law of resistance of hyperconcentration flow in open channel. *Scientia Sinica (Series A)*, 25 (12): 1332-1342.

APPENDICES

Appendices

All the flume data used are presented in this section.

The tests fluids were aqueous suspensions/solutions of CMC, bentonite and kaolin.

The data sets are for tests in the rectangular flumes (300 mm and 150 mm wide), semi-circular flumes (300 mm and 150 mm wide), trapezoidal flumes (150mm and 75 mm wide) and triangular flume (300 mm wide).

The rectangular, semi-circular, trapezoidal and triangular flume data are presented from Appendix A to D respectively.

The rheological parameters, the flume slope, the flow rate and the flow depth were tabulated for each test.

APPENDIX A: Rectangular flume data

Table A.1: 1% CMC in water solution flowing in a 300 mm rectangular flume

| | |
|-----------------------------|--------|
| Material: | CMC |
| Concentration/vol: | 1.0% |
| Density kg/m ³ : | 1006.7 |
| Ty (Pa): | 0.000 |
| k (Pa.s ²): | 0.060 |
| n: | 0.655 |
| Flume width (mm): | 300 |

| SLOPE | FLOW | DEPTH | SLOPE | FLOW | DEPTH | SLOPE | FLOW | DEPTH | SLOPE | FLOW | DEPTH | SLOPE | FLOW | DEPTH |
|-----------|----------------------|-------|-----------|----------------------|-------|-----------|----------------------|-------|-----------|----------------------|-------|-----------|----------------------|-------|
| FLUME | Q | h | FLUME | Q | h | FLUME | Q | h | FLUME | Q | h | FLUME | Q | h |
| (degrees) | (l.s ⁻¹) | (m) | (degrees) | (l.s ⁻¹) | (m) | (degrees) | (l.s ⁻¹) | (m) | (degrees) | (l.s ⁻¹) | (m) | (degrees) | (l.s ⁻¹) | (m) |
| 1 | 1.856 | 0.010 | 2 | 1.491 | 0.008 | 3 | 1.923 | 0.007 | 4 | 1.479 | 0.006 | 5 | 1.760 | 0.006 |
| 1 | 4.276 | 0.018 | 2 | 0.892 | 0.006 | 3 | 4.390 | 0.012 | 4 | 0.858 | 0.005 | 5 | 4.536 | 0.011 |
| 1 | 6.758 | 0.024 | 2 | 0.611 | 0.005 | 3 | 6.785 | 0.016 | 4 | 0.579 | 0.004 | 5 | 6.906 | 0.015 |
| 1 | 11.445 | 0.035 | 2 | 0.269 | 0.004 | 3 | 8.940 | 0.020 | 4 | 0.297 | 0.004 | 5 | 9.163 | 0.018 |
| 1 | 13.644 | 0.039 | 2 | 1.803 | 0.008 | 3 | 11.660 | 0.024 | 4 | 1.934 | 0.006 | 5 | 12.193 | 0.022 |
| 1 | 16.302 | 0.045 | 2 | 4.306 | 0.014 | 3 | 13.928 | 0.027 | 4 | 4.364 | 0.011 | 5 | 14.656 | 0.025 |
| 1 | 18.615 | 0.049 | 2 | 6.750 | 0.019 | 3 | 17.307 | 0.032 | 4 | 6.729 | 0.015 | 5 | 17.400 | 0.029 |
| 1 | 22.886 | 0.056 | 2 | 9.115 | 0.023 | 3 | 22.025 | 0.038 | 4 | 9.165 | 0.018 | 5 | 23.112 | 0.035 |
| 1 | 0.393 | 0.006 | 2 | 11.659 | 0.027 | 3 | 0.206 | 0.003 | 4 | 12.126 | 0.022 | 5 | 0.571 | 0.004 |
| 1 | 0.592 | 0.007 | 2 | 13.969 | 0.031 | 3 | 0.584 | 0.005 | 4 | 14.442 | 0.026 | 5 | 1.198 | 0.005 |
| 1 | 0.912 | 0.008 | 2 | 17.358 | 0.037 | 3 | 0.888 | 0.005 | 4 | 17.531 | 0.029 | 5 | 0.907 | 0.005 |
| 1 | 1.520 | 0.009 | 2 | 21.375 | 0.043 | 3 | 1.527 | 0.007 | 4 | 22.576 | 0.035 | 5 | 1.280 | 0.006 |

Table A.2: 1.8% CMC in water solution flowing in a 300 mm rectangular flume

| | |
|-----------------------------|--------|
| Material: | CMC |
| Concentration/vol: | 1.8% |
| Density kg/m ³ : | 1010.7 |
| Ty (Pa): | 0.000 |
| k (Pa.s ²): | 0.105 |
| n: | 0.775 |
| Flume width (mm): | 300 |

| SLOPE | FLOW | DEPTH | SLOPE | FLOW | DEPTH | SLOPE | FLOW | DEPTH | SLOPE | FLOW | DEPTH | SLOPE | FLOW | DEPTH |
|-----------|----------------------|-------|-----------|----------------------|-------|-----------|----------------------|-------|-----------|----------------------|-------|-----------|----------------------|-------|
| FLUME | Q | h | FLUME | Q | h | FLUME | Q | h | FLUME | Q | h | FLUME | Q | h |
| (degrees) | (l.s ⁻¹) | (m) | (degrees) | (l.s ⁻¹) | (m) | (degrees) | (l.s ⁻¹) | (m) | (degrees) | (l.s ⁻¹) | (m) | (degrees) | (l.s ⁻¹) | (m) |
| 1 | 2.037 | 0.015 | 2 | 0.283 | 0.007 | 3 | 1.837 | 0.010 | 4 | 1.497 | 0.007 | 5 | 6.780 | 0.013 |
| 1 | 4.265 | 0.020 | 2 | 0.578 | 0.008 | 3 | 4.425 | 0.014 | 4 | 1.177 | 0.007 | 5 | 9.055 | 0.015 |
| 1 | 3.189 | 0.018 | 2 | 0.875 | 0.009 | 3 | 6.713 | 0.017 | 4 | 0.884 | 0.006 | 5 | 11.632 | 0.020 |
| 1 | 6.666 | 0.024 | 2 | 1.194 | 0.010 | 3 | 6.729 | 0.017 | 4 | 0.590 | 0.006 | 5 | 13.406 | 0.022 |
| 1 | 9.095 | 0.030 | 2 | 1.458 | 0.011 | 3 | 9.002 | 0.020 | 4 | 0.295 | 0.005 | 5 | 15.659 | 0.025 |
| 1 | 11.752 | 0.035 | 2 | 1.891 | 0.011 | 3 | 11.476 | 0.023 | 4 | 4.714 | 0.012 | 5 | 18.114 | 0.028 |
| 1 | 13.383 | 0.039 | 2 | 4.285 | 0.015 | 3 | 13.562 | 0.026 | 4 | 6.634 | 0.013 | 5 | 20.087 | 0.032 |
| 1 | 15.686 | 0.042 | 2 | 6.687 | 0.019 | 3 | 15.627 | 0.031 | 4 | 9.056 | 0.016 | 5 | 0.299 | 0.005 |
| 1 | 17.935 | 0.047 | 2 | 9.020 | 0.023 | 3 | 17.944 | 0.035 | 4 | 11.555 | 0.020 | 5 | 0.615 | 0.005 |
| 1 | 20.241 | 0.052 | 2 | 11.539 | 0.027 | 3 | 20.043 | 0.037 | 4 | 13.311 | 0.023 | 5 | 0.882 | 0.006 |
| 1 | 7.225 | 0.026 | 2 | 13.192 | 0.029 | 3 | 0.304 | 0.006 | 4 | 15.667 | 0.027 | 5 | 1.186 | 0.007 |
| 1 | 0.306 | 0.009 | 2 | 15.712 | 0.033 | 3 | 0.617 | 0.007 | 4 | 17.904 | 0.029 | 5 | 1.456 | 0.007 |
| 1 | 0.570 | 0.010 | 2 | 17.997 | 0.036 | 3 | 0.881 | 0.008 | 4 | 19.929 | 0.033 | | | |
| 1 | 0.890 | 0.012 | 2 | 19.928 | 0.039 | 3 | 1.177 | 0.009 | 4 | 1.966 | 0.008 | | | |
| 1 | 1.183 | 0.013 | | | | 3 | 1.476 | 0.009 | | | | | | |
| 1 | 1.471 | 0.014 | | | | | | | | | | | | |

Table A.3: 2.8% CMC in water solution flowing in a 300 mm rectangular flume

| | |
|-----------------------------|-------|
| Material: | CMC |
| Concentration/vol: | 2.8% |
| Density kg/m ³ : | 1016 |
| Ty (Pa): | 0.000 |
| k (Pa.s ⁿ): | 0.368 |
| n: | 0.658 |
| Flume width (mm): | 300 |

| SLOPE | FLOW | DEPTH | SLOPE | FLOW | DEPTH | SLOPE | FLOW | DEPTH | SLOPE | FLOW | DEPTH | SLOPE | FLOW | DEPTH |
|-----------|----------------------|-------|-----------|----------------------|-------|-----------|----------------------|-------|-----------|----------------------|-------|-----------|----------------------|-------|
| FLUME | Q | h | FLUME | Q | h | FLUME | Q | h | FLUME | Q | h | FLUME | Q | h |
| (degrees) | (l.s ⁻¹) | (m) | (degrees) | (l.s ⁻¹) | (m) | (degrees) | (l.s ⁻¹) | (m) | (degrees) | (l.s ⁻¹) | (m) | (degrees) | (l.s ⁻¹) | (m) |
| 1 | 1.932 | 0.021 | 2 | 1.428 | 0.015 | 3 | 2.057 | 0.014 | 4 | 1.555 | 0.011 | 5 | 2.304 | 0.012 |
| 1 | 2.008 | 0.021 | 2 | 1.170 | 0.014 | 3 | 2.813 | 0.016 | 4 | 1.457 | 0.011 | 5 | 3.312 | 0.013 |
| 1 | 2.873 | 0.024 | 2 | 0.898 | 0.013 | 3 | 4.300 | 0.018 | 4 | 1.187 | 0.010 | 5 | 5.754 | 0.015 |
| 1 | 4.285 | 0.027 | 2 | 0.730 | 0.012 | 3 | 6.858 | 0.021 | 4 | 0.858 | 0.009 | 5 | 7.968 | 0.018 |
| 1 | 6.698 | 0.032 | 2 | 0.410 | 0.010 | 3 | 8.994 | 0.024 | 4 | 0.549 | 0.008 | 5 | 10.606 | 0.020 |
| 1 | 9.039 | 0.038 | 2 | 0.202 | 0.009 | 3 | 11.475 | 0.027 | 4 | 0.330 | 0.007 | 5 | 12.847 | 0.023 |
| 1 | 11.725 | 0.043 | 2 | 2.422 | 0.017 | 3 | 13.782 | 0.031 | 4 | 0.210 | 0.006 | 5 | 15.342 | 0.025 |
| 1 | 13.810 | 0.048 | 2 | 3.344 | 0.019 | 3 | 16.094 | 0.034 | 4 | 1.897 | 0.012 | 5 | 17.506 | 0.028 |
| 1 | 16.189 | 0.053 | 2 | 5.654 | 0.023 | 3 | 18.123 | 0.037 | 4 | 2.887 | 0.014 | 5 | 20.525 | 0.031 |
| 1 | 19.912 | 0.060 | 2 | 8.102 | 0.027 | 3 | 20.224 | 0.040 | 4 | 4.352 | 0.016 | 5 | 0.197 | 0.005 |
| 1 | 0.324 | 0.012 | 2 | 10.457 | 0.032 | 3 | 0.298 | 0.008 | 4 | 6.653 | 0.018 | 5 | 0.448 | 0.007 |
| 1 | 0.331 | 0.012 | 2 | 12.788 | 0.036 | 3 | 0.207 | 0.007 | 4 | 9.030 | 0.021 | 5 | 0.667 | 0.008 |
| 1 | 0.629 | 0.015 | 2 | 15.272 | 0.040 | 3 | 0.502 | 0.009 | 4 | 11.607 | 0.024 | 5 | 0.841 | 0.008 |
| 1 | 0.963 | 0.016 | 2 | 17.467 | 0.045 | 3 | 0.736 | 0.010 | 4 | 13.785 | 0.027 | 5 | 1.329 | 0.010 |
| 1 | 1.194 | 0.018 | 2 | 18.974 | 0.047 | 3 | 0.927 | 0.011 | 4 | 16.132 | 0.030 | 5 | 0.306 | 0.006 |
| 1 | 1.469 | 0.020 | 2 | 19.776 | 0.048 | 3 | 1.295 | 0.012 | 4 | 18.107 | 0.032 | 5 | 0.346 | 0.007 |
| | | | | | | 3 | 1.596 | 0.013 | 4 | 20.581 | 0.035 | 5 | 0.399 | 0.007 |
| | | | | | | | | | | | | 5 | 1.702 | 0.010 |

Table A.4: 3.8% CMC in water solution flowing in a 300 mm rectangular flume

| | |
|-----------------------------|-------|
| Material: | CMC |
| Concentration/vol: | 3.8% |
| Density kg/m ³ : | 1021 |
| Ty (Pa): | 0.000 |
| k (Pa.s ⁿ): | 0.606 |
| n: | 0.678 |
| Flume width (mm): | 300 |

| SLOPE | FLOW | DEPTH | SLOPE | FLOW | DEPTH | SLOPE | FLOW | DEPTH | SLOPE | FLOW | DEPTH | SLOPE | FLOW | DEPTH |
|-----------|----------------------|-------|-----------|----------------------|-------|-----------|----------------------|-------|-----------|----------------------|-------|-----------|----------------------|-------|
| FLUME | Q | h | FLUME | Q | h | FLUME | Q | h | FLUME | Q | h | FLUME | Q | h |
| (degrees) | (l.s ⁻¹) | (m) | (degrees) | (l.s ⁻¹) | (m) | (degrees) | (l.s ⁻¹) | (m) | (degrees) | (l.s ⁻¹) | (m) | (degrees) | (l.s ⁻¹) | (m) |
| 1 | 1.869 | 0.029 | 2 | 1.624 | 0.021 | 3 | 2.276 | 0.019 | 4 | 1.926 | 0.015 | 5 | 2.646 | 0.016 |
| 1 | 2.969 | 0.033 | 2 | 1.682 | 0.021 | 3 | 3.340 | 0.021 | 4 | 1.565 | 0.015 | 5 | 4.520 | 0.019 |
| 1 | 4.311 | 0.038 | 2 | 1.243 | 0.019 | 3 | 5.188 | 0.025 | 4 | 1.276 | 0.014 | 5 | 6.206 | 0.021 |
| 1 | 6.616 | 0.043 | 2 | 0.916 | 0.018 | 3 | 7.438 | 0.028 | 4 | 1.040 | 0.013 | 5 | 8.389 | 0.023 |
| 1 | 8.845 | 0.049 | 2 | 0.624 | 0.015 | 3 | 9.749 | 0.031 | 4 | 0.738 | 0.012 | 5 | 10.720 | 0.025 |
| 1 | 11.242 | 0.053 | 2 | 0.441 | 0.014 | 3 | 14.120 | 0.037 | 4 | 0.525 | 0.011 | 5 | 12.571 | 0.027 |
| 1 | 13.277 | 0.058 | 2 | 0.324 | 0.013 | 3 | 16.468 | 0.041 | 4 | 0.373 | 0.010 | 5 | 15.985 | 0.031 |
| 1 | 15.968 | 0.064 | 2 | 0.168 | 0.010 | 3 | 18.831 | 0.044 | 4 | 2.423 | 0.017 | 5 | 17.724 | 0.033 |
| 1 | 17.557 | 0.067 | 2 | 2.099 | 0.022 | 3 | 0.366 | 0.010 | 4 | 3.546 | 0.019 | 5 | 19.068 | 0.035 |
| 1 | 18.520 | 0.069 | 2 | 3.073 | 0.025 | 3 | 0.465 | 0.012 | 4 | 5.647 | 0.022 | 5 | 0.213 | 0.008 |
| 1 | 0.443 | 0.018 | 2 | 4.711 | 0.028 | 3 | 0.679 | 0.013 | 4 | 7.820 | 0.024 | 5 | 0.414 | 0.009 |
| 1 | 0.128 | 0.013 | 2 | 7.066 | 0.032 | 3 | 0.947 | 0.014 | 4 | 10.459 | 0.028 | 5 | 0.544 | 0.010 |
| 1 | 0.604 | 0.020 | 2 | 9.420 | 0.036 | 3 | 1.288 | 0.016 | 4 | 12.266 | 0.030 | 5 | 0.798 | 0.011 |
| 1 | 0.927 | 0.022 | 2 | 11.476 | 0.040 | 3 | 1.671 | 0.017 | 4 | 14.572 | 0.033 | 5 | 1.094 | 0.012 |
| 1 | 1.179 | 0.025 | 2 | 13.569 | 0.043 | | | | 4 | 17.128 | 0.036 | 5 | 1.347 | 0.013 |
| 1 | 1.526 | 0.026 | 2 | 16.085 | 0.048 | | | | 4 | 19.363 | 0.039 | 5 | 1.610 | 0.013 |
| | | | 2 | 18.561 | 0.052 | | | | | | | 5 | 1.953 | 0.014 |

Table A.5: 1% CMC in water solution flowing in a 150 mm rectangular flume

| | |
|-----------------------------|--------|
| Material: | CMC |
| Concentration/vol: | 1.0% |
| Density kg/m ³ : | 1006.7 |
| Ty (Pa): | 0.000 |
| k (Pa.s ⁿ): | 0.060 |
| n: | 0.655 |
| Flume width (mm): | 150 |

| SLOPE | FLOW | DEPTH | SLOPE | FLOW | DEPTH | SLOPE | FLOW | DEPTH | SLOPE | FLOW | DEPTH | SLOPE | FLOW | DEPTH |
|-----------|----------------------|-------|-----------|----------------------|-------|-----------|----------------------|-------|-----------|----------------------|-------|-----------|----------------------|-------|
| FLUME | Q | h | FLUME | Q | h | FLUME | Q | h | FLUME | Q | h | FLUME | Q | h |
| (degrees) | (l.s ⁻¹) | (m) | (degrees) | (l.s ⁻¹) | (m) | (degrees) | (l.s ⁻¹) | (m) | (degrees) | (l.s ⁻¹) | (m) | (degrees) | (l.s ⁻¹) | (m) |
| 1 | 1.161 | 0.011 | 2 | 0.181 | 0.005 | 3 | 1.954 | 0.009 | 4 | 0.342 | 0.004 | 5 | 2.051 | 0.010 |
| 1 | 1.925 | 0.015 | 2 | 0.291 | 0.004 | 3 | 4.549 | 0.021 | 4 | 0.643 | 0.005 | 5 | 4.512 | 0.017 |
| 1 | 4.476 | 0.029 | 2 | 0.656 | 0.006 | 3 | 6.664 | 0.027 | 4 | 0.971 | 0.006 | 5 | 6.802 | 0.022 |
| 1 | 6.741 | 0.039 | 2 | 0.938 | 0.007 | 3 | 9.227 | 0.036 | 4 | 1.267 | 0.006 | 5 | 9.258 | 0.029 |
| 1 | 9.140 | 0.052 | 2 | 1.272 | 0.009 | 3 | 11.892 | 0.041 | 4 | 1.979 | 0.010 | 5 | 11.762 | 0.034 |
| 1 | 11.755 | 0.062 | 2 | 2.102 | 0.011 | 3 | 13.464 | 0.046 | 4 | 4.351 | 0.017 | 5 | 13.644 | 0.038 |
| 1 | 13.496 | 0.069 | 2 | 4.520 | 0.024 | 3 | 16.586 | 0.054 | 4 | 6.840 | 0.024 | 5 | 16.613 | 0.045 |
| 1 | 16.278 | 0.079 | 2 | 6.753 | 0.032 | 3 | 18.275 | 0.059 | 4 | 9.231 | 0.030 | 5 | 20.410 | 0.052 |
| 1 | 18.321 | 0.088 | 2 | 9.251 | 0.040 | 3 | 20.420 | 0.066 | 4 | 11.761 | 0.037 | 5 | 0.342 | 0.004 |
| 1 | 20.280 | 0.098 | 2 | 11.982 | 0.049 | 3 | 0.313 | 0.004 | 4 | 13.495 | 0.041 | 5 | 0.624 | 0.004 |
| 1 | 0.153 | 0.006 | 2 | 13.460 | 0.056 | 3 | 0.636 | 0.005 | 4 | 16.542 | 0.049 | 5 | 0.907 | 0.005 |
| 1 | 0.323 | 0.007 | 2 | 16.585 | 0.064 | 3 | 0.906 | 0.006 | 4 | 20.389 | 0.058 | 5 | 1.280 | 0.006 |
| 1 | 0.653 | 0.009 | 2 | 18.210 | 0.074 | 3 | 1.240 | 0.007 | | | | | | |
| 1 | 0.090 | 0.005 | 2 | 20.252 | 0.075 | 3 | 1.514 | 0.008 | | | | | | |

Table A.6: 1.8% CMC in water solution flowing in a 150 mm rectangular flume

| | |
|-----------------------------|--------|
| Material: | CMC |
| Concentration/vol: | 1.8% |
| Density kg/m ³ : | 1010.7 |
| Ty (Pa): | 0.000 |
| k (Pa.s ⁿ): | 0.087 |
| n: | 0.765 |
| Flume width (mm): | 150 |

| SLOPE | FLOW | DEPTH | SLOPE | FLOW | DEPTH | SLOPE | FLOW | DEPTH | SLOPE | FLOW | DEPTH | SLOPE | FLOW | DEPTH |
|-----------|----------------------|-------|-----------|----------------------|-------|-----------|----------------------|-------|-----------|----------------------|-------|-----------|----------------------|-------|
| FLUME | Q | h | FLUME | Q | h | FLUME | Q | h | FLUME | Q | h | FLUME | Q | h |
| (degrees) | (l.s ⁻¹) | (m) | (degrees) | (l.s ⁻¹) | (m) | (degrees) | (l.s ⁻¹) | (m) | (degrees) | (l.s ⁻¹) | (m) | (degrees) | (l.s ⁻¹) | (m) |
| 5 | 2.029 | 0.011 | 4 | 1.457 | 0.010 | 3 | 1.929 | 0.012 | 2 | 1.447 | 0.013 | 1 | 2.202 | 0.020 |
| 5 | 4.361 | 0.016 | 4 | 1.150 | 0.009 | 3 | 4.264 | 0.019 | 2 | 1.185 | 0.012 | 1 | 2.821 | 0.022 |
| 5 | 6.543 | 0.021 | 4 | 0.880 | 0.008 | 3 | 6.651 | 0.025 | 2 | 0.856 | 0.011 | 1 | 4.101 | 0.028 |
| 5 | 9.038 | 0.029 | 4 | 0.626 | 0.008 | 3 | 2.891 | 0.015 | 2 | 0.543 | 0.009 | 1 | 6.473 | 0.037 |
| 5 | 11.579 | 0.036 | 4 | 0.297 | 0.006 | 3 | 9.049 | 0.033 | 2 | 0.422 | 0.009 | 1 | 8.987 | 0.049 |
| 5 | 13.082 | 0.040 | 4 | 4.398 | 0.017 | 3 | 11.465 | 0.042 | 2 | 0.287 | 0.008 | 1 | 11.395 | 0.062 |
| 5 | 15.586 | 0.047 | 4 | 6.742 | 0.024 | 3 | 13.359 | 0.047 | 2 | 2.013 | 0.014 | 1 | 13.356 | 0.070 |
| 5 | 18.131 | 0.052 | 4 | 9.098 | 0.031 | 3 | 15.650 | 0.054 | 2 | 3.006 | 0.018 | 1 | 15.785 | 0.083 |
| 5 | 20.183 | 0.057 | 4 | 11.858 | 0.038 | 3 | 18.089 | 0.060 | 2 | 4.082 | 0.021 | 1 | 17.956 | 0.089 |
| 5 | 0.293 | 0.005 | 4 | 13.161 | 0.041 | 3 | 20.104 | 0.067 | 2 | 6.465 | 0.030 | 1 | 19.866 | 0.097 |
| 5 | 0.598 | 0.006 | 4 | 15.754 | 0.049 | 3 | 0.291 | 0.006 | 2 | 9.035 | 0.039 | 1 | 0.293 | 0.010 |
| 5 | 0.920 | 0.008 | 4 | 17.958 | 0.054 | 3 | 0.589 | 0.008 | 2 | 11.545 | 0.049 | 1 | 0.435 | 0.011 |
| 5 | 1.197 | 0.009 | 4 | 20.050 | 0.060 | 3 | 0.399 | 0.007 | 2 | 13.248 | 0.054 | 1 | 0.600 | 0.012 |
| 5 | 1.477 | 0.010 | | | | 3 | 0.906 | 0.009 | 2 | 15.694 | 0.063 | 1 | 0.906 | 0.014 |
| | | | | | | 3 | 1.170 | 0.010 | 2 | 18.080 | 0.071 | 1 | 1.214 | 0.015 |
| | | | | | | 3 | 1.465 | 0.011 | 2 | 20.010 | 0.077 | 1 | 1.477 | 0.017 |

Table A.7: 2.8% CMC in water solution flowing in a 150 mm rectangular flume

| | |
|-----------------------------|-------|
| Material: | CMC |
| Concentration/vol: | 2.8% |
| Density kg/m ³ : | 1016 |
| Ty (Pa): | 0.000 |
| k (Pa.s ⁿ): | 0.769 |
| n: | 0.197 |
| Flume width (mm): | 150 |

| SLOPE FLUME | FLOW Q | DEPTH h | SLOPE FLUME | FLOW Q | DEPTH h | SLOPE FLUME | FLOW Q | DEPTH h | SLOPE FLUME | FLOW Q | DEPTH h | SLOPE FLUME | FLOW Q | DEPTH h |
|----------------|----------------------|------------|----------------|----------------------|------------|----------------|----------------------|------------|----------------|----------------------|------------|----------------|----------------------|------------|
| (degrees) | (l.s ⁻¹) | (m) | (degrees) | (l.s ⁻¹) | (m) | (degrees) | (l.s ⁻¹) | (m) | (degrees) | (l.s ⁻¹) | (m) | (degrees) | (l.s ⁻¹) | (m) |
| 1 | 1.776 | 0.027 | 2 | 1.469 | 0.019 | 3 | 1.998 | 0.017 | 4 | 1.465 | 0.013 | 5 | 2.062 | 0.014 |
| 1 | 2.830 | 0.032 | 2 | 1.186 | 0.018 | 3 | 2.831 | 0.019 | 4 | 1.219 | 0.013 | 5 | 2.777 | 0.015 |
| 1 | 4.230 | 0.039 | 2 | 0.881 | 0.016 | 3 | 4.189 | 0.023 | 4 | 0.890 | 0.011 | 5 | 4.220 | 0.019 |
| 1 | 6.616 | 0.051 | 2 | 0.603 | 0.014 | 3 | 6.624 | 0.032 | 4 | 0.586 | 0.010 | 5 | 6.618 | 0.025 |
| 1 | 9.022 | 0.063 | 2 | 0.320 | 0.011 | 3 | 8.999 | 0.038 | 4 | 0.302 | 0.008 | 5 | 8.933 | 0.030 |
| 1 | 11.585 | 0.075 | 2 | 1.945 | 0.020 | 3 | 11.350 | 0.045 | 4 | 1.868 | 0.014 | 5 | 11.473 | 0.036 |
| 1 | 13.728 | 0.085 | 2 | 2.789 | 0.022 | 3 | 13.773 | 0.051 | 4 | 4.308 | 0.021 | 5 | 13.939 | 0.041 |
| 1 | 16.185 | 0.096 | 2 | 4.344 | 0.028 | 3 | 16.350 | 0.059 | 4 | 6.569 | 0.026 | 5 | 16.142 | 0.046 |
| 1 | 18.064 | 0.105 | 2 | 6.644 | 0.036 | 3 | 18.105 | 0.064 | 4 | 9.044 | 0.034 | 5 | 18.259 | 0.052 |
| 1 | 20.044 | 0.114 | 2 | 8.994 | 0.045 | 3 | 20.095 | 0.070 | 4 | 11.587 | 0.039 | 5 | 20.076 | 0.055 |
| 1 | 0.315 | 0.015 | 2 | 11.753 | 0.055 | 3 | 0.301 | 0.009 | 4 | 13.643 | 0.045 | 5 | 0.280 | 0.007 |
| 1 | 0.600 | 0.018 | 2 | 13.753 | 0.061 | 3 | 0.621 | 0.011 | 4 | 16.154 | 0.051 | 5 | 0.662 | 0.009 |
| 1 | 0.900 | 0.021 | 2 | 16.257 | 0.069 | 3 | 0.866 | 0.013 | 4 | 17.927 | 0.056 | 5 | 0.887 | 0.010 |
| 1 | 1.191 | 0.023 | 2 | 20.161 | 0.082 | 3 | 1.188 | 0.014 | 4 | 19.974 | 0.062 | 5 | 1.171 | 0.011 |
| 1 | 1.490 | 0.025 | | | | 3 | 1.494 | 0.015 | | | | 5 | 1.488 | 0.012 |

Table A.8: 3.8% CMC in water solution flowing in a 150 mm rectangular flume

| | |
|-----------------------------|-------|
| Material: | CMC |
| Concentration/vol: | 3.8% |
| Density kg/m ³ : | 1021 |
| Ty (Pa): | 0.000 |
| k (Pa.s ⁿ): | 0.572 |
| n: | 0.690 |
| Flume width (mm): | 150 |

| SLOPE FLUME | FLOW Q | DEPTH h | SLOPE FLUME | FLOW Q | DEPTH h | SLOPE FLUME | FLOW Q | DEPTH h | SLOPE FLUME | FLOW Q | DEPTH h | SLOPE FLUME | FLOW Q | DEPTH h |
|----------------|----------------------|------------|----------------|----------------------|------------|----------------|----------------------|------------|----------------|----------------------|------------|----------------|----------------------|------------|
| (degrees) | (l.s ⁻¹) | (m) | (degrees) | (l.s ⁻¹) | (m) | (degrees) | (l.s ⁻¹) | (m) | (degrees) | (l.s ⁻¹) | (m) | (degrees) | (l.s ⁻¹) | (m) |
| 1 | 1.974 | 0.041 | 2 | 1.593 | 0.027 | 3 | 2.254 | 0.025 | 4 | 1.748 | 0.020 | 5 | 2.682 | 0.021 |
| 1 | 4.264 | 0.058 | 2 | 1.249 | 0.025 | 3 | 3.299 | 0.029 | 4 | 1.324 | 0.018 | 5 | 3.779 | 0.024 |
| 1 | 2.886 | 0.049 | 2 | 0.918 | 0.023 | 3 | 5.248 | 0.035 | 4 | 1.025 | 0.017 | 5 | 6.085 | 0.029 |
| 1 | 6.518 | 0.071 | 2 | 0.636 | 0.021 | 3 | 7.440 | 0.042 | 4 | 0.735 | 0.015 | 5 | 8.389 | 0.035 |
| 1 | 8.826 | 0.083 | 2 | 0.461 | 0.018 | 3 | 9.843 | 0.050 | 4 | 0.484 | 0.014 | 5 | 10.642 | 0.040 |
| 1 | 11.226 | 0.095 | 2 | 0.335 | 0.017 | 3 | 11.822 | 0.056 | 4 | 0.367 | 0.012 | 5 | 13.173 | 0.045 |
| 1 | 12.922 | 0.106 | 2 | 0.142 | 0.014 | 3 | 14.212 | 0.064 | 4 | 0.184 | 0.011 | 5 | 15.242 | 0.053 |
| 1 | 15.714 | 0.119 | 2 | 2.092 | 0.030 | 3 | 16.704 | 0.072 | 4 | 2.468 | 0.023 | 5 | 17.559 | 0.059 |
| 1 | 17.995 | 0.132 | 2 | 3.057 | 0.035 | 3 | 17.041 | 0.073 | 4 | 3.536 | 0.026 | 5 | 18.433 | 0.061 |
| 1 | 19.271 | 0.137 | 2 | 4.700 | 0.041 | 3 | 0.164 | 0.011 | 4 | 5.660 | 0.031 | | | |
| 1 | 0.112 | 0.018 | 2 | 6.969 | 0.049 | 3 | 0.346 | 0.013 | 4 | 7.896 | 0.038 | | | |
| 1 | 0.292 | 0.022 | 2 | 9.325 | 0.058 | 3 | 0.575 | 0.016 | 4 | 10.364 | 0.044 | | | |
| 1 | 0.651 | 0.026 | 2 | 11.471 | 0.066 | 3 | 0.731 | 0.018 | 4 | 12.149 | 0.050 | | | |
| 1 | 0.904 | 0.031 | 2 | 13.575 | 0.075 | 3 | 1.090 | 0.020 | 4 | 14.615 | 0.057 | | | |
| 1 | 1.202 | 0.033 | 2 | 16.131 | 0.084 | 3 | 1.288 | 0.021 | 4 | 17.044 | 0.064 | | | |
| 1 | 1.494 | 0.036 | 2 | 18.533 | 0.093 | 3 | 1.683 | 0.023 | 4 | 18.839 | 0.069 | | | |

Table A.9: 4.5% Bentonite in water suspension flowing in a 300 mm rectangular flume

| | |
|-----------------------------|-----------|
| Material: | Bentonite |
| Concentration/vol: | 4.5% |
| Density kg/m ³ : | 1025 |
| Ty (Pa): | 5.410 |
| k (Pa.s ⁿ): | 0.004 |
| n: | 1.000 |
| Flume width (mm): | 300 |

| SLOPE FLUME | FLOW Q | DEPTH h | SLOPE FLUME | FLOW Q | DEPTH h | SLOPE FLUME | FLOW Q | DEPTH h | SLOPE FLUME | FLOW Q | DEPTH h | SLOPE FLUME | FLOW Q | DEPTH h |
|----------------|----------------------|------------|----------------|----------------------|------------|----------------|----------------------|------------|----------------|----------------------|------------|----------------|----------------------|------------|
| (degrees) | (l.s ⁻¹) | (m) | (degrees) | (l.s ⁻¹) | (m) | (degrees) | (l.s ⁻¹) | (m) | (degrees) | (l.s ⁻¹) | (m) | (degrees) | (l.s ⁻¹) | (m) |
| 1 | 1.944 | 0.0349 | 2 | 0.300 | 0.0176 | 3 | 2.042 | 0.0125 | 4 | 0.292 | 0.0074 | 5 | 2.061 | 0.0086 |
| 1 | 1.946 | 0.0370 | 2 | 0.672 | 0.0187 | 3 | 4.596 | 0.0160 | 4 | 0.668 | 0.0087 | 5 | 4.531 | 0.0107 |
| 1 | 4.495 | 0.0366 | 2 | 1.001 | 0.0194 | 3 | 7.039 | 0.0184 | 4 | 0.952 | 0.0091 | 5 | 7.048 | 0.0134 |
| 1 | 6.985 | 0.0388 | 2 | 1.301 | 0.0197 | 3 | 9.606 | 0.0213 | 4 | 1.242 | 0.0094 | 5 | 9.630 | 0.0152 |
| 1 | 9.625 | 0.0424 | 2 | 1.968 | 0.0194 | 3 | 12.250 | 0.0246 | 4 | 2.171 | 0.0104 | 5 | 12.223 | 0.0182 |
| 1 | 12.261 | 0.0469 | 2 | 4.518 | 0.0225 | 3 | 14.230 | 0.0263 | 4 | 4.539 | 0.0128 | 5 | 14.226 | 0.0203 |
| 1 | 14.142 | 0.0460 | 2 | 7.085 | 0.0248 | 3 | 18.201 | 0.0310 | 4 | 7.201 | 0.0155 | 5 | 18.197 | 0.0238 |
| 1 | 18.229 | 0.0523 | 2 | 9.567 | 0.0277 | 3 | 21.444 | 0.0344 | 4 | 9.689 | 0.0178 | 5 | 21.566 | 0.0274 |
| 1 | 22.351 | 0.0561 | 2 | 12.495 | 0.0314 | 3 | 0.309 | 0.0099 | 4 | 12.168 | 0.0203 | 5 | 0.284 | 0.0064 |
| 1 | 1.250 | 0.0346 | 2 | 14.036 | 0.0332 | 3 | 0.614 | 0.0105 | 4 | 14.158 | 0.0226 | 5 | 0.657 | 0.0072 |
| 1 | 0.925 | 0.0336 | 2 | 18.100 | 0.0385 | 3 | 0.939 | 0.0113 | 4 | 18.238 | 0.0270 | 5 | 0.959 | 0.0068 |
| 1 | 0.577 | 0.0337 | 2 | 21.137 | 0.0416 | 3 | 1.249 | 0.0114 | 4 | 21.127 | 0.0289 | 5 | 1.252 | 0.0068 |

Table A.10: 6% Bentonite in water suspension in a 300 mm rectangular flume

| | |
|-----------------------------|-----------|
| Material: | Bentonite |
| Concentration/vol: | 6.0% |
| Density kg/m ³ : | 1034 |
| Ty (Pa): | 12.698 |
| k (Pa.s ⁿ): | 0.006 |
| n: | 1.000 |
| Flume width (mm): | 300 |

| SLOPE FLUME | FLOW Q | DEPTH h | SLOPE FLUME | FLOW Q | DEPTH h | SLOPE FLUME | FLOW Q | DEPTH h | SLOPE FLUME | FLOW Q | DEPTH h |
|----------------|----------------------|------------|----------------|----------------------|------------|----------------|----------------------|------------|----------------|----------------------|------------|
| (degrees) | (l.s ⁻¹) | (m) | (degrees) | (l.s ⁻¹) | (m) | (degrees) | (l.s ⁻¹) | (m) | (degrees) | (l.s ⁻¹) | (m) |
| 5 | 0.281 | 0.0185 | 4 | 2.081 | 0.0252 | 3 | 1.232 | 0.0335 | 2 | 2.141 | 0.0565 |
| 5 | 0.615 | 0.0191 | 4 | 3.015 | 0.0257 | 3 | 0.930 | 0.0332 | 2 | 3.048 | 0.0586 |
| 5 | 1.193 | 0.0195 | 4 | 5.084 | 0.0269 | 3 | 0.594 | 0.0334 | 2 | 5.035 | 0.0592 |
| 5 | 21.017 | 0.0332 | 4 | 7.004 | 0.0271 | 3 | 20.217 | 0.0438 | 2 | 7.086 | 0.0575 |
| 5 | 18.970 | 0.0305 | 4 | 9.009 | 0.0280 | 3 | 18.880 | 0.0430 | 2 | 9.158 | 0.0567 |
| 5 | 17.108 | 0.0287 | 4 | 11.070 | 0.0288 | 3 | 15.004 | 0.0393 | 2 | 10.937 | 0.0562 |
| 5 | 15.391 | 0.0273 | 4 | 13.138 | 0.0306 | 3 | 13.143 | 0.0382 | 2 | 12.921 | 0.0563 |
| 5 | 13.177 | 0.0256 | 4 | 15.275 | 0.0324 | 3 | 10.883 | 0.0353 | 2 | 14.952 | 0.0565 |
| 5 | 11.309 | 0.0243 | 4 | 17.053 | 0.0340 | 3 | 8.990 | 0.0343 | 2 | 17.575 | 0.0593 |
| 5 | 8.979 | 0.0230 | 4 | 19.001 | 0.0359 | 3 | 7.056 | 0.0344 | 2 | 20.464 | 0.0606 |
| 5 | 7.116 | 0.0227 | 4 | 18.985 | 0.0347 | 3 | 5.093 | 0.0346 | | | |
| 5 | 5.020 | 0.0212 | 4 | 21.165 | 0.0371 | 3 | 2.997 | 0.0343 | | | |
| 5 | 2.983 | 0.0201 | 4 | 0.310 | 0.0221 | 3 | 2.068 | 0.0337 | | | |
| 5 | 1.977 | 0.0194 | 4 | 0.756 | 0.0237 | | | | | | |
| | | | 4 | 0.946 | 0.0239 | | | | | | |
| | | | 4 | 1.212 | 0.0239 | | | | | | |

Table A.11: 4.5% Bentonite in water suspension in a 150 mm rectangular flume

| | |
|-----------------------------|-----------|
| Material: | Bentonite |
| Concentration/vol: | 3.0% |
| Density kg/m ³ : | 1014 |
| Ty (Pa): | 1.002 |
| k (Pa.s ⁿ): | 0.003 |
| n: | 1.000 |
| Flume width (mm): | 150 |

| SLOPE | FLOW | DEPTH | SLOPE | FLOW | DEPTH | SLOPE | FLOW | DEPTH | SLOPE | FLOW | DEPTH | SLOPE | FLOW | DEPTH |
|-----------|----------------------|--------|-----------|----------------------|--------|-----------|----------------------|--------|-----------|----------------------|--------|-----------|----------------------|--------|
| FLUME | Q | h | FLUME | Q | h | FLUME | Q | h | FLUME | Q | h | FLUME | Q | h |
| (degrees) | (l.s ⁻¹) | (m) | (degrees) | (l.s ⁻¹) | (m) | (degrees) | (l.s ⁻¹) | (m) | (degrees) | (l.s ⁻¹) | (m) | (degrees) | (l.s ⁻¹) | (m) |
| 1 | 4.309 | 0.0239 | 3 | 2.213 | 0.0086 | 5 | 2.089 | 0.0087 | 4 | 0.334 | 0.0030 | 2 | 0.460 | 0.0063 |
| 1 | 6.111 | 0.0326 | 3 | 4.157 | 0.0171 | 5 | 4.178 | 0.0140 | 4 | 0.430 | 0.0036 | 2 | 0.603 | 0.0062 |
| 1 | 8.117 | 0.0416 | 3 | 6.187 | 0.0235 | 5 | 6.072 | 0.0189 | 4 | 0.607 | 0.0042 | 2 | 0.816 | 0.0070 |
| 1 | 10.216 | 0.0505 | 3 | 8.254 | 0.0287 | 5 | 8.224 | 0.0238 | 4 | 0.803 | 0.0049 | 2 | 1.220 | 0.0083 |
| 1 | 13.267 | 0.0614 | 3 | 10.437 | 0.0341 | 5 | 10.423 | 0.0280 | 4 | 1.020 | 0.0052 | 2 | 1.506 | 0.0091 |
| 1 | 16.619 | 0.0722 | 3 | 13.268 | 0.0409 | 5 | 13.550 | 0.0335 | 4 | 1.261 | 0.0055 | 2 | 1.045 | 0.0075 |
| 1 | 19.333 | 0.0808 | 3 | 16.526 | 0.0493 | 5 | 16.386 | 0.0396 | 4 | 1.553 | 0.0076 | 1 | 1.324 | 0.0116 |
| 1 | 22.729 | 0.0919 | 3 | 19.328 | 0.0555 | 5 | 19.472 | 0.0447 | 3 | 1.525 | 0.0069 | 1 | 1.038 | 0.0103 |
| 2 | 2.229 | 0.0106 | 3 | 22.463 | 0.0628 | 5 | 22.352 | 0.0502 | 3 | 1.279 | 0.0063 | 1 | 0.806 | 0.0099 |
| 2 | 4.118 | 0.0171 | 4 | 1.985 | 0.0087 | 5 | 1.404 | 0.0072 | 3 | 1.018 | 0.0058 | 1 | 0.613 | 0.0093 |
| 2 | 6.100 | 0.0261 | 4 | 4.061 | 0.0153 | 5 | 1.085 | 0.0054 | 3 | 0.826 | 0.0051 | 1 | 0.417 | 0.0084 |
| 2 | 8.111 | 0.0329 | 4 | 6.176 | 0.0211 | 5 | 0.872 | 0.0039 | 3 | 0.405 | 0.0044 | 1 | 0.209 | 0.0079 |
| 2 | 10.351 | 0.0399 | 4 | 8.228 | 0.0259 | 5 | 0.660 | 0.0037 | 3 | 0.629 | 0.0045 | | | |
| 2 | 13.392 | 0.0488 | 4 | 10.509 | 0.0306 | 5 | 0.418 | 0.0029 | | | | | | |
| 2 | 16.192 | 0.0567 | 4 | 13.369 | 0.0380 | 5 | 0.287 | 0.0033 | | | | | | |
| 2 | 19.354 | 0.0646 | 4 | 16.220 | 0.0441 | | | | | | | | | |
| 2 | 22.400 | 0.0721 | 4 | 19.452 | 0.0491 | | | | | | | | | |
| | | | 4 | 22.424 | 0.0561 | | | | | | | | | |

Table A.12: 4.5% Bentonite in water suspension in a 150 mm rectangular flume

| | |
|-----------------------------|-----------|
| Material: | Bentonite |
| Concentration/vol: | 4.5% |
| Density kg/m ³ : | 1025 |
| Ty (Pa): | 4.402 |
| k (Pa.s ⁿ): | 0.006 |
| n: | 1.000 |
| Flume width (mm): | 150 |

| SLOPE | FLOW | DEPTH | SLOPE | FLOW | DEPTH | SLOPE | FLOW | DEPTH | SLOPE | FLOW | DEPTH | SLOPE | FLOW | DEPTH |
|-----------|----------------------|--------|-----------|----------------------|--------|-----------|----------------------|--------|-----------|----------------------|--------|-----------|----------------------|--------|
| FLUME | Q | h | FLUME | Q | h | FLUME | Q | h | FLUME | Q | h | FLUME | Q | h |
| (degrees) | (l.s ⁻¹) | (m) | (degrees) | (l.s ⁻¹) | (m) | (degrees) | (l.s ⁻¹) | (m) | (degrees) | (l.s ⁻¹) | (m) | (degrees) | (l.s ⁻¹) | (m) |
| 1 | 1.232 | 0.0390 | 2 | 2.225 | 0.0188 | 3 | 1.228 | 0.0135 | 4 | 1.994 | 0.0117 | 5 | 1.247 | 0.0090 |
| 1 | 0.944 | 0.0411 | 2 | 4.524 | 0.0260 | 3 | 0.946 | 0.0122 | 4 | 4.528 | 0.0177 | 5 | 0.941 | 0.0075 |
| 1 | 0.629 | 0.0414 | 2 | 7.047 | 0.0331 | 3 | 0.632 | 0.0122 | 4 | 6.931 | 0.0225 | 5 | 0.611 | 0.0074 |
| 1 | 2.272 | 0.0445 | 2 | 9.511 | 0.0396 | 3 | 0.305 | 0.0113 | 4 | 9.538 | 0.0281 | 5 | 2.273 | 0.0103 |
| 1 | 4.492 | 0.0490 | 2 | 12.299 | 0.0475 | 3 | 2.005 | 0.0143 | 4 | 12.279 | 0.0335 | 5 | 4.546 | 0.0149 |
| 1 | 6.968 | 0.0554 | 2 | 14.192 | 0.0515 | 3 | 4.591 | 0.0209 | 4 | 14.114 | 0.0384 | 5 | 6.961 | 0.0199 |
| 1 | 9.683 | 0.0643 | 2 | 18.227 | 0.0617 | 3 | 7.261 | 0.0279 | 4 | 18.082 | 0.0485 | 5 | 9.491 | 0.0252 |
| 1 | 12.423 | 0.0709 | 2 | 21.307 | 0.0707 | 3 | 9.653 | 0.0326 | 4 | 21.473 | 0.0530 | 5 | 12.322 | 0.0302 |
| 1 | 11.925 | 0.0710 | 2 | 0.337 | 0.0150 | 3 | 11.949 | 0.0383 | 4 | 0.335 | 0.0084 | 5 | 14.493 | 0.0343 |
| 1 | 14.028 | 0.0760 | 2 | 0.610 | 0.0162 | 3 | 14.226 | 0.0436 | 4 | 0.622 | 0.0088 | 5 | 18.066 | 0.0427 |
| 1 | 17.990 | 0.0839 | 2 | 0.911 | 0.0166 | 3 | 18.124 | 0.0532 | 4 | 0.976 | 0.0097 | 5 | 21.178 | 0.0490 |
| 1 | 21.103 | 0.0884 | 2 | 1.226 | 0.0170 | 3 | 21.271 | 0.0621 | 4 | 1.226 | 0.0105 | | | |

Table A.13: 6% Bentonite in water suspension in a 150 mm rectangular flume

| | |
|-----------------------------|-----------|
| Material: | Bentonite |
| Concentration/vol: | 6.0% |
| Density kg/m ³ : | 1033 |
| Ty (Pa): | 8.187 |
| k (Pa.s ⁿ): | 0.006 |
| n: | 1.000 |
| Flume width (mm): | 150 |

| SLOPE | FLOW | DEPTH | SLOPE | FLOW | DEPTH | SLOPE | FLOW | DEPTH | SLOPE | FLOW | DEPTH | SLOPE | FLOW | DEPTH |
|-----------|----------------------|--------|-----------|----------------------|--------|-----------|----------------------|--------|-----------|----------------------|--------|-----------|----------------------|--------|
| FLUME | Q | h | FLUME | Q | h | FLUME | Q | h | FLUME | Q | h | FLUME | Q | h |
| (degrees) | (l.s ⁻¹) | (m) | (degrees) | (l.s ⁻¹) | (m) | (degrees) | (l.s ⁻¹) | (m) | (degrees) | (l.s ⁻¹) | (m) | (degrees) | (l.s ⁻¹) | (m) |
| 1 | 0.363 | 0.0801 | 3 | 0.366 | 0.0242 | 5 | 0.336 | 0.0129 | 3 | 2.066 | 0.0223 | 2 | 2.007 | 0.0350 |
| 1 | 0.676 | 0.0835 | 3 | 0.640 | 0.0231 | 5 | 0.657 | 0.0133 | 3 | 4.370 | 0.0284 | 2 | 4.513 | 0.0397 |
| 1 | 0.969 | 0.0858 | 3 | 0.919 | 0.0246 | 5 | 0.940 | 0.0140 | 3 | 7.027 | 0.0340 | 2 | 6.994 | 0.0477 |
| 1 | 1.252 | 0.0858 | 3 | 1.227 | 0.0246 | 5 | 1.236 | 0.0140 | 3 | 9.534 | 0.0393 | 2 | 9.579 | 0.0533 |
| 1 | 1.585 | 0.0888 | 3 | 1.522 | 0.0257 | 5 | 1.532 | 0.0148 | 3 | 11.918 | 0.0455 | 2 | 11.852 | 0.0593 |
| 1 | 1.930 | 0.0852 | 4 | 1.520 | 0.0180 | 5 | 2.000 | 0.0146 | 3 | 16.593 | 0.0583 | 2 | 16.006 | 0.0706 |
| 2 | 1.559 | 0.0378 | 4 | 1.229 | 0.0175 | 5 | 4.470 | 0.0188 | 3 | 17.817 | 0.0599 | 2 | 18.170 | 0.0761 |
| 2 | 1.224 | 0.0384 | 4 | 0.920 | 0.0170 | 5 | 7.042 | 0.0242 | 3 | 20.803 | 0.0668 | 2 | 20.206 | 0.0815 |
| 2 | 0.931 | 0.0379 | 4 | 0.589 | 0.0163 | 5 | 9.644 | 0.0286 | 4 | 2.019 | 0.0167 | 1 | 1.965 | 0.0841 |
| 2 | 0.606 | 0.0391 | 4 | 0.283 | 0.0154 | 5 | 12.276 | 0.0322 | 4 | 4.522 | 0.0223 | 1 | 4.444 | 0.0951 |
| 2 | 0.301 | 0.0405 | | | | 5 | 15.897 | 0.0363 | 4 | 7.078 | 0.0277 | 1 | 7.111 | 0.1124 |
| | | | | | | 5 | 18.188 | 0.0460 | 4 | 9.559 | 0.0330 | 1 | 9.513 | 0.1148 |
| | | | | | | 5 | 20.647 | 0.0510 | 4 | 12.083 | 0.0382 | 1 | 12.469 | 0.1123 |
| | | | | | | | | | 4 | 16.100 | 0.0469 | 1 | 16.145 | 0.1216 |
| | | | | | | | | | 4 | 18.457 | 0.0519 | 1 | 18.527 | 0.1307 |
| | | | | | | | | | | | | 1 | 20.454 | 0.1375 |

Table A.14: 3% kaolin in water suspension in a 150 mm rectangular flume

| | |
|-----------------------------|--------|
| Material: | Kaolin |
| Concentration/vol: | 3% |
| Density kg/m ³ : | 1049 |
| Ty (Pa): | 1.843 |
| k (Pa.s ⁿ): | 0.002 |
| n: | 1.062 |
| Flume width (mm): | 150 |

| SLOPE FLUME (degrees) | FLOW Q (l.s ⁻¹) | DEPTH h (m) | SLOPE FLUME (degrees) | FLOW Q (l.s ⁻¹) | DEPTH h (m) | SLOPE FLUME (degrees) | FLOW Q (l.s ⁻¹) | DEPTH h (m) | SLOPE FLUME (degrees) | FLOW Q (l.s ⁻¹) | DEPTH h (m) |
|-----------------------------|-----------------------------------|-------------------|-----------------------------|-----------------------------------|-------------------|-----------------------------|-----------------------------------|-------------------|-----------------------------|-----------------------------------|-------------------|
| 4 | 3.052 | 0.0111 | 3 | 0.976 | 0.0069 | 2 | 1.039 | 0.0090 | 1 | 1.153 | 0.0147 |
| 4 | 4.063 | 0.0135 | 3 | 2.039 | 0.0092 | 2 | 2.225 | 0.0119 | 1 | 2.013 | 0.0171 |
| 4 | 5.160 | 0.0159 | 3 | 3.056 | 0.0115 | 2 | 3.027 | 0.0141 | 1 | 3.114 | 0.0207 |
| 4 | 6.212 | 0.0187 | 3 | 4.051 | 0.0139 | 2 | 4.239 | 0.0175 | 1 | 4.297 | 0.0255 |
| 4 | 8.190 | 0.0228 | 3 | 4.993 | 0.0168 | 2 | 6.138 | 0.0228 | 1 | 6.299 | 0.0326 |
| 4 | 10.956 | 0.0290 | 3 | 6.055 | 0.0195 | 2 | 8.249 | 0.0281 | 1 | 8.238 | 0.0372 |
| 4 | 12.225 | 0.0323 | 3 | 7.296 | 0.0232 | 2 | 10.193 | 0.0367 | 1 | 10.211 | 0.0460 |
| 4 | 14.291 | 0.0357 | 3 | 8.118 | 0.0255 | 2 | 12.574 | 0.0433 | 1 | 12.799 | 0.0569 |
| 4 | 16.382 | 0.0403 | 3 | 10.922 | 0.0324 | 2 | 14.208 | 0.0480 | 1 | 14.219 | 0.0618 |
| 4 | 20.345 | 0.0476 | 3 | 12.155 | 0.0358 | 2 | 16.483 | 0.0545 | 1 | 16.493 | 0.0705 |
| 4 | 0.773 | 0.0053 | 3 | 14.363 | 0.0420 | 2 | 18.379 | 0.0599 | 1 | 18.365 | 0.0772 |
| 4 | 0.528 | 0.0050 | 3 | 16.215 | 0.0458 | 2 | 20.452 | 0.0653 | 1 | 20.298 | 0.0832 |
| 4 | 0.306 | 0.0040 | 3 | 18.394 | 0.0521 | 2 | 0.740 | 0.0083 | 1 | 0.128 | 0.0164 |
| | | | 3 | 20.558 | 0.0569 | 2 | 0.518 | 0.0079 | 1 | 0.333 | 0.0180 |
| | | | 3 | 0.324 | 0.0044 | 2 | 0.325 | 0.0074 | 1 | 0.579 | 0.0201 |
| | | | 3 | 0.544 | 0.0060 | 2 | 0.148 | 0.0058 | 1 | 0.743 | 0.0203 |
| | | | 3 | 0.785 | 0.0063 | | | | | | |

Table A.15: 4.5% kaolin in water suspension in a 150 mm rectangular flume

| | |
|-----------------------------|--------|
| Material: | Kaolin |
| Concentration/vol: | 4.5% |
| Density kg/m ³ : | 1075 |
| Ty (Pa): | 3.510 |
| k (Pa.s ⁿ): | 0.012 |
| n: | 0.836 |
| Flume width (mm): | 150 |

| SLOPE FLUME (degrees) | FLOW Q (l.s ⁻¹) | DEPTH h (m) | SLOPE FLUME (degrees) | FLOW Q (l.s ⁻¹) | DEPTH h (m) | SLOPE FLUME (degrees) | FLOW Q (l.s ⁻¹) | DEPTH h (m) | SLOPE FLUME (degrees) | FLOW Q (l.s ⁻¹) | DEPTH h (m) | SLOPE FLUME (degrees) | FLOW Q (l.s ⁻¹) | DEPTH h (m) |
|-----------------------------|-----------------------------------|-------------------|-----------------------------|-----------------------------------|-------------------|-----------------------------|-----------------------------------|-------------------|-----------------------------|-----------------------------------|-------------------|-----------------------------|-----------------------------------|-------------------|
| 1 | 1.060 | 0.0235 | 2 | 1.028 | 0.0136 | 3 | 1.128 | 0.0106 | 4 | 1.203 | 0.0086 | 5 | 0.988 | 0.0070 |
| 1 | 2.078 | 0.0279 | 2 | 2.009 | 0.0158 | 3 | 2.245 | 0.0126 | 4 | 2.056 | 0.0106 | 5 | 2.134 | 0.0095 |
| 1 | 3.123 | 0.0306 | 2 | 3.115 | 0.0188 | 3 | 3.036 | 0.0147 | 4 | 3.140 | 0.0131 | 5 | 3.034 | 0.0114 |
| 1 | 4.103 | 0.0339 | 2 | 4.687 | 0.0235 | 3 | 4.266 | 0.0176 | 4 | 4.418 | 0.0154 | 5 | 4.184 | 0.0145 |
| 1 | 5.067 | 0.0372 | 2 | 5.393 | 0.0270 | 3 | 5.181 | 0.0200 | 4 | 5.509 | 0.0180 | 5 | 5.337 | 0.0170 |
| 1 | 6.209 | 0.0407 | 2 | 6.537 | 0.0291 | 3 | 6.042 | 0.0222 | 4 | 6.237 | 0.0193 | 5 | 6.238 | 0.0180 |
| 1 | 7.178 | 0.0449 | 2 | 8.281 | 0.0339 | 3 | 6.990 | 0.0250 | 4 | 10.611 | 0.0287 | 5 | 8.378 | 0.0231 |
| 1 | 8.288 | 0.0489 | 2 | 10.173 | 0.0394 | 3 | 8.363 | 0.0292 | 4 | 12.353 | 0.0336 | 5 | 10.461 | 0.0272 |
| 1 | 10.515 | 0.0568 | 2 | 12.482 | 0.0461 | 3 | 10.522 | 0.0339 | 4 | 14.447 | 0.0376 | 5 | 12.076 | 0.0316 |
| 1 | 12.518 | 0.0639 | 2 | 14.363 | 0.0518 | 3 | 12.730 | 0.0415 | 4 | 18.557 | 0.0476 | 5 | 14.411 | 0.0346 |
| 1 | 14.422 | 0.0708 | 2 | 16.573 | 0.0579 | 3 | 14.600 | 0.0444 | 4 | 0.371 | 0.0073 | 5 | 16.507 | 0.0407 |
| 1 | 16.284 | 0.0772 | 2 | 18.389 | 0.0626 | 3 | 16.334 | 0.0508 | 4 | 0.679 | 0.0079 | 5 | 18.907 | 0.0461 |
| 1 | 18.273 | 0.0823 | 2 | 20.469 | 0.0699 | 3 | 18.304 | 0.0548 | 4 | 0.953 | 0.0081 | 5 | 20.626 | 0.0493 |
| 1 | 20.611 | 0.0902 | 2 | 0.388 | 0.0129 | 3 | 20.471 | 0.0600 | | | | 5 | 0.946 | 0.0069 |
| 1 | 0.969 | 0.0251 | 2 | 0.633 | 0.0133 | 3 | 0.966 | 0.0103 | | | | 5 | 0.599 | 0.0065 |
| 1 | 0.606 | 0.0243 | 2 | 0.955 | 0.0136 | 3 | 0.624 | 0.0096 | | | | 5 | 0.324 | 0.0054 |
| 1 | 0.328 | 0.0239 | | | | 3 | 0.332 | 0.0094 | | | | | | |

Table A.16: 5.3% kaolin in water suspension in a 150 mm rectangular flume

| | |
|-----------------------------|--------|
| Material: | Kaolin |
| Concentration/vol: | 5.3% |
| Density kg/m ³ : | 1088 |
| Ty (Pa): | 4.400 |
| k (Pa.s ⁿ): | 0.084 |
| n: | 0.582 |
| Flume width (mm): | 150 |

| SLOPE | FLOW | DEPTH | SLOPE | FLOW | DEPTH | SLOPE | FLOW | DEPTH | SLOPE | FLOW | DEPTH | SLOPE | FLOW | DEPTH |
|-----------|----------------------|--------|-----------|----------------------|--------|-----------|----------------------|--------|-----------|----------------------|--------|-----------|----------------------|--------|
| FLUME | Q | h | FLUME | Q | h | FLUME | Q | h | FLUME | Q | h | FLUME | Q | h |
| (degrees) | (l.s ⁻¹) | (m) | (degrees) | (l.s ⁻¹) | (m) | (degrees) | (l.s ⁻¹) | (m) | (degrees) | (l.s ⁻¹) | (m) | (degrees) | (l.s ⁻¹) | (m) |
| 1 | 0.086 | 0.0298 | 2 | 0.161 | 0.0154 | 3 | 0.167 | 0.0109 | 4 | 1.040 | 0.0103 | 5 | 1.322 | 0.0093 |
| 1 | 0.189 | 0.0313 | 2 | 0.290 | 0.0164 | 3 | 0.276 | 0.0113 | 4 | 1.489 | 0.0110 | 5 | 2.129 | 0.0107 |
| 1 | 0.268 | 0.0323 | 2 | 0.385 | 0.0164 | 3 | 0.493 | 0.0118 | 4 | 2.057 | 0.0121 | 5 | 3.020 | 0.0123 |
| 1 | 0.367 | 0.0329 | 2 | 0.487 | 0.0168 | 3 | 0.579 | 0.0121 | 4 | 2.522 | 0.0132 | 5 | 4.536 | 0.0142 |
| 1 | 0.481 | 0.0334 | 2 | 0.700 | 0.0176 | 3 | 0.817 | 0.0123 | 4 | 2.994 | 0.0144 | 5 | 5.134 | 0.0163 |
| 1 | 0.703 | 0.0340 | 2 | 0.914 | 0.0177 | 3 | 1.013 | 0.0126 | 4 | 3.242 | 0.0142 | 5 | 6.102 | 0.0184 |
| 1 | 0.913 | 0.0347 | 2 | 1.532 | 0.0186 | 3 | 1.538 | 0.0137 | 4 | 4.139 | 0.0164 | 5 | 8.043 | 0.0219 |
| 1 | 1.449 | 0.0372 | 2 | 2.145 | 0.0202 | 3 | 2.011 | 0.0147 | 4 | 5.162 | 0.0186 | 5 | 10.192 | 0.0259 |
| 1 | 2.030 | 0.0377 | 2 | 2.437 | 0.0212 | 3 | 2.464 | 0.0160 | 4 | 6.908 | 0.0226 | 5 | 18.001 | 0.0411 |
| 1 | 3.356 | 0.0404 | 2 | 2.835 | 0.0221 | 3 | 2.994 | 0.0167 | 4 | 8.672 | 0.0263 | 5 | 28.125 | 0.0617 |
| 1 | 4.114 | 0.0436 | 2 | 4.846 | 0.0276 | 3 | 4.069 | 0.0194 | 4 | 10.137 | 0.0297 | 5 | 2.514 | 0.0115 |
| 1 | 5.271 | 0.0468 | 2 | 3.083 | 0.0220 | 3 | 6.114 | 0.0241 | 4 | 15.097 | 0.0401 | 5 | 3.548 | 0.0134 |
| 1 | 6.189 | 0.0496 | 2 | 3.972 | 0.0247 | 3 | 8.137 | 0.0291 | 4 | 22.202 | 0.0579 | 5 | 3.869 | 0.0143 |
| 1 | 8.098 | 0.0568 | 2 | 6.069 | 0.0307 | 3 | 10.003 | 0.0345 | 4 | 26.103 | 0.0623 | | | |
| 1 | 10.079 | 0.0631 | 2 | 7.964 | 0.0365 | 3 | 16.148 | 0.0487 | | | | | | |
| 1 | 15.116 | 0.0798 | 2 | 10.020 | 0.0420 | 3 | 22.011 | 0.0621 | | | | | | |
| 1 | 20.419 | 0.0980 | 2 | 15.186 | 0.0563 | | | | | | | | | |
| 1 | 24.363 | 0.1102 | 2 | 21.917 | 0.0764 | | | | | | | | | |

Table A.17: 6% kaolin in water suspension in a 150 mm rectangular flume

| | |
|-----------------------------|--------|
| Material: | Kaolin |
| Concentration/vol: | 6% |
| Density kg/m ³ : | 1099 |
| Ty (Pa): | 6.840 |
| k (Pa.s ⁿ): | 0.148 |
| n: | 0.517 |
| Flume width (mm): | 150 |

| SLOPE | FLOW | DEPTH | SLOPE | FLOW | DEPTH | SLOPE | FLOW | DEPTH | SLOPE | FLOW | DEPTH | SLOPE | FLOW | DEPTH |
|-----------|----------------------|--------|-----------|----------------------|--------|-----------|----------------------|--------|-----------|----------------------|--------|-----------|----------------------|--------|
| FLUME | Q | h | FLUME | Q | h | FLUME | Q | h | FLUME | Q | h | FLUME | Q | h |
| (degrees) | (l.s ⁻¹) | (m) | (degrees) | (l.s ⁻¹) | (m) | (degrees) | (l.s ⁻¹) | (m) | (degrees) | (l.s ⁻¹) | (m) | (degrees) | (l.s ⁻¹) | (m) |
| 5 | 0.103 | 0.0101 | 4 | 1.129 | 0.0146 | 3 | 0.264 | 0.0171 | 2 | 1.099 | 0.0275 | 1 | 0.959 | 0.0532 |
| 5 | 0.311 | 0.0106 | 4 | 0.699 | 0.0139 | 3 | 0.406 | 0.0175 | 2 | 0.705 | 0.0270 | 1 | 1.855 | 0.0617 |
| 5 | 0.677 | 0.0115 | 4 | 0.370 | 0.0130 | 3 | 0.685 | 0.0180 | 2 | 0.446 | 0.0256 | 1 | 3.063 | 0.0711 |
| 5 | 1.121 | 0.0120 | 4 | 0.087 | 0.0117 | 3 | 1.038 | 0.0186 | 2 | 0.097 | 0.0225 | 1 | 5.174 | 0.0822 |
| 5 | 1.760 | 0.0129 | 4 | 23.972 | 0.0574 | 3 | 1.738 | 0.0196 | 2 | 19.946 | 0.0732 | 1 | 7.062 | 0.0899 |
| 5 | 3.319 | 0.0152 | 4 | 20.863 | 0.0505 | 3 | 5.349 | 0.0259 | 2 | 23.999 | 0.0824 | 1 | 11.537 | 0.1067 |
| 5 | 5.171 | 0.0183 | 4 | 15.319 | 0.0401 | 3 | 8.496 | 0.0329 | 2 | 15.429 | 0.0614 | 1 | 15.652 | 0.1213 |
| 5 | 8.465 | 0.0231 | 4 | 10.420 | 0.0312 | 3 | 14.852 | 0.0469 | 2 | 10.472 | 0.0472 | 1 | 24.013 | 0.1466 |
| 5 | 11.234 | 0.0289 | 4 | 8.437 | 0.0270 | 3 | 17.981 | 0.0534 | 2 | 7.334 | 0.0390 | 1 | 19.897 | 0.1348 |
| 5 | 15.531 | 0.0361 | 4 | 4.938 | 0.0204 | 3 | 20.799 | 0.0591 | 2 | 4.948 | 0.0342 | | | |
| 5 | 19.757 | 0.0429 | 4 | 3.553 | 0.0176 | 3 | 23.960 | 0.0656 | 2 | 1.821 | 0.0249 | | | |
| 5 | 23.953 | 0.0496 | 4 | 1.882 | 0.0157 | | | | | | | | | |

Table A.18: 7% kaolin in water suspension in a 150 mm rectangular flume

| | |
|-----------------------------|--------|
| Material: | Kaolin |
| Concentration/vol: | 7% |
| Density kg/m ³ : | 1118.3 |
| Ty (Pa): | 9.431 |
| k (Pa.s ⁿ): | 0.625 |
| n: | 0.388 |
| Flume width (mm): | 150 |

| SLOPE FLUME | FLOW Q | DEPTH h | SLOPE FLUME | FLOW Q | DEPTH h | SLOPE FLUME | FLOW Q | DEPTH h | SLOPE FLUME | FLOW Q | DEPTH h | SLOPE FLUME | FLOW Q | DEPTH h |
|----------------|----------------------|------------|----------------|----------------------|------------|----------------|----------------------|------------|----------------|----------------------|------------|----------------|----------------------|------------|
| (degrees) | (l.s ⁻¹) | (m) | (degrees) | (l.s ⁻¹) | (m) | (degrees) | (l.s ⁻¹) | (m) | (degrees) | (l.s ⁻¹) | (m) | (degrees) | (l.s ⁻¹) | (m) |
| 1 | 1.416 | 0.0838 | 2 | 1.145 | 0.0440 | 3 | 1.032 | 0.0282 | 4 | 0.972 | 0.0210 | 5 | 1.890 | 0.0180 |
| 1 | 2.043 | 0.0888 | 2 | 2.066 | 0.0471 | 3 | 1.538 | 0.0295 | 4 | 2.155 | 0.0225 | 5 | 2.535 | 0.0189 |
| 1 | 2.497 | 0.0929 | 2 | 2.520 | 0.0493 | 3 | 2.206 | 0.0300 | 4 | 1.419 | 0.0215 | 5 | 2.987 | 0.0197 |
| 1 | 2.991 | 0.0964 | 2 | 3.050 | 0.0511 | 3 | 2.632 | 0.0316 | 4 | 2.772 | 0.0232 | 5 | 3.524 | 0.0206 |
| 1 | 4.085 | 0.1031 | 2 | 4.130 | 0.0530 | 3 | 3.136 | 0.0323 | 4 | 3.109 | 0.0242 | 5 | 4.294 | 0.0213 |
| 1 | 5.074 | 0.1087 | 2 | 5.193 | 0.0545 | 3 | 3.587 | 0.0327 | 4 | 4.160 | 0.0259 | 5 | 5.019 | 0.0228 |
| 1 | 6.231 | 0.1147 | 2 | 6.317 | 0.0562 | 3 | 4.053 | 0.0334 | 4 | 4.793 | 0.0268 | 5 | 6.104 | 0.0247 |
| 1 | 7.211 | 0.1197 | 2 | 7.071 | 0.0576 | 3 | 4.691 | 0.0340 | 4 | 5.609 | 0.0282 | 5 | 7.157 | 0.0269 |
| 1 | 8.133 | 0.1236 | 2 | 7.987 | 0.0596 | 3 | 5.351 | 0.0357 | 4 | 6.269 | 0.0297 | 5 | 8.079 | 0.0286 |
| 1 | 9.074 | 0.1284 | 2 | 9.060 | 0.0618 | 3 | 6.084 | 0.0371 | 4 | 7.100 | 0.0312 | 5 | 9.304 | 0.0309 |
| 1 | 10.107 | 0.1318 | 2 | 10.107 | 0.0644 | 3 | 7.172 | 0.0394 | 4 | 8.052 | 0.0334 | 5 | 10.187 | 0.0325 |
| 1 | 12.180 | 0.1410 | 2 | 11.822 | 0.0685 | 3 | 7.998 | 0.0413 | 4 | 8.955 | 0.0353 | 5 | 12.727 | 0.0375 |
| 1 | 14.361 | 0.1490 | 2 | 14.813 | 0.0770 | 3 | 9.067 | 0.0439 | 4 | 10.105 | 0.0378 | 5 | 16.621 | 0.0454 |
| 1 | 17.288 | 0.1592 | 2 | 19.279 | 0.0889 | 3 | 10.107 | 0.0462 | 4 | 11.967 | 0.0414 | 5 | 21.403 | 0.0550 |
| 1 | 19.022 | 0.1654 | 2 | 21.304 | 0.0949 | 3 | 12.432 | 0.0514 | 4 | 15.670 | 0.0499 | 5 | 28.511 | 0.0689 |
| 1 | 20.907 | 0.1709 | 2 | 22.923 | 0.0993 | 3 | 15.149 | 0.0579 | 4 | 20.315 | 0.0597 | | | |
| | | | 2 | 26.139 | 0.1078 | 3 | 19.034 | 0.0676 | 4 | 25.544 | 0.0710 | | | |
| | | | 2 | 17.466 | 0.0841 | 3 | 22.664 | 0.0763 | | | | | | |
| | | | | | | 3 | 27.439 | 0.0871 | | | | | | |

Table A.19: 8% kaolin in water suspension in a 150 mm rectangular flume

| | |
|-----------------------------|--------|
| Material: | Kaolin |
| Concentration/vol: | 8.0% |
| Density kg/m ³ : | 1133 |
| Ty (Pa): | 14.630 |
| k (Pa.s ⁿ): | 0.057 |
| n: | 0.694 |
| Flume width (mm): | 150 |

| SLOPE FLUME | FLOW Q | DEPTH h | SLOPE FLUME | FLOW Q | DEPTH h | SLOPE FLUME | FLOW Q | DEPTH h | SLOPE FLUME | FLOW Q | DEPTH h |
|----------------|----------------------|------------|----------------|----------------------|------------|----------------|----------------------|------------|----------------|----------------------|------------|
| (degrees) | (l.s ⁻¹) | (m) | (degrees) | (l.s ⁻¹) | (m) | (degrees) | (l.s ⁻¹) | (m) | (degrees) | (l.s ⁻¹) | (m) |
| 5 | 0.533 | 0.0205 | 4 | 0.447 | 0.0253 | 3 | 0.762 | 0.0355 | 2 | 1.209 | 0.0577 |
| 5 | 1.882 | 0.0222 | 4 | 0.851 | 0.0263 | 3 | 1.789 | 0.0376 | 2 | 2.049 | 0.0618 |
| 5 | 2.896 | 0.0235 | 4 | 1.220 | 0.0268 | 3 | 0.839 | 0.0306 | 2 | 2.859 | 0.0657 |
| 5 | 4.935 | 0.0264 | 4 | 2.829 | 0.0289 | 3 | 3.073 | 0.0397 | 2 | 3.757 | 0.0692 |
| 5 | 7.149 | 0.0305 | 4 | 5.091 | 0.0316 | 3 | 4.931 | 0.0425 | 2 | 5.288 | 0.0735 |
| 5 | 9.297 | 0.0346 | 4 | 7.216 | 0.0356 | 3 | 9.468 | 0.0507 | 2 | 7.036 | 0.0764 |
| 5 | 11.313 | 0.0386 | 4 | 9.070 | 0.0396 | 3 | 11.126 | 0.0555 | 2 | 8.984 | 0.0773 |
| 5 | 13.231 | 0.0424 | 4 | 11.403 | 0.0445 | 3 | 13.243 | 0.0605 | 2 | 11.065 | 0.0802 |
| 5 | 15.382 | 0.0462 | 4 | 13.410 | 0.0493 | 3 | 15.302 | 0.0653 | 2 | 13.073 | 0.0842 |
| 5 | 17.551 | 0.0515 | 4 | 15.438 | 0.0536 | 3 | 17.529 | 0.0705 | 2 | 15.181 | 0.0887 |
| 5 | 19.416 | 0.0548 | 4 | 17.551 | 0.0582 | 3 | 19.600 | 0.0754 | 2 | 17.210 | 0.0948 |
| 5 | 21.986 | 0.0603 | 4 | 18.582 | 0.0603 | 3 | 21.652 | 0.0806 | 2 | 19.423 | 0.0994 |
| 5 | 0.268 | 0.0196 | 4 | 21.757 | 0.0676 | 3 | 23.314 | 0.0838 | 2 | 21.477 | 0.1052 |
| 5 | 0.663 | 0.0207 | 4 | 0.688 | 0.0245 | 3 | 0.342 | 0.0313 | 2 | 0.568 | 0.0515 |
| | | | 4 | 0.332 | 0.0234 | 3 | 0.498 | 0.0327 | | | |
| | | | 4 | 0.156 | 0.0215 | | | | | | |

Table A.20: 9% kaolin in water suspension in a 150 mm rectangular flume

| | |
|-----------------------------|--------|
| Material: | Kaolin |
| Concentration/vol: | 9.0% |
| Density kg/m ³ : | 1149.4 |
| Ty (Pa): | 19.000 |
| k (Pa.s ⁿ): | 0.210 |
| n: | 0.616 |
| Flume width (mm): | 150 |

| SLOPE FLUME (degrees) | FLOW Q (l.s ⁻¹) | DEPTH h (m) | SLOPE FLUME (degrees) | FLOW Q (l.s ⁻¹) | DEPTH h (m) | SLOPE FLUME (degrees) | FLOW Q (l.s ⁻¹) | DEPTH h (m) | SLOPE FLUME (degrees) | FLOW Q (l.s ⁻¹) | DEPTH h (m) |
|-----------------------------|-----------------------------------|-------------------|-----------------------------|-----------------------------------|-------------------|-----------------------------|-----------------------------------|-------------------|-----------------------------|-----------------------------------|-------------------|
| 1 | 2.172 | 0.1515 | 3 | 2.217 | 0.0626 | 4 | 1.972 | 0.0432 | 5 | 2.167 | 0.0337 |
| 1 | 2.837 | 0.1578 | 3 | 2.994 | 0.0651 | 4 | 3.060 | 0.0456 | 5 | 3.195 | 0.0348 |
| 2 | 2.403 | 0.1019 | 3 | 4.149 | 0.0694 | 4 | 3.739 | 0.0467 | 5 | 3.926 | 0.0359 |
| 2 | 3.083 | 0.1075 | 3 | 5.102 | 0.0728 | 4 | 4.068 | 0.0481 | 5 | 5.140 | 0.0373 |
| 2 | 4.011 | 0.1128 | 3 | 6.160 | 0.0747 | 4 | 5.043 | 0.0488 | 5 | 6.283 | 0.0385 |
| 2 | 5.048 | 0.1181 | 3 | 7.224 | 0.0765 | 4 | 6.038 | 0.0498 | 5 | 7.226 | 0.0398 |
| 2 | 6.277 | 0.1179 | 3 | 8.145 | 0.0771 | 4 | 7.086 | 0.0509 | 5 | 8.503 | 0.0419 |
| 2 | 1.000 | 0.1181 | 3 | 10.081 | 0.0803 | 4 | 8.569 | 0.0530 | 5 | 10.081 | 0.0443 |
| 2 | 6.285 | 0.1236 | 3 | 13.733 | 0.0846 | 4 | 10.094 | 0.0557 | 5 | 12.204 | 0.0483 |
| 2 | 7.290 | 0.1283 | 3 | 18.102 | 0.0948 | 4 | 12.906 | 0.0612 | 5 | 15.702 | 0.0555 |
| 2 | 8.496 | 0.1336 | 3 | 23.231 | 0.1065 | 4 | 16.122 | 0.0679 | 5 | 18.528 | 0.0613 |
| 2 | 10.081 | 0.1403 | 3 | 26.755 | 0.1146 | 4 | 18.795 | 0.0738 | 5 | 22.055 | 0.0681 |
| 2 | 14.146 | 0.1544 | | | | 4 | 22.787 | 0.0826 | 5 | 28.434 | 0.0813 |
| 2 | 17.790 | 0.1680 | | | | 4 | 25.937 | 0.0895 | | | |
| 2 | 21.802 | 0.1792 | | | | | | | | | |

Table A.21: 10% kaolin in water suspension in a 150 mm rectangular flume

| | |
|-----------------------------|--------|
| Material: | Kaolin |
| Concentration/vol: | 10.0% |
| Density kg/m ³ : | 1165 |
| Ty (Pa): | 21.311 |
| k (Pa.s ⁿ): | 0.524 |
| n: | 0.468 |
| Flume width (mm): | 150 |

| SLOPE FLUME (degrees) | FLOW Q (l.s ⁻¹) | DEPTH h (m) | SLOPE FLUME (degrees) | FLOW Q (l.s ⁻¹) | DEPTH h (m) | SLOPE FLUME (degrees) | FLOW Q (l.s ⁻¹) | DEPTH h (m) | SLOPE FLUME (degrees) | FLOW Q (l.s ⁻¹) | DEPTH h (m) |
|-----------------------------|-----------------------------------|-------------------|-----------------------------|-----------------------------------|-------------------|-----------------------------|-----------------------------------|-------------------|-----------------------------|-----------------------------------|-------------------|
| 5 | 1.487 | 0.0342 | 4 | 1.133 | 0.0444 | 3 | 1.085 | 0.0618 | 2 | 1.259 | 0.1096 |
| 5 | 2.250 | 0.0352 | 4 | 2.068 | 0.0477 | 3 | 2.293 | 0.0692 | 2 | 2.163 | 0.1123 |
| 5 | 2.945 | 0.0366 | 4 | 3.458 | 0.0507 | 3 | 3.418 | 0.0745 | 2 | 3.208 | 0.1176 |
| 5 | 4.046 | 0.0380 | 4 | 4.482 | 0.0520 | 3 | 4.202 | 0.0782 | 2 | 4.241 | 0.1247 |
| 5 | 5.391 | 0.0394 | 4 | 6.089 | 0.0545 | 3 | 6.454 | 0.0836 | 2 | 6.409 | 0.1364 |
| 5 | 7.280 | 0.0414 | 4 | 8.129 | 0.0565 | 3 | 8.493 | 0.0867 | 2 | 8.299 | 0.1455 |
| 5 | 9.423 | 0.0471 | 4 | 10.328 | 0.0595 | 3 | 12.079 | 0.0892 | 2 | 12.407 | 0.1605 |
| 5 | 0.913 | 0.0340 | 4 | 12.161 | 0.0635 | 3 | 14.332 | 0.0919 | 2 | 16.267 | 0.1686 |
| 5 | 0.673 | 0.0331 | 4 | 14.250 | 0.0665 | 3 | 16.496 | 0.0948 | 2 | 0.321 | 0.0846 |
| 5 | 0.309 | 0.0312 | 4 | 17.056 | 0.0714 | 3 | 18.160 | 0.0983 | 2 | 0.303 | 0.0846 |
| 5 | 12.268 | 0.0510 | 4 | 18.386 | 0.0755 | 3 | 20.445 | 0.1029 | 2 | 0.612 | 0.0949 |
| 5 | 14.329 | 0.0529 | 4 | 20.248 | 0.0787 | 3 | 10.570 | 0.0862 | 2 | 0.930 | 0.0974 |
| 5 | 16.155 | 0.0586 | 4 | 0.323 | 0.0403 | 3 | 3.286 | 0.0738 | | | |
| 5 | 18.006 | 0.0622 | 4 | 0.654 | 0.0430 | 3 | 0.935 | 0.0637 | | | |
| 5 | 20.219 | 0.0668 | 4 | 0.940 | 0.0444 | 3 | 0.618 | 0.0603 | | | |
| | | | | | | 3 | 0.310 | 0.0560 | | | |

Table A.22: 3% kaolin in water suspension in a 300 mm rectangular flume

| | |
|-----------------------------|--------|
| Material: | Kaolin |
| Concentration/vol: | 3% |
| Density kg/m ³ : | 1050 |
| Ty (Pa): | 1.727 |
| k (Pa.s ⁿ): | 0.004 |
| n: | 0.955 |
| Flume width (mm): | 300 |

| SLOPE | FLOW | DEPTH | SLOPE | FLOW | DEPTH | SLOPE | FLOW | DEPTH | SLOPE | FLOW | DEPTH |
|-----------|----------------------|--------|-----------|----------------------|--------|-----------|----------------------|--------|-----------|----------------------|--------|
| FLUME | Q | h | FLUME | Q | h | FLUME | Q | h | FLUME | Q | h |
| (degrees) | (l.s ⁻¹) | (m) | (degrees) | (l.s ⁻¹) | (m) | (degrees) | (l.s ⁻¹) | (m) | (degrees) | (l.s ⁻¹) | (m) |
| 4 | 1.432 | 0.0067 | 3 | 2.004 | 0.0081 | 2 | 2.462 | 0.0101 | 1 | 1.984 | 0.0144 |
| 4 | 2.351 | 0.0074 | 3 | 4.159 | 0.0104 | 2 | 4.103 | 0.0130 | 1 | 4.050 | 0.0188 |
| 4 | 3.025 | 0.0095 | 3 | 6.048 | 0.0134 | 2 | 6.118 | 0.0162 | 1 | 6.106 | 0.0231 |
| 4 | 4.175 | 0.0104 | 3 | 10.251 | 0.0185 | 2 | 8.232 | 0.0193 | 1 | 8.135 | 0.0272 |
| 4 | 5.245 | 0.0114 | 3 | 15.249 | 0.0267 | 2 | 10.146 | 0.0218 | 1 | 10.264 | 0.0296 |
| 4 | 6.069 | 0.0130 | 3 | 20.439 | 0.0346 | 2 | 15.240 | 0.0313 | 1 | 15.383 | 0.0379 |
| 4 | 8.107 | 0.0142 | 3 | 0.724 | 0.0066 | 2 | 20.394 | 0.0384 | 1 | 20.438 | 0.0472 |
| 4 | 10.207 | 0.0178 | 3 | 1.124 | 0.0073 | 2 | 0.224 | 0.0081 | 1 | 0.286 | 0.0134 |
| 4 | 12.411 | 0.0211 | | | | 2 | 0.556 | 0.0079 | 1 | 0.515 | 0.0133 |
| 4 | 16.265 | 0.0256 | | | | 2 | 1.027 | 0.0089 | 1 | 1.070 | 0.0135 |
| | | | | | | 2 | 1.555 | 0.0093 | 1 | 1.550 | 0.0147 |

Table A.23: 4.5% kaolin in water suspension in a 300 mm rectangular flume

| | |
|-----------------------------|--------|
| Material: | Kaolin |
| Concentration/vol: | 4.5% |
| Density kg/m ³ : | 1075 |
| Ty (Pa): | 3.510 |
| k (Pa.s ⁿ): | 0.012 |
| n: | 0.836 |
| Flume width (mm): | 300 |

| SLOPE | FLOW | DEPTH | SLOPE | FLOW | DEPTH | SLOPE | FLOW | DEPTH | SLOPE | FLOW | DEPTH | SLOPE | FLOW | DEPTH |
|-----------|----------------------|--------|-----------|----------------------|--------|-----------|----------------------|--------|-----------|----------------------|--------|-----------|----------------------|--------|
| FLUME | Q | h | FLUME | Q | h | FLUME | Q | h | FLUME | Q | h | FLUME | Q | h |
| (degrees) | (l.s ⁻¹) | (m) | (degrees) | (l.s ⁻¹) | (m) | (degrees) | (l.s ⁻¹) | (m) | (degrees) | (l.s ⁻¹) | (m) | (degrees) | (l.s ⁻¹) | (m) |
| 1 | 1.041 | 0.0218 | 2 | 1.125 | 0.0121 | 3 | 2.022 | 0.0105 | 4 | 1.544 | 0.0080 | 5 | 1.208 | 0.0069 |
| 1 | 2.197 | 0.0237 | 2 | 2.026 | 0.0132 | 3 | 3.148 | 0.0116 | 4 | 2.224 | 0.0089 | 5 | 1.981 | 0.0075 |
| 1 | 3.088 | 0.0244 | 2 | 3.548 | 0.0151 | 3 | 4.269 | 0.0122 | 4 | 3.058 | 0.0096 | 5 | 3.140 | 0.0082 |
| 1 | 4.329 | 0.0253 | 2 | 4.046 | 0.0157 | 3 | 5.272 | 0.0134 | 4 | 4.297 | 0.0108 | 5 | 4.136 | 0.0091 |
| 1 | 5.151 | 0.0266 | 2 | 5.093 | 0.0170 | 3 | 6.159 | 0.0144 | 4 | 5.143 | 0.0114 | 5 | 5.149 | 0.0099 |
| 1 | 6.245 | 0.0278 | 2 | 6.245 | 0.0184 | 3 | 8.231 | 0.0167 | 4 | 6.213 | 0.0122 | 5 | 6.206 | 0.0105 |
| 1 | 7.287 | 0.0296 | 2 | 8.377 | 0.0212 | 3 | 12.256 | 0.0216 | 4 | 8.500 | 0.0147 | 5 | 8.335 | 0.0117 |
| 1 | 8.218 | 0.0312 | 2 | 10.422 | 0.0241 | 3 | 14.246 | 0.0241 | 4 | 10.782 | 0.0172 | 5 | 10.755 | 0.0150 |
| 1 | 9.200 | 0.0327 | 2 | 12.481 | 0.0268 | 3 | 16.651 | 0.0270 | 4 | 12.498 | 0.0185 | 5 | 12.199 | 0.0165 |
| 1 | 10.552 | 0.0354 | 2 | 12.495 | 0.0267 | 3 | 18.596 | 0.0292 | 4 | 14.273 | 0.0202 | 5 | 14.281 | 0.0182 |
| 1 | 12.516 | 0.0384 | 2 | 14.303 | 0.0291 | 3 | 20.584 | 0.0324 | 4 | 16.465 | 0.0230 | 5 | 16.359 | 0.0207 |
| 1 | 14.108 | 0.0412 | 2 | 16.505 | 0.0323 | 3 | 0.987 | 0.0095 | 4 | 18.467 | 0.0257 | 5 | 18.592 | 0.0231 |
| 1 | 16.719 | 0.0455 | 2 | 18.513 | 0.0352 | 3 | 0.598 | 0.0092 | 4 | 20.336 | 0.0277 | 5 | 20.514 | 0.0249 |
| 1 | 18.684 | 0.0487 | 2 | 20.511 | 0.0378 | 3 | 0.316 | 0.0091 | 4 | 0.588 | 0.0070 | 5 | 0.940 | 0.0065 |
| 1 | 20.967 | 0.0529 | 2 | 0.341 | 0.0124 | | | | 4 | 0.325 | 0.0073 | 5 | 0.630 | 0.0059 |
| 1 | 0.943 | 0.0228 | 2 | 0.691 | 0.0130 | | | | 4 | 1.029 | 0.0079 | 5 | 0.401 | 0.0047 |
| 1 | 0.628 | 0.0221 | 2 | 0.932 | 0.0130 | | | | | | | | | |
| 1 | 0.307 | 0.0209 | | | | | | | | | | | | |

Table A.24: 5.3% kaolin in water suspension in a 300 mm rectangular flume

| | |
|-----------------------------|--------|
| Material: | Kaolin |
| Concentration/vol: | 5.3% |
| Density kg/m ³ : | 1087.1 |
| Ty (Pa): | 4.985 |
| k (Pa.s ⁿ): | 0.030 |
| n: | 0.717 |
| Flume width (mm): | 300 |

| SLOPE | FLOW | DEPTH | SLOPE | FLOW | DEPTH | SLOPE | FLOW | DEPTH | SLOPE | FLOW | DEPTH | SLOPE | FLOW | DEPTH |
|-----------|----------------------|--------|-----------|----------------------|--------|-----------|----------------------|--------|-----------|----------------------|--------|-----------|----------------------|--------|
| FLUME | Q | h | FLUME | Q | h | FLUME | Q | h | FLUME | Q | h | FLUME | Q | h |
| (degrees) | (l.s ⁻¹) | (m) | (degrees) | (l.s ⁻¹) | (m) | (degrees) | (l.s ⁻¹) | (m) | (degrees) | (l.s ⁻¹) | (m) | (degrees) | (l.s ⁻¹) | (m) |
| 1 | 0.243 | 0.0297 | 2 | 0.241 | 0.0150 | 3 | 0.698 | 0.0111 | 4 | 1.270 | 0.0094 | 5 | 1.306 | 0.0079 |
| 1 | 0.357 | 0.0299 | 2 | 0.366 | 0.0155 | 3 | 0.915 | 0.0114 | 4 | 1.469 | 0.0097 | 5 | 2.057 | 0.0086 |
| 1 | 0.443 | 0.0300 | 2 | 0.564 | 0.0159 | 3 | 1.187 | 0.0116 | 4 | 2.106 | 0.0103 | 5 | 1.793 | 0.0085 |
| 1 | 0.522 | 0.0302 | 2 | 0.795 | 0.0164 | 3 | 1.488 | 0.0121 | 4 | 2.523 | 0.0106 | 5 | 2.434 | 0.0091 |
| 1 | 0.699 | 0.0300 | 2 | 0.986 | 0.0164 | 3 | 1.845 | 0.0124 | 4 | 3.536 | 0.0114 | 5 | 3.419 | 0.0098 |
| 1 | 0.980 | 0.0302 | 2 | 1.363 | 0.0171 | 3 | 2.394 | 0.0128 | 4 | 4.588 | 0.0123 | 5 | 4.723 | 0.0108 |
| 1 | 1.221 | 0.0298 | 2 | 1.647 | 0.0175 | 3 | 2.565 | 0.0128 | 4 | 5.475 | 0.0131 | 5 | 5.605 | 0.0116 |
| 1 | 1.422 | 0.0307 | 2 | 2.061 | 0.0178 | 3 | 3.597 | 0.0142 | 4 | 7.015 | 0.0147 | 5 | 7.095 | 0.0128 |
| 1 | 1.964 | 0.0318 | 2 | 2.993 | 0.0182 | 3 | 4.839 | 0.0152 | 4 | 8.377 | 0.0157 | 5 | 8.460 | 0.0141 |
| 1 | 3.155 | 0.0342 | 2 | 3.644 | 0.0191 | 3 | 5.729 | 0.0159 | 4 | 10.026 | 0.0177 | 5 | 10.082 | 0.0156 |
| 1 | 3.715 | 0.0349 | 2 | 4.854 | 0.0203 | 3 | 6.970 | 0.0172 | 4 | 17.417 | 0.0256 | 5 | 16.007 | 0.0215 |
| 1 | 4.637 | 0.0356 | 2 | 5.549 | 0.0211 | 3 | 8.500 | 0.0191 | 4 | 25.286 | 0.0339 | 5 | 24.692 | 0.0299 |
| 1 | 5.021 | 0.0357 | 2 | 7.208 | 0.0228 | 3 | 10.153 | 0.0208 | 4 | 35.672 | 0.0435 | 5 | 35.437 | 0.0395 |
| 1 | 6.454 | 0.0366 | 2 | 8.632 | 0.0246 | 3 | 18.124 | 0.0303 | 4 | 45.158 | 0.0527 | 5 | 44.935 | 0.0486 |
| 1 | 7.662 | 0.0379 | 2 | 10.040 | 0.0267 | 3 | 23.588 | 0.0368 | | | | | | |
| 1 | 8.817 | 0.0392 | 2 | 16.127 | 0.0348 | 3 | 34.384 | 0.0487 | | | | | | |
| 1 | 10.099 | 0.0408 | 2 | 22.458 | 0.0433 | 3 | 45.172 | 0.0599 | | | | | | |
| 1 | 14.875 | 0.0482 | 2 | 33.385 | 0.0573 | | | | | | | | | |
| 1 | 19.618 | 0.0557 | 2 | 44.725 | 0.0712 | | | | | | | | | |
| 1 | 23.881 | 0.0624 | | | | | | | | | | | | |
| 1 | 30.455 | 0.0726 | | | | | | | | | | | | |
| 1 | 36.908 | 0.0824 | | | | | | | | | | | | |
| 1 | 44.008 | 0.0933 | | | | | | | | | | | | |

Table A.25: 6% kaolin in water suspension in a 300 mm rectangular flume

| | |
|-----------------------------|--------|
| Material: | Kaolin |
| Concentration/vol: | 6% |
| Density kg/m ³ : | 1098.5 |
| Ty (Pa): | 6.840 |
| k (Pa.s ⁿ): | 0.148 |
| n: | 0.517 |
| Flume width (mm): | 300 |

| SLOPE | FLOW | DEPTH | SLOPE | FLOW | DEPTH | SLOPE | FLOW | DEPTH | SLOPE | FLOW | DEPTH | SLOPE | FLOW | DEPTH |
|-----------|----------------------|--------|-----------|----------------------|--------|-----------|----------------------|--------|-----------|----------------------|--------|-----------|----------------------|--------|
| FLUME | Q | h | FLUME | Q | h | FLUME | Q | h | FLUME | Q | h | FLUME | Q | h |
| (degrees) | (l.s ⁻¹) | (m) | (degrees) | (l.s ⁻¹) | (m) | (degrees) | (l.s ⁻¹) | (m) | (degrees) | (l.s ⁻¹) | (m) | (degrees) | (l.s ⁻¹) | (m) |
| 5 | 0.848 | 0.0112 | 4 | 0.880 | 0.0132 | 3 | 1.210 | 0.0168 | 2 | 1.192 | 0.0236 | 1 | 1.117 | 0.0428 |
| 5 | 2.978 | 0.0123 | 4 | 2.875 | 0.0142 | 3 | 2.854 | 0.0177 | 2 | 4.983 | 0.0265 | 1 | 5.198 | 0.0516 |
| 5 | 5.260 | 0.0142 | 4 | 7.216 | 0.0183 | 3 | 7.284 | 0.0216 | 2 | 10.383 | 0.0323 | 1 | 10.176 | 0.0576 |
| 5 | 7.229 | 0.0153 | 4 | 13.461 | 0.0243 | 3 | 15.470 | 0.0308 | 2 | 15.752 | 0.0390 | 1 | 15.639 | 0.0623 |
| 5 | 9.410 | 0.0176 | 4 | 17.596 | 0.0285 | 3 | 20.821 | 0.0372 | 2 | 21.012 | 0.0450 | 1 | 20.900 | 0.0686 |
| 5 | 15.650 | 0.0244 | 4 | 20.874 | 0.0341 | 3 | 0.099 | 0.0145 | 2 | 0.119 | 0.0223 | 1 | 0.135 | 0.0357 |
| 5 | 20.917 | 0.0296 | 4 | 0.122 | 0.0121 | 3 | 0.549 | 0.0161 | 2 | 1.939 | 0.0253 | 1 | 0.285 | 0.0425 |
| 5 | 0.121 | 0.0099 | 4 | 0.533 | 0.0133 | 3 | 0.705 | 0.0164 | 2 | 0.560 | 0.0222 | 1 | 0.729 | 0.0457 |
| 5 | 0.517 | 0.0114 | 4 | 0.728 | 0.0133 | | | | 2 | 0.795 | 0.0242 | | | |
| 5 | 0.710 | 0.0116 | | | | | | | | | | | | |

Table A.26: 7.1% kaolin in water suspension in a 300 mm rectangular flume

| | |
|-----------------------------|--------|
| Material: | Kaolin |
| Concentration/vol: | 7.1% |
| Density kg/m ³ : | 1118.5 |
| Ty (Pa): | 10.551 |
| k (Pa.s ⁿ): | 0.834 |
| n: | 0.387 |
| Flume width (mm): | 300 |

| SLOPE | FLOW | DEPTH | SLOPE | FLOW | DEPTH | SLOPE | FLOW | DEPTH | SLOPE | FLOW | DEPTH | SLOPE | FLOW | DEPTH |
|-----------|----------------------|--------|-----------|----------------------|--------|-----------|----------------------|--------|-----------|----------------------|--------|-----------|----------------------|--------|
| FLUME | Q | h | FLUME | Q | h | FLUME | Q | h | FLUME | Q | h | FLUME | Q | h |
| (degrees) | (l.s ⁻¹) | (m) | (degrees) | (l.s ⁻¹) | (m) | (degrees) | (l.s ⁻¹) | (m) | (degrees) | (l.s ⁻¹) | (m) | (degrees) | (l.s ⁻¹) | (m) |
| 1 | 1.206 | 0.0633 | 2 | 1.044 | 0.0353 | 3 | 0.965 | 0.0249 | 4 | 0.917 | 0.0184 | 5 | 1.507 | 0.0160 |
| 1 | 2.054 | 0.0675 | 2 | 2.172 | 0.0378 | 3 | 2.016 | 0.0260 | 4 | 1.635 | 0.0194 | 5 | 2.040 | 0.0166 |
| 1 | 2.584 | 0.0691 | 2 | 3.093 | 0.0391 | 3 | 2.990 | 0.0268 | 4 | 2.099 | 0.0198 | 5 | 2.565 | 0.0173 |
| 1 | 3.038 | 0.0703 | 2 | 4.131 | 0.0404 | 3 | 4.149 | 0.0278 | 4 | 2.561 | 0.0207 | 5 | 3.105 | 0.0178 |
| 1 | 4.135 | 0.0732 | 2 | 5.399 | 0.0417 | 3 | 5.089 | 0.0286 | 4 | 3.377 | 0.0210 | 5 | 3.492 | 0.0177 |
| 1 | 5.140 | 0.0756 | 2 | 6.042 | 0.0416 | 3 | 6.119 | 0.0292 | 4 | 4.076 | 0.0217 | 5 | 3.929 | 0.0183 |
| 1 | 6.063 | 0.0774 | 2 | 7.170 | 0.0423 | 3 | 7.138 | 0.0296 | 4 | 4.557 | 0.0219 | 5 | 4.888 | 0.0185 |
| 1 | 7.007 | 0.0796 | 2 | 8.103 | 0.0428 | 3 | 8.110 | 0.0303 | 4 | 5.020 | 0.0224 | 5 | 5.603 | 0.0191 |
| 1 | 8.065 | 0.0813 | 2 | 9.052 | 0.0432 | 3 | 9.042 | 0.0311 | 4 | 6.165 | 0.0232 | 5 | 6.726 | 0.0197 |
| 1 | 9.082 | 0.0830 | 2 | 10.153 | 0.0444 | 3 | 10.247 | 0.0318 | 4 | 6.963 | 0.0235 | 5 | 7.555 | 0.0203 |
| 1 | 10.158 | 0.0849 | 2 | 12.713 | 0.0457 | 3 | 13.100 | 0.0345 | 4 | 7.618 | 0.0241 | 5 | 8.505 | 0.0210 |
| 1 | 13.634 | 0.0897 | 2 | 15.924 | 0.0490 | 3 | 17.043 | 0.0386 | 4 | 8.577 | 0.0247 | 5 | 9.421 | 0.0218 |
| 1 | 19.849 | 0.1023 | 2 | 17.800 | 0.0509 | 3 | 18.962 | 0.0405 | 4 | 9.437 | 0.0254 | 5 | 10.123 | 0.0224 |
| 1 | 22.889 | 0.0978 | 2 | 20.168 | 0.0542 | 3 | 23.351 | 0.0454 | 4 | 10.159 | 0.0260 | 5 | 13.860 | 0.0252 |
| 1 | 28.571 | 0.1044 | 2 | 24.059 | 0.0591 | 3 | 27.316 | 0.0499 | 4 | 12.422 | 0.0278 | 5 | 12.500 | 0.0241 |
| 1 | 33.360 | 0.1102 | 2 | 27.408 | 0.0625 | 3 | 30.588 | 0.0535 | 4 | 16.255 | 0.0314 | 5 | 18.345 | 0.0294 |
| 1 | 38.570 | 0.1170 | 2 | 30.089 | 0.0662 | 3 | 35.379 | 0.0589 | 4 | 15.299 | 0.0305 | 5 | 25.222 | 0.0360 |
| 1 | 44.609 | 0.1254 | 2 | 34.154 | 0.0715 | 3 | 39.500 | 0.0633 | 4 | 19.676 | 0.0349 | 5 | 35.567 | 0.0459 |
| | | | 2 | 38.813 | 0.0772 | 3 | 42.162 | 0.0665 | 4 | 22.668 | 0.0378 | 5 | 39.398 | 0.0496 |
| | | | 2 | 44.036 | 0.0837 | | | | 4 | 25.454 | 0.0407 | | | |
| | | | | | | | | | 4 | 29.940 | 0.0454 | | | |
| | | | | | | | | | 4 | 35.637 | 0.0512 | | | |
| | | | | | | | | | 4 | 39.557 | 0.0559 | | | |
| | | | | | | | | | 4 | 42.539 | 0.0576 | | | |

Table A.27: 8% kaolin in water suspension in a 300 mm rectangular flume

| | |
|-----------------------------|--------|
| Material: | Kaolin |
| Concentration/vol: | 8.0% |
| Density kg/m ³ : | 1133 |
| Ty (Pa): | 14.630 |
| k (Pa.s ⁿ): | 0.057 |
| n: | 0.694 |
| Flume width (mm): | 300 |

| SLOPE | FLOW | DEPTH | SLOPE | FLOW | DEPTH | SLOPE | FLOW | DEPTH | SLOPE | FLOW | DEPTH | SLOPE | FLOW | DEPTH |
|-----------|----------------------|--------|-----------|----------------------|--------|-----------|----------------------|--------|-----------|----------------------|--------|-----------|----------------------|--------|
| FLUME | Q | h | FLUME | Q | h | FLUME | Q | h | FLUME | Q | h | FLUME | Q | h |
| (degrees) | (l.s ⁻¹) | (m) | (degrees) | (l.s ⁻¹) | (m) | (degrees) | (l.s ⁻¹) | (m) | (degrees) | (l.s ⁻¹) | (m) | (degrees) | (l.s ⁻¹) | (m) |
| 5 | 0.994 | 0.0192 | 4 | 0.442 | 0.0216 | 3 | 0.969 | 0.0300 | 2 | 0.557 | 0.0426 | 1 | 20.890 | 0.1137 |
| 5 | 0.745 | 0.0188 | 4 | 0.712 | 0.0228 | 3 | 0.757 | 0.0294 | 2 | 0.753 | 0.0436 | 1 | 17.648 | 0.1089 |
| 5 | 0.466 | 0.0183 | 4 | 1.013 | 0.0235 | 3 | 0.479 | 0.0284 | 2 | 0.975 | 0.0442 | 1 | 14.464 | 0.1043 |
| 5 | 1.654 | 0.0194 | 4 | 2.274 | 0.0242 | 3 | 1.877 | 0.0308 | 2 | 2.017 | 0.0461 | 1 | 11.074 | 0.0990 |
| 5 | 3.923 | 0.0207 | 4 | 4.266 | 0.0253 | 3 | 4.364 | 0.0329 | 2 | 4.040 | 0.0497 | 1 | 8.195 | 0.0936 |
| 5 | 5.792 | 0.0218 | 4 | 6.196 | 0.0263 | 3 | 6.114 | 0.0339 | 2 | 6.444 | 0.0516 | 1 | 5.042 | 0.0877 |
| 5 | 8.078 | 0.0230 | 4 | 8.219 | 0.0274 | 3 | 8.205 | 0.0351 | 2 | 8.312 | 0.0521 | 1 | 1.670 | 0.0784 |
| 5 | 10.260 | 0.0242 | 4 | 10.552 | 0.0290 | 3 | 10.516 | 0.0364 | 2 | 10.417 | 0.0529 | 1 | 0.640 | 0.0737 |
| 5 | 12.692 | 0.0257 | 4 | 12.267 | 0.0302 | 3 | 12.602 | 0.0377 | 2 | 12.553 | 0.0535 | | | |
| 5 | 14.704 | 0.0274 | 4 | 14.405 | 0.0319 | 3 | 14.429 | 0.0391 | 2 | 14.717 | 0.0547 | | | |
| 5 | 16.376 | 0.0292 | 4 | 16.205 | 0.0333 | 3 | 16.350 | 0.0408 | 2 | 16.751 | 0.0560 | | | |
| 5 | 18.599 | 0.0309 | 4 | 18.692 | 0.0355 | 3 | 18.569 | 0.0425 | 2 | 18.704 | 0.0577 | | | |
| 5 | 20.806 | 0.0328 | 4 | 20.751 | 0.0374 | 3 | 20.700 | 0.0448 | 2 | 20.593 | 0.0593 | | | |

Table A.28: 10% kaolin in water suspension in a 300 mm rectangular flume

| | |
|----------------------------------|---------------|
| Material: | Kaolin |
| Concentration/vol: | 10.0% |
| Density kg/m³: | 1165 |
| Ty (Pa): | 21.311 |
| k (Pa.sⁿ): | 0.524 |
| n: | 0.468 |
| Flume width (mm): | 300 |

| SLOPE | FLOW | DEPTH | SLOPE | FLOW | DEPTH | SLOPE | FLOW | DEPTH | SLOPE | FLOW | DEPTH |
|------------------|---------------------------|--------------|------------------|---------------------------|--------------|------------------|---------------------------|--------------|------------------|---------------------------|--------------|
| FLUME | Q | h | FLUME | Q | h | FLUME | Q | h | FLUME | Q | h |
| (degrees) | (l.s⁻¹) | (m) | (degrees) | (l.s⁻¹) | (m) | (degrees) | (l.s⁻¹) | (m) | (degrees) | (l.s⁻¹) | (m) |
| 5 | 0.986 | 0.0285 | 4 | 0.800 | 0.0344 | 3 | 1.103 | 0.0474 | 2 | 1.399 | 0.0718 |
| 5 | 2.184 | 0.0307 | 4 | 1.527 | 0.0364 | 3 | 2.369 | 0.0507 | 2 | 2.086 | 0.0759 |
| 5 | 3.119 | 0.0313 | 4 | 1.965 | 0.0379 | 3 | 3.257 | 0.0526 | 2 | 3.134 | 0.0791 |
| 5 | 3.970 | 0.0320 | 4 | 3.016 | 0.0387 | 3 | 4.228 | 0.0534 | 2 | 3.844 | 0.0805 |
| 5 | 5.651 | 0.0328 | 4 | 4.358 | 0.0402 | 3 | 6.121 | 0.0565 | 2 | 6.112 | 0.0854 |
| 5 | 6.126 | 0.0333 | 4 | 5.092 | 0.0411 | 3 | 8.107 | 0.0577 | 2 | 8.193 | 0.0888 |
| 5 | 7.323 | 0.0336 | 4 | 6.253 | 0.0412 | 3 | 10.322 | 0.0585 | 2 | 10.201 | 0.0910 |
| 5 | 8.192 | 0.0339 | 4 | 7.085 | 0.0419 | 3 | 12.127 | 0.0586 | 2 | 12.267 | 0.0932 |
| 5 | 9.330 | 0.0347 | 4 | 8.123 | 0.0420 | 3 | 14.197 | 0.0592 | 2 | 14.385 | 0.0951 |
| 5 | 10.582 | 0.0349 | 4 | 9.306 | 0.0427 | 3 | 16.304 | 0.0598 | 2 | 16.431 | 0.0963 |
| 5 | 11.099 | 0.0356 | 4 | 10.228 | 0.0430 | 3 | 18.200 | 0.0606 | 2 | 18.348 | 0.0969 |
| 5 | 12.207 | 0.0361 | 4 | 11.289 | 0.0431 | 3 | 20.503 | 0.0620 | 2 | 20.747 | 0.0973 |
| 5 | 13.085 | 0.0365 | 4 | 12.129 | 0.0435 | 3 | 0.561 | 0.0450 | 2 | 0.302 | 0.0616 |
| 5 | 14.270 | 0.0368 | 4 | 13.139 | 0.0442 | 3 | 0.280 | 0.0426 | 2 | 0.655 | 0.0650 |
| 5 | 15.228 | 0.0377 | 4 | 14.043 | 0.0444 | | | | | | |
| 5 | 16.167 | 0.0379 | 4 | 15.252 | 0.0451 | | | | | | |
| 5 | 17.345 | 0.0387 | 4 | 16.005 | 0.0457 | | | | | | |
| 5 | 18.362 | 0.0396 | 4 | 17.286 | 0.0467 | | | | | | |
| 5 | 19.268 | 0.0405 | 4 | 18.261 | 0.0469 | | | | | | |
| 5 | 20.072 | 0.0406 | 4 | 19.949 | 0.0483 | | | | | | |
| 5 | 0.615 | 0.0285 | 4 | 0.230 | 0.0356 | | | | | | |
| 5 | 0.298 | 0.0262 | | | | | | | | | |

APPENDIX B: Semi-circular flume data

Table B.1: 1.5% CMC in water solution in a 300 mm semi-circular flume

| | |
|-----------------------------|-------|
| Material: | CMC |
| Concentration/vol: | 1.5% |
| Density kg/m ³ : | 1008 |
| Ty (Pa): | 0.000 |
| k (Pa.s ²): | 0.015 |
| n: | 0.944 |
| Flume width (mm): | 300 |

| SLOPE FLUME | FLOW Q | DEPTH h | SLOPE FLUME | FLOW Q | DEPTH h | SLOPE FLUME | FLOW Q | DEPTH h | SLOPE FLUME | FLOW Q | DEPTH h | SLOPE FLUME | FLOW Q | DEPTH h |
|----------------|----------------------|------------|----------------|----------------------|------------|----------------|----------------------|------------|----------------|----------------------|------------|----------------|----------------------|------------|
| (degrees) | (l.s ⁻¹) | (m) | (degrees) | (l.s ⁻¹) | (m) | (degrees) | (l.s ⁻¹) | (m) | (degrees) | (l.s ⁻¹) | (m) | (degrees) | (l.s ⁻¹) | (m) |
| 1 | 0.156 | 0.009 | 2 | 0.171 | 0.007 | 3 | 0.513 | 0.009 | 4 | 0.357 | 0.007 | 5 | 0.458 | 0.007 |
| 1 | 0.212 | 0.009 | 2 | 0.270 | 0.008 | 3 | 0.712 | 0.010 | 4 | 0.505 | 0.008 | 5 | 0.602 | 0.008 |
| 1 | 0.325 | 0.011 | 2 | 0.325 | 0.009 | 3 | 1.039 | 0.011 | 4 | 0.620 | 0.008 | 5 | 0.794 | 0.009 |
| 1 | 0.413 | 0.012 | 2 | 0.416 | 0.009 | 3 | 1.267 | 0.012 | 4 | 0.753 | 0.009 | 5 | 1.535 | 0.012 |
| 1 | 0.514 | 0.012 | 2 | 0.486 | 0.010 | 3 | 1.540 | 0.013 | 4 | 0.835 | 0.010 | 5 | 2.109 | 0.014 |
| 1 | 0.615 | 0.013 | 2 | 0.620 | 0.011 | 3 | 2.016 | 0.016 | 4 | 1.043 | 0.011 | 5 | 3.183 | 0.016 |
| 1 | 0.837 | 0.015 | 2 | 0.618 | 0.011 | 3 | 3.805 | 0.025 | 4 | 1.521 | 0.013 | 5 | 4.143 | 0.022 |
| 1 | 1.032 | 0.016 | 2 | 0.715 | 0.011 | 3 | 6.126 | 0.030 | 4 | 2.062 | 0.015 | 5 | 8.007 | 0.029 |
| 1 | 1.442 | 0.018 | 2 | 0.941 | 0.012 | 3 | 8.075 | 0.034 | 4 | 3.024 | 0.019 | 5 | 5.747 | 0.026 |
| 1 | 2.080 | 0.022 | 2 | 1.240 | 0.014 | 3 | 10.043 | 0.038 | 4 | 4.147 | 0.023 | 5 | 10.094 | 0.033 |
| 1 | 3.346 | 0.026 | 2 | 1.435 | 0.015 | 3 | 19.790 | 0.055 | 4 | 6.032 | 0.027 | 5 | 20.031 | 0.049 |
| 1 | 4.067 | 0.031 | 2 | 2.156 | 0.018 | 3 | 31.564 | 0.073 | 4 | 8.045 | 0.031 | 5 | 29.310 | 0.062 |
| 1 | 4.525 | 0.033 | 2 | 2.515 | 0.020 | 3 | 39.954 | 0.085 | 4 | 10.068 | 0.036 | 5 | 39.827 | 0.074 |
| 1 | 6.316 | 0.039 | 2 | 3.494 | 0.023 | | | | 4 | 17.356 | 0.047 | | | |
| 1 | 8.024 | 0.045 | 2 | 4.969 | 0.029 | | | | 4 | 28.980 | 0.065 | | | |
| 1 | 10.072 | 0.051 | 2 | 6.149 | 0.032 | | | | 4 | 39.561 | 0.081 | | | |
| 1 | 16.866 | 0.069 | 2 | 8.086 | 0.037 | | | | | | | | | |
| 1 | 32.374 | 0.101 | 2 | 10.020 | 0.042 | | | | | | | | | |
| 1 | 41.781 | 0.117 | 2 | 20.032 | 0.064 | | | | | | | | | |

Table B.2: 3% CMC in water solution in a 300 mm semi-circular flume

| | |
|-----------------------------|-------|
| Material: | CMC |
| Concentration/vol: | 3.0% |
| Density kg/m ³ : | 1017 |
| Ty (Pa): | 0.000 |
| k (Pa.s ²): | 0.126 |
| n: | 0.780 |
| Flume width (mm): | 300 |

| SLOPE FLUME | FLOW Q | DEPTH h | SLOPE FLUME | FLOW Q | DEPTH h | SLOPE FLUME | FLOW Q | DEPTH h | SLOPE FLUME | FLOW Q | DEPTH h | SLOPE FLUME | FLOW Q | DEPTH h |
|----------------|----------------------|------------|----------------|----------------------|------------|----------------|----------------------|------------|----------------|----------------------|------------|----------------|----------------------|------------|
| (degrees) | (l.s ⁻¹) | (m) | (degrees) | (l.s ⁻¹) | (m) | (degrees) | (l.s ⁻¹) | (m) | (degrees) | (l.s ⁻¹) | (m) | (degrees) | (l.s ⁻¹) | (m) |
| 1 | 0.088 | 0.000 | 2 | 0.106 | 0.010 | 3 | 0.256 | 0.011 | 4 | 0.237 | 0.010 | 5 | 0.658 | 0.012 |
| 1 | 0.195 | 0.009 | 2 | 0.178 | 0.011 | 3 | 0.314 | 0.011 | 4 | 0.376 | 0.011 | 5 | 0.750 | 0.012 |
| 1 | 0.418 | 0.009 | 2 | 0.195 | 0.012 | 3 | 0.450 | 0.013 | 4 | 0.574 | 0.012 | 5 | 0.839 | 0.013 |
| 1 | 0.500 | 0.011 | 2 | 0.286 | 0.013 | 3 | 0.607 | 0.014 | 4 | 0.677 | 0.013 | 5 | 0.954 | 0.013 |
| 1 | 0.602 | 0.012 | 2 | 0.387 | 0.014 | 3 | 0.818 | 0.015 | 4 | 0.844 | 0.014 | 5 | 1.088 | 0.014 |
| 1 | 0.868 | 0.012 | 2 | 0.528 | 0.015 | 3 | 1.039 | 0.016 | 4 | 0.953 | 0.014 | 5 | 1.314 | 0.014 |
| 1 | 1.023 | 0.013 | 2 | 0.605 | 0.016 | 3 | 1.213 | 0.017 | 4 | 1.128 | 0.015 | 5 | 1.486 | 0.015 |
| 1 | 1.556 | 0.015 | 2 | 0.827 | 0.017 | 3 | 1.326 | 0.017 | 4 | 1.350 | 0.016 | 5 | 2.059 | 0.017 |
| 1 | 1.841 | 0.016 | 2 | 1.307 | 0.020 | 3 | 1.574 | 0.018 | 4 | 1.559 | 0.016 | 5 | 2.813 | 0.018 |
| 1 | 2.265 | 0.018 | 2 | 2.068 | 0.023 | 3 | 1.876 | 0.019 | 4 | 1.989 | 0.018 | 5 | 4.407 | 0.023 |
| 1 | 2.717 | 0.022 | 2 | 3.429 | 0.028 | 3 | 2.381 | 0.021 | 4 | 2.475 | 0.020 | 5 | 5.502 | 0.026 |
| 1 | 3.555 | 0.026 | 2 | 5.164 | 0.033 | 3 | 3.062 | 0.023 | 4 | 2.868 | 0.021 | 5 | 6.418 | 0.028 |
| 1 | 4.029 | 0.031 | 2 | 6.686 | 0.038 | 3 | 3.836 | 0.025 | 4 | 3.241 | 0.022 | 5 | 8.158 | 0.032 |
| 1 | 4.825 | 0.033 | 2 | 8.464 | 0.043 | 3 | 5.680 | 0.031 | 4 | 4.280 | 0.025 | 5 | 9.477 | 0.035 |
| 1 | 5.720 | 0.039 | 2 | 11.889 | 0.051 | 3 | 7.526 | 0.036 | 4 | 6.099 | 0.029 | 5 | 15.818 | 0.044 |
| 1 | 6.707 | 0.045 | | | | 3 | 9.471 | 0.041 | 4 | 7.202 | 0.032 | 5 | 24.236 | 0.057 |
| 1 | 8.495 | 0.051 | | | | 3 | 16.963 | 0.054 | 4 | 9.489 | 0.037 | 5 | 33.925 | 0.068 |
| 1 | 9.509 | 0.069 | | | | 3 | 25.462 | 0.067 | 4 | 22.436 | 0.056 | | | |
| 1 | 20.236 | 0.101 | | | | 3 | 35.361 | 0.081 | 4 | 32.681 | 0.070 | | | |
| 1 | 25.757 | 0.117 | | | | | | | 4 | 41.163 | 0.082 | | | |
| 1 | 32.210 | 0.105 | | | | | | | | | | | | |
| 1 | 35.580 | 0.111 | | | | | | | | | | | | |
| 1 | 42.286 | 0.121 | | | | | | | | | | | | |
| 1 | 44.730 | 0.125 | | | | | | | | | | | | |

Table B.3: 1.5% CMC in water solution in a 150 mm semi-circular flume

| | |
|-----------------------------|-------|
| Material: | CMC |
| Concentration/vol: | 1.5% |
| Density kg/m ³ : | 1009 |
| Ty (Pa): | 0.000 |
| k (Pa.s ⁿ): | 0.014 |
| n: | 0.944 |
| Flume width (mm): | 150 |

| SLOPE | FLOW | DEPTH | SLOPE | FLOW | DEPTH | SLOPE | FLOW | DEPTH | SLOPE | FLOW | DEPTH | SLOPE | FLOW | DEPTH |
|-----------|----------------------|-------|-----------|----------------------|-------|-----------|----------------------|-------|-----------|----------------------|-------|-----------|----------------------|-------|
| FLUME | Q | h | FLUME | Q | h | FLUME | Q | h | FLUME | Q | h | FLUME | Q | h |
| (degrees) | (l.s ⁻¹) | (m) | (degrees) | (l.s ⁻¹) | (m) | (degrees) | (l.s ⁻¹) | (m) | (degrees) | (l.s ⁻¹) | (m) | (degrees) | (l.s ⁻¹) | (m) |
| 1 | 0.172 | 0.010 | 2 | 0.172 | 0.008 | 3 | 0.199 | 0.007 | 4 | 0.088 | 0.005 | 5 | 0.117 | 0.005 |
| 1 | 0.212 | 0.010 | 2 | 0.124 | 0.007 | 3 | 0.261 | 0.008 | 4 | 0.133 | 0.006 | 5 | 0.142 | 0.006 |
| 1 | 0.257 | 0.011 | 2 | 0.219 | 0.008 | 3 | 0.318 | 0.008 | 4 | 0.177 | 0.006 | 5 | 0.212 | 0.007 |
| 1 | 0.343 | 0.012 | 2 | 0.266 | 0.009 | 3 | 0.426 | 0.009 | 4 | 0.217 | 0.007 | 5 | 0.254 | 0.007 |
| 1 | 0.433 | 0.013 | 2 | 0.323 | 0.009 | 3 | 0.520 | 0.010 | 4 | 0.271 | 0.007 | 5 | 0.362 | 0.008 |
| 1 | 0.518 | 0.014 | 2 | 0.414 | 0.010 | 3 | 0.630 | 0.011 | 4 | 0.318 | 0.008 | 5 | 0.455 | 0.008 |
| 1 | 0.637 | 0.015 | 2 | 0.506 | 0.011 | 3 | 0.764 | 0.012 | 4 | 0.358 | 0.008 | 5 | 0.634 | 0.009 |
| 1 | 0.729 | 0.016 | 2 | 0.621 | 0.012 | 3 | 0.923 | 0.013 | 4 | 0.424 | 0.008 | 5 | 0.755 | 0.010 |
| 1 | 0.818 | 0.017 | 2 | 0.818 | 0.014 | 3 | 1.053 | 0.013 | 4 | 0.512 | 0.009 | 5 | 0.923 | 0.010 |
| 1 | 0.929 | 0.018 | 2 | 0.921 | 0.015 | 3 | 1.516 | 0.015 | 4 | 0.617 | 0.010 | 5 | 1.474 | 0.013 |
| 1 | 1.147 | 0.020 | 2 | 1.368 | 0.017 | 3 | 2.004 | 0.018 | 4 | 0.724 | 0.010 | 5 | 1.991 | 0.015 |
| 1 | 2.001 | 0.027 | 2 | 2.061 | 0.021 | 3 | 2.983 | 0.025 | 4 | 0.871 | 1.000 | 5 | 2.786 | 0.021 |
| 1 | 3.173 | 0.034 | 2 | 2.536 | 0.024 | 3 | 3.906 | 0.031 | 4 | 1.030 | 0.012 | 5 | 4.025 | 0.026 |
| 1 | 3.952 | 0.039 | 2 | 3.223 | 0.032 | 3 | 5.785 | 0.038 | 4 | 1.496 | 0.014 | 5 | 5.941 | 0.033 |
| 1 | 4.629 | 0.043 | 2 | 4.087 | 0.035 | 3 | 8.100 | 0.044 | 4 | 2.056 | 0.017 | 5 | 8.020 | 0.038 |
| 1 | 5.941 | 0.050 | 2 | 6.290 | 0.042 | 3 | 10.117 | 0.050 | 4 | 3.486 | 0.025 | 5 | 10.054 | 0.043 |
| 1 | 7.930 | 0.060 | 2 | 7.976 | 0.050 | 3 | 17.232 | 0.071 | 4 | 5.018 | 0.031 | 5 | 15.853 | 0.059 |
| 1 | 10.241 | 0.069 | 2 | 10.074 | 0.057 | 3 | 26.123 | 0.093 | 4 | 8.055 | 0.042 | 5 | 18.437 | 0.063 |
| 1 | 14.740 | 0.087 | | | | | | | 4 | 10.116 | 0.048 | | | |
| 1 | 18.882 | 0.102 | | | | | | | 4 | 18.135 | 0.068 | | | |
| 1 | 22.585 | 0.116 | | | | | | | 4 | 25.389 | 0.085 | | | |

Table B.4: 3% CMC in water solution in a 150 mm semi-circular flume

| | |
|-----------------------------|-------|
| Material: | CMC |
| Concentration/vol: | 3.0% |
| Density kg/m ³ : | 1018 |
| Ty (Pa): | 0.000 |
| k (Pa.s ⁿ): | 0.175 |
| n: | 0.768 |
| Flume width (mm): | 150 |

| SLOPE | FLOW | DEPTH | SLOPE | FLOW | DEPTH | SLOPE | FLOW | DEPTH | SLOPE | FLOW | DEPTH | SLOPE | FLOW | DEPTH |
|-----------|----------------------|-------|-----------|----------------------|-------|-----------|----------------------|-------|-----------|----------------------|-------|-----------|----------------------|-------|
| FLUME | Q | h | FLUME | Q | h | FLUME | Q | h | FLUME | Q | h | FLUME | Q | h |
| (degrees) | (l.s ⁻¹) | (m) | (degrees) | (l.s ⁻¹) | (m) | (degrees) | (l.s ⁻¹) | (m) | (degrees) | (l.s ⁻¹) | (m) | (degrees) | (l.s ⁻¹) | (m) |
| 1 | 0.128 | 0.016 | 2 | 0.144 | 0.013 | 3 | 0.506 | 0.016 | 4 | 0.121 | 0.010 | 5 | 0.328 | 0.012 |
| 1 | 0.219 | 0.018 | 2 | 0.247 | 0.015 | 3 | 0.603 | 0.017 | 4 | 0.193 | 0.011 | 5 | 0.429 | 0.013 |
| 1 | 0.288 | 0.020 | 2 | 0.342 | 0.016 | 3 | 0.803 | 0.018 | 4 | 0.298 | 0.012 | 5 | 0.522 | 0.014 |
| 1 | 0.402 | 0.022 | 2 | 0.402 | 0.017 | 3 | 1.013 | 0.019 | 4 | 0.401 | 0.013 | 5 | 0.636 | 0.014 |
| 1 | 0.558 | 0.024 | 2 | 0.512 | 0.018 | 3 | 1.295 | 0.021 | 4 | 0.500 | 0.014 | 5 | 0.719 | 0.015 |
| 1 | 0.866 | 0.027 | 2 | 0.643 | 0.020 | 3 | 1.608 | 0.023 | 4 | 0.592 | 0.015 | 5 | 0.884 | 0.015 |
| 1 | 0.993 | 0.028 | 2 | 0.877 | 0.022 | 3 | 2.100 | 0.025 | 4 | 0.751 | 0.016 | 5 | 1.026 | 0.016 |
| 1 | 1.246 | 0.030 | 2 | 1.004 | 0.023 | 3 | 2.531 | 0.027 | 4 | 0.997 | 0.017 | 5 | 1.309 | 0.018 |
| 1 | 1.539 | 0.033 | 2 | 1.300 | 0.025 | 3 | 3.609 | 0.031 | 4 | 1.260 | 0.019 | 5 | 1.613 | 0.019 |
| 1 | 2.023 | 0.036 | 2 | 1.695 | 0.027 | 3 | 4.766 | 0.036 | 4 | 1.519 | 0.020 | 5 | 2.040 | 0.021 |
| 1 | 2.846 | 0.041 | 2 | 2.270 | 0.030 | 3 | 6.446 | 0.042 | 4 | 1.897 | 0.022 | 5 | 2.994 | 0.024 |
| 1 | 4.020 | 0.047 | 2 | 2.640 | 0.032 | 3 | 8.112 | 0.047 | 4 | 2.257 | 0.024 | 5 | 4.141 | 0.028 |
| 1 | 4.948 | 0.052 | 2 | 3.645 | 0.036 | 3 | 10.162 | 0.053 | 4 | 3.034 | 0.026 | 5 | 5.008 | 0.031 |
| 1 | 5.893 | 0.057 | 2 | 4.267 | 0.039 | 3 | 15.479 | 0.069 | 4 | 4.125 | 0.030 | 5 | 6.131 | 0.034 |
| 1 | 6.769 | 0.061 | 2 | 5.185 | 0.043 | 3 | 19.412 | 0.079 | 4 | 5.044 | 0.034 | 5 | 7.070 | 0.037 |
| 1 | 8.013 | 0.067 | 2 | 6.285 | 0.047 | | | | 4 | 6.066 | 0.037 | 5 | 9.924 | 0.045 |
| 1 | 10.019 | 0.076 | 2 | 7.476 | 0.052 | | | | 4 | 8.050 | 0.043 | 5 | 15.833 | 0.059 |
| 1 | 15.564 | 0.097 | 2 | 9.483 | 0.059 | | | | 4 | 10.120 | 0.049 | 5 | 19.941 | 0.069 |
| 1 | 19.738 | 0.114 | 2 | 12.447 | 0.069 | | | | 4 | 14.414 | 0.060 | | | |
| | | | 2 | 14.934 | 0.077 | | | | 4 | 19.349 | 0.072 | | | |

Table B.5: 4% CMC in water solution in a 150 mm semi-circular flume

| | |
|-----------------------------|-------|
| Material: | CMC |
| Concentration/vol: | 4.0% |
| Density kg/m ³ : | 1022 |
| Ty (Pa): | 0.000 |
| k (Pa.s ⁿ): | 0.278 |
| n: | 0.749 |
| Flume width (mm): | 150 |

| SLOPE | FLOW | DEPTH | SLOPE | FLOW | DEPTH | SLOPE | FLOW | DEPTH | SLOPE | FLOW | DEPTH | SLOPE | FLOW | DEPTH |
|-----------|----------------------|-------|-----------|----------------------|-------|-----------|----------------------|-------|-----------|----------------------|-------|-----------|----------------------|-------|
| FLUME | Q | h | FLUME | Q | h | FLUME | Q | h | FLUME | Q | h | FLUME | Q | h |
| (degrees) | (l.s ⁻¹) | (m) | (degrees) | (l.s ⁻¹) | (m) | (degrees) | (l.s ⁻¹) | (m) | (degrees) | (l.s ⁻¹) | (m) | (degrees) | (l.s ⁻¹) | (m) |
| 1 | 0.148 | 0.020 | 2 | 0.141 | 0.016 | 3 | 0.392 | 0.018 | 4 | 0.101 | 0.011 | 5 | 0.113 | 0.011 |
| 1 | 0.195 | 0.021 | 2 | 0.274 | 0.018 | 3 | 0.500 | 0.019 | 4 | 0.252 | 0.014 | 5 | 0.201 | 0.012 |
| 1 | 0.293 | 0.024 | 2 | 0.382 | 0.020 | 3 | 0.599 | 0.020 | 4 | 0.406 | 0.016 | 5 | 0.290 | 0.013 |
| 1 | 0.393 | 0.026 | 2 | 0.491 | 0.022 | 3 | 0.802 | 0.021 | 4 | 0.546 | 0.017 | 5 | 0.395 | 0.015 |
| 1 | 0.496 | 0.028 | 2 | 0.592 | 0.023 | 3 | 0.995 | 0.023 | 4 | 0.613 | 0.018 | 5 | 0.581 | 0.016 |
| 1 | 0.684 | 0.031 | 2 | 0.697 | 0.024 | 3 | 1.489 | 0.026 | 4 | 0.792 | 0.019 | 5 | 0.587 | 0.016 |
| 1 | 0.889 | 0.033 | 2 | 0.888 | 0.026 | 3 | 1.943 | 0.028 | 4 | 0.988 | 0.021 | 5 | 0.786 | 0.017 |
| 1 | 1.179 | 0.036 | 2 | 1.041 | 0.027 | 3 | 2.492 | 0.031 | 4 | 0.994 | 0.021 | 5 | 0.984 | 0.019 |
| 1 | 1.480 | 0.039 | 2 | 1.455 | 0.030 | 3 | 3.505 | 0.035 | 4 | 1.489 | 0.023 | 5 | 1.487 | 0.021 |
| 1 | 1.788 | 0.041 | 2 | 2.000 | 0.033 | 3 | 4.161 | 0.037 | 4 | 1.975 | 0.026 | 5 | 1.990 | 0.024 |
| 1 | 1.994 | 0.043 | 2 | 2.911 | 0.037 | 3 | 6.054 | 0.044 | 4 | 2.554 | 0.028 | 5 | 2.945 | 0.027 |
| 1 | 2.902 | 0.048 | 2 | 3.504 | 0.040 | 3 | 7.122 | 0.048 | 4 | 3.053 | 0.030 | 5 | 4.136 | 0.031 |
| 1 | 3.539 | 0.052 | 2 | 4.075 | 0.043 | 3 | 8.019 | 0.051 | 4 | 3.972 | 0.033 | 5 | 5.002 | 0.034 |
| 1 | 4.057 | 0.055 | 2 | 5.011 | 0.047 | 3 | 10.275 | 0.058 | 4 | 5.106 | 0.037 | 5 | 5.984 | 0.037 |
| 1 | 5.037 | 0.060 | 2 | 6.105 | 0.051 | 3 | 14.606 | 0.072 | 4 | 6.118 | 0.040 | 5 | 8.079 | 0.043 |
| 1 | 6.102 | 0.065 | 2 | 8.040 | 0.058 | 3 | 18.807 | 0.083 | 4 | 8.083 | 0.046 | 5 | 10.046 | 0.048 |
| 1 | 8.104 | 0.075 | 2 | 10.080 | 0.066 | 3 | 24.286 | 0.098 | 4 | 10.245 | 0.052 | 5 | 16.390 | 0.064 |
| 1 | 10.035 | 0.084 | 2 | 15.325 | 0.084 | | | | 4 | 17.063 | 0.070 | 5 | 19.792 | 0.071 |
| 1 | 15.259 | 0.108 | | | | | | | 4 | 21.080 | 0.080 | 5 | 23.078 | 0.079 |
| 1 | 19.299 | 0.125 | | | | | | | | | | | | |
| 1 | 22.241 | 0.137 | | | | | | | | | | | | |

Table B.6: 5.3% CMC in water solution in a 150 mm semi-circular flume

| | |
|-----------------------------|-------|
| Material: | CMC |
| Concentration/vol: | 5.3% |
| Density kg/m ³ : | 1028 |
| Ty (Pa): | 0.000 |
| k (Pa.s ⁿ): | 0.920 |
| n: | 0.678 |
| Flume width (mm): | 150 |

| SLOPE | FLOW | DEPTH | SLOPE | FLOW | DEPTH | SLOPE | FLOW | DEPTH |
|-----------|----------------------|-------|-----------|----------------------|-------|-----------|----------------------|-------|
| FLUME | Q | h | FLUME | Q | h | FLUME | Q | h |
| (degrees) | (l.s ⁻¹) | (m) | (degrees) | (l.s ⁻¹) | (m) | (degrees) | (l.s ⁻¹) | (m) |
| 1 | 10.053 | 0.074 | 3 | 0.116 | 0.019 | 5 | 0.121 | 0.015 |
| 1 | 11.044 | 0.077 | 3 | 0.211 | 0.020 | 5 | 0.212 | 0.017 |
| 1 | 11.923 | 0.080 | 3 | 0.307 | 0.024 | 5 | 0.330 | 0.020 |
| 1 | 2.247 | 0.067 | 3 | 0.404 | 0.026 | 5 | 0.420 | 0.021 |
| 1 | 3.491 | 0.080 | 3 | 0.511 | 0.028 | 5 | 0.506 | 0.022 |
| 1 | 4.355 | 0.087 | 3 | 0.605 | 0.030 | 5 | 0.608 | 0.024 |
| 1 | 5.746 | 0.098 | 3 | 0.698 | 0.031 | 5 | 0.693 | 0.025 |
| 1 | 7.437 | 0.111 | 3 | 0.801 | 0.032 | 5 | 0.821 | 0.026 |
| 1 | 13.369 | 0.146 | 3 | 0.898 | 0.033 | 5 | 0.883 | 0.075 |
| 1 | 15.390 | 0.156 | 3 | 0.996 | 0.034 | 5 | 0.997 | 0.027 |
| 1 | 18.017 | 0.172 | 3 | 1.192 | 0.036 | 5 | 1.196 | 0.029 |
| 1 | 0.227 | 0.033 | 3 | 1.391 | 0.037 | 5 | 1.410 | 0.030 |
| 1 | 0.454 | 0.040 | 3 | 2.526 | 0.045 | 5 | 1.761 | 0.031 |
| 1 | 0.359 | 0.038 | 3 | 2.999 | 0.048 | 5 | 1.693 | 0.033 |
| 1 | 0.671 | 0.045 | 3 | 3.877 | 0.052 | 5 | 2.078 | 0.034 |
| 1 | 0.737 | 0.046 | 3 | 4.325 | 0.054 | 5 | 2.228 | 0.034 |
| 1 | 0.816 | 0.047 | 3 | 4.739 | 0.056 | 5 | 2.651 | 0.036 |
| 1 | 0.976 | 0.050 | 3 | 5.745 | 0.060 | 5 | 2.895 | 0.037 |
| 1 | 0.980 | 0.050 | 3 | 6.572 | 0.063 | 5 | 3.159 | 0.038 |
| 1 | 1.092 | 0.052 | 3 | 7.502 | 0.067 | 5 | 3.526 | 0.040 |
| 1 | 1.414 | 0.057 | 3 | 9.023 | 0.070 | 5 | 4.421 | 0.043 |
| 1 | 1.542 | 0.058 | 3 | 12.020 | 0.080 | 5 | 5.373 | 0.046 |
| 1 | 2.177 | 0.065 | 3 | 12.850 | 0.082 | 5 | 6.247 | 0.049 |
| 1 | 2.399 | 0.068 | 3 | 15.990 | 0.092 | | | |
| 1 | 2.485 | 0.068 | 3 | 16.710 | 0.095 | | | |
| 1 | 3.026 | 0.073 | 3 | 19.785 | 0.105 | | | |
| 1 | 3.159 | 0.074 | 3 | 21.999 | 0.111 | | | |

Table B.7: 4.6% Bentonite in water suspension in a 300 mm semi-circular flume

| | |
|-----------------------------|-----------|
| Material: | Bentonite |
| Concentration/vol: | 4.6% |
| Density kg/m ³ : | 1027.8 |
| Ty (Pa): | 4.680 |
| k (Pa.s ⁿ): | 0.003 |
| n: | 1.000 |
| Flume width (mm): | 300 |
| Flume Shape | H-Round |

| SLOPE FLUME (degrees) | FLOW Q (l.s ⁻¹) | DEPTH h (m) | SLOPE FLUME (degrees) | FLOW Q (l.s ⁻¹) | DEPTH h (m) | SLOPE FLUME (degrees) | FLOW Q (l.s ⁻¹) | DEPTH h (m) | SLOPE FLUME (degrees) | FLOW Q (l.s ⁻¹) | DEPTH h (m) | SLOPE FLUME (degrees) | FLOW Q (l.s ⁻¹) | DEPTH h (m) |
|-----------------------------|-----------------------------------|-------------------|-----------------------------|-----------------------------------|-------------------|-----------------------------|-----------------------------------|-------------------|-----------------------------|-----------------------------------|-------------------|-----------------------------|-----------------------------------|-------------------|
| 1 | 0.669 | 0.0420 | 2 | 0.824 | 0.0191 | 3 | 0.876 | 0.0152 | 4 | 0.54 | 0.0113 | 5 | 0.50 | 0.0108 |
| 1 | 0.752 | 0.0435 | 2 | 1.056 | 0.0206 | 3 | 1.006 | 0.0158 | 4 | 0.76 | 0.0122 | 5 | 0.54 | 0.0103 |
| 1 | 1.001 | 0.0452 | 2 | 1.263 | 0.0212 | 3 | 1.312 | 0.0168 | 4 | 0.66 | 0.0119 | 5 | 0.81 | 0.0114 |
| 1 | 1.241 | 0.0445 | 2 | 1.569 | 0.0222 | 3 | 1.208 | 0.0169 | 4 | 0.92 | 0.0131 | 5 | 0.73 | 0.0116 |
| 1 | 1.567 | 0.0451 | 2 | 1.866 | 0.0239 | 3 | 1.532 | 0.0181 | 4 | 1.24 | 0.0148 | 5 | 0.99 | 0.0123 |
| 1 | 1.861 | 0.0446 | 2 | 2.229 | 0.0249 | 3 | 1.943 | 0.0198 | 4 | 1.05 | 0.0140 | 5 | 1.43 | 0.0133 |
| 1 | 2.131 | 0.0440 | 2 | 2.635 | 0.0257 | 3 | 2.282 | 0.0206 | 4 | 1.40 | 0.0155 | 5 | 1.22 | 0.0130 |
| 1 | 2.445 | 0.0411 | 2 | 2.847 | 0.0261 | 3 | 2.675 | 0.0211 | 4 | 1.69 | 0.0159 | 5 | 1.63 | 0.0142 |
| 1 | 3.029 | 0.0427 | 2 | 3.857 | 0.0296 | 3 | 3.041 | 0.0224 | 4 | 1.52 | 0.0157 | | | |
| 1 | 3.612 | 0.0453 | 2 | 4.827 | 0.0322 | 3 | 3.535 | 0.0242 | 4 | 1.94 | 0.0170 | | | |
| 1 | 4.228 | 0.0469 | 2 | 6.057 | 0.0352 | 3 | 4.248 | 0.0258 | 4 | 2.23 | 0.0177 | | | |
| 1 | 4.701 | 0.0481 | 2 | 7.082 | 0.0379 | 3 | 4.646 | 0.0269 | 4 | 2.54 | 0.0188 | | | |
| 1 | 5.240 | 0.0496 | 2 | 8.194 | 0.0404 | 3 | 5.186 | 0.0286 | 4 | 3.03 | 0.0200 | | | |
| 1 | 6.066 | 0.0520 | 2 | 9.049 | 0.0423 | 3 | 6.091 | 0.0304 | 4 | 3.53 | 0.0213 | | | |
| 1 | 7.164 | 0.0554 | 2 | 10.157 | 0.0448 | 3 | 7.100 | 0.0331 | 4 | 4.14 | 0.0226 | | | |
| 1 | 7.612 | 0.0553 | 2 | 12.397 | 0.0493 | 3 | 8.140 | 0.0352 | 4 | 4.49 | 0.0236 | | | |
| 1 | 8.123 | 0.0570 | 2 | 18.854 | 0.0619 | 3 | 10.079 | 0.0396 | 4 | 5.18 | 0.0252 | | | |
| 1 | 9.282 | 0.0598 | 2 | 21.851 | 0.0674 | 3 | 11.995 | 0.0420 | 4 | 6.12 | 0.0272 | | | |
| 1 | 10.147 | 0.0617 | 2 | 26.257 | 0.0759 | 3 | 16.163 | 0.0495 | 4 | 7.08 | 0.0293 | | | |
| 1 | 11.734 | 0.0622 | | | | 3 | 20.947 | 0.0576 | 4 | 8.03 | 0.0310 | | | |
| 1 | 15.678 | 0.0711 | | | | 3 | 26.915 | 0.0656 | 4 | 10.08 | 0.0350 | | | |
| 1 | 18.159 | 0.0766 | | | | 3 | 32.225 | 0.0740 | 4 | 14.22 | 0.0421 | | | |
| 1 | 22.846 | 0.0854 | | | | | | | 4 | 18.52 | 0.0487 | | | |
| 1 | 28.247 | 0.0967 | | | | | | | 4 | 23.16 | 0.0559 | | | |
| 1 | 33.630 | 0.1027 | | | | | | | | | | | | |
| 1 | 38.434 | 0.1119 | | | | | | | | | | | | |

Table B.8: 6.2% Bentonite in water suspension in a 300 mm semi-circular flume

| | |
|-----------------------------|-----------|
| Material: | Bentonite |
| Concentration/vol: | 6.2% |
| Density kg/m ³ : | 0 |
| Ty (Pa): | 18.340 |
| k (Pa.s ⁿ): | 0.008 |
| n: | 1.000 |
| Flume width (mm): | 300 |
| Flume Shape | H-Round |

| SLOPE FLUME (degrees) | FLOW Q (l.s ⁻¹) | DEPTH h (m) | SLOPE FLUME (degrees) | FLOW Q (l.s ⁻¹) | DEPTH h (m) | SLOPE FLUME (degrees) | FLOW Q (l.s ⁻¹) | DEPTH h (m) | SLOPE FLUME (degrees) | FLOW Q (l.s ⁻¹) | DEPTH h (m) |
|-----------------------------|-----------------------------------|-------------------|-----------------------------|-----------------------------------|-------------------|-----------------------------|-----------------------------------|-------------------|-----------------------------|-----------------------------------|-------------------|
| 2 | 1.631 | 0.1072 | 3 | 2.111 | 0.0580 | 4 | 1.36 | 0.0416 | 5 | 1.97 | 0.0316 |
| 2 | 2.635 | 0.1051 | 3 | 3.471 | 0.0595 | 4 | 2.29 | 0.0416 | 5 | 2.90 | 0.0340 |
| 2 | 1.996 | 0.0991 | 3 | 4.147 | 0.0611 | 4 | 3.02 | 0.0462 | 5 | 3.95 | 0.0353 |
| 2 | 3.062 | 0.1022 | 3 | 4.963 | 0.0610 | 4 | 4.01 | 0.0435 | 5 | 4.96 | 0.0374 |
| 2 | 4.027 | 0.1037 | 3 | 6.068 | 0.0627 | 4 | 5.02 | 0.0452 | 5 | 6.10 | 0.0391 |
| 2 | 4.988 | 0.1013 | 3 | 7.030 | 0.0621 | 4 | 6.10 | 0.0465 | 5 | 7.27 | 0.0405 |
| 2 | 6.059 | 0.1014 | 3 | 8.490 | 0.0620 | 4 | 7.07 | 0.0476 | 5 | 8.43 | 0.0417 |
| 2 | 6.897 | 0.1007 | 3 | 10.224 | 0.0645 | 4 | 8.46 | 0.0496 | 5 | 10.16 | 0.0444 |
| 2 | 8.443 | 0.0995 | 3 | 12.711 | 0.0666 | 4 | 10.22 | 0.0523 | 5 | 11.99 | 0.0459 |
| 2 | 12.468 | 0.1001 | 3 | 14.507 | 0.0682 | 4 | 12.73 | 0.0542 | 5 | 14.29 | 0.0507 |
| 2 | 14.463 | 0.1048 | 3 | 16.723 | 0.0719 | 4 | 14.49 | 0.0570 | 5 | 15.94 | 0.0526 |
| 2 | 17.642 | 0.1093 | 3 | 21.384 | 0.0778 | 4 | 16.62 | 0.0599 | 5 | 19.67 | 0.0579 |
| 2 | 22.975 | 0.1112 | 3 | 25.676 | 0.0841 | 4 | 21.21 | 0.0666 | 5 | 25.02 | 0.0647 |
| 2 | 30.217 | 0.1157 | 3 | 32.294 | 0.0944 | 4 | 25.70 | 0.0720 | 5 | 29.46 | 0.0708 |
| 2 | 34.629 | 0.1184 | 3 | 36.650 | 0.0989 | 4 | 31.68 | 0.0810 | | | |
| 2 | 40.516 | 0.1258 | 3 | 41.754 | 0.1047 | 4 | 36.57 | 0.0869 | | | |

Table B.9: 4.6% Bentonite in water suspension in a 150 mm semi-circular flume

| | |
|-----------------------------|-----------|
| Material: | Bentonite |
| Concentration/vol: | 4.6% |
| Density kg/m ³ : | 1028.1 |
| Ty (Pa): | 5.660 |
| k (Pa.s ⁿ): | 0.010 |
| n: | 1.000 |
| Flume width (mm): | 150 |
| Flume Shape | H-Round |

| SLOPE | FLOW | DEPTH | SLOPE | FLOW | DEPTH | SLOPE | FLOW | DEPTH | SLOPE | FLOW | DEPTH | SLOPE | FLOW | DEPTH |
|-----------|----------------------|--------|-----------|----------------------|--------|-----------|----------------------|--------|-----------|----------------------|--------|-----------|----------------------|--------|
| FLUME | Q | h | FLUME | Q | h | FLUME | Q | h | FLUME | Q | h | FLUME | Q | h |
| (degrees) | (l.s ⁻¹) | (m) | (degrees) | (l.s ⁻¹) | (m) | (degrees) | (l.s ⁻¹) | (m) | (degrees) | (l.s ⁻¹) | (m) | (degrees) | (l.s ⁻¹) | (m) |
| 1 | 0.451 | 0.0644 | 2 | 0.504 | 0.0271 | 3 | 0.623 | 0.0186 | 4 | 0.63 | 0.0154 | 5 | 0.65 | 0.0133 |
| 1 | 0.690 | 0.0648 | 2 | 0.822 | 0.0292 | 3 | 0.934 | 0.0203 | 4 | 1.04 | 0.0175 | 5 | 1.00 | 0.0152 |
| 1 | 0.936 | 0.0637 | 2 | 1.365 | 0.0308 | 3 | 1.505 | 0.0228 | 4 | 1.50 | 0.0201 | 5 | 1.56 | 0.0183 |
| 1 | 1.319 | 0.0620 | 2 | 1.760 | 0.0307 | 3 | 2.055 | 0.0259 | 4 | 2.09 | 0.0229 | 5 | 2.10 | 0.0207 |
| 1 | 1.715 | 0.0656 | 2 | 2.256 | 0.0331 | 3 | 2.650 | 0.0291 | 4 | 2.58 | 0.0249 | 5 | 2.50 | 0.0220 |
| 1 | 2.413 | 0.0641 | 2 | 2.735 | 0.0338 | 3 | 3.009 | 0.0292 | 4 | 3.00 | 0.0249 | 5 | 2.99 | 0.0221 |
| 1 | 3.009 | 0.0679 | 2 | 3.023 | 0.0351 | 3 | 3.615 | 0.0310 | 4 | 3.52 | 0.0266 | 5 | 3.53 | 0.0242 |
| 1 | 3.509 | 0.0693 | 2 | 3.656 | 0.0391 | 3 | 4.117 | 0.0329 | 4 | 4.11 | 0.0288 | 5 | 4.49 | 0.0271 |
| 1 | 4.662 | 0.0705 | 2 | 4.409 | 0.0418 | 3 | 4.976 | 0.0359 | 4 | 5.34 | 0.0325 | 5 | 5.14 | 0.0293 |
| 1 | 5.551 | 0.0726 | 2 | 5.587 | 0.0455 | 3 | 6.054 | 0.0394 | 4 | 6.12 | 0.0354 | 5 | 6.28 | 0.0324 |
| 1 | 6.583 | 0.0758 | 2 | 7.403 | 0.0517 | 3 | 8.074 | 0.0459 | 4 | 8.13 | 0.0414 | 5 | 8.21 | 0.0380 |
| 1 | 7.599 | 0.0786 | 2 | 9.068 | 0.0572 | 3 | 10.232 | 0.0519 | 4 | 10.20 | 0.0470 | 5 | 10.19 | 0.0433 |
| 1 | 8.891 | 0.0811 | 2 | 10.168 | 0.0613 | 3 | 14.448 | 0.0641 | 4 | 14.49 | 0.0577 | 5 | 14.39 | 0.0532 |
| 1 | 10.162 | 0.0847 | 2 | 14.123 | 0.0723 | 3 | 21.963 | 0.0824 | 4 | 20.08 | 0.0707 | 5 | 19.62 | 0.0645 |
| 1 | 11.909 | 0.0906 | 2 | 21.573 | 0.0933 | | | | 4 | 25.26 | 0.0804 | | | |
| 1 | 11.943 | 0.0873 | | | | | | | | | | | | |
| 1 | 13.162 | 0.0935 | | | | | | | | | | | | |
| 1 | 17.664 | 0.1071 | | | | | | | | | | | | |
| 1 | 20.065 | 0.1143 | | | | | | | | | | | | |

Table B.10: 6.2% Bentonite in water suspension in a 150 mm semi-circular flume

| | |
|-----------------------------|-----------|
| Material: | Bentonite |
| Concentration/vol: | 6.2% |
| Density kg/m ³ : | 1037.9 |
| Ty (Pa): | 18.340 |
| k (Pa.s ⁿ): | 0.008 |
| n: | 1.000 |
| Flume width (mm): | 150 |
| Flume Shape | H-Round |

| SLOPE | FLOW | DEPTH | SLOPE | FLOW | DEPTH | SLOPE | FLOW | DEPTH | SLOPE | FLOW | DEPTH |
|-----------|----------------------|--------|-----------|----------------------|--------|-----------|----------------------|--------|-----------|----------------------|--------|
| FLUME | Q | h | FLUME | Q | h | FLUME | Q | h | FLUME | Q | h |
| (degrees) | (l.s ⁻¹) | (m) | (degrees) | (l.s ⁻¹) | (m) | (degrees) | (l.s ⁻¹) | (m) | (degrees) | (l.s ⁻¹) | (m) |
| 2 | 0.794 | 0.0972 | 3 | 1.066 | 0.0622 | 4 | 3.27 | 0.0478 | 5 | 2.99 | 0.0366 |
| 2 | 1.424 | 0.1069 | 3 | 1.233 | 0.0658 | 4 | 4.17 | 0.0484 | 5 | 1.97 | 0.0355 |
| 2 | 1.817 | 0.1125 | 3 | 1.546 | 0.0697 | 4 | 4.58 | 0.0496 | 5 | 1.28 | 0.0342 |
| 2 | 2.481 | 0.1178 | 3 | 1.855 | 0.0692 | 4 | 4.93 | 0.0498 | 5 | 1.79 | 0.0351 |
| 2 | 3.053 | 0.1213 | 3 | 2.010 | 0.0682 | 4 | 5.36 | 0.0509 | 5 | 2.71 | 0.0367 |
| 2 | 5.378 | 0.1312 | 3 | 2.345 | 0.0685 | 4 | 5.85 | 0.0517 | 5 | 3.53 | 0.0388 |
| 2 | 5.773 | 0.1204 | 3 | 2.862 | 0.0685 | 4 | 6.45 | 0.0524 | 5 | 4.35 | 0.0399 |
| 2 | 6.288 | 0.1222 | 3 | 3.611 | 0.0693 | 4 | 7.40 | 0.0543 | 5 | 5.46 | 0.0424 |
| 2 | 7.134 | 0.1230 | 3 | 4.324 | 0.0696 | 4 | 8.10 | 0.0557 | 5 | 6.34 | 0.0443 |
| 2 | 8.096 | 0.1238 | 3 | 5.688 | 0.0702 | 4 | 8.31 | 0.0556 | 5 | 7.89 | 0.0478 |
| 2 | 8.731 | 0.1244 | 3 | 6.474 | 0.0689 | 4 | 10.47 | 0.0609 | 5 | 9.16 | 0.0518 |
| 2 | 9.248 | 0.1244 | 3 | 7.537 | 0.0704 | 4 | 11.57 | 0.0639 | 5 | 10.86 | 0.0540 |
| 2 | 13.805 | 0.1244 | 3 | 8.420 | 0.0719 | 4 | 13.73 | 0.0688 | 5 | 9.98 | 0.0522 |
| 2 | 11.102 | 0.1279 | 3 | 9.657 | 0.0745 | 4 | 15.12 | 0.0713 | 5 | 12.60 | 0.0586 |
| 2 | 12.007 | 0.1294 | 3 | 10.345 | 0.0756 | | | | 5 | 14.49 | 0.0629 |
| 2 | 14.225 | 0.1322 | 3 | 13.480 | 0.0826 | | | | | | |
| 2 | 15.359 | 0.1333 | 3 | 18.033 | 0.0940 | | | | | | |
| 2 | 18.577 | 0.1369 | 3 | 21.167 | 0.1005 | | | | | | |

Table B.11: 3.5% kaolin in water suspension in a 300 mm semi-circular flume

| | |
|-----------------------------|---------|
| Material: | Kaolin |
| Concentration/vol: | 3.5% |
| Density kg/m ³ : | 1057.8 |
| Ty (Pa): | 0.463 |
| k (Pa.s ⁿ): | 0.061 |
| n: | 0.560 |
| Flume width (mm): | 300 |
| Flume Shape | H-Round |

| SLOPE | FLOW | DEPTH | SLOPE | FLOW | DEPTH | SLOPE | FLOW | DEPTH | SLOPE | FLOW | DEPTH | SLOPE | FLOW | DEPTH |
|-----------|----------------------|--------|-----------|----------------------|--------|-----------|----------------------|--------|-----------|----------------------|--------|-----------|----------------------|--------|
| FLUME | Q | h | FLUME | Q | h | FLUME | Q | h | FLUME | Q | h | FLUME | Q | h |
| (degrees) | (l.s ⁻¹) | (m) | (degrees) | (l.s ⁻¹) | (m) | (degrees) | (l.s ⁻¹) | (m) | (degrees) | (l.s ⁻¹) | (m) | (degrees) | (l.s ⁻¹) | (m) |
| 1 | 0.122 | 0.0104 | 2 | 0.066 | 0.0065 | 3 | 0.231 | 0.0065 | 4 | 0.32 | 0.0059 | 5 | 0.49 | 0.0074 |
| 1 | 0.158 | 0.0109 | 2 | 0.159 | 0.0072 | 3 | 0.385 | 0.0073 | 4 | 0.42 | 0.0065 | 5 | 0.67 | 0.0084 |
| 1 | 0.218 | 0.0114 | 2 | 0.105 | 0.0068 | 3 | 0.320 | 0.0070 | 4 | 0.53 | 0.0071 | 5 | 1.03 | 0.0104 |
| 1 | 0.264 | 0.0119 | 2 | 0.219 | 0.0077 | 3 | 0.465 | 0.0075 | 4 | 0.63 | 0.0075 | 5 | 1.57 | 0.0121 |
| 1 | 0.374 | 0.0125 | 2 | 0.262 | 0.0081 | 3 | 0.584 | 0.0093 | 4 | 0.77 | 0.0080 | 5 | 1.45 | 0.0117 |
| 1 | 0.311 | 0.0122 | 2 | 0.318 | 0.0085 | 3 | 0.668 | 0.0100 | 4 | 0.98 | 0.0088 | 5 | 2.04 | 0.0141 |
| 1 | 0.424 | 0.0130 | 2 | 0.383 | 0.0090 | 3 | 0.804 | 0.0105 | 4 | 1.49 | 0.0128 | 5 | 3.23 | 0.0179 |
| 1 | 0.478 | 0.0135 | 2 | 0.482 | 0.0096 | 3 | 1.047 | 0.0112 | 4 | 2.14 | 0.0148 | 5 | 4.11 | 0.0201 |
| 1 | 0.526 | 0.0138 | 2 | 0.576 | 0.0100 | 3 | 1.538 | 0.0138 | 4 | 3.58 | 0.0198 | 5 | 6.93 | 0.0263 |
| 1 | 0.586 | 0.0141 | 2 | 0.683 | 0.0106 | 3 | 2.116 | 0.0161 | 4 | 5.37 | 0.0237 | 5 | 10.10 | 0.0325 |
| 1 | 0.690 | 0.0148 | 2 | 0.765 | 0.0109 | 3 | 3.143 | 0.0196 | 4 | 7.06 | 0.0289 | 5 | 23.78 | 0.0560 |
| 1 | 0.801 | 0.0154 | 2 | 0.807 | 0.0112 | 3 | 4.235 | 0.0229 | 4 | 10.09 | 0.0349 | 5 | 34.72 | 0.0669 |
| 1 | 0.943 | 0.0160 | 2 | 0.916 | 0.0118 | 3 | 5.467 | 0.0260 | 4 | 19.11 | 0.0495 | 5 | 44.29 | 0.0791 |
| 1 | 1.013 | 0.0164 | 2 | 1.215 | 0.0131 | 3 | 8.093 | 0.0337 | 4 | 33.51 | 0.0695 | | | |
| 1 | 1.499 | 0.0193 | 2 | 2.185 | 0.0181 | 3 | 10.158 | 0.0380 | 4 | 45.47 | 0.0851 | | | |
| 1 | 2.071 | 0.0215 | 2 | 3.180 | 0.0219 | 3 | 17.676 | 0.0515 | | | | | | |
| 1 | 3.119 | 0.0259 | 2 | 4.128 | 0.0254 | 3 | 28.609 | 0.0682 | | | | | | |
| 1 | 4.072 | 0.0296 | 2 | 5.102 | 0.0286 | 3 | 46.740 | 0.0944 | | | | | | |
| 1 | 5.081 | 0.0327 | 2 | 6.140 | 0.0317 | | | | | | | | | |
| 1 | 6.119 | 0.0359 | 2 | 7.098 | 0.0340 | | | | | | | | | |
| 1 | 7.208 | 0.0386 | 2 | 8.232 | 0.0368 | | | | | | | | | |
| 1 | 8.429 | 0.0436 | 2 | 10.099 | 0.0419 | | | | | | | | | |
| 1 | 9.562 | 0.0479 | 2 | 17.287 | 0.0569 | | | | | | | | | |
| 1 | 10.105 | 0.0493 | 2 | 30.715 | 0.0789 | | | | | | | | | |
| 1 | 15.782 | 0.0633 | 2 | 45.267 | 0.1019 | | | | | | | | | |
| 1 | 22.294 | 0.0796 | | | | | | | | | | | | |
| 1 | 30.832 | 0.0946 | | | | | | | | | | | | |
| 1 | 43.733 | 0.1160 | | | | | | | | | | | | |

Table B.12: 5.3% kaolin in water suspension in a 300 mm semi-circular flume

| | |
|-----------------------------|---------|
| Material: | Kaolin |
| Concentration/vol: | 5.3% |
| Density kg/m ³ : | 1088.6 |
| Ty (Pa): | 4.448 |
| k (Pa.s ⁿ): | 0.018 |
| n: | 0.781 |
| Flume width (mm): | 300 |
| Flume Shape | H-Round |

| SLOPE | FLOW | DEPTH | SLOPE | FLOW | DEPTH | SLOPE | FLOW | DEPTH | SLOPE | FLOW | DEPTH | SLOPE | FLOW | DEPTH |
|-----------|----------------------|--------|-----------|----------------------|--------|-----------|----------------------|--------|-----------|----------------------|--------|-----------|----------------------|--------|
| FLUME | Q | h | FLUME | Q | h | FLUME | Q | h | FLUME | Q | h | FLUME | Q | h |
| (degrees) | (l.s ⁻¹) | (m) | (degrees) | (l.s ⁻¹) | (m) | (degrees) | (l.s ⁻¹) | (m) | (degrees) | (l.s ⁻¹) | (m) | (degrees) | (l.s ⁻¹) | (m) |
| 1 | 0.192 | 0.0358 | 2 | 0.257 | 0.0189 | 3 | 0.356 | 0.0141 | 4 | 1.21 | 0.0143 | 5 | 1.04 | 0.0119 |
| 1 | 0.276 | 0.0372 | 2 | 0.510 | 0.0198 | 3 | 0.406 | 0.0141 | 4 | 1.47 | 0.0151 | 5 | 1.31 | 0.0128 |
| 1 | 0.384 | 0.0382 | 2 | 0.390 | 0.0197 | 3 | 0.491 | 0.0145 | 4 | 1.70 | 0.0159 | 5 | 1.55 | 0.0139 |
| 1 | 0.548 | 0.0386 | 2 | 0.586 | 0.0204 | 3 | 0.576 | 0.0148 | 4 | 1.98 | 0.0169 | 5 | 1.89 | 0.0148 |
| 1 | 0.638 | 0.0391 | 2 | 0.697 | 0.0207 | 3 | 0.688 | 0.0152 | 4 | 2.45 | 0.0181 | 5 | 2.41 | 0.0161 |
| 1 | 0.842 | 0.0394 | 2 | 0.942 | 0.0211 | 3 | 0.907 | 0.0158 | 4 | 3.06 | 0.0196 | 5 | 3.01 | 0.0176 |
| 1 | 0.991 | 0.0406 | 2 | 0.782 | 0.0209 | 3 | 0.804 | 0.0153 | 4 | 3.97 | 0.0222 | 5 | 4.01 | 0.0199 |
| 1 | 1.531 | 0.0423 | 2 | 1.006 | 0.0216 | 3 | 1.018 | 0.0160 | 4 | 5.17 | 0.0245 | 5 | 5.30 | 0.0228 |
| 1 | 1.341 | 0.0420 | 2 | 1.312 | 0.0227 | 3 | 1.396 | 0.0176 | 4 | 6.17 | 0.0268 | 5 | 6.13 | 0.0245 |
| 1 | 2.129 | 0.0422 | 2 | 1.667 | 0.0237 | 3 | 1.649 | 0.0183 | 4 | 7.98 | 0.0306 | 5 | 8.22 | 0.0284 |
| 1 | 2.669 | 0.0423 | 2 | 2.069 | 0.0248 | 3 | 2.087 | 0.0197 | 4 | 10.19 | 0.0349 | 5 | 10.08 | 0.0322 |
| 1 | 2.925 | 0.0425 | 2 | 2.538 | 0.0262 | 3 | 2.559 | 0.0209 | 4 | 13.87 | 0.0412 | 5 | 14.86 | 0.0395 |
| 1 | 3.702 | 0.0460 | 2 | 2.956 | 0.0271 | 3 | 3.046 | 0.0224 | 4 | 22.48 | 0.0546 | 5 | 22.01 | 0.0499 |
| 1 | 4.604 | 0.0481 | 2 | 4.584 | 0.0314 | 3 | 4.032 | 0.0251 | 4 | 31.76 | 0.0658 | 5 | 31.44 | 0.0605 |
| 1 | 5.625 | 0.0502 | 2 | 3.825 | 0.0303 | 3 | 5.004 | 0.0275 | 4 | 42.13 | 0.0768 | | | |
| 1 | 6.754 | 0.0529 | 2 | 6.219 | 0.0364 | 3 | 6.109 | 0.0302 | 4 | 46.22 | 0.0822 | | | |
| 1 | 8.079 | 0.0562 | 2 | 7.092 | 0.0386 | 3 | 7.038 | 0.0323 | | | | | | |
| 1 | 9.326 | 0.0585 | 2 | 10.096 | 0.0457 | 3 | 8.540 | 0.0357 | | | | | | |
| 1 | 10.222 | 0.0610 | 2 | 14.297 | 0.0539 | 3 | 10.168 | 0.0389 | | | | | | |
| 1 | 14.770 | 0.0712 | 2 | 22.181 | 0.0681 | 3 | 14.114 | 0.0459 | | | | | | |
| 1 | 21.056 | 0.0838 | 2 | 33.603 | 0.0865 | 3 | 21.353 | 0.0582 | | | | | | |
| 1 | 31.780 | 0.1036 | 2 | 42.322 | 0.0986 | 3 | 31.829 | 0.0731 | | | | | | |
| 1 | 41.910 | 0.1203 | 2 | 46.015 | 0.1022 | 3 | 42.089 | 0.0864 | | | | | | |
| 1 | 45.596 | 0.1259 | | | | 3 | 46.358 | 0.0895 | | | | | | |

Table B.13: 7.1% kaolin in water suspension in a 300 mm semi-circular flume

| | |
|-----------------------------|---------|
| Material: | Kaolin |
| Concentration/vol: | 7.1% |
| Density kg/m ³ : | 1117.4 |
| Ty (Pa): | 8.100 |
| k (Pa.s ⁿ): | 1.140 |
| n: | 0.320 |
| Flume width (mm): | 300 |
| Flume Shape | H-Round |

| SLOPE FLUME (degrees) | FLOW Q (L.s ⁻¹) | DEPTH h (m) | SLOPE FLUME (degrees) | FLOW Q (L.s ⁻¹) | DEPTH h (m) | SLOPE FLUME (degrees) | FLOW Q (L.s ⁻¹) | DEPTH h (m) | SLOPE FLUME (degrees) | FLOW Q (L.s ⁻¹) | DEPTH h (m) | SLOPE FLUME (degrees) | FLOW Q (L.s ⁻¹) | DEPTH h (m) |
|-----------------------------|-----------------------------------|-------------------|-----------------------------|-----------------------------------|-------------------|-----------------------------|-----------------------------------|-------------------|-----------------------------|-----------------------------------|-------------------|-----------------------------|-----------------------------------|-------------------|
| 1 | 0.273 | 0.0738 | 2 | 1.557 | 0.0488 | 3 | 1.005 | 0.0319 | 4 | 1.27 | 0.0241 | 5 | 1.29 | 0.0202 |
| 1 | 0.408 | 0.0747 | 2 | 1.113 | 0.0479 | 3 | 1.610 | 0.0332 | 4 | 1.11 | 0.0246 | 5 | 1.45 | 0.0211 |
| 1 | 0.615 | 0.0765 | 2 | 1.973 | 0.0505 | 3 | 1.310 | 0.0323 | 4 | 1.56 | 0.0253 | 5 | 2.11 | 0.0223 |
| 1 | 0.821 | 0.0781 | 2 | 2.637 | 0.0515 | 3 | 2.119 | 0.0335 | 4 | 2.11 | 0.0264 | 5 | 1.79 | 0.0217 |
| 1 | 1.020 | 0.0797 | 2 | 3.095 | 0.0522 | 3 | 2.583 | 0.0344 | 4 | 1.97 | 0.0262 | 5 | 2.57 | 0.0232 |
| 1 | 2.034 | 0.0855 | 2 | 3.522 | 0.0528 | 3 | 3.130 | 0.0356 | 4 | 2.56 | 0.0273 | 5 | 3.12 | 0.0241 |
| 1 | 1.536 | 0.0826 | 2 | 4.119 | 0.0530 | 3 | 3.449 | 0.0364 | 4 | 3.18 | 0.0285 | 5 | 3.63 | 0.0251 |
| 1 | 2.608 | 0.0877 | 2 | 4.515 | 0.0527 | 3 | 4.005 | 0.0373 | 4 | 3.56 | 0.0292 | 5 | 4.23 | 0.0263 |
| 1 | 3.471 | 0.0894 | 2 | 5.710 | 0.0537 | 3 | 4.953 | 0.0385 | 4 | 3.92 | 0.0302 | 5 | 4.77 | 0.0277 |
| 1 | 4.140 | 0.0926 | 2 | 6.653 | 0.0547 | 3 | 4.525 | 0.0379 | 4 | 4.42 | 0.0311 | 5 | 5.50 | 0.0292 |
| 1 | 4.998 | 0.0965 | 2 | 7.596 | 0.0562 | 3 | 5.600 | 0.0399 | 4 | 5.22 | 0.0321 | 5 | 6.55 | 0.0308 |
| 1 | 6.369 | 0.1009 | 2 | 8.573 | 0.0579 | 3 | 6.485 | 0.0416 | 4 | 6.03 | 0.0341 | 5 | 7.48 | 0.0327 |
| 1 | 7.195 | 0.1032 | 2 | 9.449 | 0.0596 | 3 | 7.553 | 0.0435 | 4 | 6.49 | 0.0350 | 5 | 8.57 | 0.0345 |
| 1 | 8.031 | 0.1052 | 2 | 10.158 | 0.0609 | 3 | 8.558 | 0.0452 | 4 | 7.94 | 0.0374 | 5 | 9.36 | 0.0359 |
| 1 | 9.161 | 0.1078 | 2 | 12.464 | 0.0647 | 3 | 9.608 | 0.0473 | 4 | 7.55 | 0.0369 | 5 | 10.19 | 0.0371 |
| 1 | 10.187 | 0.1101 | 2 | 11.992 | 0.0637 | 3 | 10.191 | 0.0481 | 4 | 8.64 | 0.0386 | 5 | 15.11 | 0.0446 |
| 1 | 14.932 | 0.1195 | 2 | 15.829 | 0.0707 | 3 | 12.467 | 0.0519 | 4 | 9.65 | 0.0406 | 5 | 11.81 | 0.0397 |
| 1 | 12.716 | 0.1154 | 2 | 17.791 | 0.0734 | 3 | 14.904 | 0.0558 | 4 | 10.19 | 0.0415 | 5 | 18.41 | 0.0493 |
| 1 | 17.446 | 0.1236 | 2 | 22.233 | 0.0802 | 3 | 18.114 | 0.0607 | 4 | 12.71 | 0.0455 | 5 | 22.67 | 0.0546 |
| 1 | 21.805 | 0.1284 | 2 | 25.512 | 0.0854 | 3 | 21.242 | 0.0657 | 4 | 15.90 | 0.0503 | 5 | 25.41 | 0.0588 |
| 1 | 26.207 | 0.1329 | 2 | 29.170 | 0.0907 | 3 | 24.731 | 0.0705 | 4 | 17.51 | 0.0531 | 5 | 28.95 | 0.0632 |
| 1 | 30.996 | 0.1387 | 2 | 35.167 | 0.0996 | 3 | 27.586 | 0.0750 | 4 | 24.59 | 0.0628 | 5 | 35.71 | 0.0711 |
| 1 | 35.020 | 0.1432 | 2 | 42.063 | 0.1100 | 3 | 31.253 | 0.0797 | 4 | 28.39 | 0.0682 | 5 | 42.50 | 0.0776 |
| 1 | 40.066 | 0.1490 | | | | 3 | 37.297 | 0.0874 | 4 | 33.75 | 0.0748 | | | |
| 1 | 43.151 | 0.1531 | | | | | | | 4 | 42.18 | 0.0847 | | | |

Table B.14: 5.3% kaolin in water suspension in a 150 mm semi-circular flume

| | |
|-----------------------------|---------|
| Material: | Kaolin |
| Concentration/vol: | 5.3% |
| Density kg/m ³ : | 1088.4 |
| Ty (Pa): | 4.400 |
| k (Pa.s ⁿ): | 0.018 |
| n: | 0.781 |
| Flume width (mm): | 150 |
| Flume Shape | H-Round |

| SLOPE FLUME (degrees) | FLOW Q (L.s ⁻¹) | DEPTH h (m) | SLOPE FLUME (degrees) | FLOW Q (L.s ⁻¹) | DEPTH h (m) | SLOPE FLUME (degrees) | FLOW Q (L.s ⁻¹) | DEPTH h (m) | SLOPE FLUME (degrees) | FLOW Q (L.s ⁻¹) | DEPTH h (m) | SLOPE FLUME (degrees) | FLOW Q (L.s ⁻¹) | DEPTH h (m) |
|-----------------------------|-----------------------------------|-------------------|-----------------------------|-----------------------------------|-------------------|-----------------------------|-----------------------------------|-------------------|-----------------------------|-----------------------------------|-------------------|-----------------------------|-----------------------------------|-------------------|
| 1 | 0.094 | 0.0400 | 2 | 0.129 | 0.0205 | 3 | 0.377 | 0.0157 | 4 | 0.44 | 0.0130 | 5 | 1.10 | 0.0135 |
| 1 | 0.159 | 0.0415 | 2 | 0.154 | 0.0214 | 3 | 0.477 | 0.0163 | 4 | 0.58 | 0.0137 | 5 | 1.45 | 0.0156 |
| 1 | 0.214 | 0.0419 | 2 | 0.401 | 0.0224 | 3 | 0.596 | 0.0167 | 4 | 0.70 | 0.0143 | 5 | 1.95 | 0.0180 |
| 1 | 0.269 | 0.0425 | 2 | 0.296 | 0.0221 | 3 | 0.751 | 0.0173 | 4 | 0.90 | 0.0151 | 5 | 2.90 | 0.0206 |
| 1 | 0.324 | 0.0431 | 2 | 0.425 | 0.0225 | 3 | 0.922 | 0.0178 | 4 | 1.13 | 0.0159 | 5 | 3.09 | 0.0214 |
| 1 | 0.471 | 0.0442 | 2 | 0.470 | 0.0228 | 3 | 1.089 | 0.0185 | 4 | 1.50 | 0.0176 | 5 | 2.18 | 0.0182 |
| 1 | 0.579 | 0.0450 | 2 | 0.599 | 0.0234 | 3 | 1.338 | 0.0196 | 4 | 2.01 | 0.0197 | 5 | 1.52 | 0.0159 |
| 1 | 0.790 | 0.0471 | 2 | 0.697 | 0.0237 | 3 | 1.598 | 0.0210 | 4 | 1.29 | 0.0167 | 5 | 3.50 | 0.0229 |
| 1 | 1.039 | 0.0489 | 2 | 0.794 | 0.0243 | 3 | 1.863 | 0.0223 | 4 | 1.80 | 0.0185 | 5 | 5.31 | 0.0283 |
| 1 | 1.504 | 0.0525 | 2 | 1.031 | 0.0253 | 3 | 2.118 | 0.0234 | 4 | 2.48 | 0.0215 | 5 | 6.55 | 0.0316 |
| 1 | 2.018 | 0.0547 | 2 | 1.538 | 0.0272 | 3 | 2.633 | 0.0252 | 4 | 3.12 | 0.0235 | 5 | 8.07 | 0.0355 |
| 1 | 3.103 | 0.0571 | 2 | 1.256 | 0.0259 | 3 | 3.013 | 0.0266 | 4 | 3.51 | 0.0252 | 5 | 10.08 | 0.0410 |
| 1 | 2.795 | 0.0562 | 2 | 2.029 | 0.0289 | 3 | 4.069 | 0.0304 | 4 | 4.24 | 0.0271 | 5 | 14.73 | 0.0513 |
| 1 | 3.808 | 0.0573 | 2 | 2.594 | 0.0313 | 3 | 5.143 | 0.0342 | 4 | 5.07 | 0.0303 | | | |
| 1 | 4.027 | 0.0579 | 2 | 1.835 | 0.0282 | 3 | 6.985 | 0.0401 | 4 | 6.24 | 0.0336 | | | |
| 1 | 4.554 | 0.0594 | 2 | 3.160 | 0.0327 | 3 | 8.359 | 0.0442 | 4 | 7.08 | 0.0360 | | | |
| 1 | 4.955 | 0.0609 | 2 | 2.845 | 0.0325 | 3 | 10.198 | 0.0494 | 4 | 8.57 | 0.0403 | | | |
| 1 | 5.555 | 0.0623 | 2 | 3.458 | 0.0352 | 3 | 16.611 | 0.0662 | 4 | 10.29 | 0.0220 | | | |
| 1 | 6.642 | 0.0663 | 2 | 4.394 | 0.0380 | 3 | 21.997 | 0.0794 | 4 | 15.17 | 0.0565 | | | |
| 1 | 7.565 | 0.0697 | 2 | 5.075 | 0.0413 | | | | 4 | 21.39 | 0.0704 | | | |
| 1 | 8.651 | 0.0740 | 2 | 7.927 | 0.0513 | | | | | | | | | |
| 1 | 10.074 | 0.0794 | 2 | 10.054 | 0.0576 | | | | | | | | | |
| 1 | 15.511 | 0.0982 | 2 | 15.193 | 0.0727 | | | | | | | | | |
| 1 | 20.435 | 0.1151 | 2 | 19.450 | 0.0848 | | | | | | | | | |
| 1 | 25.306 | 0.1317 | 2 | 23.667 | 0.0968 | | | | | | | | | |

Table B.15: 7.14% kaolin in water suspension in a 150 mm semi-circular flume

| | |
|-----------------------------|---------|
| Material: | Kaolin |
| Concentration/vol: | 7.14% |
| Density kg/m ³ : | 1117.8 |
| Ty (Pa): | 8.100 |
| k (Pa.s ⁿ): | 1.141 |
| n: | 0.320 |
| Flume width (mm): | 150 |
| Flume Shape | H-Round |

| SLOPE | FLOW | DEPTH | SLOPE | FLOW | DEPTH | SLOPE | FLOW | DEPTH | SLOPE | FLOW | DEPTH | SLOPE | FLOW | DEPTH |
|-----------|----------------------|--------|-----------|----------------------|--------|-----------|----------------------|--------|-----------|----------------------|--------|-----------|----------------------|--------|
| FLUME | Q | h | FLUME | Q | h | FLUME | Q | h | FLUME | Q | h | FLUME | Q | h |
| (degrees) | (l.s ⁻¹) | (m) | (degrees) | (l.s ⁻¹) | (m) | (degrees) | (l.s ⁻¹) | (m) | (degrees) | (l.s ⁻¹) | (m) | (degrees) | (l.s ⁻¹) | (m) |
| 1 | 0.999 | 0.0933 | 2 | 1.041 | 0.0547 | 3 | 1.817 | 0.0381 | 4 | 1.28 | 0.0277 | 5 | 1.95 | 0.0250 |
| 1 | 1.475 | 0.0985 | 2 | 1.935 | 0.0594 | 3 | 1.017 | 0.0361 | 4 | 2.14 | 0.0299 | 5 | 2.66 | 0.0269 |
| 1 | 1.883 | 0.1023 | 2 | 2.624 | 0.0608 | 3 | 2.064 | 0.0389 | 4 | 1.79 | 0.0291 | 5 | 2.92 | 0.0280 |
| 1 | 3.102 | 0.1111 | 2 | 3.144 | 0.0633 | 3 | 3.297 | 0.0421 | 4 | 2.81 | 0.0325 | 5 | 3.52 | 0.0299 |
| 1 | 3.595 | 0.1145 | 2 | 3.597 | 0.0641 | 3 | 2.628 | 0.0407 | 4 | 3.34 | 0.0338 | 5 | 4.05 | 0.0313 |
| 1 | 4.532 | 0.1207 | 2 | 4.421 | 0.0645 | 3 | 4.180 | 0.0438 | 4 | 3.83 | 0.0351 | 5 | 4.98 | 0.0340 |
| 1 | 5.498 | 0.1267 | 2 | 4.951 | 0.0653 | 3 | 4.664 | 0.0452 | 4 | 4.40 | 0.0365 | 5 | 5.90 | 0.0365 |
| 1 | 6.817 | 0.1330 | 2 | 5.621 | 0.0665 | 3 | 5.032 | 0.0464 | 4 | 4.94 | 0.0385 | 5 | 7.11 | 0.0396 |
| 1 | 7.863 | 0.1388 | 2 | 6.058 | 0.0675 | 3 | 5.826 | 0.0486 | 4 | 6.29 | 0.0420 | 5 | 8.30 | 0.0426 |
| 1 | 8.987 | 0.1439 | 2 | 6.594 | 0.0686 | 3 | 6.835 | 0.0516 | 4 | 7.11 | 0.0442 | 5 | 10.01 | 0.0469 |
| 1 | 10.072 | 0.1493 | 2 | 7.175 | 0.0702 | 3 | 7.844 | 0.0544 | 4 | 7.91 | 0.0465 | 5 | 12.32 | 0.0520 |
| 1 | 12.258 | 0.1580 | 2 | 7.869 | 0.0721 | 3 | 8.785 | 0.0570 | 4 | 9.45 | 0.0502 | 5 | 15.15 | 0.0583 |
| 1 | 14.994 | 0.1691 | 2 | 9.177 | 0.0756 | 3 | 10.010 | 0.0603 | 4 | 10.24 | 0.0522 | 5 | 18.01 | 0.0645 |
| | | | 2 | 10.126 | 0.0782 | 3 | 11.929 | 0.0650 | 4 | 11.93 | 0.0566 | 5 | 20.26 | 0.0691 |
| | | | 2 | 12.627 | 0.0850 | 3 | 14.075 | 0.0707 | 4 | 14.73 | 0.0633 | 5 | 22.99 | 0.0750 |
| | | | 2 | 12.216 | 0.0840 | 3 | 17.326 | 0.0788 | 4 | 17.22 | 0.0689 | | | |
| | | | 2 | 14.496 | 0.0905 | 3 | 19.659 | 0.0852 | 4 | 20.20 | 0.0759 | | | |
| | | | 2 | 15.746 | 0.0942 | 3 | 22.658 | 0.0922 | 4 | 23.04 | 0.0820 | | | |
| | | | 2 | 17.865 | 0.1000 | | | | | | | | | |
| | | | 2 | 20.264 | 0.1065 | | | | | | | | | |
| | | | 2 | 23.121 | 0.1144 | | | | | | | | | |

Table B.16: 9% kaolin in water suspension in a 150 mm semi-circular flume

| | |
|-----------------------------|---------|
| Material: | Kaolin |
| Concentration/vol: | 9.0% |
| Density kg/m ³ : | 1147.8 |
| Ty (Pa): | 19.000 |
| k (Pa.s ⁿ): | 0.497 |
| n: | 0.472 |
| Flume width (mm): | 150 |
| Flume Shape | H-Round |

| SLOPE | FLOW | DEPTH | SLOPE | FLOW | DEPTH | SLOPE | FLOW | DEPTH | SLOPE | FLOW | DEPTH |
|-----------|----------------------|--------|-----------|----------------------|--------|-----------|----------------------|--------|-----------|----------------------|--------|
| FLUME | Q | h | FLUME | Q | h | FLUME | Q | h | FLUME | Q | h |
| (degrees) | (l.s ⁻¹) | (m) | (degrees) | (l.s ⁻¹) | (m) | (degrees) | (l.s ⁻¹) | (m) | (degrees) | (l.s ⁻¹) | (m) |
| 2 | 2.138 | 0.1139 | 3 | 2.042 | 0.0805 | 4 | 2.14 | 0.0581 | 5 | 2.37 | 0.0460 |
| 2 | 2.707 | 0.1198 | 3 | 3.034 | 0.0848 | 4 | 2.95 | 0.0597 | 5 | 3.31 | 0.0474 |
| 2 | 3.917 | 0.1266 | 3 | 4.074 | 0.0895 | 4 | 3.75 | 0.0616 | 5 | 4.06 | 0.0489 |
| 2 | 5.415 | 0.1349 | 3 | 5.062 | 0.0915 | 4 | 4.91 | 0.0638 | 5 | 4.99 | 0.0506 |
| 2 | 6.664 | 0.1421 | 3 | 6.548 | 0.0937 | 4 | 6.16 | 0.0651 | 5 | 6.02 | 0.0522 |
| 2 | 7.633 | 0.1469 | 3 | 7.838 | 0.0967 | 4 | 7.31 | 0.0671 | 5 | 6.97 | 0.0539 |
| 2 | 8.816 | 0.1524 | 3 | 8.975 | 0.0978 | 4 | 13.85 | 0.0686 | 5 | 7.85 | 0.0556 |
| 2 | 10.045 | 0.1572 | 3 | 9.991 | 0.0986 | 4 | 9.35 | 0.0707 | 5 | 8.77 | 0.0576 |
| 2 | 12.186 | 0.1667 | 3 | 12.195 | 0.1016 | 4 | 10.08 | 0.0722 | 5 | 9.39 | 0.0589 |
| 2 | 15.371 | 0.1859 | 3 | 14.174 | 0.1051 | 4 | 11.55 | 0.0752 | 5 | 10.05 | 0.0604 |
| | | | 3 | 16.127 | 0.1095 | 4 | 13.18 | 0.0785 | 5 | 11.80 | 0.0637 |
| | | | 3 | 18.364 | 0.1146 | 4 | 15.16 | 0.0827 | 5 | 14.08 | 0.0688 |
| | | | 3 | 20.549 | 0.1195 | 4 | 18.02 | 0.0890 | 5 | 16.03 | 0.0728 |
| | | | 3 | 23.805 | 0.1274 | 4 | 20.30 | 0.0945 | 5 | 18.44 | 0.0780 |
| | | | | | | 4 | 24.31 | 0.1036 | 5 | 20.05 | 0.0814 |
| | | | | | | | | | 5 | 25.41 | 0.0926 |

APPENDIX C: Trapezoidal flume data

Table C.1: 4% CMC in water solution in a 150 mm trapezoidal flume

| | |
|-----------------------------|-----------|
| Material: | CMC |
| Concentration/vol: | 4.0% |
| Density kg/m ³ : | 1022.60 |
| Ty (Pa): | 0.000 |
| k (Pa.s): | 0.330 |
| n: | 0.727 |
| Flume base width (mm) | 150 |
| Flume Shape | Trapezoid |

| SLOPE | FLOW | DEPTH | SLOPE | FLOW | DEPTH | SLOPE | FLOW | DEPTH | SLOPE | FLOW | DEPTH | SLOPE | FLOW | DEPTH |
|-----------|----------------------|--------|-----------|----------------------|--------|-----------|----------------------|--------|-----------|----------------------|--------|-----------|----------------------|--------|
| FLUME | Q | h | FLUME | Q | h | FLUME | Q | h | FLUME | Q | h | FLUME | Q | h |
| (degrees) | (l.s ⁻¹) | (m) | (degrees) | (l.s ⁻¹) | (m) | (degrees) | (l.s ⁻¹) | (m) | (degrees) | (l.s ⁻¹) | (m) | (degrees) | (l.s ⁻¹) | (m) |
| 1 | 0.086 | 0.0124 | 2 | 0.088 | 0.0097 | 3 | 0.189 | 0.0101 | 4 | 0.39 | 0.0111 | 5 | 0.50 | 0.0113 |
| 1 | 0.203 | 0.0156 | 2 | 0.184 | 0.0117 | 3 | 0.291 | 0.0114 | 4 | 0.60 | 0.0125 | 5 | 0.61 | 0.0119 |
| 1 | 0.288 | 0.0174 | 2 | 0.284 | 0.0133 | 3 | 0.389 | 0.0124 | 4 | 0.84 | 0.0140 | 5 | 0.70 | 0.0125 |
| 1 | 0.406 | 0.0193 | 2 | 0.395 | 0.0147 | 3 | 0.518 | 0.0134 | 4 | 1.01 | 0.0148 | 5 | 0.90 | 0.0134 |
| 1 | 0.494 | 0.0206 | 2 | 0.485 | 0.0157 | 3 | 0.684 | 0.0146 | 4 | 1.44 | 0.0165 | 5 | 1.03 | 0.0140 |
| 1 | 0.672 | 0.0226 | 2 | 0.744 | 0.0178 | 3 | 0.892 | 0.0159 | 4 | 2.01 | 0.0182 | 5 | 1.95 | 0.0167 |
| 1 | 0.877 | 0.0247 | 2 | 0.874 | 0.0187 | 3 | 1.081 | 0.0169 | 4 | 3.01 | 0.0205 | 5 | 1.44 | 0.0154 |
| 1 | 1.039 | 0.0262 | 2 | 1.125 | 0.0203 | 3 | 1.460 | 0.0185 | 4 | 4.00 | 0.0228 | 5 | 3.04 | 0.0192 |
| 1 | 1.287 | 0.0279 | 2 | 1.457 | 0.0220 | 3 | 2.065 | 0.0206 | 4 | 4.89 | 0.0247 | 5 | 4.06 | 0.0213 |
| 1 | 1.619 | 0.0299 | 2 | 2.016 | 0.0244 | 3 | 3.010 | 0.0231 | 4 | 6.00 | 0.0268 | 5 | 5.17 | 0.0233 |
| 1 | 2.081 | 0.0326 | 2 | 2.483 | 0.0259 | 3 | 4.166 | 0.0258 | 4 | 8.04 | 0.0307 | 5 | 6.25 | 0.0251 |
| 1 | 2.656 | 0.0350 | 2 | 3.475 | 0.0289 | 3 | 6.008 | 0.0301 | 4 | 10.30 | 0.0353 | 5 | 8.05 | 0.0285 |
| 1 | 3.671 | 0.0391 | 2 | 4.498 | 0.0317 | 3 | 8.106 | 0.0346 | 4 | 15.63 | 0.0457 | 5 | 10.30 | 0.0328 |
| 1 | 4.473 | 0.0421 | 2 | 5.378 | 0.0341 | 3 | 10.271 | 0.0395 | 4 | 25.08 | 0.0625 | 5 | 16.16 | 0.0437 |
| 1 | 5.378 | 0.0451 | 2 | 6.817 | 0.0379 | 3 | 15.777 | 0.0515 | 4 | 31.03 | 0.0720 | 5 | 29.52 | 0.0638 |
| 1 | 7.010 | 0.0505 | 2 | 8.534 | 0.0423 | 3 | 21.056 | 0.0621 | 4 | 38.32 | 0.0833 | 5 | 35.64 | 0.0741 |
| 1 | 8.527 | 0.0553 | 2 | 10.147 | 0.0462 | 3 | 28.421 | 0.0755 | 4 | 0.29 | 0.0093 | 5 | 41.13 | 0.0820 |
| 1 | 10.064 | 0.0600 | 2 | 17.023 | 0.0621 | 3 | 38.474 | 0.0925 | 4 | 0.39 | 0.0105 | | | |
| 1 | 16.275 | 0.0780 | 2 | 31.159 | 0.0921 | | | | | | | | | |
| 1 | 20.961 | 0.0904 | 2 | 42.994 | 0.1125 | | | | | | | | | |
| 1 | 29.455 | 0.1107 | | | | | | | | | | | | |
| 1 | 35.456 | 0.1225 | | | | | | | | | | | | |
| 1 | 44.609 | 0.1392 | | | | | | | | | | | | |
| 1 | 44.967 | 0.1390 | | | | | | | | | | | | |

Table C.2: 1.5% CMC in water solution in a 75 mm trapezoidal flume

| | |
|-----------------------------|-----------|
| Material: | CMC |
| Concentration/vol: | 1.5% |
| Density kg/m ³ : | 1008.19 |
| Ty (Pa): | 0.000 |
| k (Pa.s ⁿ): | 0.517 |
| n: | 0.014 |
| Flume base width (mm) | 75 |
| Flume Shape | Trapezoid |

| SLOPE | FLOW | DEPTH | SLOPE | FLOW | DEPTH | SLOPE | FLOW | DEPTH | SLOPE | FLOW | DEPTH | SLOPE | FLOW | DEPTH |
|-----------|----------------------|--------|-----------|----------------------|--------|-----------|----------------------|--------|-----------|----------------------|--------|-----------|----------------------|--------|
| FLUME | Q | h | FLUME | Q | h | FLUME | Q | h | FLUME | Q | h | FLUME | Q | h |
| (degrees) | (L.s ⁻¹) | (m) | (degrees) | (L.s ⁻¹) | (m) | (degrees) | (L.s ⁻¹) | (m) | (degrees) | (L.s ⁻¹) | (m) | (degrees) | (L.s ⁻¹) | (m) |
| 1 | 0.127 | 0.0069 | 2 | 0.135 | 0.0056 | 3 | 0.322 | 0.0063 | 4 | 0.599 | 0.0072 | 5 | 0.62 | 0.0067 |
| 1 | 0.241 | 0.0086 | 2 | 0.211 | 0.0063 | 3 | 0.534 | 0.0076 | 4 | 0.751 | 0.0078 | 5 | 0.81 | 0.0072 |
| 1 | 0.276 | 0.0092 | 2 | 0.263 | 0.0068 | 3 | 0.619 | 0.0081 | 4 | 0.910 | 0.0083 | 5 | 1.09 | 0.0084 |
| 1 | 0.341 | 0.0096 | 2 | 0.304 | 0.0073 | 3 | 0.727 | 0.0085 | 4 | 1.174 | 0.0095 | 5 | 1.54 | 0.0096 |
| 1 | 0.421 | 0.0103 | 2 | 0.432 | 0.0083 | 3 | 0.836 | 0.0091 | 4 | 1.508 | 0.0108 | 5 | 1.51 | 0.0127 |
| 1 | 0.510 | 0.0112 | 2 | 0.521 | 0.0089 | 3 | 0.922 | 0.0098 | 4 | 2.357 | 0.0179 | 5 | 2.14 | 0.0157 |
| 1 | 0.559 | 0.0116 | 2 | 0.610 | 0.0094 | 3 | 1.071 | 0.0104 | 4 | 2.85 | 0.0191 | 5 | 4.90 | 0.0256 |
| 1 | 0.605 | 0.0121 | 2 | 0.709 | 0.0101 | 3 | 1.553 | 0.0124 | 4 | 5.14 | 0.0290 | 5 | 7.84 | 0.0372 |
| 1 | 0.712 | 0.0129 | 2 | 0.817 | 0.0107 | 3 | 2.084 | 0.0150 | 4 | 7.62 | 0.0369 | 5 | 10.13 | 0.0411 |
| 1 | 0.828 | 0.0139 | 2 | 0.918 | 0.0112 | 3 | 3.007 | 0.0234 | 4 | 9.75 | 0.0440 | 5 | 15.85 | 0.0553 |
| 1 | 0.908 | 0.0147 | 2 | 1.454 | 0.0146 | 3 | 4.784 | 0.0316 | 4 | 9.76 | 0.0440 | 5 | 23.69 | 0.0754 |
| 1 | 1.026 | 0.0155 | 2 | 1.316 | 0.0136 | 3 | 5.780 | 0.0350 | 4 | 21.72 | 0.0728 | | | |
| 1 | 1.456 | 0.0186 | 2 | 2.193 | 0.0205 | 3 | 7.666 | 0.0441 | | | | | | |
| 1 | 1.781 | 0.0212 | 2 | 2.778 | 0.0242 | 3 | 9.757 | 0.0494 | | | | | | |
| 1 | 2.324 | 0.0268 | 2 | 4.170 | 0.0325 | 3 | 20.387 | 0.0787 | | | | | | |
| 1 | 3.381 | 0.0354 | 2 | 5.808 | 0.0400 | 3 | 23.248 | 0.0861 | | | | | | |
| 1 | 4.200 | 0.0413 | 2 | 7.822 | 0.0479 | | | | | | | | | |
| 1 | 5.591 | 0.0501 | 2 | 9.755 | 0.0556 | | | | | | | | | |
| 1 | 7.561 | 0.0583 | 2 | 17.428 | 0.0787 | | | | | | | | | |
| 1 | 9.754 | 0.0668 | 2 | 23.744 | 0.0974 | | | | | | | | | |
| 1 | 15.543 | 0.0892 | | | | | | | | | | | | |
| 1 | 20.979 | 0.1092 | | | | | | | | | | | | |

Table C.3: 3% CMC in water solution in a 75 mm trapezoidal flume

| | |
|-----------------------------|-----------|
| Material: | CMC |
| Concentration/vol: | 3.0% |
| Density kg/m ³ : | 1017.50 |
| Ty (Pa): | 0.000 |
| k (Pa.s ⁿ): | 0.517 |
| n: | 0.145 |
| Flume base width (mm) | 75 |
| Flume Shape | Trapezoid |

| SLOPE | FLOW | DEPTH | SLOPE | FLOW | DEPTH | SLOPE | FLOW | DEPTH | SLOPE | FLOW | DEPTH | SLOPE | FLOW | DEPTH |
|-----------|----------------------|--------|-----------|----------------------|--------|-----------|----------------------|--------|-----------|----------------------|--------|-----------|----------------------|--------|
| FLUME | Q | h | FLUME | Q | h | FLUME | Q | h | FLUME | Q | h | FLUME | Q | h |
| (degrees) | (L.s ⁻¹) | (m) | (degrees) | (L.s ⁻¹) | (m) | (degrees) | (L.s ⁻¹) | (m) | (degrees) | (L.s ⁻¹) | (m) | (degrees) | (L.s ⁻¹) | (m) |
| 1 | 0.109 | 0.0124 | 2 | 0.111 | 0.0097 | 3 | 0.158 | 0.0091 | 4 | 0.126 | 0.0078 | 5 | 0.28 | 0.0088 |
| 1 | 0.205 | 0.0152 | 2 | 0.204 | 0.0113 | 3 | 0.247 | 0.0106 | 4 | 0.211 | 0.0087 | 5 | 0.34 | 0.0093 |
| 1 | 0.308 | 0.0170 | 2 | 0.293 | 0.0126 | 3 | 0.348 | 0.0115 | 4 | 0.317 | 0.0099 | 5 | 0.45 | 0.0101 |
| 1 | 0.411 | 0.0187 | 2 | 0.403 | 0.0140 | 3 | 0.450 | 0.0126 | 4 | 0.414 | 0.0109 | 5 | 0.59 | 0.0111 |
| 1 | 0.503 | 0.0201 | 2 | 0.501 | 0.0151 | 3 | 0.641 | 0.0140 | 4 | 0.511 | 0.0116 | 5 | 0.75 | 0.0119 |
| 1 | 0.717 | 0.0229 | 2 | 0.634 | 0.0164 | 3 | 0.832 | 0.0154 | 4 | 0.608 | 0.0122 | 5 | 0.91 | 0.0129 |
| 1 | 0.937 | 0.0254 | 2 | 0.822 | 0.0179 | 3 | 1.041 | 0.0166 | 4 | 0.72 | 0.0130 | 5 | 1.02 | 0.0134 |
| 1 | 1.214 | 0.0279 | 2 | 0.975 | 0.0190 | 3 | 1.300 | 0.0180 | 4 | 0.85 | 0.0138 | 5 | 1.29 | 0.0145 |
| 1 | 1.566 | 0.0306 | 2 | 1.300 | 0.0212 | 3 | 1.602 | 0.0197 | 4 | 1.04 | 0.0148 | 5 | 1.43 | 0.0152 |
| 1 | 2.258 | 0.0353 | 2 | 1.654 | 0.0235 | 3 | 2.112 | 0.0220 | 4 | 1.26 | 0.0156 | 5 | 1.53 | 0.0156 |
| 1 | 3.068 | 0.0403 | 2 | 2.220 | 0.0264 | 3 | 3.056 | 0.0262 | 4 | 1.52 | 0.0172 | 5 | 1.73 | 0.0164 |
| 1 | 4.097 | 0.0467 | 2 | 3.087 | 0.0309 | 3 | 4.077 | 0.0309 | 4 | 1.81 | 0.0183 | 5 | 2.12 | 0.0179 |
| 1 | 5.246 | 0.0532 | 2 | 4.075 | 0.0365 | 3 | 5.143 | 0.0351 | 4 | 2.09 | 0.0195 | 5 | 2.53 | 0.0194 |
| 1 | 6.129 | 0.0580 | 2 | 5.056 | 0.0408 | 3 | 8.097 | 0.0470 | 4 | 2.52 | 0.0213 | 5 | 2.91 | 0.0207 |
| 1 | 8.072 | 0.0683 | 2 | 6.680 | 0.0480 | 3 | 10.186 | 0.0540 | 4 | 3.02 | 0.0231 | 5 | 3.36 | 0.0223 |
| 1 | 10.096 | 0.0774 | 2 | 7.979 | 0.0532 | 3 | 19.171 | 0.0787 | 4 | 4.05 | 0.0271 | 5 | 3.97 | 0.0246 |
| 1 | 20.032 | 0.1176 | 2 | 10.165 | 0.0615 | 3 | 25.179 | 0.0928 | 4 | 5.02 | 0.0310 | 5 | 4.84 | 0.0275 |
| 1 | 13.120 | 0.0866 | 2 | 14.756 | 0.0755 | 3 | 1.884 | 0.0208 | 4 | 6.14 | 0.0348 | 5 | 6.11 | 0.0316 |
| | | | 2 | 19.735 | 0.0907 | 3 | 2.471 | 0.0238 | 4 | 8.08 | 0.0419 | 5 | 7.63 | 0.0364 |
| | | | 2 | 21.653 | 0.0961 | 3 | 14.878 | 0.0672 | 4 | 10.03 | 0.0479 | 5 | 10.10 | 0.0438 |
| | | | | | | | | | 4 | 12.09 | 0.0535 | 5 | 13.94 | 0.0537 |
| | | | | | | | | | 4 | 16.04 | 0.0642 | 5 | 21.05 | 0.0705 |
| | | | | | | | | | 4 | 19.63 | 0.0727 | 5 | 27.17 | 0.0834 |

Table C.4: 4% CMC in water solution in a 75 mm trapezoidal flume

| | |
|-----------------------------|-----------|
| Material: | CMC |
| Concentration/vol: | 4.0% |
| Density kg/m ³ : | 1022.80 |
| Ty (Pa): | 0.000 |
| k (Pa.s ²): | 0.330 |
| n: | 0.727 |
| Flume base width (mm) | 75 |
| Flume Shape | Trapezoid |

| SLOPE | FLOW | DEPTH | SLOPE | FLOW | DEPTH | SLOPE | FLOW | DEPTH | SLOPE | FLOW | DEPTH | SLOPE | FLOW | DEPTH |
|-----------|----------------------|--------|-----------|----------------------|--------|-----------|----------------------|--------|-----------|----------------------|--------|-----------|----------------------|--------|
| FLUME | Q | h | FLUME | Q | h | FLUME | Q | h | FLUME | Q | h | FLUME | Q | h |
| (degrees) | (L.s ⁻¹) | (m) | (degrees) | (L.s ⁻¹) | (m) | (degrees) | (L.s ⁻¹) | (m) | (degrees) | (L.s ⁻¹) | (m) | (degrees) | (L.s ⁻¹) | (m) |
| 1 | 0.173 | 0.0191 | 2 | 0.096 | 0.0119 | 3 | 0.143 | 0.0113 | 4 | 0.16 | 0.0104 | 5 | 0.17 | 0.0097 |
| 1 | 0.206 | 0.0199 | 2 | 0.194 | 0.0148 | 3 | 0.197 | 0.0126 | 4 | 0.20 | 0.0111 | 5 | 0.20 | 0.0103 |
| 1 | 0.344 | 0.0237 | 2 | 0.300 | 0.0167 | 3 | 0.294 | 0.0143 | 4 | 0.29 | 0.0125 | 5 | 0.39 | 0.0124 |
| 1 | 0.498 | 0.0267 | 2 | 0.397 | 0.0184 | 3 | 0.391 | 0.0154 | 4 | 0.39 | 0.0137 | 5 | 0.49 | 0.0134 |
| 1 | 0.605 | 0.0286 | 2 | 0.490 | 0.0197 | 3 | 0.498 | 0.0167 | 4 | 0.49 | 0.0146 | 5 | 0.59 | 0.0143 |
| 1 | 0.803 | 0.0311 | 2 | 0.595 | 0.0210 | 3 | 0.593 | 0.0176 | 4 | 0.59 | 0.0156 | 5 | 0.70 | 0.0151 |
| 1 | 0.981 | 0.0334 | 2 | 0.704 | 0.0222 | 3 | 0.703 | 0.0186 | 4 | 0.71 | 0.0164 | 5 | 0.81 | 0.0158 |
| 1 | 1.220 | 0.0360 | 2 | 0.810 | 0.0233 | 3 | 0.800 | 0.0195 | 4 | 0.84 | 0.0175 | 5 | 1.05 | 0.0170 |
| 1 | 1.403 | 0.0378 | 2 | 1.048 | 0.0253 | 3 | 1.005 | 0.0209 | 4 | 1.07 | 0.0188 | 5 | 1.49 | 0.0192 |
| 1 | 1.992 | 0.0430 | 2 | 1.436 | 0.0284 | 3 | 1.504 | 0.0240 | 4 | 1.43 | 0.0208 | 5 | 2.00 | 0.0213 |
| 1 | 2.525 | 0.0464 | 2 | 2.079 | 0.0324 | 3 | 2.001 | 0.0264 | 4 | 2.00 | 0.0233 | 5 | 2.55 | 0.0234 |
| 1 | 3.140 | 0.0506 | 2 | 2.524 | 0.0350 | 3 | 2.490 | 0.0291 | 4 | 3.05 | 0.0276 | 5 | 3.56 | 0.0270 |
| 1 | 3.911 | 0.0552 | 2 | 3.427 | 0.0392 | 3 | 3.515 | 0.0331 | 4 | 4.04 | 0.0315 | 5 | 4.52 | 0.0304 |
| 1 | 4.757 | 0.0592 | 2 | 5.427 | 0.0485 | 3 | 4.515 | 0.0376 | 4 | 5.00 | 0.0352 | 5 | 5.53 | 0.0336 |
| 1 | 5.392 | 0.0633 | 2 | 5.063 | 0.0470 | 3 | 5.509 | 0.0416 | 4 | 6.09 | 0.0389 | 5 | 7.05 | 0.0380 |
| 1 | 6.601 | 0.0690 | 2 | 6.500 | 0.0533 | 3 | 6.978 | 0.0475 | 4 | 7.56 | 0.0435 | 5 | 8.49 | 0.0424 |
| 1 | 8.089 | 0.0762 | 2 | 8.055 | 0.0597 | 3 | 8.032 | 0.0511 | 4 | 10.32 | 0.0517 | 5 | 10.30 | 0.0478 |
| 1 | 10.035 | 0.0855 | 2 | 10.023 | 0.0673 | 3 | 10.030 | 0.0578 | 4 | 13.88 | 0.0623 | 5 | 13.48 | 0.0571 |
| 1 | 16.306 | 0.1133 | 2 | 16.638 | 0.0893 | 3 | 14.579 | 0.0706 | 4 | 19.67 | 0.0766 | 5 | 16.38 | 0.0633 |
| 1 | 19.957 | 0.1292 | 2 | 19.732 | 0.0992 | 3 | 18.761 | 0.0822 | 4 | 21.53 | 0.0812 | 5 | 20.51 | 0.0732 |
| 1 | 22.546 | 0.1395 | 2 | 23.716 | 0.1123 | 3 | 21.380 | 0.0897 | 4 | 25.37 | 0.0898 | 5 | 26.46 | 0.0843 |
| | | | | | | 3 | 24.686 | 0.0982 | | | | | | |

Table C.5: 1.5% CMC in water solution in a 150 mm trapezoidal flume

| | |
|-----------------------------|-----------|
| Material: | CMC |
| Concentration/vol: | 1.5% |
| Density kg/m ³ : | 1008.32 |
| Ty (Pa): | 0.000 |
| k (Pa.s ²): | 0.014 |
| n: | 0.944 |
| Flume base width (mm) | 150 |
| Flume Shape | Trapezoid |

| SLOPE | FLOW | DEPTH | SLOPE | FLOW | DEPTH | SLOPE | FLOW | DEPTH | SLOPE | FLOW | DEPTH | SLOPE | FLOW | DEPTH |
|-----------|----------------------|--------|-----------|----------------------|--------|-----------|----------------------|--------|-----------|----------------------|--------|-----------|----------------------|--------|
| FLUME | Q | h | FLUME | Q | h | FLUME | Q | h | FLUME | Q | h | FLUME | Q | h |
| (degrees) | (L.s ⁻¹) | (m) | (degrees) | (L.s ⁻¹) | (m) | (degrees) | (L.s ⁻¹) | (m) | (degrees) | (L.s ⁻¹) | (m) | (degrees) | (L.s ⁻¹) | (m) |
| 1 | 0.163 | 0.0060 | 2 | 0.132 | 0.0043 | 3 | 0.276 | 0.0048 | 4 | 0.470 | 0.0049 | 5 | 0.56 | 0.0050 |
| 1 | 0.207 | 0.0065 | 2 | 0.223 | 0.0052 | 3 | 0.352 | 0.0053 | 4 | 0.535 | 0.0054 | 5 | 0.68 | 0.0053 |
| 1 | 0.270 | 0.0071 | 2 | 0.310 | 0.0058 | 3 | 0.429 | 0.0056 | 4 | 0.602 | 0.0056 | 5 | 0.87 | 0.0058 |
| 1 | 0.317 | 0.0075 | 2 | 0.423 | 0.0066 | 3 | 0.586 | 0.0062 | 4 | 0.814 | 0.0061 | 5 | 1.08 | 0.0063 |
| 1 | 0.364 | 0.0078 | 2 | 0.520 | 0.0070 | 3 | 0.751 | 0.0067 | 4 | 0.923 | 0.0064 | 5 | 1.33 | 0.0066 |
| 1 | 0.464 | 0.0085 | 2 | 0.743 | 0.0077 | 3 | 0.848 | 0.0072 | 4 | 1.052 | 0.0067 | 5 | 1.54 | 0.0072 |
| 1 | 0.554 | 0.0090 | 2 | 0.950 | 0.0085 | 3 | 1.106 | 0.0078 | 4 | 3.11 | 0.0146 | 5 | 2.06 | 0.0097 |
| 1 | 0.615 | 0.0094 | 2 | 1.565 | 0.0102 | 3 | 2.271 | 0.0110 | 4 | 4.82 | 0.0191 | 5 | 3.41 | 0.0128 |
| 1 | 0.714 | 0.0099 | 2 | 2.064 | 0.0120 | 3 | 3.138 | 0.0144 | 4 | 7.60 | 0.0244 | 5 | 4.85 | 0.0160 |
| 1 | 0.827 | 0.0103 | 2 | 2.994 | 0.0156 | 3 | 4.013 | 0.0186 | 4 | 10.14 | 0.0304 | 5 | 7.74 | 0.0221 |
| 1 | 0.936 | 0.0108 | 2 | 3.930 | 0.0191 | 3 | 5.765 | 0.0224 | 4 | 17.15 | 0.0436 | 5 | 10.13 | 0.0268 |
| 1 | 1.438 | 0.0128 | 2 | 6.024 | 0.0261 | 3 | 7.794 | 0.0281 | 4 | 30.79 | 0.0661 | 5 | 15.43 | 0.0380 |
| 1 | 1.838 | 0.0144 | 2 | 8.024 | 0.0315 | 3 | 10.252 | 0.0338 | 4 | 43.14 | 0.0837 | 5 | 29.95 | 0.0588 |
| 1 | 2.209 | 0.0160 | 2 | 10.114 | 0.0366 | 3 | 18.732 | 0.0505 | 4 | 0.42 | 0.0045 | 5 | 43.55 | 0.0789 |
| 1 | 2.948 | 0.0186 | 2 | 16.718 | 0.0532 | 3 | 25.098 | 0.0629 | 4 | 0.48 | 0.0048 | | | |
| 1 | 3.511 | 0.0231 | 2 | 25.562 | 0.0719 | 3 | 41.860 | 0.0894 | | | | | | |
| 1 | 4.510 | 0.0277 | 2 | 39.995 | 0.0966 | | | | | | | | | |
| 1 | 5.997 | 0.0336 | | | | | | | | | | | | |
| 1 | 7.907 | 0.0406 | | | | | | | | | | | | |
| 1 | 10.105 | 0.0473 | | | | | | | | | | | | |
| 1 | 17.084 | 0.0664 | | | | | | | | | | | | |
| 1 | 22.740 | 0.0798 | | | | | | | | | | | | |
| 1 | 44.691 | 0.1248 | | | | | | | | | | | | |

Table C.6: 3% CMC in water solution in a 150 mm trapezoidal flume

| | |
|-----------------------------|-----------|
| Material: | CMC |
| Concentration/vol: | 3.0% |
| Density kg/m ³ : | 1017.49 |
| Ty (Pa): | 0.000 |
| k (Pa.s ⁿ): | 0.126 |
| n: | 0.780 |
| Flume base width (mm) | 150 |
| Flume Shape | Trapezoid |

| SLOPE | FLOW | DEPTH | SLOPE | FLOW | DEPTH | SLOPE | FLOW | DEPTH | SLOPE | FLOW | DEPTH | SLOPE | FLOW | DEPTH |
|-----------|----------------------|--------|-----------|----------------------|--------|-----------|----------------------|--------|-----------|----------------------|--------|-----------|----------------------|--------|
| FLUME | Q | h | FLUME | Q | h | FLUME | Q | h | FLUME | Q | h | FLUME | Q | h |
| (degrees) | (l.s ⁻¹) | (m) | (degrees) | (l.s ⁻¹) | (m) | (degrees) | (l.s ⁻¹) | (m) | (degrees) | (l.s ⁻¹) | (m) | (degrees) | (l.s ⁻¹) | (m) |
| 1 | 0.107 | 0.0097 | 2 | 0.092 | 0.0068 | 3 | 0.098 | 0.0061 | 4 | 0.527 | 0.0089 | 5 | 1.49 | 0.0114 |
| 1 | 0.196 | 0.0112 | 2 | 0.145 | 0.0079 | 3 | 0.194 | 0.0074 | 4 | 0.652 | 0.0096 | 5 | 2.03 | 0.0126 |
| 1 | 0.309 | 0.0129 | 2 | 0.214 | 0.0089 | 3 | 0.335 | 0.0088 | 4 | 0.820 | 0.0103 | 5 | 3.08 | 0.0145 |
| 1 | 0.403 | 0.0141 | 2 | 0.308 | 0.0099 | 3 | 0.437 | 0.0095 | 4 | 1.003 | 0.0110 | 5 | 4.98 | 0.0182 |
| 1 | 0.608 | 0.0161 | 2 | 0.409 | 0.0108 | 3 | 0.608 | 0.0105 | 4 | 1.530 | 0.0126 | 5 | 7.04 | 0.0222 |
| 1 | 0.815 | 0.0176 | 2 | 0.493 | 0.0115 | 3 | 0.808 | 0.0116 | 4 | 2.048 | 0.0138 | 5 | 9.99 | 0.0273 |
| 1 | 1.047 | 0.0188 | 2 | 0.670 | 0.0127 | 3 | 1.106 | 0.0127 | 4 | 3.187 | 0.0161 | 5 | 20.19 | 0.0444 |
| 1 | 1.577 | 0.0215 | 2 | 0.842 | 0.0135 | 3 | 2.318 | 0.0161 | 4 | 5.073 | 0.0200 | 5 | 30.04 | 0.0593 |
| 1 | 2.090 | 0.0238 | 2 | 1.053 | 0.0146 | 3 | 3.159 | 0.0180 | 4 | 7.146 | 0.0246 | 5 | 40.16 | 0.0718 |
| 1 | 2.303 | 0.0247 | 2 | 1.310 | 0.0158 | 3 | 5.023 | 0.0222 | 4 | 31.33 | 0.0665 | | | |
| 1 | 2.917 | 0.0271 | 2 | 1.637 | 0.0168 | 3 | 7.269 | 0.0274 | 4 | 0.78 | 0.0092 | | | |
| 1 | 4.377 | 0.0326 | 2 | 2.340 | 0.0191 | 3 | 10.056 | 0.0336 | 4 | 1.02 | 0.0103 | | | |
| 1 | 5.717 | 0.0377 | 2 | 2.919 | 0.0204 | 3 | 17.512 | 0.0489 | | | | | | |
| 1 | 7.452 | 0.0443 | 2 | 4.450 | 0.0247 | 3 | 27.723 | 0.0674 | | | | | | |
| 1 | 9.446 | 0.0516 | 2 | 5.942 | 0.0287 | 3 | 37.272 | 0.0829 | | | | | | |
| 1 | 21.012 | 0.0802 | 2 | 10.247 | 0.0398 | | | | | | | | | |
| 1 | 27.352 | 0.0956 | 2 | 21.025 | 0.0641 | | | | | | | | | |
| 1 | 42.648 | 0.1258 | 2 | 39.095 | 0.0975 | | | | | | | | | |
| 1 | 44.918 | 0.1285 | 2 | 41.556 | 0.1017 | | | | | | | | | |

Table C.7: 4.6% Bentonite in water suspension in a 75 mm trapezoidal flume

| | |
|-----------------------------|-----------|
| Material: | Bentonite |
| Concentration/vol: | 4.6% |
| Density kg/m ³ : | 1028.10 |
| Ty (Pa): | 5.697 |
| k (Pa.s ⁿ): | 0.010 |
| n: | 1.000 |
| Flume base width (mm) | 75 |
| Flume Shape | Trapezoid |

| SLOPE | FLOW | DEPTH | SLOPE | FLOW | DEPTH | SLOPE | FLOW | DEPTH | SLOPE | FLOW | DEPTH | SLOPE | FLOW | DEPTH |
|-----------|----------------------|--------|-----------|----------------------|--------|-----------|----------------------|--------|-----------|----------------------|--------|-----------|----------------------|--------|
| FLUME | Q | h | FLUME | Q | h | FLUME | Q | h | FLUME | Q | h | FLUME | Q | h |
| (degrees) | (l.s ⁻¹) | (m) | (degrees) | (l.s ⁻¹) | (m) | (degrees) | (l.s ⁻¹) | (m) | (degrees) | (l.s ⁻¹) | (m) | (degrees) | (l.s ⁻¹) | (m) |
| 1 | 0.592 | 0.0520 | 2 | 0.649 | 0.0223 | 3 | 0.640 | 0.0152 | 4 | 0.49 | 0.0117 | 5 | 0.70 | 0.0104 |
| 1 | 0.680 | 0.0537 | 2 | 0.818 | 0.0235 | 3 | 0.924 | 0.0167 | 4 | 0.73 | 0.0130 | 5 | 0.88 | 0.0114 |
| 1 | 1.024 | 0.0555 | 2 | 1.235 | 0.0251 | 3 | 1.221 | 0.0186 | 4 | 1.05 | 0.0148 | 5 | 1.25 | 0.0120 |
| 1 | 1.391 | 0.0557 | 2 | 1.711 | 0.0274 | 3 | 1.584 | 0.0204 | 4 | 1.29 | 0.0154 | 5 | 1.05 | 0.0114 |
| 1 | 1.742 | 0.0575 | 2 | 2.235 | 0.0297 | 3 | 1.908 | 0.0219 | 4 | 1.77 | 0.0168 | 5 | 1.56 | 0.0137 |
| 1 | 2.494 | 0.0575 | 2 | 2.707 | 0.0307 | 3 | 2.172 | 0.0224 | 4 | 2.20 | 0.0187 | 5 | 1.85 | 0.0148 |
| 1 | 2.990 | 0.0534 | 2 | 4.090 | 0.0363 | 3 | 2.647 | 0.0241 | 4 | 2.74 | 0.0209 | 5 | 1.94 | 0.0151 |
| 1 | 3.561 | 0.0576 | 2 | 5.200 | 0.0409 | 3 | 3.135 | 0.0251 | 4 | 3.08 | 0.0214 | 5 | 2.28 | 0.0160 |
| 1 | 4.125 | 0.0595 | 2 | 5.652 | 0.0426 | 3 | 3.593 | 0.0270 | 4 | 3.81 | 0.0228 | 5 | 2.57 | 0.0172 |
| 1 | 4.986 | 0.0619 | 2 | 6.525 | 0.0453 | 3 | 4.176 | 0.0293 | 4 | 5.68 | 0.0313 | 5 | 2.98 | 0.0189 |
| 1 | 6.008 | 0.0655 | 2 | 7.462 | 0.0489 | 3 | 4.678 | 0.0311 | 4 | 3.78 | 0.0236 | 5 | 3.51 | 0.0207 |
| 1 | 7.320 | 0.0697 | 2 | 9.932 | 0.0574 | 3 | 5.545 | 0.0345 | 4 | 6.41 | 0.0338 | 5 | 4.04 | 0.0224 |
| 1 | 8.473 | 0.0735 | 2 | 12.383 | 0.0649 | 3 | 6.627 | 0.0380 | 4 | 7.97 | 0.0389 | 5 | 5.01 | 0.0252 |
| 1 | 9.377 | 0.0753 | 2 | 17.166 | 0.0784 | 3 | 8.078 | 0.0431 | 4 | 9.52 | 0.0439 | 5 | 6.04 | 0.0300 |
| 1 | 10.146 | 0.0784 | 2 | 21.896 | 0.0901 | 3 | 10.18 | 0.0496 | 4 | 13.51 | 0.0523 | 5 | 8.20 | 0.0365 |
| 1 | 13.627 | 0.0904 | | | | 3 | 13.30 | 0.0581 | 4 | 19.61 | 0.0667 | 5 | 10.16 | 0.0405 |
| 1 | 16.144 | 0.0966 | | | | 3 | 19.44 | 0.0734 | | | | 5 | 10.15 | 0.0405 |
| 1 | 20.920 | 0.1115 | | | | 3 | 24.08 | 0.0836 | | | | 5 | 12.95 | 0.0474 |
| 1 | 23.585 | 0.1186 | | | | | | | | | | 5 | 16.92 | 0.0567 |
| | | | | | | | | | | | | 5 | 21.63 | 0.0664 |
| | | | | | | | | | | | | 5 | 25.77 | 0.0735 |

Table C.8: 6.2% Bentonite in water suspension in a 75 mm trapezoidal flume

| | |
|-----------------------------|-----------|
| Material: | Bentonite |
| Concentration/vol: | 6.2% |
| Density kg/m ³ : | 1038.00 |
| Ty (Pa): | 15.777 |
| k (Pa.s ⁿ): | 0.006 |
| n: | 1.000 |
| Flume base width (mm) | 75 |
| Flume Shape | Trapezoid |

| SLOPE | FLOW | DEPTH | SLOPE | FLOW | DEPTH | SLOPE | FLOW | DEPTH | SLOPE | FLOW | DEPTH |
|-----------|----------------------|--------|-----------|----------------------|--------|-----------|----------------------|--------|-----------|----------------------|--------|
| FLUME | Q | h | FLUME | Q | h | FLUME | Q | h | FLUME | Q | h |
| (degrees) | (l.s ⁻¹) | (m) | (degrees) | (l.s ⁻¹) | (m) | (degrees) | (l.s ⁻¹) | (m) | (degrees) | (l.s ⁻¹) | (m) |
| 2 | 1.795 | 0.1182 | 3 | 0.985 | 0.0656 | 4 | 1.005 | 0.0446 | 5 | 0.92 | 0.0314 |
| 2 | 2.654 | 0.1210 | 3 | 2.523 | 0.0669 | 4 | 2.105 | 0.0466 | 5 | 1.49 | 0.0334 |
| 2 | 3.579 | 0.1235 | 3 | 1.642 | 0.0657 | 4 | 1.380 | 0.0446 | 5 | 2.10 | 0.0355 |
| 2 | 4.574 | 0.1034 | 3 | 2.880 | 0.0697 | 4 | 3.037 | 0.0492 | 5 | 3.06 | 0.0374 |
| 2 | 5.795 | 0.1267 | 3 | 3.993 | 0.0716 | 4 | 4.001 | 0.0503 | 5 | 4.05 | 0.0392 |
| 2 | 5.795 | 0.1267 | 3 | 5.120 | 0.0730 | 4 | 5.203 | 0.0515 | 5 | 5.00 | 0.0413 |
| 2 | 6.956 | 0.1310 | 3 | 6.165 | 0.0723 | 4 | 6.105 | 0.0532 | 5 | 6.14 | 0.0434 |
| 2 | 8.102 | 0.1313 | 3 | 7.121 | 0.0728 | 4 | 7.134 | 0.0551 | 5 | 7.10 | 0.0456 |
| 2 | 10.037 | 0.1305 | 3 | 8.023 | 0.0731 | 4 | 8.153 | 0.0573 | 5 | 8.10 | 0.0474 |
| 2 | 11.647 | 0.1349 | 3 | 9.084 | 0.0743 | 4 | 10.147 | 0.0609 | 5 | 9.01 | 0.0499 |
| 2 | 12.650 | 0.1437 | 3 | 10.073 | 0.0761 | 4 | 11.836 | 0.0649 | 5 | 10.16 | 0.0524 |
| 2 | 13.829 | 0.1434 | 3 | 12.083 | 0.0802 | 4 | 14.427 | 0.0707 | 5 | 12.78 | 0.0582 |
| 2 | 16.140 | 0.1428 | 3 | 14.336 | 0.0848 | 4 | 17.459 | 0.0775 | 5 | 15.91 | 0.0653 |
| 2 | 17.949 | 0.1468 | 3 | 16.951 | 0.0910 | 4 | 21.313 | 0.0861 | 5 | 23.75 | 0.0811 |
| 2 | 19.978 | 0.1492 | 3 | 19.300 | 0.0967 | 4 | 23.736 | 0.0909 | | | |
| 2 | 22.564 | 0.1560 | 3 | 21.587 | 0.1015 | | | | | | |
| | | | 3 | 23.844 | 0.1072 | | | | | | |

Table C.9: 4.6% Bentonite in water suspension in a 150 mm trapezoidal flume

| | |
|-----------------------------|-----------|
| Material: | Bentonite |
| Concentration/vol: | 4.6% |
| Density kg/m ³ : | 1028.20 |
| Ty (Pa): | 4.680 |
| k (Pa.s ⁿ): | 0.003 |
| n: | 1.000 |
| Flume base width (mm) | 150 |
| Flume Shape | Trapezoid |

| SLOPE | FLOW | DEPTH | SLOPE | FLOW | DEPTH | SLOPE | FLOW | DEPTH | SLOPE | FLOW | DEPTH | SLOPE | FLOW | DEPTH |
|-----------|----------------------|--------|-----------|----------------------|--------|-----------|----------------------|--------|-----------|----------------------|--------|-----------|----------------------|--------|
| FLUME | Q | h | FLUME | Q | h | FLUME | Q | h | FLUME | Q | h | FLUME | Q | h |
| (degrees) | (l.s ⁻¹) | (m) | (degrees) | (l.s ⁻¹) | (m) | (degrees) | (l.s ⁻¹) | (m) | (degrees) | (l.s ⁻¹) | (m) | (degrees) | (l.s ⁻¹) | (m) |
| 1 | 0.645 | 0.0351 | 2 | 0.585 | 0.0156 | 3 | 0.617 | 0.0116 | 4 | 0.59 | 0.0090 | 5 | 1.18 | 0.0088 |
| 1 | 0.806 | 0.0351 | 2 | 0.793 | 0.0161 | 3 | 0.809 | 0.0117 | 4 | 1.03 | 0.0098 | 5 | 0.65 | 0.0081 |
| 1 | 1.049 | 0.0399 | 2 | 1.043 | 0.0168 | 3 | 1.027 | 0.0122 | 4 | 0.78 | 0.0096 | 5 | 0.88 | 0.0085 |
| 1 | 1.214 | 0.0404 | 2 | 1.403 | 0.0175 | 3 | 1.49 | 0.0131 | 4 | 1.39 | 0.0107 | 5 | 1.34 | 0.0097 |
| 1 | 1.357 | 0.0403 | 2 | 1.796 | 0.0192 | 3 | 2.07 | 0.0148 | 4 | 1.53 | 0.0113 | 5 | 1.53 | 0.0102 |
| 1 | 1.905 | 0.0412 | 2 | 2.290 | 0.0198 | 3 | 2.32 | 0.0152 | 4 | 1.81 | 0.0117 | 5 | 2.13 | 0.0111 |
| 1 | 2.631 | 0.0415 | 2 | 2.826 | 0.0199 | 3 | 2.58 | 0.0150 | 4 | 1.99 | 0.0120 | 5 | 1.82 | 0.0107 |
| 1 | 3.039 | 0.0375 | 2 | 3.501 | 0.0217 | 3 | 1.76 | 0.0137 | 4 | 0.95 | 0.0106 | 5 | 2.63 | 0.0120 |
| 1 | 3.814 | 0.0394 | 2 | 4.107 | 0.0236 | 3 | 2.99 | 0.0163 | 4 | 1.39 | 0.0117 | 5 | 3.09 | 0.0128 |
| 1 | 5.007 | 0.0412 | 2 | 4.563 | 0.0241 | 3 | 4.12 | 0.0188 | 4 | 2.47 | 0.0135 | 5 | 4.30 | 0.0145 |
| 1 | 6.181 | 0.0451 | 2 | 5.244 | 1.0000 | 3 | 5.03 | 0.0207 | 4 | 3.12 | 0.0147 | 5 | 5.01 | 0.0163 |
| 1 | 7.180 | 0.0472 | 2 | 6.240 | 0.0286 | 3 | 6.19 | 0.0229 | 4 | 3.94 | 0.0160 | 5 | 6.17 | 0.0178 |
| 1 | 8.033 | 0.0486 | 2 | 7.064 | 0.0309 | 3 | 7.20 | 0.0253 | 4 | 5.10 | 0.0180 | 5 | 8.24 | 0.0216 |
| 1 | 9.977 | 0.0532 | 2 | 8.044 | 0.0333 | 3 | 8.07 | 0.0271 | 4 | 6.13 | 0.0202 | 5 | 10.15 | 0.0252 |
| 1 | 12.575 | 0.0597 | 2 | 9.988 | 0.0376 | 3 | 9.83 | 0.0307 | 4 | 8.08 | 0.0240 | 5 | 12.71 | 0.0294 |
| 1 | 15.058 | 0.0650 | 2 | 12.213 | 0.0419 | 3 | 12.11 | 0.0353 | 4 | 10.06 | 0.0276 | 5 | 17.59 | 0.0374 |
| 1 | 20.047 | 0.0765 | 2 | 15.088 | 0.0486 | 3 | 15.57 | 0.0420 | 4 | 13.14 | 0.0330 | 5 | 22.84 | 0.0463 |
| 1 | 26.220 | 0.0900 | 2 | 19.935 | 0.0582 | 3 | 20.34 | 0.0508 | 4 | 16.64 | 0.0391 | 5 | 30.43 | 0.0560 |
| 1 | 32.134 | 0.1011 | 2 | 25.364 | 0.0679 | 3 | 30.68 | 0.0687 | 4 | 22.69 | 0.0490 | | | |
| 1 | 40.205 | 0.1141 | 2 | 30.287 | 0.0773 | 3 | 40.00 | 0.0826 | 4 | 30.32 | 0.0619 | | | |
| | | | 2 | 39.882 | 0.0934 | | | | | | | | | |

Table C.10: 6.2% Bentonite in water suspension in a 150 mm trapezoidal flume

| | |
|-----------------------------|-----------|
| Material: | Bentonite |
| Concentration/vol: | 6.2% |
| Density kg/m ³ : | 1041.60 |
| Ty (Pa): | 18.340 |
| k (Pa.s ⁿ): | 0.008 |
| n: | 1.000 |
| Flume base width (mm) | 150 |
| Flume Shape | Trapezoid |

| SLOPE | FLOW | DEPTH | SLOPE | FLOW | DEPTH | SLOPE | FLOW | DEPTH | SLOPE | FLOW | DEPTH |
|-----------|----------------------|--------|-----------|----------------------|--------|-----------|----------------------|--------|-----------|----------------------|--------|
| FLUME | Q | h | FLUME | Q | h | FLUME | Q | h | FLUME | Q | h |
| (degrees) | (l.s ⁻¹) | (m) | (degrees) | (l.s ⁻¹) | (m) | (degrees) | (l.s ⁻¹) | (m) | (degrees) | (l.s ⁻¹) | (m) |
| 2 | 4.569 | 0.0865 | 3 | 1.454 | 0.0475 | 4 | 1.388 | 0.0356 | 5 | 1.39 | 0.0272 |
| 2 | 2.408 | 0.0835 | 3 | 2.336 | 0.0508 | 4 | 2.472 | 0.0422 | 5 | 2.34 | 0.0285 |
| 2 | 1.336 | 0.0845 | 3 | 3.353 | 0.0525 | 4 | 3.305 | 0.0351 | 5 | 3.28 | 0.0295 |
| 2 | 5.117 | 0.0917 | 3 | 4.198 | 0.0540 | 4 | 5.121 | 0.0389 | 5 | 4.07 | 0.0304 |
| 2 | 7.313 | 0.0931 | 3 | 6.094 | 0.0560 | 4 | 7.092 | 0.0416 | 5 | 5.56 | 0.0326 |
| 2 | 8.573 | 0.0917 | 3 | 7.470 | 0.0556 | 4 | 8.530 | 0.0424 | 5 | 7.03 | 0.0338 |
| 2 | 10.125 | 0.0909 | 3 | 9.754 | 0.0563 | 4 | 10.159 | 0.0446 | 5 | 8.54 | 0.0361 |
| 2 | 12.354 | 0.0931 | 3 | 10.182 | 0.0559 | 4 | 13.174 | 0.0482 | 5 | 10.09 | 0.0377 |
| 2 | 15.463 | 0.0932 | 3 | 13.213 | 0.0596 | 4 | 16.236 | 0.0527 | 5 | 17.03 | 0.0471 |
| 2 | 17.938 | 0.0936 | 3 | 16.244 | 0.0632 | 4 | 20.007 | 0.0582 | 5 | 12.60 | 0.0409 |
| 2 | 21.851 | 0.0967 | 3 | 20.680 | 0.0707 | 4 | 25.087 | 0.0650 | 5 | 20.39 | 0.0528 |
| 2 | 24.952 | 0.1016 | 3 | 25.858 | 0.0771 | 4 | 30.997 | 0.0753 | 5 | 25.97 | 0.0599 |
| 2 | 30.981 | 0.1096 | 3 | 30.599 | 0.0844 | 4 | 35.504 | 0.0798 | 5 | 31.75 | 0.0681 |
| 2 | 35.048 | 0.1130 | 3 | 35.321 | 0.0922 | | | | | | |
| 2 | 39.905 | 0.1162 | 3 | 40.194 | 0.0988 | | | | | | |
| 2 | 39.824 | 0.1184 | | | | | | | | | |

Table C.11: 5.4% kaolin in water suspension in a 75 mm trapezoidal flume

| | |
|-----------------------------|-----------|
| Material: | Kaolin |
| Concentration/vol: | 5.4% |
| Density kg/m ³ : | 1088.20 |
| Ty (Pa): | 4.448 |
| k (Pa.s ⁿ): | 0.018 |
| n: | 0.781 |
| Flume base width (mm) | 75 |
| Flume Shape | Trapezoid |

| SLOPE | FLOW | DEPTH | SLOPE | FLOW | DEPTH | SLOPE | FLOW | DEPTH | SLOPE | FLOW | DEPTH | SLOPE | FLOW | DEPTH |
|-----------|----------------------|--------|-----------|----------------------|--------|-----------|----------------------|--------|-----------|----------------------|--------|-----------|----------------------|--------|
| FLUME | Q | h | FLUME | Q | h | FLUME | Q | h | FLUME | Q | h | FLUME | Q | h |
| (degrees) | (l.s ⁻¹) | (m) | (degrees) | (l.s ⁻¹) | (m) | (degrees) | (l.s ⁻¹) | (m) | (degrees) | (l.s ⁻¹) | (m) | (degrees) | (l.s ⁻¹) | (m) |
| 1 | 0.093 | 0.0363 | 2 | 0.220 | 0.0171 | 3 | 0.161 | 0.0125 | 4 | 0.859 | 0.0120 | 5 | 0.79 | 0.0104 |
| 1 | 0.292 | 0.0373 | 2 | 0.265 | 0.0194 | 3 | 0.272 | 0.0130 | 4 | 0.96 | 0.0123 | 5 | 0.98 | 0.0105 |
| 1 | 0.312 | 0.0396 | 2 | 0.373 | 0.0199 | 3 | 0.377 | 0.0138 | 4 | 1.17 | 0.0131 | 5 | 1.09 | 0.0112 |
| 1 | 0.326 | 0.0392 | 2 | 0.486 | 0.0201 | 3 | 0.482 | 0.0142 | 4 | 1.31 | 0.0137 | 5 | 1.21 | 0.0111 |
| 1 | 0.472 | 0.0412 | 2 | 0.600 | 0.0208 | 3 | 0.583 | 0.0146 | 4 | 1.62 | 0.0148 | 5 | 1.52 | 0.0128 |
| 1 | 0.611 | 0.0416 | 2 | 0.784 | 0.0212 | 3 | 0.783 | 0.0148 | 4 | 2.06 | 0.0167 | 5 | 1.95 | 0.0140 |
| 1 | 0.578 | 0.0419 | 2 | 1.076 | 0.0221 | 3 | 1.027 | 0.0158 | 4 | 2.77 | 0.0189 | 5 | 2.31 | 0.0148 |
| 1 | 0.818 | 0.0436 | 2 | 1.587 | 0.0241 | 3 | 1.530 | 0.0178 | 4 | 3.08 | 0.0207 | 5 | 3.10 | 0.0185 |
| 1 | 1.001 | 0.0453 | 2 | 2.191 | 0.0263 | 3 | 2.061 | 0.0198 | 4 | 4.06 | 0.0247 | 5 | 4.18 | 0.0224 |
| 1 | 1.326 | 0.0472 | 2 | 2.977 | 0.0298 | 3 | 1.226 | 0.0165 | 4 | 5.42 | 0.0287 | 5 | 5.21 | 0.0257 |
| 1 | 1.624 | 0.0485 | 2 | 4.023 | 0.0352 | 3 | 2.950 | 0.0237 | 4 | 6.41 | 0.0327 | 5 | 6.27 | 0.0288 |
| 1 | 2.115 | 0.0502 | 2 | 5.485 | 0.0407 | 3 | 4.882 | 0.0318 | 4 | 8.20 | 0.0384 | 5 | 8.04 | 0.0338 |
| 1 | 3.104 | 0.0504 | 2 | 6.536 | 0.0450 | 3 | 5.413 | 0.0334 | 4 | 10.15 | 0.0440 | 5 | 10.10 | 0.0401 |
| 1 | 4.068 | 0.0543 | 2 | 8.084 | 0.0512 | 3 | 6.326 | 0.0369 | 4 | 13.32 | 0.0510 | 5 | 13.31 | 0.0489 |
| 1 | 5.097 | 0.0593 | 2 | 10.129 | 0.0580 | 3 | 8.121 | 0.0429 | 4 | 13.36 | 0.0522 | 5 | 25.47 | 0.0750 |
| 1 | 6.495 | 0.0645 | 2 | 14.209 | 0.0700 | 3 | 10.122 | 0.0495 | 4 | 18.23 | 0.0649 | | | |
| 1 | 8.245 | 0.0711 | 2 | 18.696 | 0.0824 | 3 | 14.551 | 0.0618 | | | | | | |
| 1 | 10.025 | 0.0780 | 2 | 24.286 | 0.1021 | 3 | 20.192 | 0.0743 | | | | | | |
| 1 | 14.032 | 4.2370 | | | | 3 | 23.573 | 0.0826 | | | | | | |
| 1 | 19.989 | 0.1116 | | | | | | | | | | | | |
| 1 | 20.793 | 0.1143 | | | | | | | | | | | | |

Table C.12: 7.2% kaolin in water suspension in a 75 mm trapezoidal flume

| | |
|-----------------------------|-----------|
| Material: | Kaolin |
| Concentration/vol: | 7.1% |
| Density kg/m ³ : | 1117.60 |
| Ty (Pa): | 8.100 |
| k (Pa.s ⁿ): | 1.140 |
| n: | 0.320 |
| Flume base width (mm) | 75 |
| Flume Shape | Trapezoid |

| SLOPE FLUME (degrees) | FLOW Q (l.s ⁻¹) | DEPTH h (m) | SLOPE FLUME (degrees) | FLOW Q (l.s ⁻¹) | DEPTH h (m) | SLOPE FLUME (degrees) | FLOW Q (l.s ⁻¹) | DEPTH h (m) | SLOPE FLUME (degrees) | FLOW Q (l.s ⁻¹) | DEPTH h (m) | SLOPE FLUME (degrees) | FLOW Q (l.s ⁻¹) | DEPTH h (m) |
|-----------------------------|-----------------------------------|-------------------|-----------------------------|-----------------------------------|-------------------|-----------------------------|-----------------------------------|-------------------|-----------------------------|-----------------------------------|-------------------|-----------------------------|-----------------------------------|-------------------|
| 1 | 1.314 | 0.0972 | 2 | 0.666 | 0.0528 | 3 | 0.941 | 0.0343 | 4 | 1.16 | 0.0256 | 5 | 1.01 | 0.0201 |
| 1 | 1.929 | 0.1029 | 2 | 1.983 | 0.0595 | 3 | 1.702 | 0.0360 | 4 | 1.67 | 0.0263 | 5 | 1.62 | 0.0213 |
| 1 | 2.226 | 0.1059 | 2 | 1.717 | 0.0591 | 3 | 1.393 | 0.0349 | 4 | 1.36 | 0.0255 | 5 | 1.13 | 0.0206 |
| 1 | 2.800 | 0.1117 | 2 | 2.500 | 0.0627 | 3 | 2.199 | 0.0367 | 4 | 2.06 | 0.0273 | 5 | 1.41 | 0.0210 |
| 1 | 4.324 | 0.1185 | 2 | 2.991 | 0.0638 | 3 | 2.678 | 0.0388 | 4 | 2.68 | 0.0290 | 5 | 1.79 | 0.0218 |
| 1 | 4.652 | 0.1227 | 2 | 3.453 | 0.0648 | 3 | 3.140 | 0.0399 | 4 | 3.11 | 0.0305 | 5 | 2.11 | 0.0226 |
| 1 | 5.654 | 0.1278 | 2 | 4.166 | 0.0661 | 3 | 3.667 | 0.0412 | 4 | 3.69 | 0.0325 | 5 | 2.52 | 0.0239 |
| 1 | 6.614 | 0.1326 | 2 | 4.412 | 0.0660 | 3 | 4.067 | 0.0425 | 4 | 4.19 | 0.0338 | 5 | 2.78 | 0.0248 |
| 1 | 8.044 | 0.1400 | 2 | 4.942 | 0.0669 | 3 | 4.719 | 0.0442 | 4 | 4.57 | 0.0350 | 5 | 2.99 | 0.0253 |
| 1 | 8.976 | 0.1439 | 2 | 5.891 | 0.0686 | 3 | 5.350 | 0.0465 | 4 | 5.26 | 0.0370 | 5 | 4.34 | 0.0289 |
| 1 | 10.121 | 0.1488 | 2 | 6.711 | 0.0697 | 3 | 6.024 | 0.0485 | 4 | 6.07 | 0.0396 | 5 | 4.04 | 0.0284 |
| 1 | 12.923 | 0.1612 | 2 | 7.384 | 0.0714 | 3 | 6.607 | 0.0504 | 4 | 7.01 | 0.0428 | 5 | 3.20 | 0.0258 |
| 1 | 14.554 | 0.1670 | 2 | 8.598 | 0.0745 | 3 | 7.264 | 0.0521 | 4 | 7.94 | 0.0457 | 5 | 4.74 | 0.0296 |
| 1 | 16.365 | 0.1743 | 2 | 9.612 | 0.0770 | 3 | 7.969 | 0.0545 | 4 | 10.12 | 0.0517 | 5 | 5.03 | 0.0313 |
| 1 | 18.143 | 0.1802 | 2 | 10.139 | 0.0783 | 3 | 9.215 | 0.0578 | 4 | 12.08 | 0.0571 | 5 | 6.15 | 0.0344 |
| | | | 2 | 12.053 | 0.0833 | 3 | 10.158 | 0.0606 | 4 | 14.90 | 0.0638 | 5 | 7.02 | 0.0375 |
| | | | 2 | 13.890 | 0.0884 | 3 | 13.572 | 0.0696 | 4 | 17.76 | 0.0703 | 5 | 8.01 | 0.0404 |
| | | | 2 | 15.104 | 0.0917 | 3 | 11.939 | 0.0653 | 4 | 22.06 | 0.0792 | 5 | 8.86 | 0.0428 |
| | | | 2 | 16.460 | 0.0951 | 3 | 16.520 | 0.0770 | 4 | 24.15 | 0.0834 | 5 | 10.19 | 0.0460 |
| | | | 2 | 17.529 | 0.0986 | 3 | 18.920 | 0.0827 | | | | 5 | 12.31 | 0.0517 |
| | | | 2 | 19.205 | 0.1021 | 3 | 23.657 | 0.0944 | | | | 5 | 16.01 | 0.0599 |
| | | | 2 | 20.693 | 0.1068 | | | | | | | 5 | 20.52 | 0.0697 |
| | | | 2 | 23.764 | 0.1149 | | | | | | | | | |

Table C.13: 5.4% kaolin in water suspension in a 150 mm trapezoidal flume

| | |
|-----------------------------|-----------|
| Material: | Kaolin |
| Concentration/vol: | 5.4% |
| Density kg/m ³ : | 1090.00 |
| Ty (Pa): | 5.500 |
| k (Pa.s ⁿ): | 0.018 |
| n: | 0.781 |
| Flume base width (mm) | 150 |
| Flume Shape | Trapezoid |

| SLOPE FLUME (degrees) | FLOW Q (l.s ⁻¹) | DEPTH h (m) | SLOPE FLUME (degrees) | FLOW Q (l.s ⁻¹) | DEPTH h (m) | SLOPE FLUME (degrees) | FLOW Q (l.s ⁻¹) | DEPTH h (m) | SLOPE FLUME (degrees) | FLOW Q (l.s ⁻¹) | DEPTH h (m) | SLOPE FLUME (degrees) | FLOW Q (l.s ⁻¹) | DEPTH h (m) |
|-----------------------------|-----------------------------------|-------------------|-----------------------------|-----------------------------------|-------------------|-----------------------------|-----------------------------------|-------------------|-----------------------------|-----------------------------------|-------------------|-----------------------------|-----------------------------------|-------------------|
| 1 | 0.096 | 0.0304 | 2 | 0.152 | 0.0155 | 3 | 0.197 | 0.0114 | 4 | 1.01 | 0.0104 | 5 | 1.54 | 0.0098 |
| 1 | 0.108 | 0.0314 | 2 | 0.228 | 0.0163 | 3 | 0.387 | 0.0118 | 4 | 1.49 | 0.0110 | 5 | 2.07 | 0.0105 |
| 1 | 0.223 | 0.0327 | 2 | 0.311 | 0.0166 | 3 | 0.469 | 0.0122 | 4 | 2.00 | 0.0121 | 5 | 3.29 | 0.0124 |
| 1 | 0.296 | 0.0337 | 2 | 0.631 | 0.0174 | 3 | 0.675 | 0.0126 | 4 | 3.16 | 0.0141 | 5 | 4.07 | 0.0140 |
| 1 | 0.389 | 0.0345 | 2 | 0.695 | 0.0174 | 3 | 0.733 | 0.0129 | 4 | 4.10 | 0.0158 | 5 | 5.17 | 0.0160 |
| 1 | 0.519 | 0.0349 | 2 | 0.877 | 0.0177 | 3 | 0.873 | 0.0131 | 4 | 5.21 | 0.0181 | 5 | 6.39 | 0.0182 |
| 1 | 0.612 | 0.0354 | 2 | 1.181 | 0.0182 | 3 | 0.926 | 0.0133 | 4 | 6.15 | 0.0200 | 5 | 8.29 | 0.0216 |
| 1 | 0.788 | 0.0360 | 2 | 1.455 | 0.0186 | 3 | 1.660 | 0.0145 | 4 | 7.96 | 0.0237 | 5 | 10.12 | 0.0248 |
| 1 | 0.955 | 0.0361 | 2 | 2.048 | 0.0200 | 3 | 1.472 | 0.0140 | 4 | 10.11 | 0.0276 | 5 | 15.11 | 0.0328 |
| 1 | 1.188 | 0.0366 | 2 | 2.965 | 0.0216 | 3 | 2.091 | 0.0150 | 4 | 16.29 | 0.0388 | 5 | 15.06 | 0.0328 |
| 1 | 1.513 | 0.0378 | 2 | 3.724 | 0.0238 | 3 | 2.436 | 0.0208 | 4 | 25.96 | 0.0571 | 5 | 25.22 | 0.0495 |
| 1 | 2.164 | 0.0390 | 2 | 4.677 | 0.0260 | 3 | 2.594 | 0.0217 | 4 | 35.55 | 0.0693 | 5 | 35.46 | 0.0638 |
| 1 | 2.955 | 0.0399 | 2 | 6.002 | 0.0291 | 3 | 3.022 | 0.0167 | 4 | 43.34 | 0.0802 | 5 | 41.79 | 0.0722 |
| 1 | 4.034 | 0.0416 | 2 | 8.060 | 0.0340 | 3 | 3.953 | 0.0188 | | | | | | |
| 1 | 4.859 | 0.0432 | 2 | 9.994 | 0.0386 | 3 | 5.119 | 0.0213 | | | | | | |
| 1 | 5.999 | 0.0459 | 2 | 17.193 | 0.0542 | 3 | 5.666 | 0.0228 | | | | | | |
| 1 | 6.884 | 0.0480 | 2 | 23.909 | 0.0673 | 3 | 7.750 | 0.0271 | | | | | | |
| 1 | 8.126 | 0.0507 | 2 | 34.592 | 0.0848 | 3 | 10.180 | 0.0320 | | | | | | |
| 1 | 9.803 | 0.0557 | 2 | 42.768 | 0.0986 | 3 | 15.266 | 0.0423 | | | | | | |
| 1 | 16.843 | 0.0731 | | | | 3 | 21.751 | 0.0567 | | | | | | |
| 1 | 23.392 | 0.0873 | | | | 3 | 32.035 | 0.0703 | | | | | | |
| 1 | 34.372 | 0.1095 | | | | 3 | 38.45 | 0.0791 | | | | | | |
| 1 | 42.678 | 0.1240 | | | | | | | | | | | | |
| 1 | 45.561 | 0.1264 | | | | | | | | | | | | |

Table C.14: 7.1% kaolin in water suspension in a 150 mm trapezoidal flume

| | |
|-----------------------------|-----------|
| Material: | Kaolin |
| Concentration/vol: | 7.1% |
| Density kg/m ³ : | 1117.60 |
| Ty (Pa): | 8.100 |
| k (Pa.s ⁿ): | 1.140 |
| n: | 0.320 |
| Flume base width (mm) | 150 |
| Flume Shape | Trapezoid |

| SLOPE | FLOW | DEPTH | SLOPE | FLOW | DEPTH | SLOPE | FLOW | DEPTH | SLOPE | FLOW | DEPTH | SLOPE | FLOW | DEPTH |
|-----------|----------------------|--------|-----------|----------------------|--------|-----------|----------------------|--------|-----------|----------------------|--------|-----------|----------------------|--------|
| FLUME | Q | h | FLUME | Q | h | FLUME | Q | h | FLUME | Q | h | FLUME | Q | h |
| (degrees) | (L.s ⁻¹) | (m) | (degrees) | (L.s ⁻¹) | (m) | (degrees) | (L.s ⁻¹) | (m) | (degrees) | (L.s ⁻¹) | (m) | (degrees) | (L.s ⁻¹) | (m) |
| 1 | 0.545 | 0.0688 | 2 | 0.500 | 0.0386 | 3 | 0.636 | 0.0261 | 4 | 1.01 | 0.0211 | 5 | 1.50 | 0.0176 |
| 1 | 0.826 | 0.0712 | 2 | 0.730 | 0.0397 | 3 | 0.860 | 0.0270 | 4 | 1.71 | 0.0221 | 5 | 1.80 | 0.0180 |
| 1 | 1.041 | 0.0726 | 2 | 0.918 | 0.0408 | 3 | 1.089 | 0.0276 | 4 | 1.32 | 0.0218 | 5 | 2.12 | 0.0187 |
| 1 | 2.051 | 0.0784 | 2 | 1.126 | 0.0416 | 3 | 1.522 | 0.0284 | 4 | 1.30 | 0.0218 | 5 | 2.43 | 0.0189 |
| 1 | 2.566 | 0.0811 | 2 | 1.595 | 0.0431 | 3 | 2.119 | 0.0291 | 4 | 2.04 | 0.0227 | 5 | 2.85 | 0.0195 |
| 1 | 3.267 | 0.0826 | 2 | 2.175 | 0.0444 | 3 | 2.566 | 0.0293 | 4 | 2.50 | 0.0232 | 5 | 3.52 | 0.0203 |
| 1 | 4.191 | 0.0868 | 2 | 2.596 | 0.0450 | 3 | 3.037 | 0.0294 | 4 | 3.01 | 0.0238 | 5 | 4.08 | 0.0213 |
| 1 | 5.077 | 0.0904 | 2 | 3.072 | 0.0453 | 3 | 4.110 | 0.0313 | 4 | 4.42 | 0.0252 | 5 | 4.44 | 0.0217 |
| 1 | 6.017 | 0.0939 | 2 | 4.181 | 0.0464 | 3 | 5.103 | 0.0328 | 4 | 4.05 | 0.0251 | 5 | 5.09 | 0.0226 |
| 1 | 8.041 | 0.0997 | 2 | 4.686 | 0.0474 | 3 | 6.160 | 0.0345 | 4 | 5.05 | 0.0265 | 5 | 6.26 | 0.0244 |
| 1 | 10.057 | 0.1044 | 2 | 5.251 | 0.0481 | 3 | 7.998 | 0.0377 | 4 | 6.16 | 0.0280 | 5 | 7.15 | 0.0257 |
| 1 | 15.411 | 0.1135 | 2 | 6.102 | 0.0489 | 3 | 7.147 | 0.0362 | 4 | 7.07 | 0.0296 | 5 | 8.05 | 0.0273 |
| 1 | 20.825 | 0.1209 | 2 | 6.960 | 0.0498 | 3 | 8.790 | 0.0362 | 4 | 8.11 | 0.0315 | 5 | 9.18 | 0.0291 |
| 1 | 24.689 | 0.1249 | 2 | 8.056 | 0.0515 | 3 | 9.338 | 0.0402 | 4 | 9.15 | 0.0333 | 5 | 10.17 | 0.0309 |
| 1 | 28.576 | 0.1293 | 2 | 9.106 | 0.0530 | 3 | 10.199 | 0.0416 | 4 | 10.25 | 0.0349 | 5 | 13.86 | 0.0363 |
| 1 | 33.534 | 0.1363 | 2 | 10.093 | 0.0548 | 3 | 16.291 | 0.0529 | 4 | 12.65 | 0.0392 | 5 | 22.05 | 0.0497 |
| 1 | 37.774 | 0.1424 | 2 | 16.086 | 0.0660 | 3 | 20.038 | 0.0597 | 4 | 16.01 | 0.0450 | 5 | 27.98 | 0.0581 |
| 1 | 40.948 | 0.1463 | 2 | 13.102 | 0.0603 | 3 | 14.379 | 0.0491 | 4 | 22.26 | 0.0554 | 5 | 35.19 | 0.0681 |
| | | | 2 | 22.680 | 0.0787 | 3 | 12.533 | 0.0459 | 4 | 24.77 | 0.0596 | | | |
| | | | 2 | 28.563 | 0.0892 | 3 | 22.484 | 0.0639 | 4 | 30.66 | 0.0680 | | | |
| | | | 2 | 33.090 | 0.0962 | 3 | 28.507 | 0.0739 | 4 | 35.97 | 0.0754 | | | |
| | | | 2 | 38.588 | 0.1044 | 3 | 33.039 | 0.0812 | 4 | 39.92 | 0.0805 | | | |
| | | | 2 | 44.308 | 0.1136 | 3 | 40.076 | 0.0910 | 4 | 43.34 | 0.0846 | | | |
| | | | | | | | | | 4 | 45.82 | 0.0874 | | | |

APPENDIX D: Triangular flume data

Table D.1: 2% CMC in water solution in a 300 mm triangular flume

| | |
|-----------------------------|--------|
| Material: | CMC |
| Concentration/vol: | 2.0% |
| Density kg/m ³ : | 1012.9 |
| Ty (Pa): | 0.000 |
| k (Pa.s): | 0.035 |
| n: | 0.776 |
| Flume width (mm): | 300 |
| Flume Shape | Vee |

| SLOPE | FLOW | DEPTH | SLOPE | FLOW | DEPTH | SLOPE | FLOW | DEPTH | SLOPE | FLOW | DEPTH | SLOPE | FLOW | DEPTH |
|-----------|----------------------|--------|-----------|----------------------|--------|-----------|----------------------|--------|-----------|----------------------|--------|-----------|----------------------|--------|
| FLUME | Q | h | FLUME | Q | h | FLUME | Q | h | FLUME | Q | h | FLUME | Q | h |
| (degrees) | (l.s ⁻¹) | (m) | (degrees) | (l.s ⁻¹) | (m) | (degrees) | (l.s ⁻¹) | (m) | (degrees) | (l.s ⁻¹) | (m) | (degrees) | (l.s ⁻¹) | (m) |
| 1 | 10.15 | 0.0899 | 2 | 0.04 | 0.0123 | 3 | 0.252 | 0.0160 | 4 | 0.446 | 0.0206 | 5 | 0.028 | 0.0093 |
| 1 | 8.13 | 0.0817 | 2 | 0.06 | 0.0132 | 3 | 0.198 | 0.0151 | 4 | 0.340 | 0.0188 | 5 | 0.051 | 0.0102 |
| 1 | 5.83 | 0.0713 | 2 | 0.08 | 0.0136 | 3 | 0.150 | 0.0142 | 4 | 0.269 | 0.0152 | 5 | 0.072 | 0.0110 |
| 1 | 4.05 | 0.0624 | 2 | 0.10 | 0.0147 | 3 | 0.103 | 0.0133 | 4 | 0.171 | 0.0135 | 5 | 0.202 | 0.0142 |
| 1 | 3.04 | 0.0554 | 2 | 0.18 | 0.0167 | 3 | 0.282 | 0.0113 | 4 | 0.122 | 0.0125 | 5 | 9.657 | 0.0652 |
| 1 | 2.45 | 0.0507 | 2 | 0.29 | 0.0190 | 3 | 0.506 | 0.0196 | 4 | 0.090 | 0.0115 | 5 | 7.867 | 0.0596 |
| 1 | 2.02 | 0.0477 | 2 | 0.38 | 0.0208 | 3 | 0.430 | 0.0182 | 4 | 0.061 | 0.0104 | 5 | 6.009 | 0.0536 |
| 1 | 1.50 | 0.0428 | 2 | 0.49 | 0.0226 | 3 | 0.357 | 0.0173 | 4 | 0.037 | 0.0095 | 5 | 4.035 | 0.0462 |
| 1 | 1.06 | 0.0376 | 2 | 0.69 | 0.0249 | 3 | 35.468 | 0.1238 | 4 | 0.626 | 0.0237 | 5 | 2.004 | 0.0357 |
| 1 | 0.78 | 0.0339 | 2 | 0.97 | 0.0291 | 3 | 27.075 | 0.1110 | 4 | 0.834 | 0.0264 | 5 | 1.511 | 0.0320 |
| 1 | 0.58 | 0.0289 | 2 | 1.52 | 0.0338 | 3 | 20.459 | 0.0997 | 4 | 1.049 | 0.0284 | 5 | 1.013 | 0.0272 |
| 1 | 0.39 | 0.0251 | 2 | 8.43 | 0.0732 | 3 | 15.238 | 0.0884 | 4 | 1.503 | 0.0326 | 5 | 0.595 | 0.0227 |
| 1 | 0.29 | 0.0229 | 2 | 5.99 | 0.0645 | 3 | 10.816 | 0.0752 | 4 | 1.989 | 0.0367 | 5 | 0.755 | 0.0248 |
| 1 | 0.19 | 0.0203 | 2 | 4.08 | 0.0564 | 3 | 8.161 | 0.0664 | 4 | 2.468 | 0.0393 | 5 | 0.281 | 0.0167 |
| 1 | 0.09 | 0.0176 | 2 | 3.04 | 0.0495 | 3 | 5.983 | 0.0599 | 4 | 3.040 | 0.0427 | 5 | 0.380 | 0.0193 |
| 1 | 0.13 | 0.0184 | 2 | 10.10 | 0.0794 | 3 | 8.025 | 0.0667 | 4 | 4.099 | 0.0482 | 5 | 0.494 | 0.0213 |
| 1 | 0.06 | 0.0160 | 2 | 14.51 | 0.0915 | 3 | 4.056 | 0.0524 | 4 | 6.087 | 0.0561 | 5 | 0.153 | 0.0128 |
| 1 | 14.44 | 0.1042 | 2 | 19.93 | 0.1064 | 3 | 3.066 | 0.0462 | 4 | 8.086 | 0.0636 | 5 | 0.112 | 0.0121 |
| 1 | 19.88 | 0.1190 | 2 | 25.43 | 0.1173 | 3 | 2.490 | 0.0425 | 4 | 10.022 | 0.0685 | 5 | 17.202 | 0.0142 |
| 1 | 24.80 | 0.1318 | 2 | 32.17 | 0.1301 | 3 | 1.978 | 0.0386 | 4 | 14.547 | 0.0795 | 5 | 18.202 | 0.0142 |
| 1 | 33.64 | 0.1502 | 2 | 40.54 | 0.1417 | 3 | 1.524 | 0.0341 | 4 | 19.141 | 0.0903 | 5 | 19.202 | 0.0142 |
| | | | | | | 3 | 1.105 | 0.0294 | 4 | 25.330 | 0.1001 | 5 | 20.202 | 0.0142 |
| | | | | | | | | | 4 | 28.979 | 0.1067 | 5 | 21.202 | 0.0142 |
| | | | | | | | | | 4 | 32.794 | 0.1128 | 5 | 22.202 | 0.0142 |
| | | | | | | | | | | | | 5 | 23.202 | 0.0142 |

Table D.2: 3.1% CMC in water solution in a 300 mm triangular flume

| | |
|-----------------------------|-------|
| Material: | CMC |
| Concentration/vol: | 3.1% |
| Density kg/m ³ : | 1018 |
| Ty (Pa): | 0.000 |
| k (Pa.s ⁿ): | 0.091 |
| n: | 0.823 |
| Flume width (mm): | 300 |
| Flume Shape | Vee |

| SLOPE | FLOW | DEPTH | SLOPE | FLOW | DEPTH | SLOPE | FLOW | DEPTH | SLOPE | FLOW | DEPTH | SLOPE | FLOW | DEPTH |
|-----------|----------------------|--------|-----------|----------------------|--------|-----------|----------------------|--------|-----------|----------------------|--------|-----------|----------------------|--------|
| FLUME | Q | h | FLUME | Q | h | FLUME | Q | h | FLUME | Q | h | FLUME | Q | h |
| (degrees) | (L.s ⁻¹) | (m) | (degrees) | (L.s ⁻¹) | (m) | (degrees) | (L.s ⁻¹) | (m) | (degrees) | (L.s ⁻¹) | (m) | (degrees) | (L.s ⁻¹) | (m) |
| 1 | 0.051 | 0.0219 | 2 | 0.087 | 0.0193 | 3 | 0.084 | 0.0171 | 4 | 0.09 | 0.0164 | 5 | 0.07 | 0.0138 |
| 1 | 0.076 | 0.0237 | 2 | 0.133 | 0.0209 | 3 | 0.139 | 0.0188 | 4 | 0.21 | 0.0191 | 5 | 0.13 | 0.0160 |
| 1 | 0.091 | 0.0247 | 2 | 0.196 | 0.0228 | 3 | 0.193 | 0.0204 | 4 | 0.31 | 0.0209 | 5 | 0.19 | 0.0176 |
| 1 | 0.188 | 0.0288 | 2 | 0.285 | 0.0248 | 3 | 0.282 | 0.0223 | 4 | 0.13 | 0.0174 | 5 | 0.29 | 0.0194 |
| 1 | 0.291 | 0.0317 | 2 | 0.396 | 0.0269 | 3 | 0.380 | 0.0240 | 4 | 0.39 | 0.0223 | 5 | 0.38 | 0.0206 |
| 1 | 0.384 | 0.0335 | 2 | 0.530 | 0.0293 | 3 | 0.573 | 0.0267 | 4 | 0.64 | 0.0251 | 5 | 0.58 | 0.0230 |
| 1 | 0.610 | 0.0376 | 2 | 0.783 | 0.0322 | 3 | 0.772 | 0.0288 | 4 | 0.82 | 0.0272 | 5 | 0.78 | 0.0253 |
| 1 | 0.797 | 0.0400 | 2 | 1.054 | 0.0356 | 3 | 1.055 | 0.0321 | 4 | 1.01 | 0.0289 | 5 | 1.04 | 0.0280 |
| 1 | 1.095 | 0.0436 | 2 | 1.474 | 0.0393 | 3 | 1.479 | 0.0356 | 4 | 1.40 | 0.0323 | 5 | 1.36 | 0.0298 |
| 1 | 1.504 | 0.0479 | 2 | 1.937 | 0.0428 | 3 | 1.961 | 0.0390 | 4 | 2.04 | 0.0368 | 5 | 2.02 | 0.0349 |
| 1 | 2.073 | 0.0527 | 2 | 2.549 | 0.0474 | 3 | 2.789 | 0.0444 | 4 | 3.05 | 0.0421 | 5 | 2.63 | 0.0372 |
| 1 | 2.480 | 0.0560 | 2 | 3.082 | 0.0500 | 3 | 3.994 | 0.0506 | 4 | 4.03 | 0.0463 | 5 | 6.02 | 0.0522 |
| 1 | 3.218 | 0.0608 | 2 | 3.962 | 0.0551 | 3 | 5.329 | 0.0557 | 4 | 6.02 | 0.0556 | 5 | 4.03 | 0.0443 |
| 1 | 4.118 | 0.0667 | 2 | 6.025 | 0.0652 | 3 | 6.456 | 0.0601 | 4 | 8.00 | 0.0618 | 5 | 6.06 | 0.0525 |
| 1 | 6.141 | 0.0772 | 2 | 7.940 | 0.0724 | 3 | 10.131 | 0.0730 | 4 | 10.14 | 0.0680 | 5 | 11.77 | 0.0685 |
| 1 | 8.127 | 0.0857 | 2 | 9.900 | 0.0794 | 3 | 14.274 | 0.0825 | 4 | 14.80 | 0.0779 | 5 | 13.27 | 0.0715 |
| 1 | 10.107 | 0.0936 | 2 | 14.072 | 0.0908 | 3 | 20.305 | 0.0949 | 4 | 19.36 | 0.0869 | 5 | 10.10 | 0.0644 |
| 1 | 14.159 | 0.1063 | 2 | 19.023 | 0.1024 | 3 | 30.823 | 0.1141 | | | | 5 | 18.27 | 0.0809 |
| 1 | 21.976 | 0.1264 | 2 | 24.939 | 0.1139 | | | | | | | 5 | 23.21 | 0.0889 |
| 1 | 32.003 | 0.1475 | 2 | 30.150 | 0.1225 | | | | | | | | | |
| | | | 2 | 36.000 | 0.1327 | | | | | | | | | |
| | | | 2 | 30.107 | 0.1229 | | | | | | | | | |

Table D.3: 4% CMC in water solution in a 300 mm triangular flume

| | |
|-----------------------------|--------|
| Material: | CMC |
| Concentration/vol: | 4.0% |
| Density kg/m ³ : | 1027.6 |
| Ty (Pa): | 0.000 |
| k (Pa.s ⁿ): | 0.599 |
| n: | 0.690 |
| Flume width (mm): | 300 |
| Flume Shape | Vee |

| SLOPE | FLOW | DEPTH | SLOPE | FLOW | DEPTH | SLOPE | FLOW | DEPTH | SLOPE | FLOW | DEPTH | SLOPE | FLOW | DEPTH |
|-----------|----------------------|--------|-----------|----------------------|--------|-----------|----------------------|--------|-----------|----------------------|--------|-----------|----------------------|--------|
| FLUME | Q | h | FLUME | Q | h | FLUME | Q | h | FLUME | Q | h | FLUME | Q | h |
| (degrees) | (L.s ⁻¹) | (m) | (degrees) | (L.s ⁻¹) | (m) | (degrees) | (L.s ⁻¹) | (m) | (degrees) | (L.s ⁻¹) | (m) | (degrees) | (L.s ⁻¹) | (m) |
| 1 | 0.10 | 0.0324 | 2 | 0.08 | 0.0251 | 3 | 0.121 | 0.0240 | 4 | 0.093 | 0.0201 | 5 | 1.053 | 0.0336 |
| 1 | 0.17 | 0.0357 | 2 | 0.13 | 0.0271 | 3 | 0.175 | 0.0259 | 4 | 0.142 | 0.0224 | 5 | 0.169 | 0.0211 |
| 1 | 0.29 | 0.0403 | 2 | 0.19 | 0.0295 | 3 | 0.275 | 0.0285 | 4 | 0.195 | 0.0240 | 5 | 0.198 | 0.0219 |
| 1 | 0.40 | 0.0437 | 2 | 0.30 | 0.0322 | 3 | 0.391 | 0.0307 | 4 | 0.291 | 0.0261 | 5 | 0.294 | 0.0241 |
| 1 | 0.60 | 0.0475 | 2 | 0.44 | 0.0350 | 3 | 0.579 | 0.0340 | 4 | 0.410 | 0.0283 | 5 | 0.387 | 0.0258 |
| 1 | 0.78 | 0.0511 | 2 | 0.62 | 0.0383 | 3 | 0.779 | 0.0366 | 4 | 0.588 | 0.0314 | 5 | 0.597 | 0.0290 |
| 1 | 1.11 | 0.0548 | 2 | 0.80 | 0.0414 | 3 | 1.125 | 0.0397 | 4 | 0.793 | 0.0335 | 5 | 0.790 | 0.0311 |
| 1 | 1.50 | 0.0590 | 2 | 1.05 | 0.0436 | 3 | 1.577 | 0.0436 | 4 | 1.048 | 0.0358 | 5 | 1.372 | 0.0360 |
| 1 | 2.12 | 0.0639 | 2 | 1.48 | 0.0481 | 3 | 2.067 | 0.0471 | 4 | 1.454 | 0.0390 | 5 | 1.996 | 0.0400 |
| 1 | 2.48 | 0.0668 | 2 | 2.01 | 0.0522 | 3 | 2.489 | 0.0495 | 4 | 2.106 | 0.0436 | 5 | 2.487 | 0.0427 |
| 1 | 3.21 | 0.0714 | 2 | 2.59 | 0.0559 | 3 | 3.101 | 0.0523 | 4 | 2.571 | 0.0460 | 5 | 3.015 | 0.0452 |
| 1 | 4.02 | 0.0762 | 2 | 3.11 | 0.0587 | 3 | 4.022 | 0.0573 | 4 | 3.024 | 0.0483 | 5 | 3.974 | 0.0490 |
| 1 | 6.05 | 0.0859 | 2 | 4.01 | 0.0635 | 3 | 5.045 | 0.0616 | 4 | 3.971 | 0.0529 | 5 | 5.912 | 0.0574 |
| 1 | 8.04 | 0.0954 | 2 | 5.02 | 0.0681 | 3 | 6.048 | 0.0650 | 4 | 6.078 | 0.0608 | 5 | 8.045 | 0.0642 |
| 1 | 10.19 | 0.1035 | 2 | 6.06 | 0.0726 | 3 | 8.110 | 0.0730 | 4 | 8.034 | 0.0686 | 5 | 10.220 | 0.0699 |
| 1 | 14.28 | 0.1172 | 2 | 8.16 | 0.0810 | 3 | 10.227 | 0.0804 | 4 | 5.118 | 0.0569 | 5 | 14.165 | 0.0791 |
| 1 | 20.24 | 0.1326 | 2 | 10.20 | 0.0877 | 3 | 14.314 | 0.0910 | 4 | 10.183 | 0.0746 | 5 | 19.291 | 0.0898 |
| 1 | 27.25 | 0.1487 | 2 | 15.18 | 0.1026 | 3 | 19.085 | 0.1009 | 4 | 14.257 | 0.0841 | 5 | 24.568 | 0.0992 |
| | | | 2 | 20.58 | 0.1148 | 3 | 24.221 | 0.1108 | 4 | 19.061 | 0.0940 | 5 | 30.569 | 0.1101 |
| | | | 2 | 26.11 | 0.1255 | 3 | 32.245 | 0.1248 | 4 | 23.962 | 0.1035 | 5 | 40.784 | 0.1229 |
| | | | 2 | 33.69 | 0.1379 | 3 | 41.333 | 0.1381 | 4 | 30.824 | 0.1140 | | | |
| | | | | | | | | | 4 | 41.821 | 0.1315 | | | |

Table D.4: 4.9% CMC in water solution in a 300 mm triangular flume

| | |
|-----------------------------|--------|
| Material: | CMC |
| Concentration/vol: | 4.9% |
| Density kg/m ³ : | 1027.6 |
| Ty (Pa): | 0.000 |
| k (Pa.s ⁿ): | 0.599 |
| n: | 0.690 |
| Flume width (mm): | 300 |
| Flume Shape | Vee |

| SLOPE | FLOW | DEPTH | SLOPE | FLOW | DEPTH | SLOPE | FLOW | DEPTH | SLOPE | FLOW | DEPTH | SLOPE | FLOW | DEPTH |
|-----------|----------------------|--------|-----------|----------------------|--------|-----------|----------------------|--------|-----------|----------------------|--------|-----------|----------------------|--------|
| FLUME | Q | h | FLUME | Q | h | FLUME | Q | h | FLUME | Q | h | FLUME | Q | h |
| (degrees) | (L.s ⁻¹) | (m) | (degrees) | (L.s ⁻¹) | (m) | (degrees) | (L.s ⁻¹) | (m) | (degrees) | (L.s ⁻¹) | (m) | (degrees) | (L.s ⁻¹) | (m) |
| 1 | 0.19 | 0.0451 | 2 | 0.18 | 0.0359 | 3 | 0.082 | 0.0273 | 4 | 0.089 | 0.0257 | 5 | 0.084 | 0.0234 |
| 1 | 0.29 | 0.0498 | 2 | 0.29 | 0.0398 | 3 | 0.188 | 0.0317 | 4 | 0.091 | 0.0253 | 5 | 0.186 | 0.0269 |
| 1 | 0.39 | 0.0537 | 2 | 0.44 | 0.0439 | 3 | 0.283 | 0.0351 | 4 | 0.185 | 0.0288 | 5 | 0.285 | 0.0303 |
| 1 | 0.53 | 0.0578 | 2 | 0.59 | 0.0466 | 3 | 0.433 | 0.0386 | 4 | 0.288 | 0.0320 | 5 | 0.426 | 0.0332 |
| 1 | 0.68 | 0.0613 | 2 | 0.83 | 0.0506 | 3 | 0.586 | 0.0411 | 4 | 0.395 | 0.0344 | 5 | 0.581 | 0.0355 |
| 1 | 0.88 | 0.0648 | 2 | 1.03 | 0.0534 | 3 | 0.782 | 0.0442 | 4 | 0.535 | 0.0372 | 5 | 0.737 | 0.0377 |
| 1 | 1.08 | 0.0681 | 2 | 1.53 | 0.0586 | 3 | 1.005 | 0.0466 | 4 | 0.726 | 0.0397 | 5 | 0.877 | 0.0390 |
| 1 | 1.48 | 0.0729 | 2 | 2.10 | 0.0629 | 3 | 1.341 | 0.0500 | 4 | 0.930 | 0.0420 | 5 | 1.127 | 0.0412 |
| 1 | 1.98 | 0.0779 | 2 | 2.77 | 0.0674 | 3 | 1.748 | 0.0532 | 4 | 1.186 | 0.0446 | 5 | 1.414 | 0.0435 |
| 1 | 2.48 | 0.0820 | 2 | 3.54 | 0.0712 | 3 | 2.196 | 0.0562 | 4 | 1.476 | 0.0468 | 5 | 1.676 | 0.0452 |
| 1 | 3.00 | 0.0856 | 2 | 4.53 | 0.0757 | 3 | 2.479 | 0.0581 | 4 | 2.043 | 0.0505 | 5 | 1.968 | 0.0471 |
| 1 | 4.02 | 0.0911 | 2 | 6.00 | 0.0821 | 3 | 3.537 | 0.0633 | 4 | 3.056 | 0.0558 | 5 | 2.478 | 0.0499 |
| 1 | 5.01 | 0.0959 | 2 | 7.60 | 0.0879 | 3 | 4.510 | 0.0675 | 4 | 4.023 | 0.0602 | 5 | 3.178 | 0.0533 |
| 1 | 6.99 | 0.1047 | 2 | 10.05 | 0.0958 | 3 | 6.054 | 0.0737 | 4 | 5.524 | 0.0661 | 5 | 4.015 | 0.0567 |
| 1 | 9.01 | 0.1121 | 2 | 14.45 | 0.1089 | 3 | 7.566 | 0.0787 | 4 | 7.012 | 0.0708 | 5 | 5.011 | 0.0603 |
| 1 | 13.27 | 0.1266 | 2 | 20.24 | 0.1234 | 3 | 10.116 | 0.0866 | 4 | 8.586 | 0.0762 | 5 | 6.480 | 0.0654 |
| 1 | 20.70 | 0.1469 | 2 | 25.53 | 0.1340 | 3 | 12.551 | 0.0943 | 4 | 10.179 | 0.0811 | 5 | 8.005 | 0.0707 |
| | | | 2 | 30.34 | 0.1420 | 3 | 20.547 | 0.1116 | 4 | 14.865 | 0.0923 | 5 | 10.022 | 0.0763 |
| | | | 2 | 35.46 | 0.1498 | 3 | 15.057 | 0.1002 | 4 | 20.027 | 0.1027 | 5 | 14.420 | 0.0860 |
| | | | | | | 3 | 25.407 | 0.1203 | 4 | 25.171 | 0.1118 | 5 | 20.074 | 0.0974 |
| | | | | | | 3 | 30.297 | 0.1281 | 4 | 30.150 | 0.1201 | 5 | 25.179 | 0.1067 |
| | | | | | | 3 | 35.331 | 0.1365 | 4 | 35.459 | 0.1280 | 5 | 30.511 | 0.1150 |
| | | | | | | | | | 4 | 40.000 | 0.1352 | 5 | 35.864 | 0.1234 |

Table D.5: 3.5% Bentonite in water suspension in a 300 mm triangular flume

| | |
|-----------------------------|-----------|
| Material: | Bentonite |
| Concentration/vol: | 3.5% |
| Density kg/m ³ : | 1032.7 |
| Ty (Pa): | 2.982 |
| k (Pa.s ⁿ): | 0.0036 |
| n: | 1.000 |
| Flume width (mm): | 300 |
| Flume Shape | Vee |

| SLOPE | FLOW | DEPTH | SLOPE | FLOW | DEPTH | SLOPE | FLOW | DEPTH | SLOPE | FLOW | DEPTH | SLOPE | FLOW | DEPTH |
|-----------|----------------------|--------|-----------|----------------------|--------|-----------|----------------------|--------|-----------|----------------------|--------|-----------|----------------------|--------|
| FLUME | Q | h | FLUME | Q | h | FLUME | Q | h | FLUME | Q | h | FLUME | Q | h |
| (degrees) | (L.s ⁻¹) | (m) | (degrees) | (L.s ⁻¹) | (m) | (degrees) | (L.s ⁻¹) | (m) | (degrees) | (L.s ⁻¹) | (m) | (degrees) | (L.s ⁻¹) | (m) |
| 1 | 0.11 | 0.0505 | 2 | 0.08 | 0.0249 | 3 | 0.076 | 0.0177 | 4 | 0.145 | 0.0160 | 5 | 0.110 | 0.0128 |
| 1 | 0.15 | 0.0468 | 2 | 0.16 | 0.0260 | 3 | 0.235 | 0.0201 | 4 | 0.237 | 0.0177 | 5 | 0.217 | 0.0153 |
| 1 | 0.19 | 0.0470 | 2 | 0.11 | 0.0256 | 3 | 0.170 | 0.0190 | 4 | 0.325 | 0.0186 | 5 | 0.164 | 0.0141 |
| 1 | 0.23 | 0.0472 | 2 | 0.13 | 0.0260 | 3 | 0.108 | 0.0182 | 4 | 0.431 | 0.0199 | 5 | 0.294 | 0.0168 |
| 1 | 0.28 | 0.0484 | 2 | 0.20 | 0.0265 | 3 | 0.346 | 0.0216 | 4 | 0.598 | 0.0220 | 5 | 0.390 | 0.0179 |
| 1 | 0.40 | 0.0489 | 2 | 0.24 | 0.0269 | 3 | 0.408 | 0.0225 | 4 | 0.794 | 0.0241 | 5 | 0.606 | 0.0206 |
| 1 | 0.58 | 0.0496 | 2 | 0.28 | 0.0273 | 3 | 0.602 | 0.0247 | 4 | 1.005 | 0.0263 | 5 | 0.797 | 0.0226 |
| 1 | 0.79 | 0.0506 | 2 | 0.39 | 0.0285 | 3 | 0.816 | 0.0269 | 4 | 1.170 | 0.0277 | 5 | 1.015 | 0.0245 |
| 1 | 1.00 | 0.0517 | 2 | 0.60 | 0.0313 | 3 | 1.183 | 0.0307 | 4 | 1.401 | 0.0292 | 5 | 1.373 | 0.0271 |
| 1 | 1.47 | 0.0534 | 2 | 0.79 | 0.0332 | 3 | 1.395 | 0.0327 | 4 | 1.635 | 0.0310 | 5 | 1.695 | 0.0291 |
| 1 | 1.98 | 0.0567 | 2 | 1.17 | 0.0367 | 3 | 1.785 | 0.0352 | 4 | 2.147 | 0.0341 | 5 | 2.527 | 0.0341 |
| 1 | 2.58 | 0.0602 | 2 | 1.58 | 0.0400 | 3 | 2.409 | 0.0391 | 4 | 3.659 | 0.0418 | 5 | 3.494 | 0.0380 |
| 1 | 3.05 | 0.0610 | 2 | 2.08 | 0.0424 | 3 | 4.012 | 0.0472 | 4 | 4.416 | 0.0452 | 5 | 4.430 | 0.0420 |
| 1 | 4.05 | 0.0668 | 2 | 2.49 | 0.0447 | 3 | 6.306 | 0.0562 | 4 | 6.058 | 0.0521 | 5 | 6.647 | 0.0500 |
| 1 | 6.00 | 0.0761 | 2 | 3.09 | 0.0485 | 3 | 8.202 | 0.0634 | 4 | 8.180 | 0.0589 | 5 | 8.305 | 0.0557 |
| 1 | 8.03 | 0.0839 | 2 | 4.06 | 0.0538 | 3 | 10.053 | 0.0692 | 4 | 10.044 | 0.0640 | 5 | 10.042 | 0.0598 |
| 1 | 10.03 | 0.0913 | 2 | 6.05 | 0.0631 | 3 | 14.639 | 0.0798 | 4 | 15.430 | 0.0766 | 5 | 14.587 | 0.0724 |
| 1 | 14.87 | 0.1054 | 2 | 8.06 | 0.0705 | 3 | 22.065 | 0.0935 | 4 | 24.016 | 0.0957 | 5 | 25.179 | 0.0943 |
| 1 | 20.26 | 0.1197 | 2 | 10.06 | 0.0774 | | | | 4 | 31.984 | 0.1104 | 5 | 30.418 | 0.1030 |
| 1 | 30.40 | 0.1398 | 2 | 14.18 | 0.0882 | | | | | | | | | |
| | | | 2 | 20.58 | 0.1031 | | | | | | | | | |
| | | | 2 | 30.02 | 0.1228 | | | | | | | | | |

Table D.6: 4.6% Bentonite in water suspension in a 300 mm triangular flume

| | |
|-----------------------------|-----------|
| Material: | Bentonite |
| Concentration/vol: | 4.6% |
| Density kg/m ³ : | 1029.4 |
| Ty (Pa): | 5.500 |
| k (Pa.s ⁿ): | 0.0070 |
| n: | 1.000 |
| Flume width (mm): | 300 |
| Flume Shape | Vee |

| SLOPE | FLOW | DEPTH | SLOPE | FLOW | DEPTH | SLOPE | FLOW | DEPTH | SLOPE | FLOW | DEPTH | SLOPE | FLOW | DEPTH |
|-----------|----------------------|--------|-----------|----------------------|--------|-----------|----------------------|--------|-----------|----------------------|--------|-----------|----------------------|--------|
| FLUME | Q | h | FLUME | Q | h | FLUME | Q | h | FLUME | Q | h | FLUME | Q | h |
| (degrees) | (L.s ⁻¹) | (m) | (degrees) | (L.s ⁻¹) | (m) | (degrees) | (L.s ⁻¹) | (m) | (degrees) | (L.s ⁻¹) | (m) | (degrees) | (L.s ⁻¹) | (m) |
| 1 | 0.17 | 0.0708 | 2 | 1.00 | 0.0429 | 3 | 1.013 | 0.0325 | 4 | 0.185 | 0.0213 | 5 | 0.345 | 0.0206 |
| 1 | 0.26 | 0.0732 | 2 | 0.39 | 0.0397 | 3 | 0.124 | 0.0253 | 4 | 0.412 | 0.0233 | 5 | 0.469 | 0.0222 |
| 1 | 0.34 | 0.0740 | 2 | 0.30 | 0.0396 | 3 | 0.186 | 0.0264 | 4 | 0.334 | 0.0230 | 5 | 0.605 | 0.0233 |
| 1 | 0.40 | 0.0744 | 2 | 0.22 | 0.0394 | 3 | 0.292 | 0.0271 | 4 | 0.593 | 0.0250 | 5 | 0.782 | 0.0253 |
| 1 | 0.61 | 0.0768 | 2 | 0.13 | 0.0384 | 3 | 0.467 | 0.0282 | 4 | 0.837 | 0.0274 | 5 | 0.983 | 0.0269 |
| 1 | 0.80 | 0.0765 | 2 | 0.64 | 0.0414 | 3 | 0.608 | 0.0297 | 4 | 1.030 | 0.0287 | 5 | 1.044 | 0.0265 |
| 1 | 1.03 | 0.0773 | 2 | 0.83 | 0.0418 | 3 | 0.833 | 0.0318 | 4 | 1.411 | 0.0317 | 5 | 1.427 | 0.0294 |
| 1 | 1.33 | 0.0772 | 2 | 1.37 | 0.0455 | 3 | 1.487 | 0.0358 | 4 | 3.247 | 0.0415 | 5 | 3.025 | 0.0388 |
| 1 | 2.72 | 0.0799 | 2 | 2.82 | 0.0517 | 3 | 2.036 | 0.0395 | 4 | 2.495 | 0.0381 | 5 | 4.090 | 0.0439 |
| 1 | 2.07 | 0.0805 | 2 | 1.95 | 0.0476 | 3 | 3.129 | 0.0463 | 4 | 2.074 | 0.0360 | 5 | 6.012 | 0.0512 |
| 1 | 3.60 | 0.0846 | 2 | 4.32 | 0.0598 | 3 | 4.062 | 0.0510 | 4 | 4.295 | 0.0462 | 5 | 8.146 | 0.0580 |
| 1 | 4.53 | 0.0862 | 2 | 6.02 | 0.0667 | 3 | 6.293 | 0.0594 | 4 | 6.066 | 0.0534 | 5 | 10.145 | 0.0629 |
| 1 | 6.34 | 0.0904 | 2 | 8.16 | 0.0740 | 3 | 8.319 | 0.0662 | 4 | 8.176 | 0.0604 | 5 | 15.781 | 0.0773 |
| 1 | 8.03 | 0.0959 | 2 | 10.06 | 0.0801 | 3 | 10.026 | 0.0714 | 4 | 10.149 | 0.0661 | 5 | 23.179 | 0.0909 |
| 1 | 9.99 | 0.1007 | 2 | 14.36 | 0.0919 | 3 | 14.935 | 0.0842 | 4 | 15.161 | 0.0782 | 5 | 31.913 | 0.1058 |
| 1 | 14.36 | 0.1113 | 2 | 25.52 | 0.1146 | 3 | 24.727 | 0.1037 | 4 | 25.499 | 0.0976 | | | |
| 1 | 24.45 | 0.1336 | 2 | 30.59 | 0.1246 | 3 | 34.112 | 0.1192 | 4 | 38.420 | 0.1183 | | | |
| 1 | 33.46 | 0.1495 | | | | | | | | | | | | |

Table D.7: 5.4% Bentonite in water suspension in a 300 mm triangular flume

| | |
|-----------------------------|-----------|
| Material: | Bentonite |
| Concentration/vol: | 5.4% |
| Density kg/m ³ : | 1032.7 |
| Ty (Pa): | 8.153 |
| k (Pa.s ⁿ): | 0.0033 |
| n: | 1.000 |
| Flume width (mm): | 300 |
| Flume Shape | Vee |

| SLOPE | FLOW | DEPTH | SLOPE | FLOW | DEPTH | SLOPE | FLOW | DEPTH | SLOPE | FLOW | DEPTH | SLOPE | FLOW | DEPTH |
|-----------|----------------------|--------|-----------|----------------------|--------|-----------|----------------------|--------|-----------|----------------------|--------|-----------|----------------------|--------|
| FLUME | Q | h | FLUME | Q | h | FLUME | Q | h | FLUME | Q | h | FLUME | Q | h |
| (degrees) | (L.s ⁻¹) | (m) | (degrees) | (L.s ⁻¹) | (m) | (degrees) | (L.s ⁻¹) | (m) | (degrees) | (L.s ⁻¹) | (m) | (degrees) | (L.s ⁻¹) | (m) |
| 1 | 0.132 | 0.1045 | 2 | 0.233 | 0.0612 | 3 | 0.236 | 0.0389 | 4 | 0.36 | 0.0307 | 5 | 0.26 | 0.0255 |
| 1 | 0.342 | 0.1045 | 2 | 0.421 | 0.0628 | 3 | 0.436 | 0.0399 | 4 | 0.52 | 0.0316 | 5 | 0.49 | 0.0268 |
| 1 | 0.483 | 0.1047 | 2 | 0.630 | 0.0632 | 3 | 0.642 | 0.0400 | 4 | 0.72 | 0.0323 | 5 | 0.73 | 0.0283 |
| 1 | 0.686 | 0.1093 | 2 | 0.827 | 0.0652 | 3 | 0.831 | 0.0405 | 4 | 0.90 | 0.0336 | 5 | 0.99 | 0.0297 |
| 1 | 0.783 | 0.1081 | 2 | 1.132 | 0.0628 | 3 | 1.070 | 0.0415 | 4 | 1.35 | 0.0364 | 5 | 1.26 | 0.0316 |
| 1 | 0.957 | 0.1101 | 2 | 1.408 | 0.0627 | 3 | 1.519 | 0.0438 | 4 | 2.04 | 0.0400 | 5 | 1.61 | 0.0341 |
| 1 | 1.462 | 0.1151 | 2 | 1.853 | 0.0629 | 3 | 2.056 | 0.0468 | 4 | 3.01 | 0.0443 | 5 | 2.28 | 0.0375 |
| 1 | 2.064 | 0.1170 | 2 | 2.428 | 0.0631 | 3 | 2.986 | 0.0497 | 4 | 4.02 | 0.0496 | 5 | 2.98 | 0.0410 |
| 1 | 2.518 | 0.1164 | 2 | 3.450 | 0.0654 | 3 | 4.205 | 0.0562 | 4 | 6.17 | 0.0575 | 5 | 4.06 | 0.0455 |
| 1 | 3.069 | 0.1127 | 2 | 4.323 | 0.0668 | 3 | 6.084 | 0.0627 | 4 | 8.07 | 0.0634 | 5 | 6.33 | 0.0538 |
| 1 | 3.929 | 0.1177 | 2 | 6.384 | 0.0752 | 3 | 8.028 | 0.0690 | 4 | 10.19 | 0.0692 | 5 | 8.08 | 0.0591 |
| 1 | 6.113 | 0.1209 | 2 | 8.107 | 0.0804 | 3 | 10.208 | 0.0755 | 4 | 12.31 | 0.0743 | 5 | 10.20 | 0.0651 |
| 1 | 8.086 | 0.1235 | 2 | 10.209 | 0.0863 | 3 | 13.842 | 0.0844 | 4 | 15.37 | 0.0815 | 5 | 11.95 | 0.0691 |
| 1 | 10.221 | 0.1245 | 2 | 12.367 | 0.0918 | 3 | 18.480 | 0.0949 | 4 | 20.00 | 0.0913 | 5 | 14.86 | 0.0756 |
| 1 | 14.753 | 0.1308 | 2 | 14.980 | 0.0990 | 3 | 25.110 | 0.1076 | 4 | 26.50 | 0.1015 | 5 | 20.76 | 0.0870 |
| 1 | 12.640 | 0.1289 | 2 | 20.006 | 0.1105 | 3 | 35.284 | 0.1231 | 4 | 34.92 | 0.1156 | 5 | 31.90 | 0.1054 |
| 1 | 18.878 | 0.1418 | 2 | 26.208 | 0.1214 | | | | | | | | | |
| 1 | 23.839 | 0.1485 | 2 | 35.557 | 0.1360 | | | | | | | | | |
| 1 | 27.665 | 0.1551 | 2 | 43.315 | 0.1466 | | | | | | | | | |
| 1 | 41.022 | 0.1756 | | | | | | | | | | | | |

Table D.8: 3.4% kaolin in water suspension in a 300 mm triangular flume

| | |
|-----------------------------|--------|
| Material: | Kaolin |
| Concentration/vol: | 3.4% |
| Density kg/m ³ : | 1055.5 |
| Ty (Pa): | 1.281 |
| k (Pa.s ⁿ): | 0.051 |
| n: | 0.568 |
| Flume width (mm): | 300 |
| Flume Shape | Vee |

| SLOPE | FLOW | DEPTH | SLOPE | FLOW | DEPTH | SLOPE | FLOW | DEPTH | SLOPE | FLOW | DEPTH | SLOPE | FLOW | DEPTH |
|-----------|----------------------|---------|-----------|----------------------|---------|-----------|----------------------|--------|-----------|----------------------|--------|-----------|----------------------|--------|
| FLUME | Q | h | FLUME | Q | h | FLUME | Q | h | FLUME | Q | h | FLUME | Q | h |
| (degrees) | (l.s ⁻¹) | (m) | (degrees) | (l.s ⁻¹) | (m) | (degrees) | (l.s ⁻¹) | (m) | (degrees) | (l.s ⁻¹) | (m) | (degrees) | (l.s ⁻¹) | (m) |
| 1 | 0.05 | 0.02609 | 2 | 0.08 | 0.0174 | 3 | 0.503 | 0.0203 | 4 | 0.074 | 0.0109 | 5 | 0.178 | 0.0128 |
| 1 | 0.14 | 0.02846 | 2 | 0.14 | 0.01789 | 3 | 0.105 | 0.0139 | 4 | 0.150 | 0.0125 | 5 | 0.273 | 0.0150 |
| 1 | 0.09 | 0.02686 | 2 | 0.18 | 0.01869 | 3 | 0.186 | 0.0150 | 4 | 0.110 | 0.0120 | 5 | 0.325 | 0.0158 |
| 1 | 0.19 | 0.02816 | 2 | 0.28 | 0.02046 | 3 | 0.131 | 0.0143 | 4 | 0.192 | 0.0133 | 5 | 0.433 | 0.0179 |
| 1 | 0.28 | 0.03007 | 2 | 0.38 | 0.02221 | 3 | 0.289 | 0.0173 | 4 | 0.237 | 0.0145 | 5 | 0.584 | 0.0201 |
| 1 | 0.39 | 0.03166 | 2 | 0.59 | 0.02518 | 3 | 0.386 | 0.0187 | 4 | 0.322 | 0.0162 | 5 | 0.785 | 0.0222 |
| 1 | 0.58 | 0.03356 | 2 | 0.79 | 0.02768 | 3 | 0.795 | 0.0246 | 4 | 0.468 | 0.0184 | 5 | 0.994 | 0.0245 |
| 1 | 0.79 | 0.0357 | 2 | 1.02 | 0.03018 | 3 | 1.005 | 0.0268 | 4 | 0.730 | 0.0223 | 5 | 1.476 | 0.0287 |
| 1 | 1.03 | 0.03808 | 2 | 1.53 | 0.03459 | 3 | 1.494 | 0.0315 | 4 | 1.005 | 0.0256 | 5 | 1.991 | 0.0326 |
| 1 | 1.49 | 0.04265 | 2 | 2.04 | 0.03852 | 3 | 1.989 | 0.0351 | 4 | 1.367 | 0.0284 | 5 | 3.005 | 0.0387 |
| 1 | 2.05 | 0.04737 | 2 | 3.02 | 0.04419 | 3 | 4.058 | 0.0465 | 4 | 1.958 | 0.0325 | 5 | 4.045 | 0.0428 |
| 1 | 2.94 | 0.05385 | 2 | 4.08 | 0.05038 | 3 | 7.932 | 0.0620 | 4 | 2.462 | 0.0357 | 5 | 6.069 | 0.0514 |
| 1 | 4.02 | 0.06037 | 2 | 6.08 | 0.0595 | 3 | 9.734 | 0.0671 | 4 | 4.128 | 0.0440 | 5 | 8.043 | 0.0574 |
| 1 | 6.01 | 0.07046 | 2 | 9.77 | 0.07336 | 3 | 14.918 | 0.0806 | 4 | 5.616 | 0.0507 | 5 | 9.822 | 0.0620 |
| 1 | 8.08 | 0.07935 | 2 | 14.20 | 0.08687 | 3 | 22.135 | 0.0962 | 4 | 7.986 | 0.0593 | 5 | 14.435 | 0.0736 |
| 1 | 9.74 | 0.08545 | 2 | 22.20 | 0.10497 | 3 | 32.670 | 0.1155 | 4 | 9.691 | 0.0648 | 5 | 20.128 | 0.0844 |
| 1 | 14.50 | 0.10024 | 2 | 32.05 | 0.12349 | | | | 4 | 14.237 | 0.0750 | | | |
| 1 | 22.12 | 0.11971 | | | | | | | 4 | 21.933 | 0.0905 | | | |
| 1 | 32.22 | 0.13976 | | | | | | | | | | | | |

Table D.9: 5% kaolin in water suspension in a 300 mm triangular flume

| | |
|-----------------------------|--------|
| Material: | Kaolin |
| Concentration/vol: | 5.0% |
| Density kg/m ³ : | 1082.3 |
| Ty (Pa): | 4.188 |
| k (Pa.s ⁿ): | 0.024 |
| n: | 0.747 |
| Flume width (mm): | 300 |
| Flume Shape | Vee |

| SLOPE | FLOW | DEPTH | SLOPE | FLOW | DEPTH | SLOPE | FLOW | DEPTH | SLOPE | FLOW | DEPTH | SLOPE | FLOW | DEPTH |
|-----------|----------------------|---------|-----------|----------------------|---------|-----------|----------------------|--------|-----------|----------------------|--------|-----------|----------------------|--------|
| FLUME | Q | h | FLUME | Q | h | FLUME | Q | h | FLUME | Q | h | FLUME | Q | h |
| (degrees) | (l.s ⁻¹) | (m) | (degrees) | (l.s ⁻¹) | (m) | (degrees) | (l.s ⁻¹) | (m) | (degrees) | (l.s ⁻¹) | (m) | (degrees) | (l.s ⁻¹) | (m) |
| 1 | 0.08 | 0.04789 | 2 | 0.09 | 0.02855 | 3 | 0.098 | 0.0216 | 4 | 0.101 | 0.0185 | 5 | 0.072 | 0.0167 |
| 1 | 0.19 | 0.05048 | 2 | 0.22 | 0.0305 | 3 | 0.188 | 0.0225 | 4 | 0.223 | 0.0201 | 5 | 0.197 | 0.0178 |
| 1 | 0.31 | 0.05344 | 2 | 0.31 | 0.03107 | 3 | 0.315 | 0.0244 | 4 | 0.142 | 0.0189 | 5 | 0.113 | 0.0165 |
| 1 | 0.41 | 0.05477 | 2 | 0.40 | 0.03188 | 3 | 0.429 | 0.0257 | 4 | 0.288 | 0.0205 | 5 | 0.304 | 0.0188 |
| 1 | 0.61 | 0.05732 | 2 | 0.62 | 0.03351 | 3 | 0.632 | 0.0276 | 4 | 0.424 | 0.0220 | 5 | 0.404 | 0.0200 |
| 1 | 0.85 | 0.05907 | 2 | 0.81 | 0.03548 | 3 | 0.927 | 0.0296 | 4 | 0.593 | 0.0237 | 5 | 0.594 | 0.0219 |
| 1 | 1.31 | 0.06163 | 2 | 1.23 | 0.0389 | 3 | 1.184 | 0.0325 | 4 | 0.814 | 0.0258 | 5 | 0.844 | 0.0237 |
| 1 | 1.55 | 0.06225 | 2 | 1.41 | 0.0404 | 3 | 1.417 | 0.0340 | 4 | 1.196 | 0.0291 | 5 | 1.197 | 0.0274 |
| 1 | 1.97 | 0.06321 | 2 | 1.65 | 0.0421 | 3 | 1.751 | 0.0365 | 4 | 1.385 | 0.0305 | 5 | 1.382 | 0.0288 |
| 1 | 3.35 | 0.06777 | 2 | 2.08 | 0.04525 | 3 | 2.571 | 0.0413 | 4 | 1.863 | 0.0333 | 5 | 1.832 | 0.0316 |
| 1 | 4.28 | 0.07277 | 2 | 3.55 | 0.05331 | 3 | 4.012 | 0.0486 | 4 | 3.435 | 0.0417 | 5 | 3.046 | 0.0374 |
| 1 | 6.14 | 0.08187 | 2 | 4.48 | 0.05786 | 3 | 4.862 | 0.0520 | 4 | 4.218 | 0.0456 | 5 | 4.059 | 0.0420 |
| 1 | 8.47 | 0.09021 | 2 | 6.03 | 0.0645 | 3 | 6.159 | 0.0578 | 4 | 6.240 | 0.0531 | 5 | 6.322 | 0.0507 |
| 1 | 10.07 | 0.09648 | 2 | 8.32 | 0.073 | 3 | 8.261 | 0.0645 | 4 | 8.038 | 0.0593 | 5 | 8.235 | 0.0565 |
| 1 | 16.48 | 0.11317 | 2 | 10.00 | 0.07879 | 3 | 10.032 | 0.0706 | 4 | 10.192 | 0.0656 | 5 | 10.075 | 0.0617 |
| 1 | 28.12 | 0.14072 | 2 | 16.68 | 0.0961 | 3 | 15.134 | 0.0836 | 4 | 14.873 | 0.0771 | 5 | 14.626 | 0.0720 |
| 1 | 36.69 | 0.15505 | 2 | 26.07 | 0.11694 | 3 | 25.049 | 0.1069 | 4 | 22.261 | 0.0923 | 5 | 20.447 | 0.0837 |
| | | | 2 | 35.67 | 0.1313 | 3 | 36.435 | 0.1258 | 4 | 32.844 | 0.1096 | 5 | 25.342 | 0.0925 |
| | | | | | | | | | 4 | 40.157 | 0.1187 | 5 | 34.950 | 0.1014 |

Table D.10: 7% kaolin in water suspension in a 300 mm triangular flume

| | |
|-----------------------------|--------|
| Material: | Kaolin |
| Concentration/vol: | 7.0% |
| Density kg/m ³ : | 1115.3 |
| Ty (Pa): | 8.175 |
| k (Pa.s ⁿ): | 0.142 |
| n: | 0.570 |
| Flume width (mm): | 300 |
| Flume Shape | Vee |

| SLOPE | FLOW | DEPTH | SLOPE | FLOW | DEPTH | SLOPE | FLOW | DEPTH | SLOPE | FLOW | DEPTH | SLOPE | FLOW | DEPTH |
|-----------|----------------------|---------|-----------|----------------------|---------|-----------|----------------------|--------|-----------|----------------------|--------|-----------|----------------------|--------|
| FLUME | Q | h | FLUME | Q | h | FLUME | Q | h | FLUME | Q | h | FLUME | Q | h |
| (degrees) | (L.s ⁻¹) | (m) | (degrees) | (L.s ⁻¹) | (m) | (degrees) | (L.s ⁻¹) | (m) | (degrees) | (L.s ⁻¹) | (m) | (degrees) | (L.s ⁻¹) | (m) |
| 1 | 1.13 | 0.10148 | 2 | 0.17 | 0.05566 | 3 | 0.112 | 0.0395 | 4 | 0.179 | 0.0329 | 5 | 0.104 | 0.0255 |
| 1 | 1.29 | 0.1028 | 2 | 0.35 | 0.05941 | 3 | 0.342 | 0.0428 | 4 | 0.399 | 0.0351 | 5 | 0.168 | 0.0269 |
| 1 | 1.49 | 0.10427 | 2 | 0.28 | 0.05839 | 3 | 0.247 | 0.0426 | 4 | 0.204 | 0.0334 | 5 | 0.311 | 0.0288 |
| 1 | 1.71 | 0.10599 | 2 | 0.54 | 0.06209 | 3 | 0.536 | 0.0453 | 4 | 0.279 | 0.0344 | 5 | 0.409 | 0.0295 |
| 1 | 2.08 | 0.10836 | 2 | 0.79 | 0.06408 | 3 | 0.710 | 0.0464 | 4 | 0.556 | 0.0360 | 5 | 0.571 | 0.0307 |
| 1 | 3.15 | 0.1131 | 2 | 1.03 | 0.06543 | 3 | 0.936 | 0.0471 | 4 | 0.761 | 0.0368 | 5 | 0.792 | 0.0316 |
| 1 | 4.48 | 0.12002 | 2 | 1.42 | 0.0667 | 3 | 1.372 | 0.0483 | 4 | 1.012 | 0.0380 | 5 | 0.992 | 0.0326 |
| 1 | 6.23 | 0.12712 | 2 | 1.67 | 0.06779 | 3 | 1.845 | 0.0501 | 4 | 1.219 | 0.0392 | 5 | 1.198 | 0.0337 |
| 1 | 8.37 | 0.13272 | 2 | 1.99 | 0.06893 | 3 | 2.725 | 0.0534 | 4 | 1.457 | 0.0404 | 5 | 1.429 | 0.0345 |
| 1 | 9.97 | 0.1364 | 2 | 2.62 | 0.06962 | 3 | 4.531 | 0.0607 | 4 | 1.457 | 0.0404 | 5 | 1.748 | 0.0369 |
| 1 | 16.67 | 0.14511 | 2 | 6.11 | 0.07932 | 3 | 5.995 | 0.0658 | 4 | 1.749 | 0.0417 | 5 | 2.255 | 0.0395 |
| 1 | 26.97 | 0.16259 | 2 | 4.17 | 0.07412 | 3 | 7.690 | 0.0716 | 4 | 2.291 | 0.0441 | 5 | 3.208 | 0.0433 |
| 1 | 36.11 | 0.17496 | 2 | 7.97 | 0.0861 | 3 | 9.763 | 0.0774 | 4 | 3.387 | 0.0480 | 5 | 4.268 | 0.0481 |
| 1 | 13.44 | 0.13881 | 2 | 9.88 | 0.09188 | 3 | 15.766 | 0.0926 | 4 | 4.334 | 0.0528 | 5 | 6.135 | 0.0542 |
| | | | 2 | 16.03 | 0.10645 | 3 | 24.477 | 0.1100 | 4 | 6.160 | 0.0596 | 5 | 8.277 | 0.0615 |
| | | | 2 | 26.21 | 0.12765 | 3 | 34.185 | 0.1259 | 4 | 8.132 | 0.0660 | 5 | 10.023 | 0.0662 |
| | | | 2 | 36.20 | 0.14354 | | | | 4 | 9.993 | 0.0714 | 5 | 15.310 | 0.0783 |
| | | | | | | | | | 4 | 15.404 | 0.0841 | 5 | 25.184 | 0.0970 |
| | | | | | | | | | 4 | 27.124 | 0.1063 | 5 | 34.149 | 0.1109 |
| | | | | | | | | | 4 | 36.256 | 0.1199 | | | |

Table D.11: 9.2% kaolin in water suspension in a 300 mm triangular flume

| | |
|-----------------------------|--------|
| Material: | Kaolin |
| Concentration/vol: | 9.2% |
| Density kg/m ³ : | 1152.2 |
| Ty (Pa): | 17.767 |
| k (Pa.s ⁿ): | 0.139 |
| n: | 0.630 |
| Flume width (mm): | 300 |
| Flume Shape | Vee |

| SLOPE | FLOW | DEPTH | SLOPE | FLOW | DEPTH | SLOPE | FLOW | DEPTH | SLOPE | FLOW | DEPTH | SLOPE | FLOW | DEPTH |
|-----------|----------------------|---------|-----------|----------------------|---------|-----------|----------------------|---------|-----------|----------------------|--------|-----------|----------------------|--------|
| FLUME | Q | h | FLUME | Q | h | FLUME | Q | h | FLUME | Q | h | FLUME | Q | h |
| (degrees) | (L.s ⁻¹) | (m) | (degrees) | (L.s ⁻¹) | (m) | (degrees) | (L.s ⁻¹) | (m) | (degrees) | (L.s ⁻¹) | (m) | (degrees) | (L.s ⁻¹) | (m) |
| 1 | 0.99 | 0.14214 | 2 | 1.06 | 0.1063 | 3 | 0.26 | 0.0711 | 4 | 0.154 | 0.0551 | 5 | 0.232 | 0.0488 |
| 1 | 1.11 | 0.1449 | 2 | 1.31 | 0.10907 | 3 | 0.36 | 0.07325 | 4 | 0.275 | 0.0575 | 5 | 0.108 | 0.0467 |
| 1 | 1.20 | 0.14627 | 2 | 1.54 | 0.11013 | 3 | 0.45 | 0.07476 | 4 | 0.435 | 0.0586 | 5 | 0.130 | 0.0468 |
| 1 | 1.48 | 0.14891 | 2 | 1.80 | 0.11147 | 3 | 0.60 | 0.07631 | 4 | 0.385 | 0.0593 | 5 | 0.188 | 0.0485 |
| 1 | 1.84 | 0.15166 | 2 | 2.30 | 0.1141 | 3 | 0.78 | 0.07709 | 4 | 0.550 | 0.0607 | 5 | 0.326 | 0.0505 |
| 1 | 2.21 | 0.1546 | 2 | 0.85 | 0.10531 | 3 | 0.99 | 0.07849 | 4 | 0.671 | 0.0615 | 5 | 0.407 | 0.0503 |
| 1 | 2.65 | 0.15784 | 2 | 0.64 | 0.10265 | 3 | 1.19 | 0.07987 | 4 | 0.819 | 0.0625 | 5 | 0.629 | 0.0521 |
| 1 | 4.23 | 0.16491 | 2 | 0.44 | 0.10044 | 3 | 1.36 | 0.08061 | 4 | 0.955 | 0.0631 | 5 | 0.729 | 0.0527 |
| 1 | 3.77 | 0.16394 | 2 | 3.13 | 0.11585 | 3 | 1.59 | 0.08106 | 4 | 1.135 | 0.0637 | 5 | 0.878 | 0.0529 |
| 1 | 5.10 | 0.17046 | 2 | 4.31 | 0.12079 | 3 | 1.79 | 0.08205 | 4 | 1.295 | 0.0645 | 5 | 1.030 | 0.0533 |
| 1 | 7.36 | 0.17987 | 2 | 6.39 | 0.12679 | 3 | 2.09 | 0.08314 | 4 | 1.467 | 0.0654 | 5 | 1.148 | 0.0537 |
| 1 | 9.84 | 0.18844 | 2 | 8.16 | 0.13061 | 3 | 2.38 | 0.08418 | 4 | 1.688 | 0.0661 | 5 | 1.337 | 0.0542 |
| 1 | 15.19 | 0.2007 | 2 | 14.28 | 0.13606 | 3 | 2.86 | 0.0852 | 4 | 1.885 | 0.0668 | 5 | 1.571 | 0.0545 |
| 1 | 25.94 | 0.22188 | 2 | 11.21 | 0.13268 | 3 | 3.63 | 0.08777 | 4 | 2.034 | 0.0660 | 5 | 1.771 | 0.0548 |
| 1 | 35.96 | 0.23724 | 2 | 27.59 | 0.15353 | 3 | 5.25 | 0.0904 | 4 | 2.452 | 0.0665 | 5 | 2.002 | 0.0551 |
| | | | 2 | 35.81 | 0.16505 | 3 | 7.24 | 0.09281 | 4 | 2.923 | 0.0684 | 5 | 2.320 | 0.0559 |
| | | | 2 | 20.24 | 0.14168 | 3 | 9.06 | 0.09603 | 4 | 4.086 | 0.0707 | 5 | 3.795 | 0.0592 |
| | | | | | | 3 | 15.86 | 0.10923 | 4 | 5.027 | 0.0729 | 5 | 3.051 | 0.0583 |
| | | | | | | 3 | 25.42 | 0.12594 | 4 | 5.986 | 0.0754 | 5 | 4.950 | 0.0632 |
| | | | | | | 3 | 34.84 | 0.14001 | 4 | 7.127 | 0.0779 | 5 | 6.473 | 0.0672 |
| | | | | | | | | | 4 | 8.449 | 0.0809 | 5 | 8.068 | 0.0717 |
| | | | | | | | | | 4 | 15.026 | 0.0952 | 5 | 9.905 | 0.0763 |
| | | | | | | | | | 4 | 22.726 | 0.1091 | 5 | 15.789 | 0.0881 |
| | | | | | | | | | 4 | 28.415 | 0.1187 | 5 | 22.134 | 0.1002 |
| | | | | | | | | | 4 | 34.483 | 0.1270 | 5 | 28.730 | 0.1105 |
| | | | | | | | | | | | | 5 | 35.966 | 0.1203 |